

---

# A Comparative Analysis of LWR Fuel Designs

---

Prepared by D. L. Acey, J. C. Voglewede

Office of  
Nuclear Reactor Regulation

U.S. Nuclear Regulatory  
Commission



Available from

GPO Sales Program  
Division of Technical Information and Document Control  
U. S. Nuclear Regulatory Commission  
Washington, D. C. 20555

Printed copy price: \$5.50

and

National Technical Information Service  
Springfield, Virginia 22161

---

# A Comparative Analysis of LWR Fuel Designs

---

Manuscript Completed: June 1980  
Date Published: July 1980

Prepared by D. L. Acey, J. C. Voglewede

Division of Systems Integration  
Office of Nuclear Reactor Regulation  
U.S. Nuclear Regulatory Commission  
Washington, D.C. 20555



## ABSTRACT

The computer code GAPCON-THERMAL-2 was used to generate thermal performance predictions for the spectrum of commercial light water reactor fuel designs at four different steady-state power levels. The input parameters for the code were obtained from design data that are non-proprietary and are tabulated in this report. Calculated values of maximum fuel temperature, average fuel temperature, stored energy, gap conductance, fission gas release and rod internal pressure are plotted as a function of burnup. Radial fuel pellet temperatures are also plotted at one burnup level.

## TABLE OF CONTENTS

I.	INTRODUCTION . . . . .	1
II.	THE COMPARATIVE PROCESS. . . . .	4
III.	LIMITATIONS OF THE STUDY . . . . .	8
1.	Operating Histories . . . . .	8
2.	Fission Gas Release. . . . .	9
3.	Cladding Creep . . . . .	25
4.	Fuel Restructuring . . . . .	33
IV.	SUMMARY. . . . .	34
V.	REFERENCES . . . . .	35
APPENDIX A	Input Parameter Source List. . . . .	A-1
APPENDIX B	Fuel Assembly Parameter List . . . . .	B-1
APPENDIX C	Legend for Multi-Fuel Design Graphs. . . . .	C-1
APPENDIX D	Fuel Centerline Temperature Graphs . . . . .	D-1
APPENDIX E	Fuel Radial Temperature Graphs . . . . .	E-1
APPENDIX F	Fuel Average Temperature Graphs . . . . .	F-1
APPENDIX G	Stored Energy Graphs . . . . .	G-1
APPENDIX H	Gap Conductance Graphs . . . . .	H-1
APPENDIX I	Fission Gas Release Graphs . . . . .	I-1
APPENDIX J	Rod Internal Pressure Graphs . . . . .	J-1

## LIST OF FIGURES

<u>Figure</u>	<u>Page</u>
1 PWR Axial Power Profile . . . . .	6
2 BWR Axial Power Profile . . . . .	7
3 Fuel Centerline Temperature for Standard and Burnup Independent Fission Gas Release Models. . . . .	10
4 Fuel Radial Temperature for Standard and Burnup Independent Fission Gas Release Models. . . . .	11
5 Fuel Average Temperature for Standard and Burnup Independent Fission Gas Release Models. . . . .	12
6 Stored Energy for Standard and Burnup Independent Fission Gas Release Models. . . . .	13
7 Gap Conductance for Standard and Burnup Independent Fission Gas Release Models. . . . .	14
8 Fission Gas Release for Standard and Burnup Independent Fission Gas Release Models. . . . .	15
9 Rod Internal Pressure for Standard and Burnup Independent Fission Gas Release Models. . . . .	16
10 Fuel Centerline Temperature for Two Burnup Dependent Fission Gas Release Models. . . . .	18
11 Fuel Radial Temperature for Two Burnup Dependent Fission Gas Release Models. . . . .	19
12 Fuel Average Temperature for Two Burnup Dependent Fission Gas Release Models. . . . .	20
13 Stored Energy for Two Burnup Dependent Fission Gas Release Models. . . . .	21
14 Gap Conductance for Two Burnup Dependent Fission Gas Release Models. . . . .	22
15 Fission Gas Release for Two Burnup Dependent Fission Gas Release Models . . . . .	23
16 Rod Internal Pressure for Two Burnup Dependent Fission Gas Release Models. . . . .	24

<u>Figure</u>		<u>Page</u>
17	Fuel Centerline Temperature with and without Cladding Creepdown. . . . .	26
18	Fuel Radial Temperature with and without Cladding Creepdown. . . . .	27
19	Fuel Average Temperature with and without Cladding Creepdown. . . . .	28
20	Stored Energy with and without Cladding Creepdown . . . . .	29
21	Gap Conductance with and without Cladding Creepdown . . . . .	30
22	Fission Gas Release with and without Cladding Creepdown. . . . .	31
23	Rod Internal Pressure with and without Cladding Creepdown. . . . .	32

## I. Introduction

A thermal performance analysis of light water reactor (LWR) fuel designs was performed using the digital computer code, GAPCON-THERMAL-2 (Refs. 1-2). Code predictions were generated for 13 commercial LWR fuel designs, at various steady-state linear power levels. The input parameters for the code were obtained from design data that are non-proprietary and are tabulated in this report. Calculated values of maximum fuel temperature, average fuel temperature, stored energy, gap conductance, fission gas release and rod internal pressure were plotted as a function of burnup. Radial fuel pellet temperature was also plotted at one burnup level.

This study was prepared for two reasons. First, it serves as an example of the fuel performance code predictions required by the NRC staff as part of the safety analysis submitted in support of a license application for a nuclear power plant. Secondly, the report serves as a reference document from which the effect of fuel design differences can be determined.

All the runs were made using the same computer code and the only variations were the input parameters. Therefore, relative differences in the results were due to changes in the input parameters, and thus the design differences. Where different model options were available within the code, best-estimate rather than conservative models were selected.

Therefore, the results are best-estimate predictions within the limits of the code. The GAPCON-THERMAL-2 code is believed to be representative of a number of similar codes used by the nuclear industry for fuel thermal performance analysis.



Fuel thermal performance analyses are performed as part of each nuclear power plant safety analysis in order to provide fuel design values such as stored energy, fuel centerline temperature and rod internal pressure. Each of these parameters has a design limit which must not be exceeded during the operation of the plant. A number of these fuel design limits are discussed below.

Appendix K to Part 50, Title 10, of the Code of Federal Regulations (10 CFR 50, Appendix K (Ref. 3)) states that the initial stored energy and fuel temperatures shall be calculated for a hypothetical loss-of-coolant accident. Historically, the peak stored energy values have been shown to occur at beginning of operation or soon after for current fuel designs. This study has demonstrated that that conclusion is not always true and may be applicable only under low and moderate burnup conditions.

Additional fuel temperature limits are given in both 10 CFR 50.46 and Section 4.2 of the NRC Standard Review Plan (Ref. 4). The Standard Review Plan states that it must be shown that "fuel melting does not occur" during normal operation. The study demonstrates that melting does not occur for the power levels considered.

Section 4.2 of the Standard Review Plan also requires the rod internal pressure to "remain below the normal system pressure during normal operation unless otherwise justified." System pressure is a known quantity for each fuel design considered in this study. Calculated values of the rod internal pressure were compared with systems pressure for all cases. For constant power operation, it was concluded that the rod internal

pressure will eventually exceed system pressure at some point in time.

The study demonstrates that this occurs only for high burnup conditions.

## II. The Comparative Process

For this study, the GAPCON-THERMAL-2, Revision 1 (March 1980) code was used. Although calculations were performed for each axial segment, only the results for the hottest axial node of each rod were plotted. This was done as a function of burnup in the peak axial segment. Depending on the fuel design and power level selected, the actual in-reactor time necessary to attain the maximum burnup considered (50,000 MWd/MtU) varied from 482 to 3298 days. Results were obtained for the following 13 fuel designs: Babcock and Wilcox 15x15 and 17x17; Combustion Engineering 14x14 and 16x16; Westinghouse 14x14, 15x15, and 17x17; Exxon 15x15 and 8x8; and General Electric 7x7, 8x8, 8x8R and prepressurized 8x8R fuel designs. For each design, four steady-state constant-peak-power levels were selected. These were 5 kW/ft, 10 kW/ft, 15 kW/ft peak power, and also a rod power level equal to that of an average rod in the core. The last value therefore represents the hot spot of an average rod in the core.

A list of the input parameters required by the GAPCON-THERMAL-2 code is shown in Appendix A. Included in the list are information references used to generate each value. The principal source of this information was a list of fuel assembly parameters, which is included as Appendix B.

A number of input parameters are based on simplified formulations rather than real data. As one example, rather than using a realistic, time-varying axial power profile, an axially symmetric, truncated cosine curve was developed with an appropriate peaking factor. The simplified profile was held constant as function of time and rod power. The method

and equations are presented below with the results plotted in Figures 1 and 2 for PWR and BWR plants respectively.

$$Y = a \cos (k(x+b))$$

where:  $Y$  = local normalized power  
 $a$  = axial peaking factor  
 $k$  = a constant (shape factor)  
 $x$  = core elevation  
 $b$  = -(core height)/2

This equation was used in conjunction with the relation

$$\int Y dx / \int dx = 1$$

in order to determine the value of  $k$  for the normalized cosine curve. The implications of using this simplified axial power profile, as well as other code input assumptions, are discussed in Section III of this report. The resulting code predictions were organized into graphs which are presented in the remaining appendices. These are:

- Appendix C - Legend for Multi-Fuel Design Graphs
- Appendix D - Fuel Centerline Temperature vs Burnup
- Appendix E - Fuel Temperature vs Radius at 10000 MWd/MtU
- Appendix F - Fuel Average Temperature vs Burnup
- Appendix G - Stored Energy vs Burnup
- Appendix H - Gap Conductance vs Burnup
- Appendix I - Fission Gas Release vs Burnup
- Appendix J - Rod Internal Pressure vs Burnup

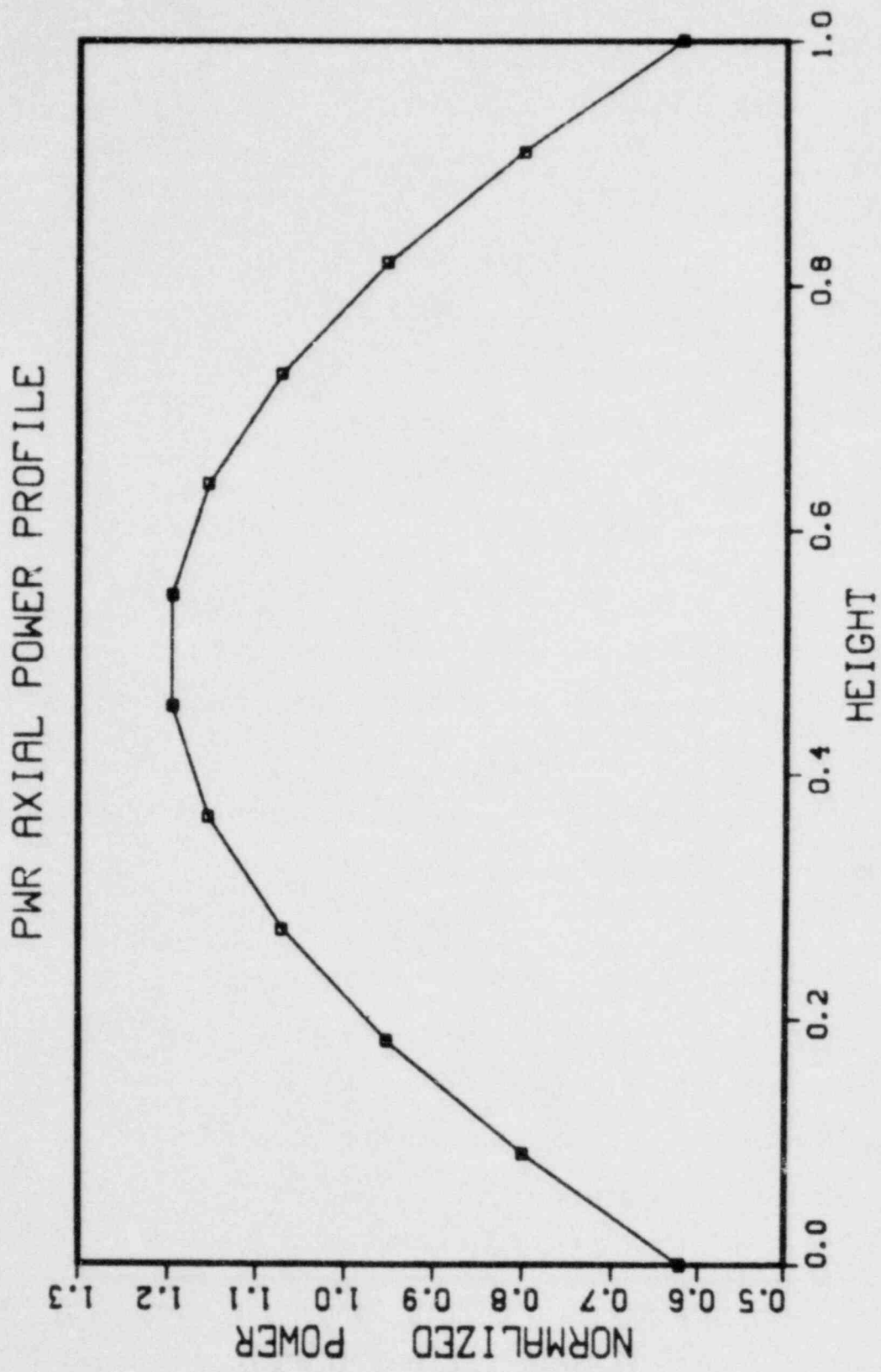


Fig. 1 PWR Axial Power Profile

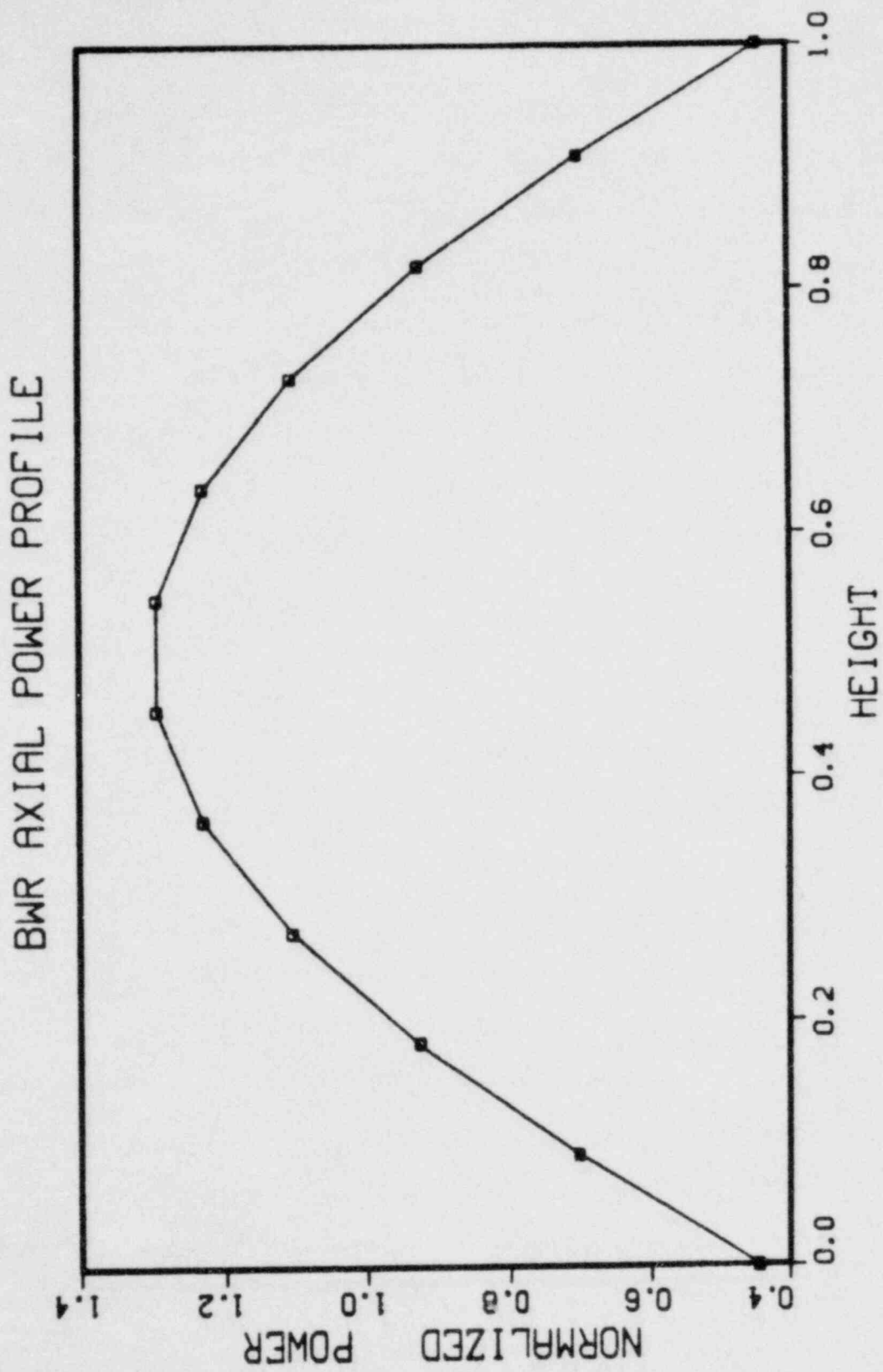


Fig. 2 BWR Axial Power Profile

### III. Limitations of the Study

A result of using an analytical computer code is that certain qualifications of the predictions must be made. The general limitations recognized in this study are the result of two factors. First, the code itself is subject to some intrinsic inaccuracies because of the inexactness of the analytical methods used. Second, a number of input simplifications have been made as mentioned previously. In safety analyses, these simplifications may be intentionally biased with respect to more realistic, and possibly more complex, assumptions. The biased assumptions are also called conservatisms. Throughout this study, the use of traditional or licensing-oriented conservatisms has been avoided. Within the limitations of the basic GAPCON-THERMAL-2 code, the results should be considered best-estimate. Several of the remaining limitations are discussed below.

#### 1. Operating Histories

The power level of a nuclear fuel rod fluctuates as a function of time and generally decreases toward end of life. In this study, a constant power history was used. A criticism of this approach is that a constant power history, rather than a time-varying power history, may exaggerate power-dependent effects at end-of-life. The effect of decreasing power on the code predictions was examined. It was found that instantaneous power is of primary importance while constant or decreasing power history is a second-order effect in the code predictions. The emphasis in this study has, therefore,

been placed on power level rather than power history. In addition, it is difficult to determine time-varying, but realistic, power histories which, when used in the code, will preserve a common comparative basis.

## 2. Fission Gas Release

Incorporated into the GAPCON-THERMAL-2 code is a fission gas release model developed by Beyer and Hann (Ref. 1). For reasons described in Reference 5, an NRC correction function for this and other models was developed to correct gas release predictions at burnup values greater than 20,000 MWd/MtU. The correction function is used to account for fission gas release data taken at high burnups. At the time they were derived, neither the Beyer-Hann model, nor those used in fuel vendor codes, had access to high burnup fission gas release data. Further discussion of the correction factor and its derivation is also found in Reference 5.

Figures 3-9 give comparative plots of the Beyer-Hann model with and without the NRC correction for a representative fuel design (B&W 15x15). It can be seen that gap conductance, fission gas release and rod internal pressure are affected to a large extent by the addition of the correction function. The Beyer-Hann model with the NRC correction gave values of fission gas release nearly 7 times as large and rod internal pressure values more than twice as large as the corresponding values obtained from the uncorrected Beyer-Hann model. Yet fuel temperatures and stored energy showed differences of less than 10%. This indicates that thermal conditions of the



# B&W 15X15

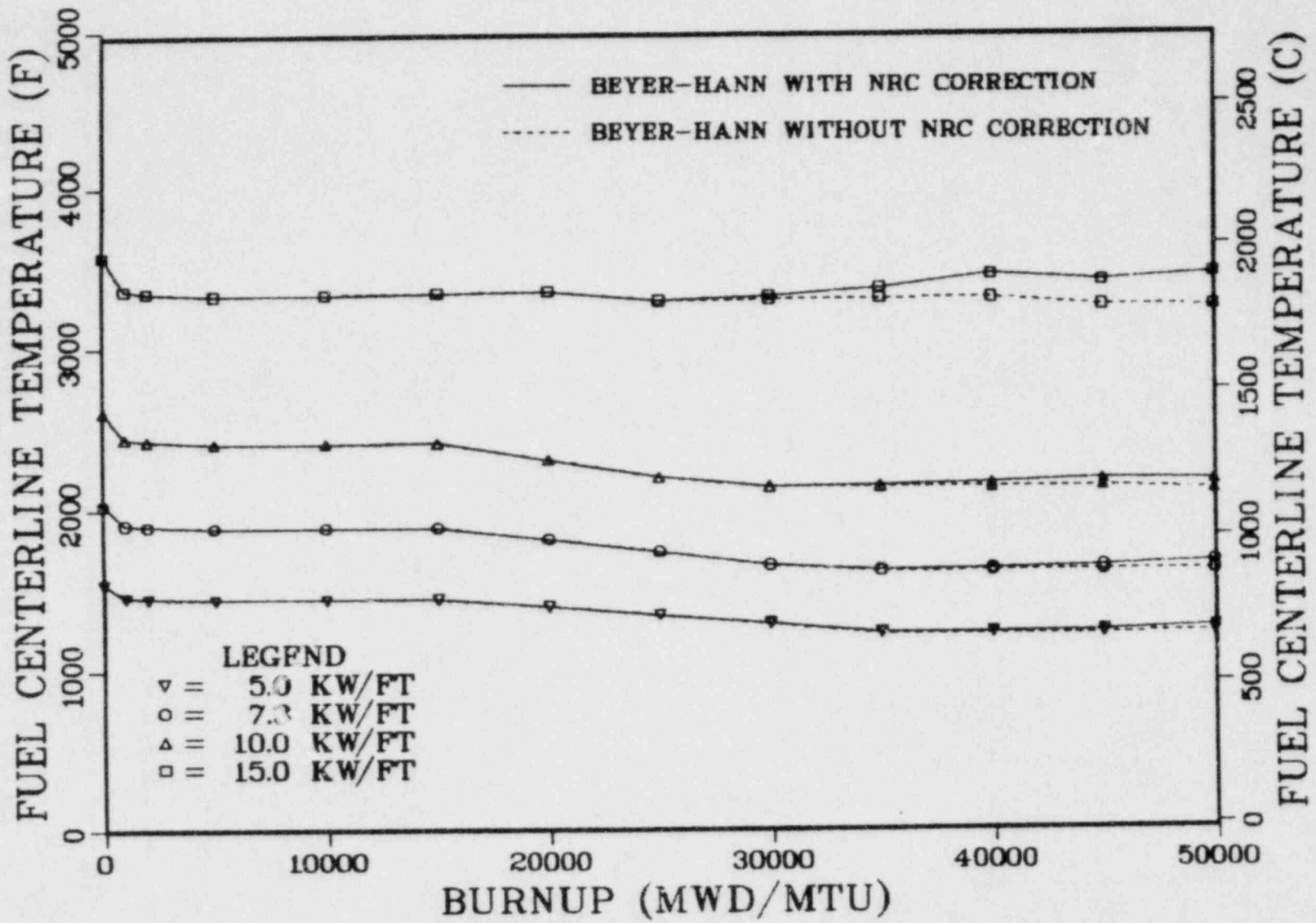


Fig. 3 Fuel Centerline Temperature for Standard and Burnup Independent Fission Gas Release Models.

# B&W 15X15

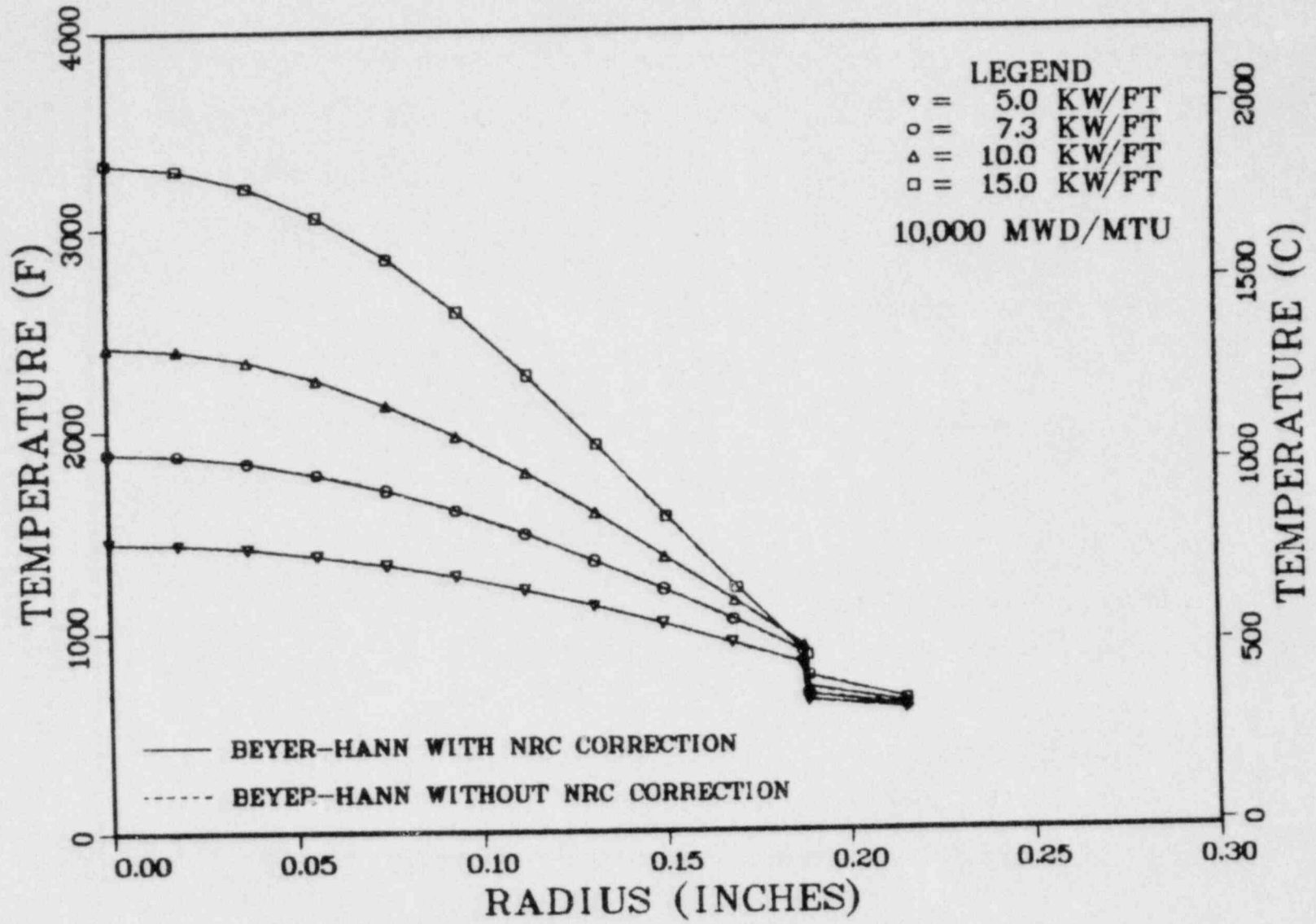


Fig. 4 Fuel Radial Temperature for Standard and Burnup Independent Fission Gas Release Models.

# B&W 15X15

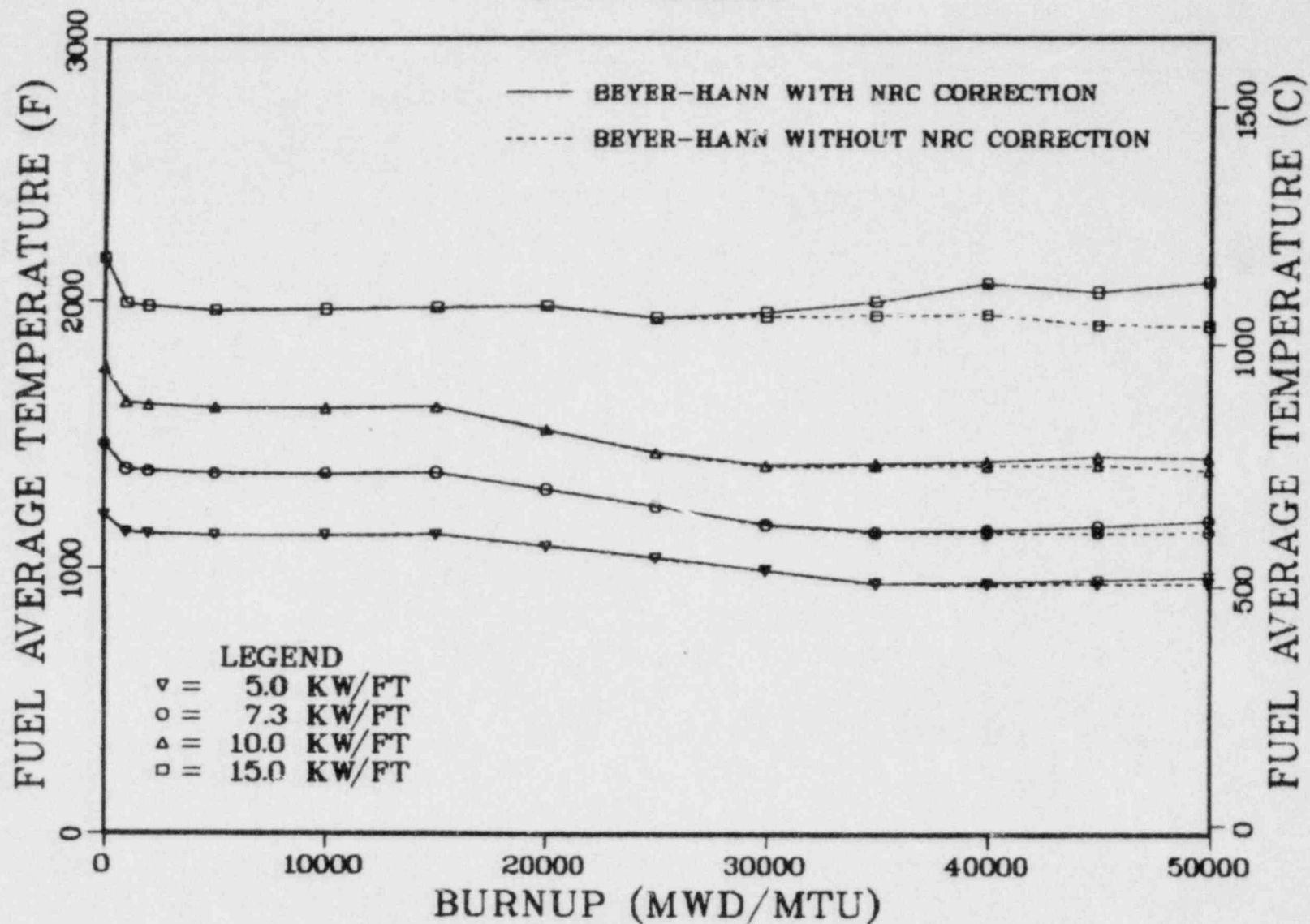


Fig. 5 Fuel Average Temperature for Standard and Burnup Independent Fission Gas Release Models.

### B&W 15X15

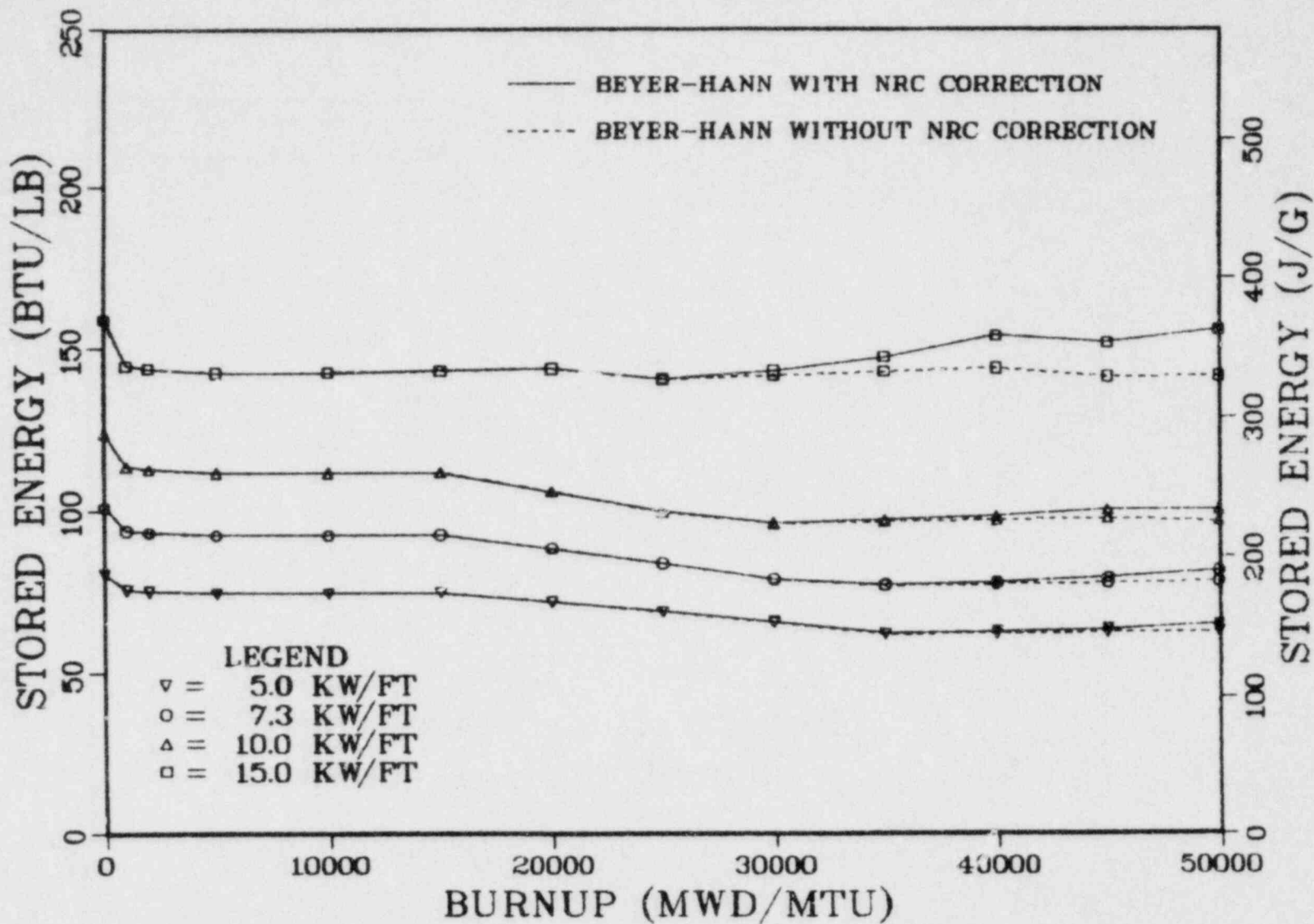


Fig. 6 Stored Energy for Standard and Burnup Independent Fission Gas Release Models.

# B&W 15X15

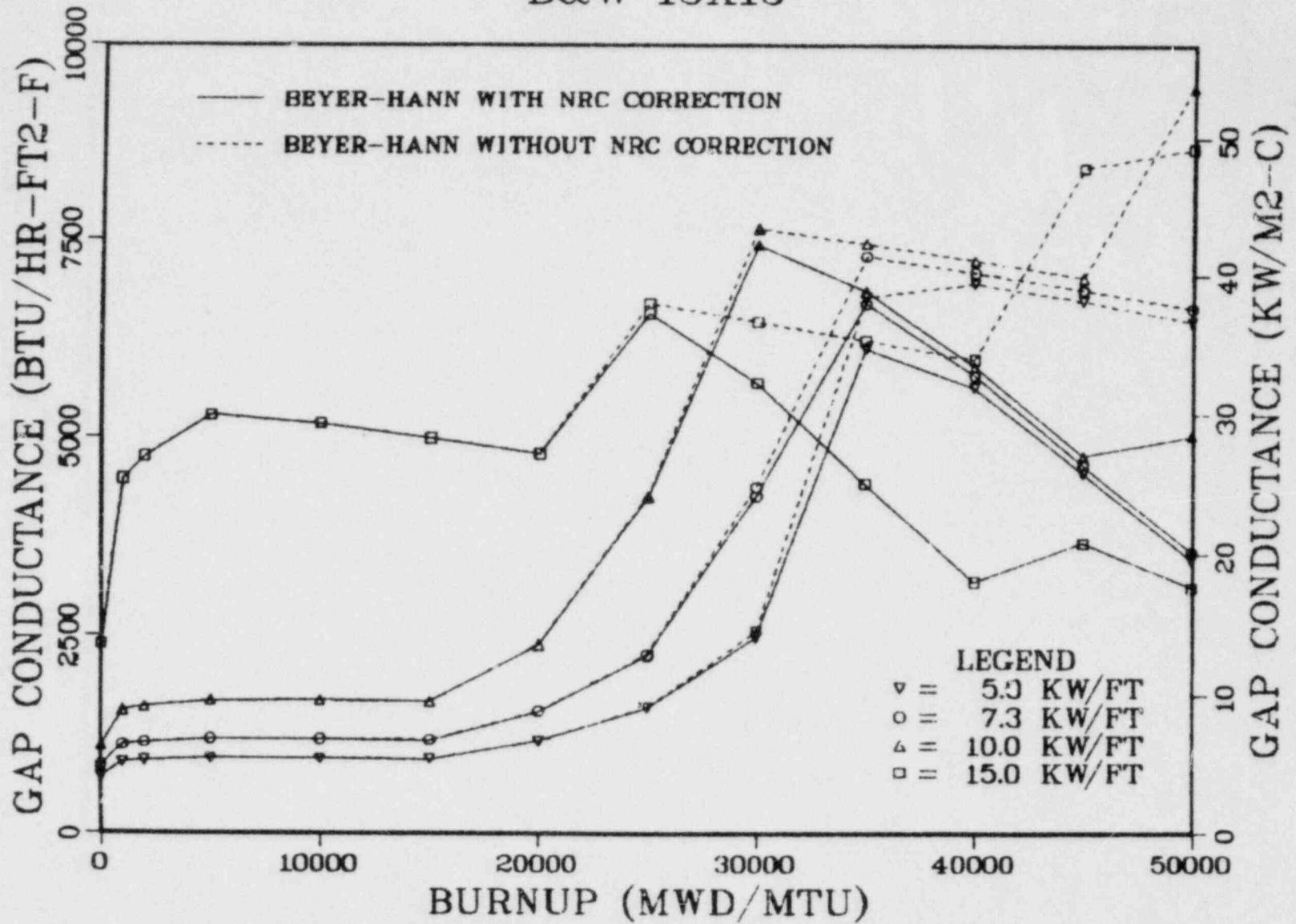


Fig. 7 Gap Conductance for Standard and Burnup Independent Fission Gas Release Models.

# B&W 15X15

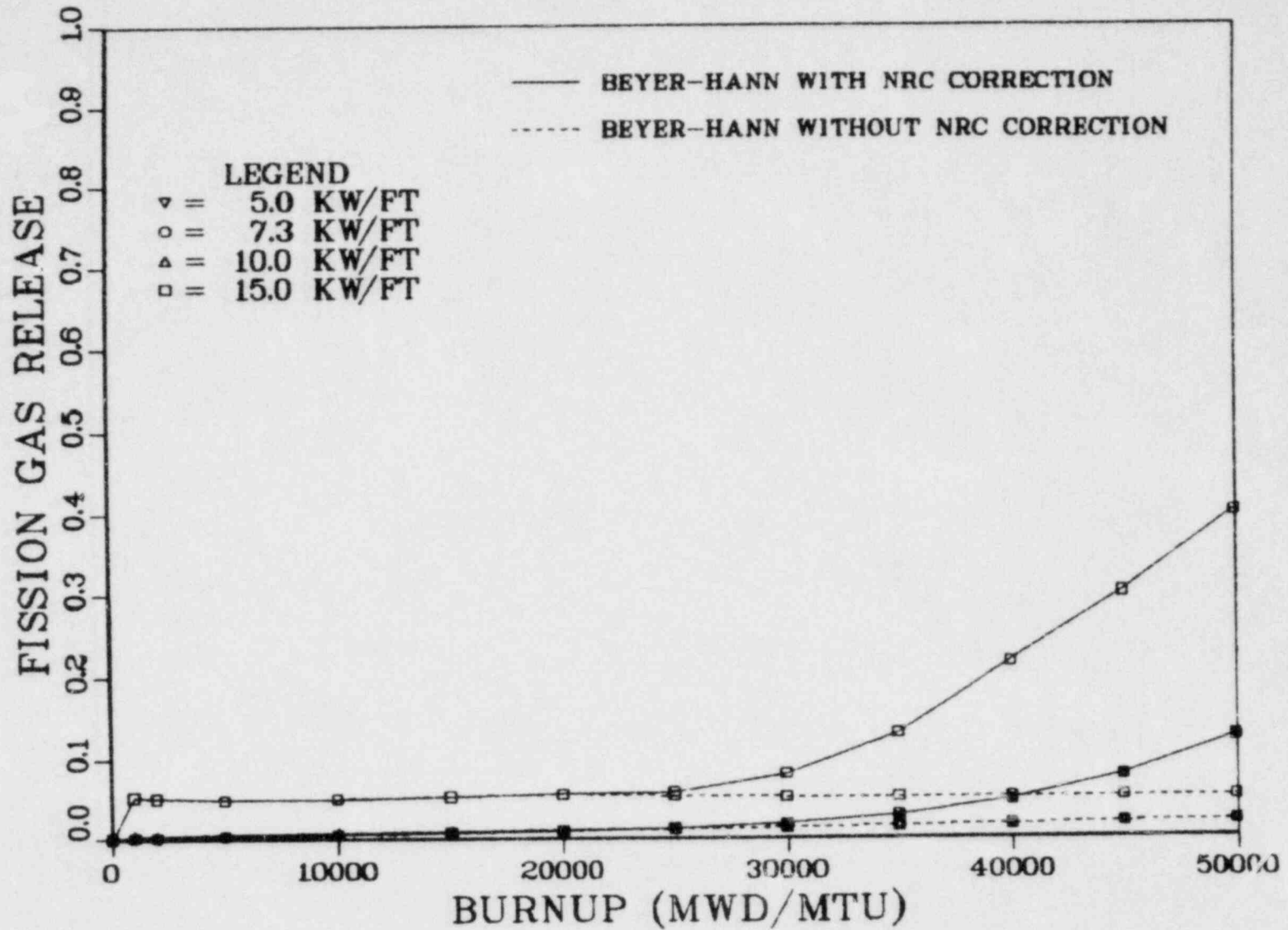


Fig. 8 Fission Gas Release for Standard and Burnup Independent Fission Gas Release Models.

# B&W 15X15

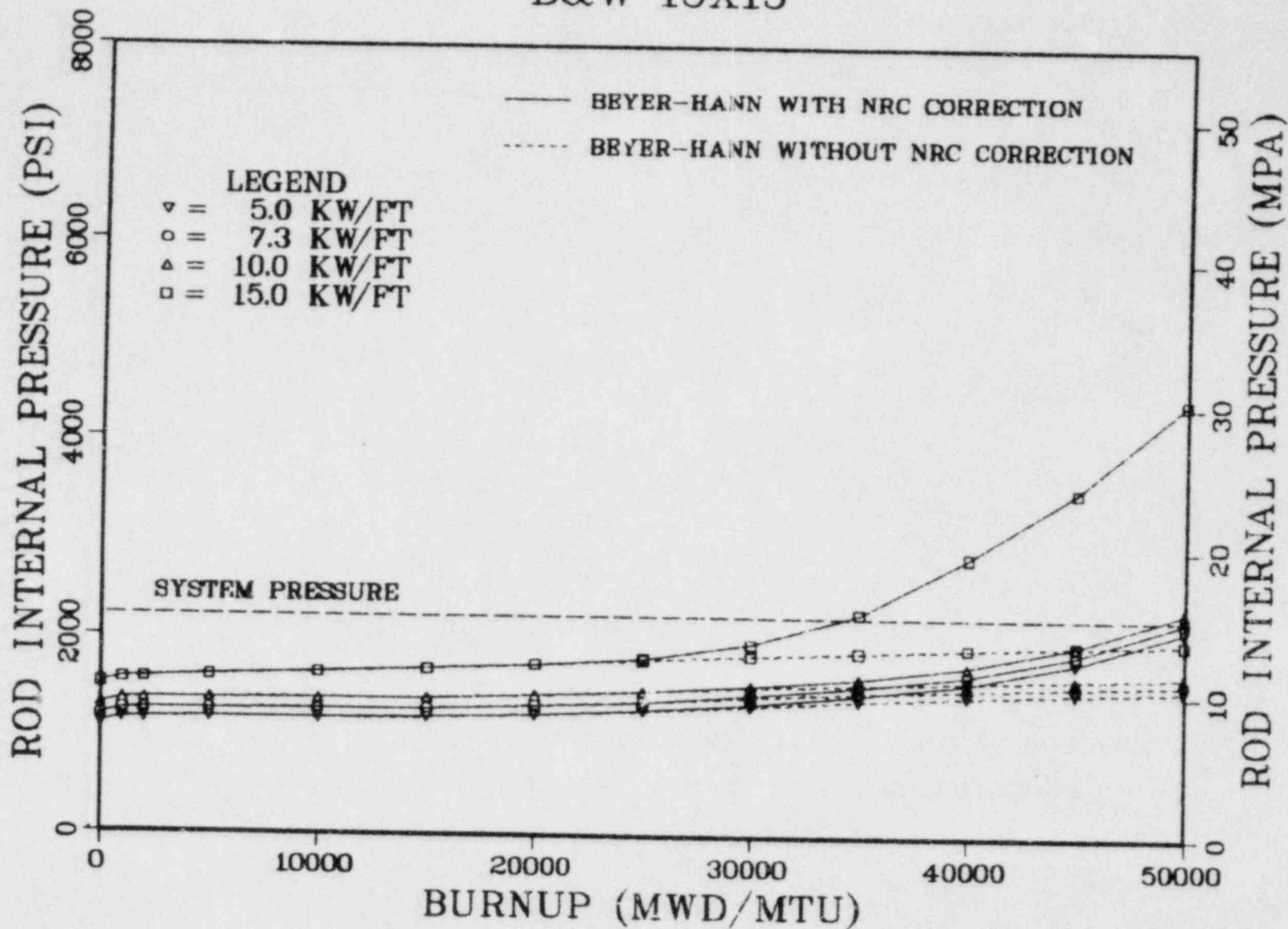


Fig. 9 Rod Internal Pressure for Standard and Burnup Independent Fission Gas Release Models.

fuel are not a direct function of fission gas release, particularly at high power and high burnup conditions where the fuel-to-cladding gap is very small. Under these conditions, fuel temperatures are largely determined by the thermal resistance of the fuel itself rather than the fuel-to-cladding gap.

Recently, work has been progressing on a new fission gas release model, known as the ANS-5.4 model (Ref. 6-7). This model was developed under the auspices of the American Nuclear Society because a standard method for determining radioactive fission gas release did not exist. Calculations with this model were made using the representative fuel design (B&W 15x15) mentioned above. The results of the ANS-5.4 model compared with the Beyer-Hann model with NRC correction are shown in Figures 10-16.

It can be seen from these graphs that the ANS-5.4 model predicts fission gas release values that are generally much the same as those predicted by the NRC corrected Beyer-Hann model at low power levels. The exception are those values generated at 15 kW/ft where large release fractions are predicted by both models. At nearly all burnups, the ANS model predicts release fractions larger than the corresponding values generated by the Beyer-Hann model. Smaller differences are found in examining the rod internal pressure predictions, where the ANS values are higher than those predicted by the NRC corrected Beyer-Hann model. Little variation between the two runs is evident when examining fuel temperatures and stored energy, again demonstrating the second-order effect which fission



### B&W 15X15

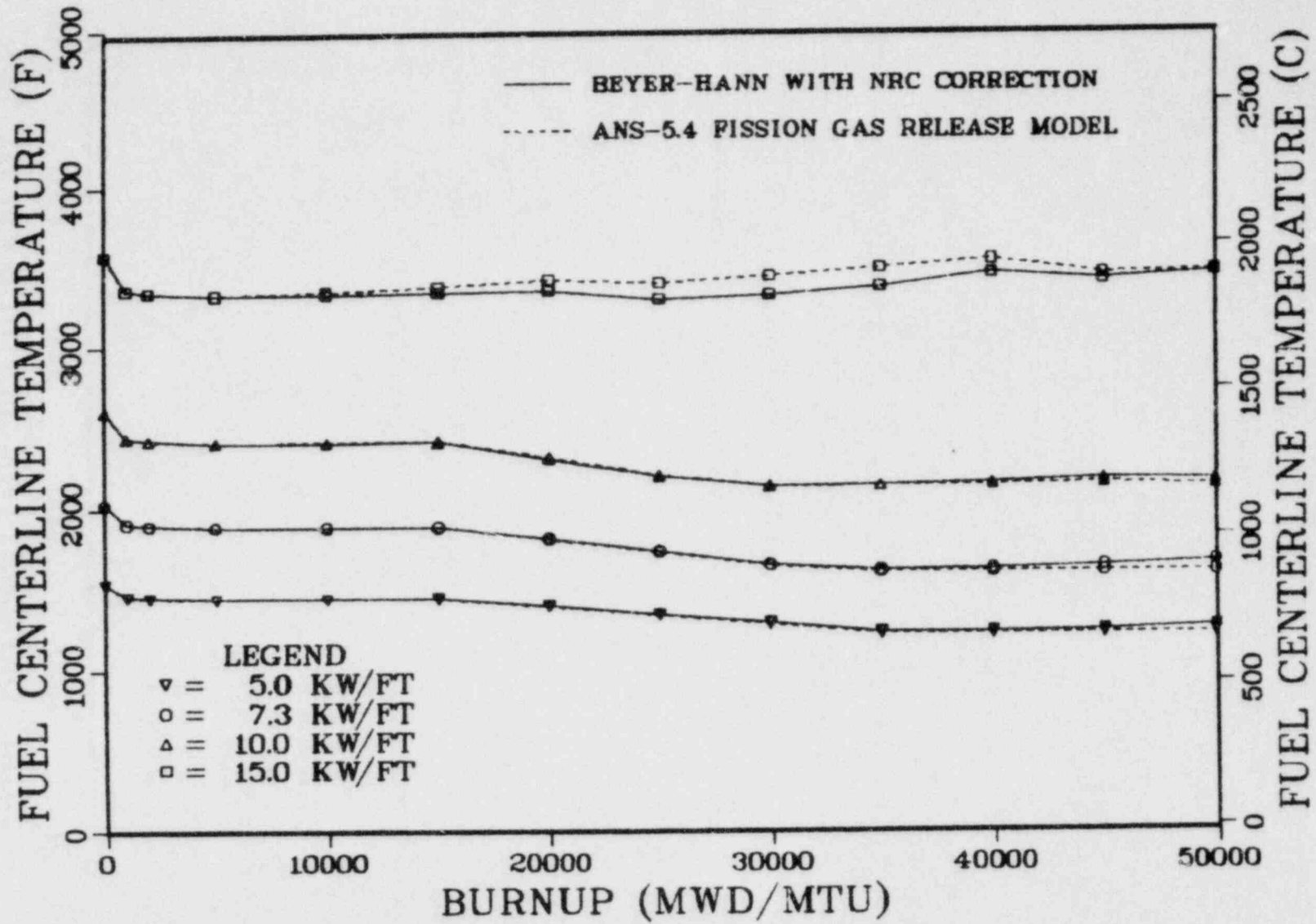


Fig. 10 Fuel Centerline Temperature for Two Burnup Dependent Fission Gas Release Models.

# B&W 15X15

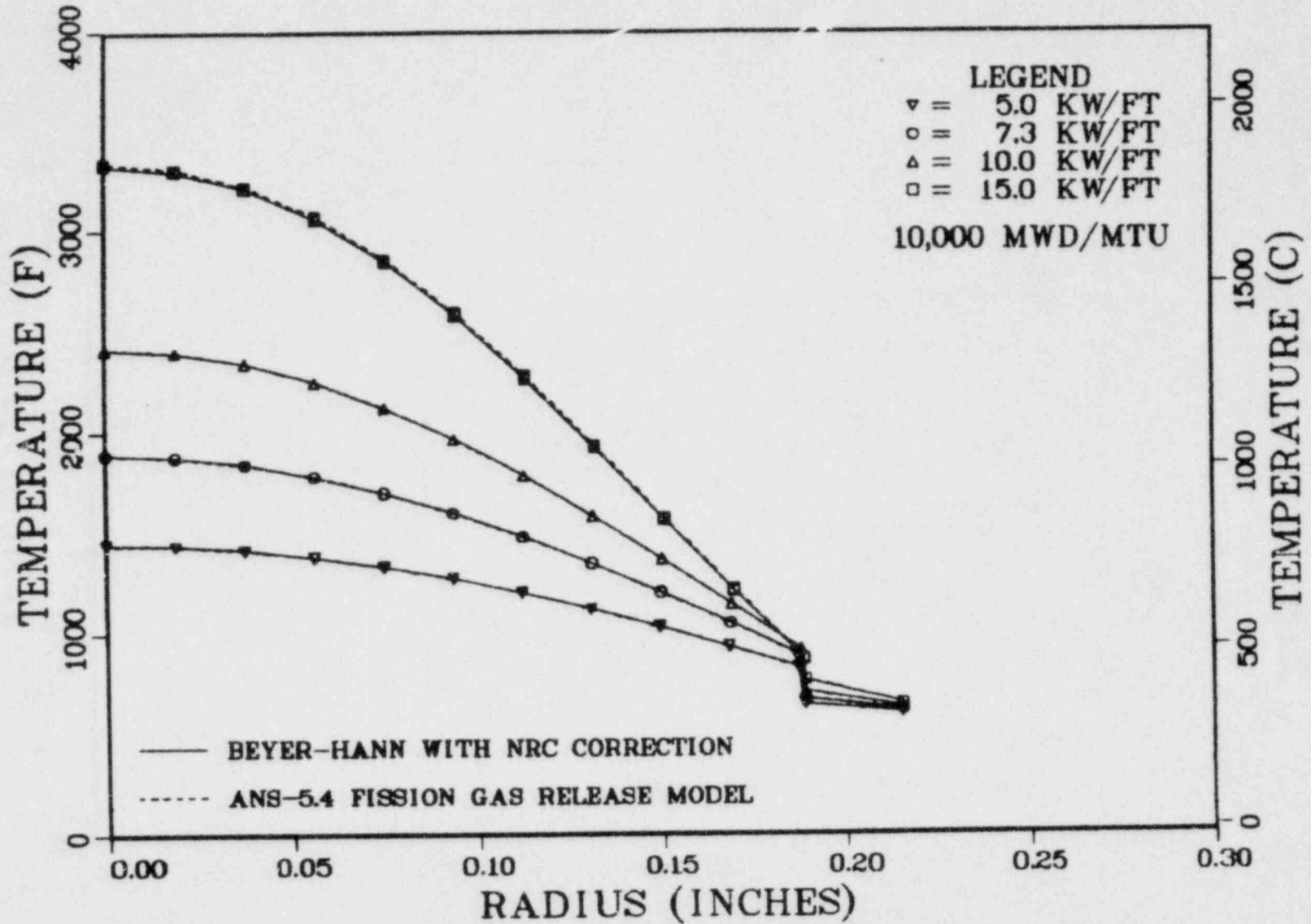


Fig. 11 Fuel Radial Temperature for Two Burnup Dependent Fission Gas Release Models.

# B&W 15X15

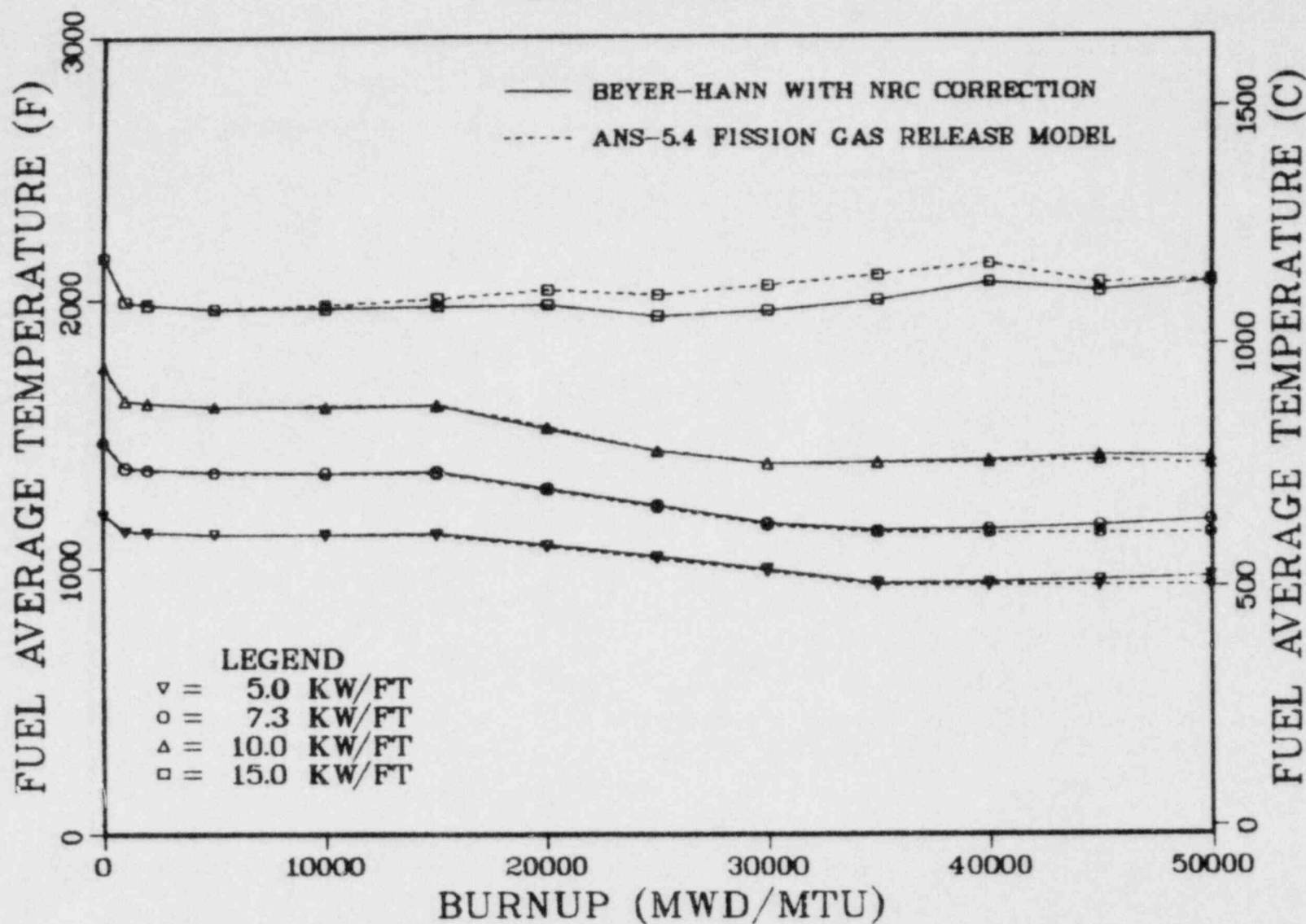


Fig. 12 Fuel Average Temperature for Two Burnup Dependent Fission Gas Release Models.

# B&W 15X15

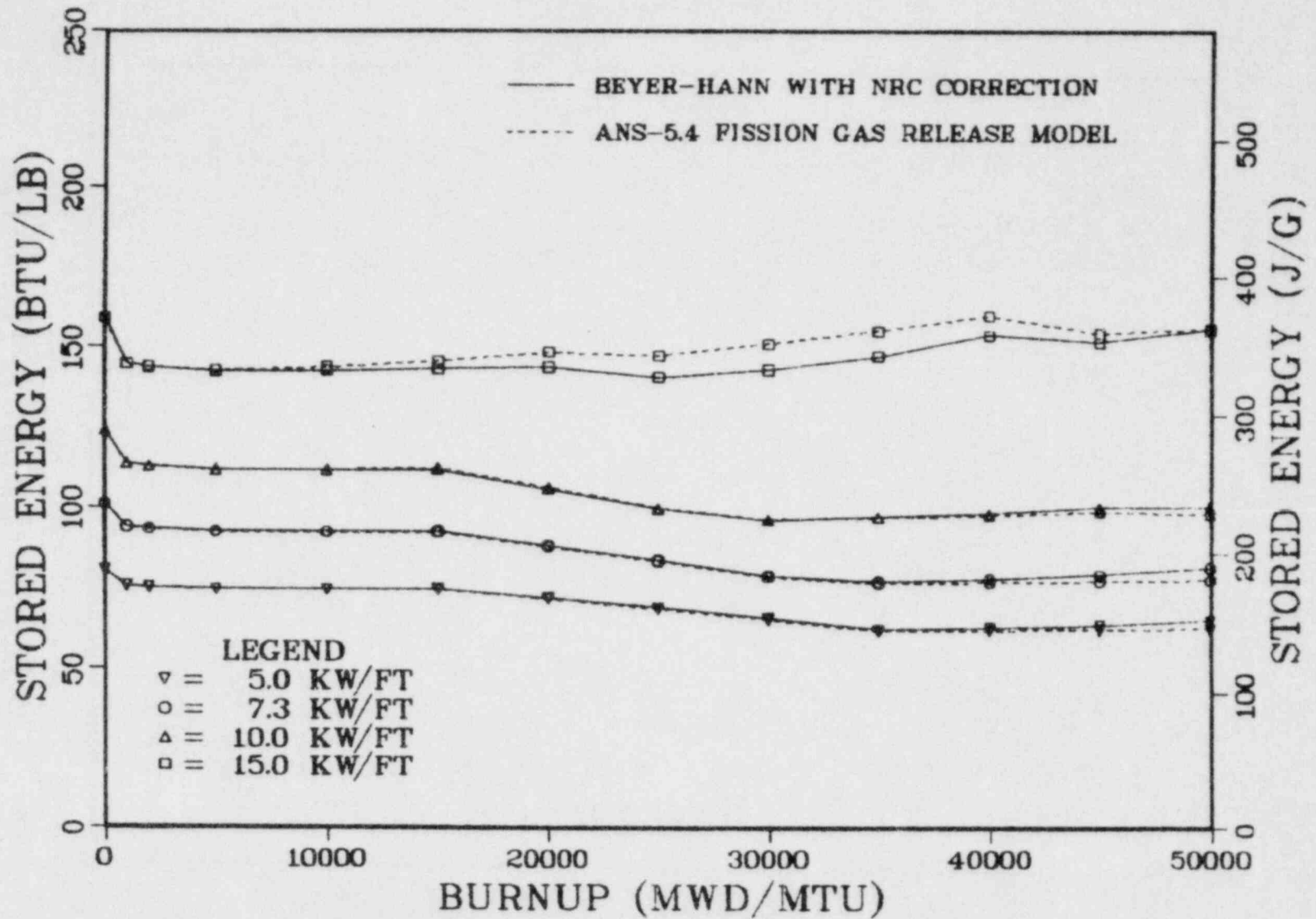


Fig. 13 Stored Energy for Two Burnup Dependent Fission Gas Release Models.

# B&W 15X15

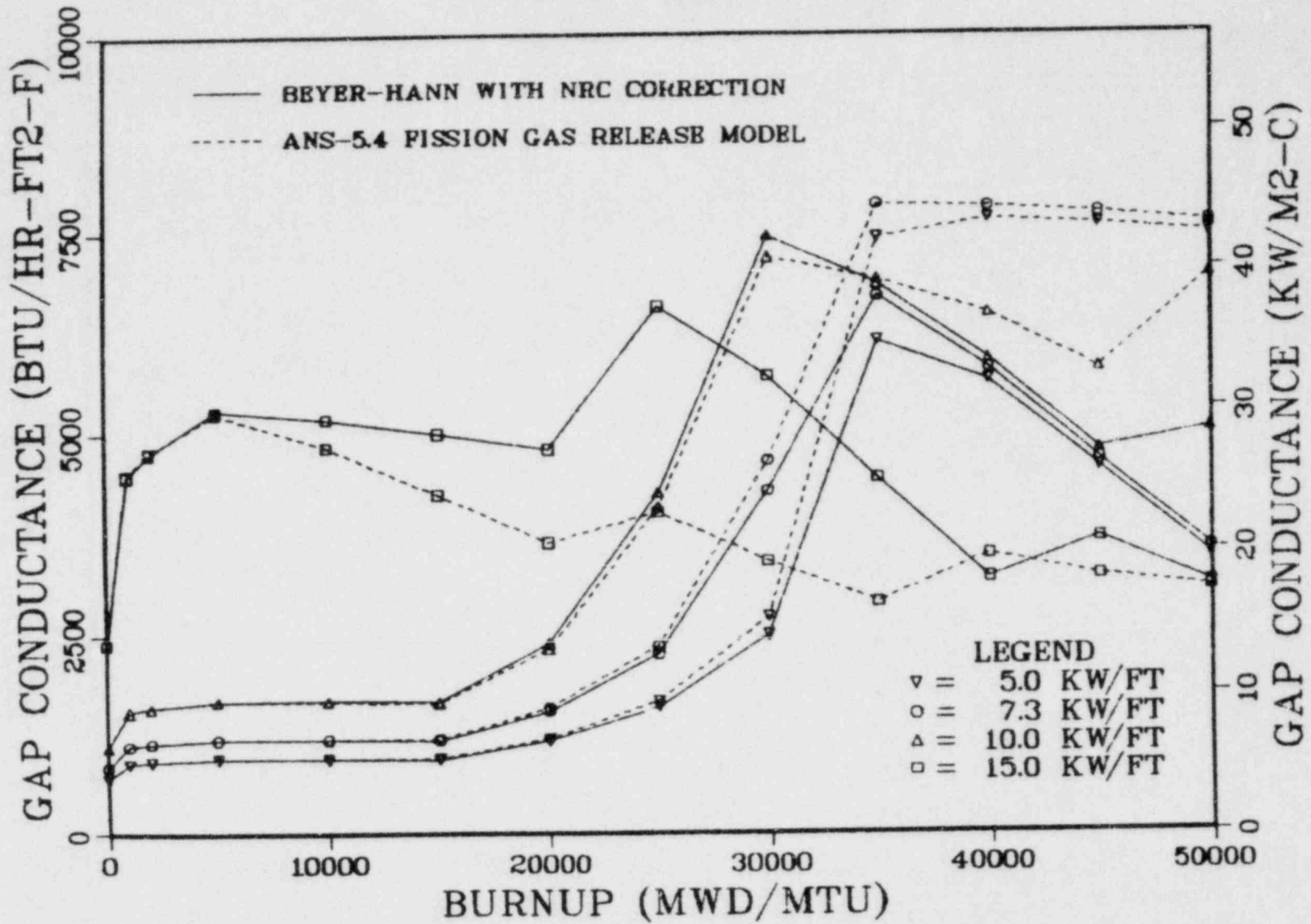


Fig. 14 Gap Conductance for Two Burnup Dependent Fission Gas Release Models.

# B&W 15X15

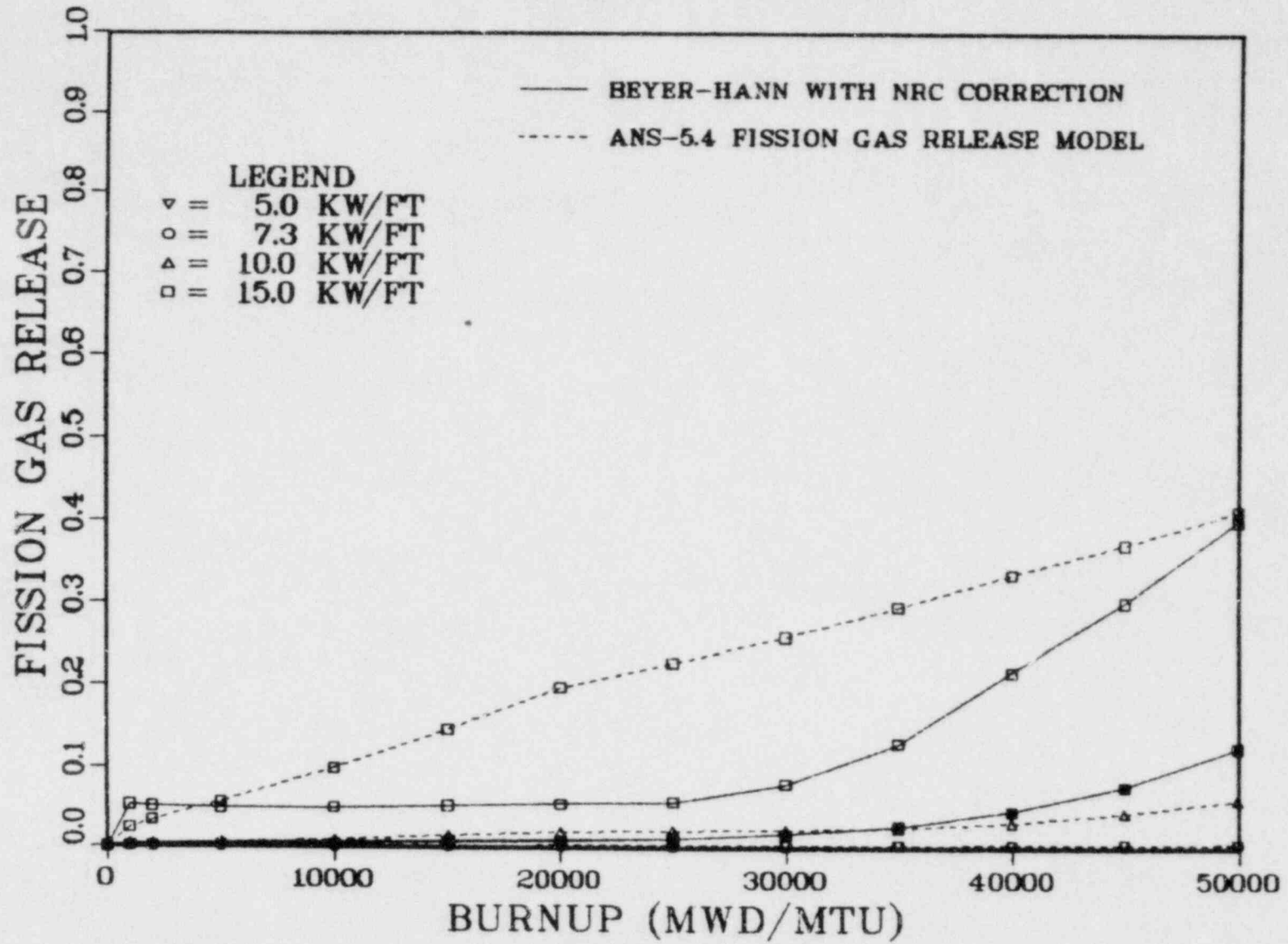


Fig. 15 Fission Gas Release for Two Burnup Dependent Fission Gas Release Models.

# B&W 15X15

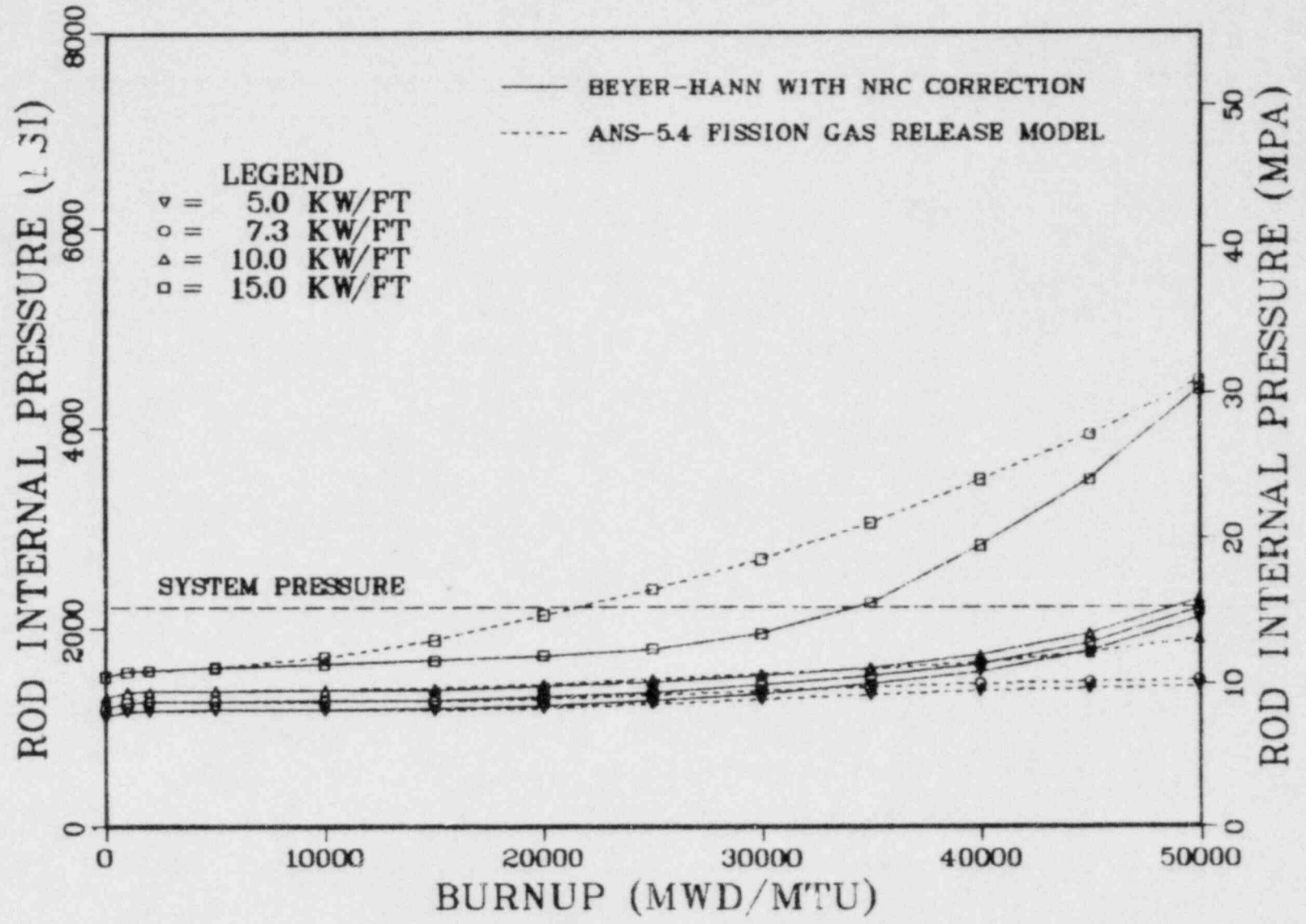


Fig. 16 Rod Internal Pressure for Two Burnup Dependent Fission Gas Release Models.

gas release has on fuel thermal conditions at high burnup when the fuel-to-cladding gap is small.

### 3. Cladding Creep

The GAPCON-THERMAL-2 code does not possess a self-contained cladding creep model. The code requires values of creep-down as input if the effect is to be considered. For most of the cases in this study, cladding creep was not considered.

In order to evaluate the effect of cladding creep on fuel rod performance, computer runs were made by iteratively using GAPCON-THERMAL-2 and a second code, BUCKLE (Ref. 8), which calculates values of cladding creepdown. The previous test case, a B&W 15x15 rod, was run with and without cladding creepdown values generated by the BUCKLE code. The standard Beyer-Hann gas release model with the NRC correction was used in both cases. The results of this comparison are shown in Figures 17-23.

The graphs of fuel centerline, radial, and average temperature and stored energy demonstrate the expected effect of cladding creep, which is to decrease temperature for low and mid-life burnups due to more rapid gap closure. The gap conductance values predicted by the code show significant differences when cladding creepdown is considered, particularly at high burnups. However, these differences are not reflected in the thermal response of the fuel because fuel-to-cladding gap conductance has little effect above 2500 Btu/hr-ft<sup>2</sup>-°F. We conclude that the lack of cladding creepdown model in the GAPCON-THERMAL-2 code does not invalidate the code predictions.



# B&W 15X15

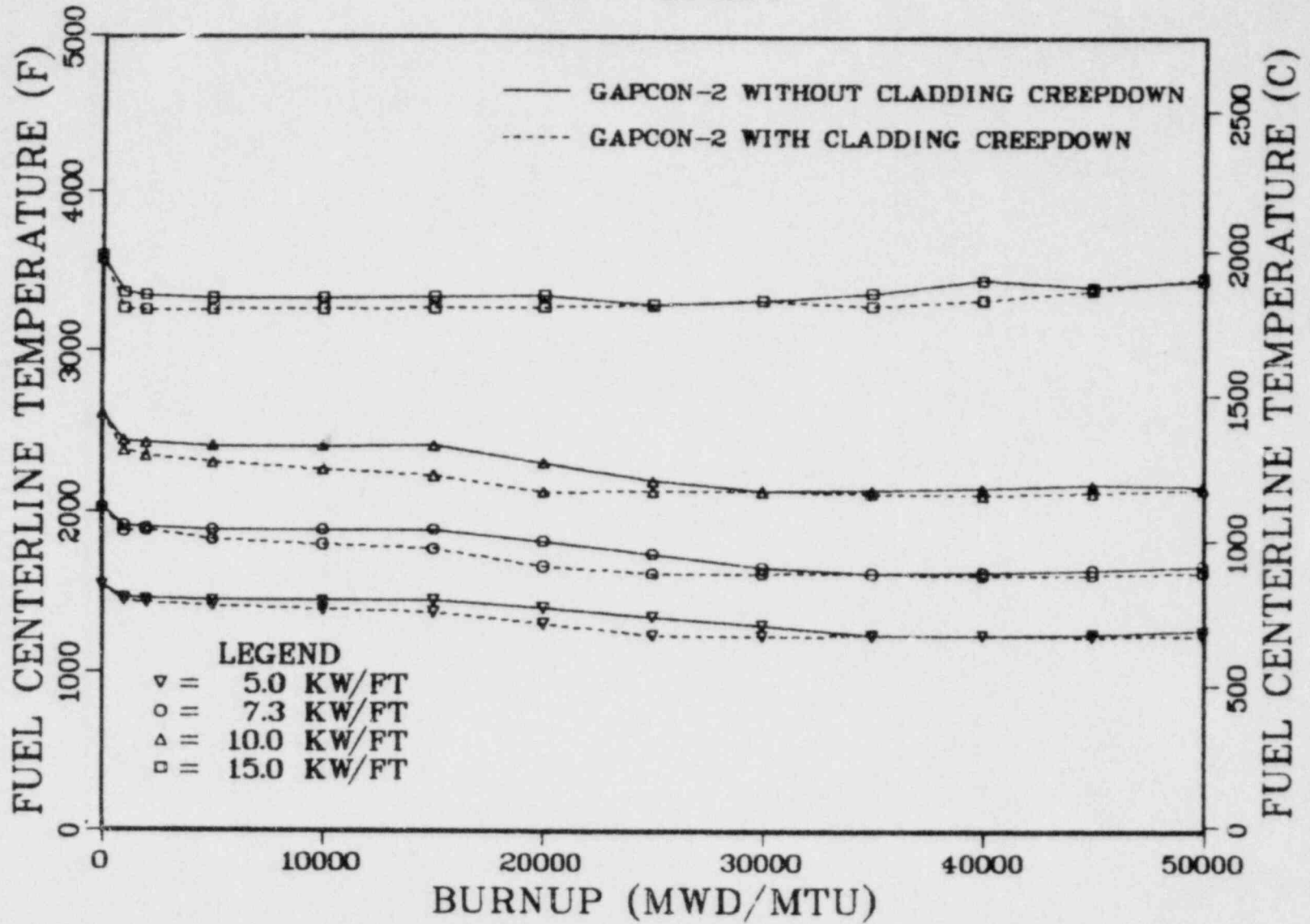


Fig. 17 Fuel Centerline Temperature with and without Cladding Creepdown.

# B&W 15X15

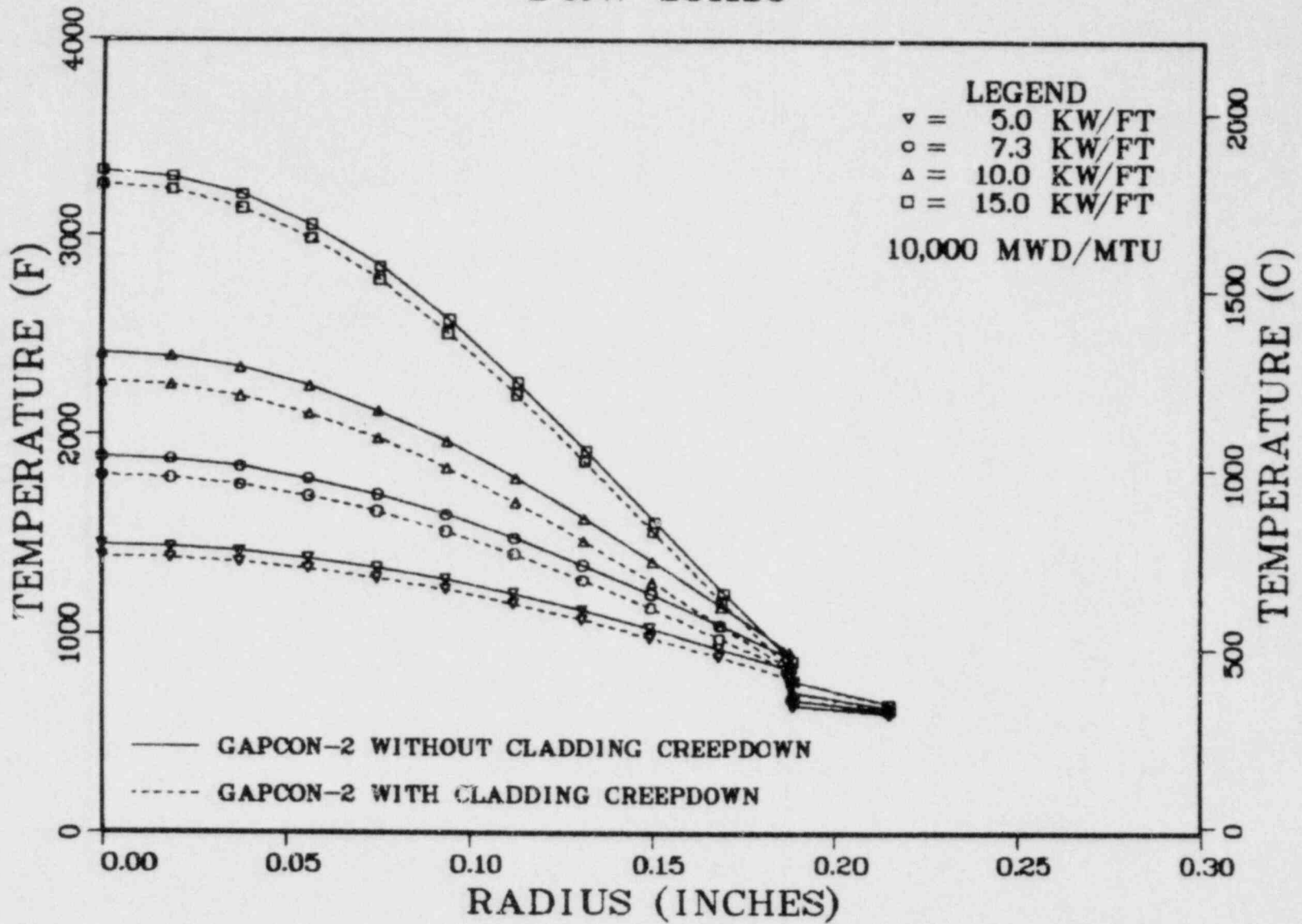


Fig. 18 Fuel Average Temperature with and without Cladding Creepdown.

# B&W 15X15

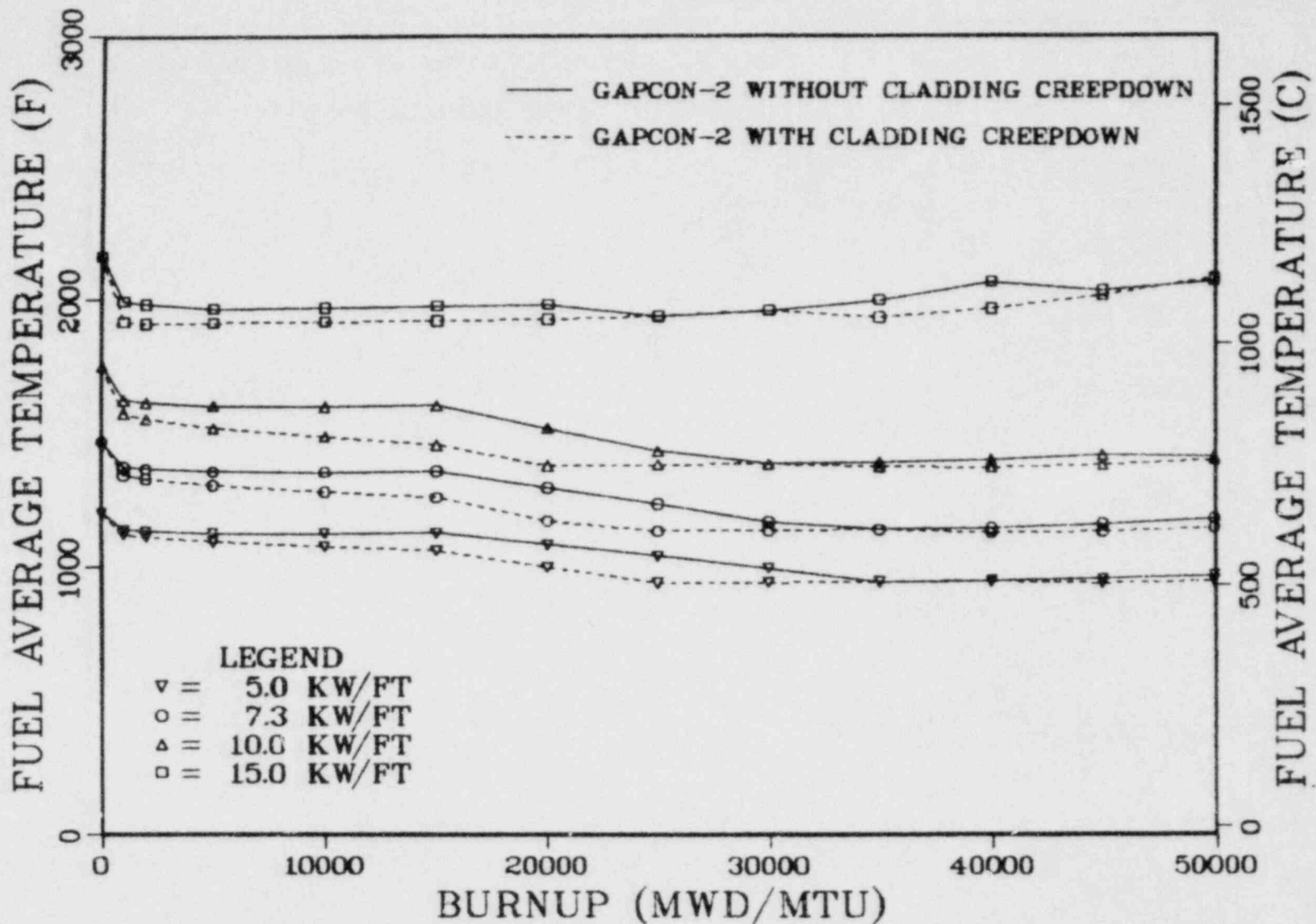


Fig. 19 Fuel Average Temperature with and without Cladding Creepdown.

# B&W 15X15

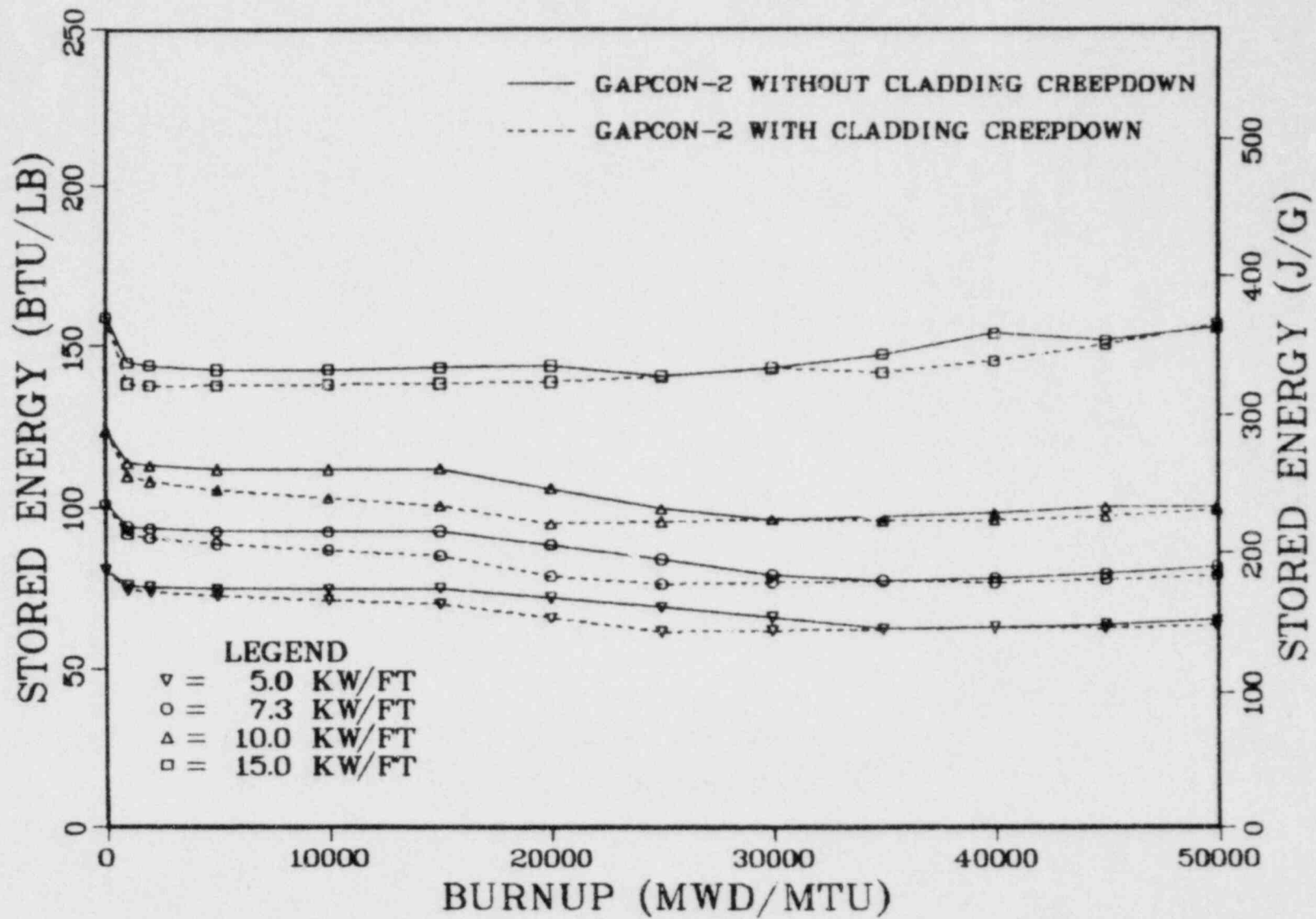


Fig. 20 Stored Energy with and without Cladding Creepdown.

# B&W 15X15

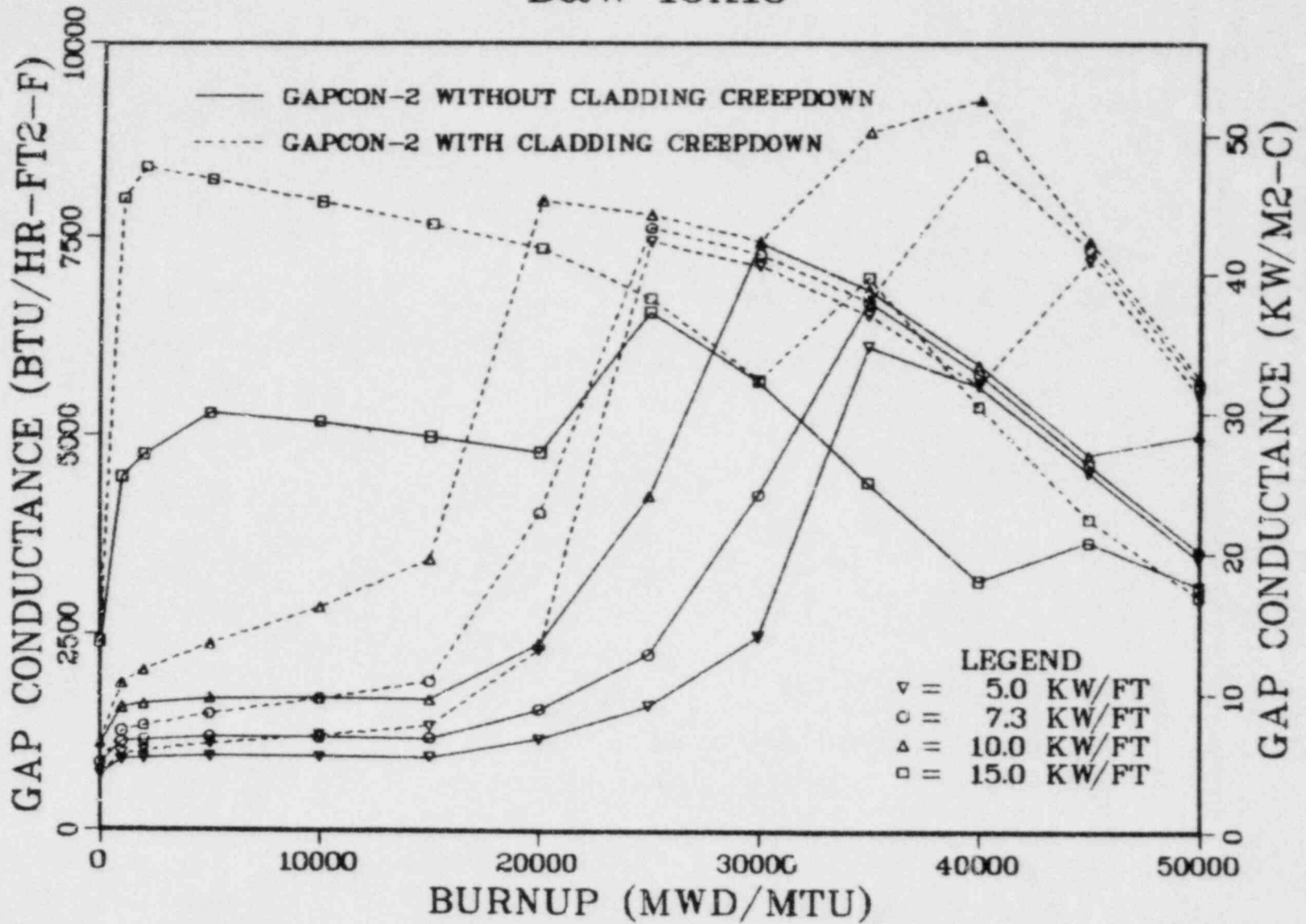


Fig. 21 Gap Conductance with and without Cladding Creepdown.

# B&W 15X15

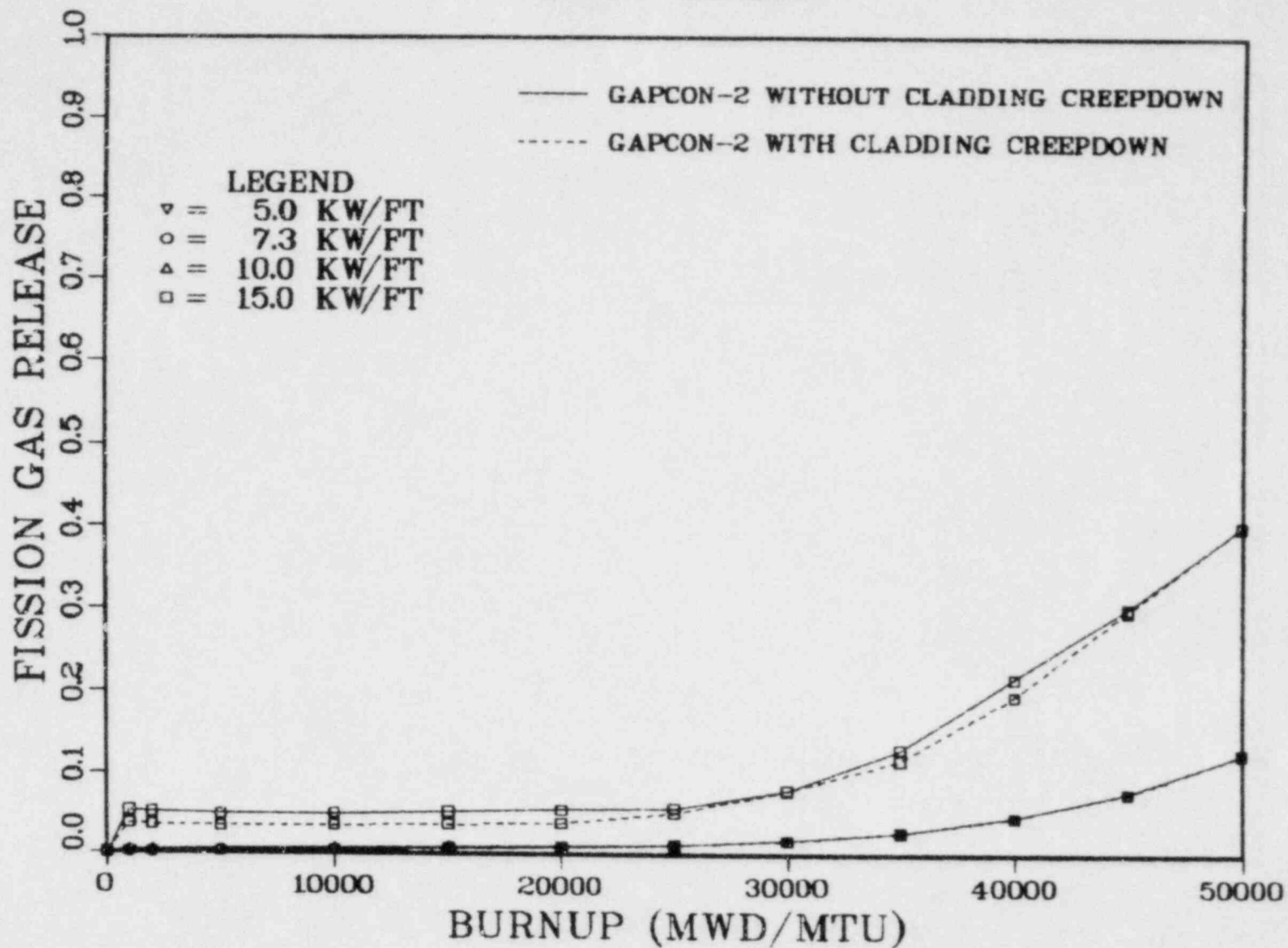


Fig. 22 Fission Gas Release with and without Cladding Creepdown.

# B&W 15X15

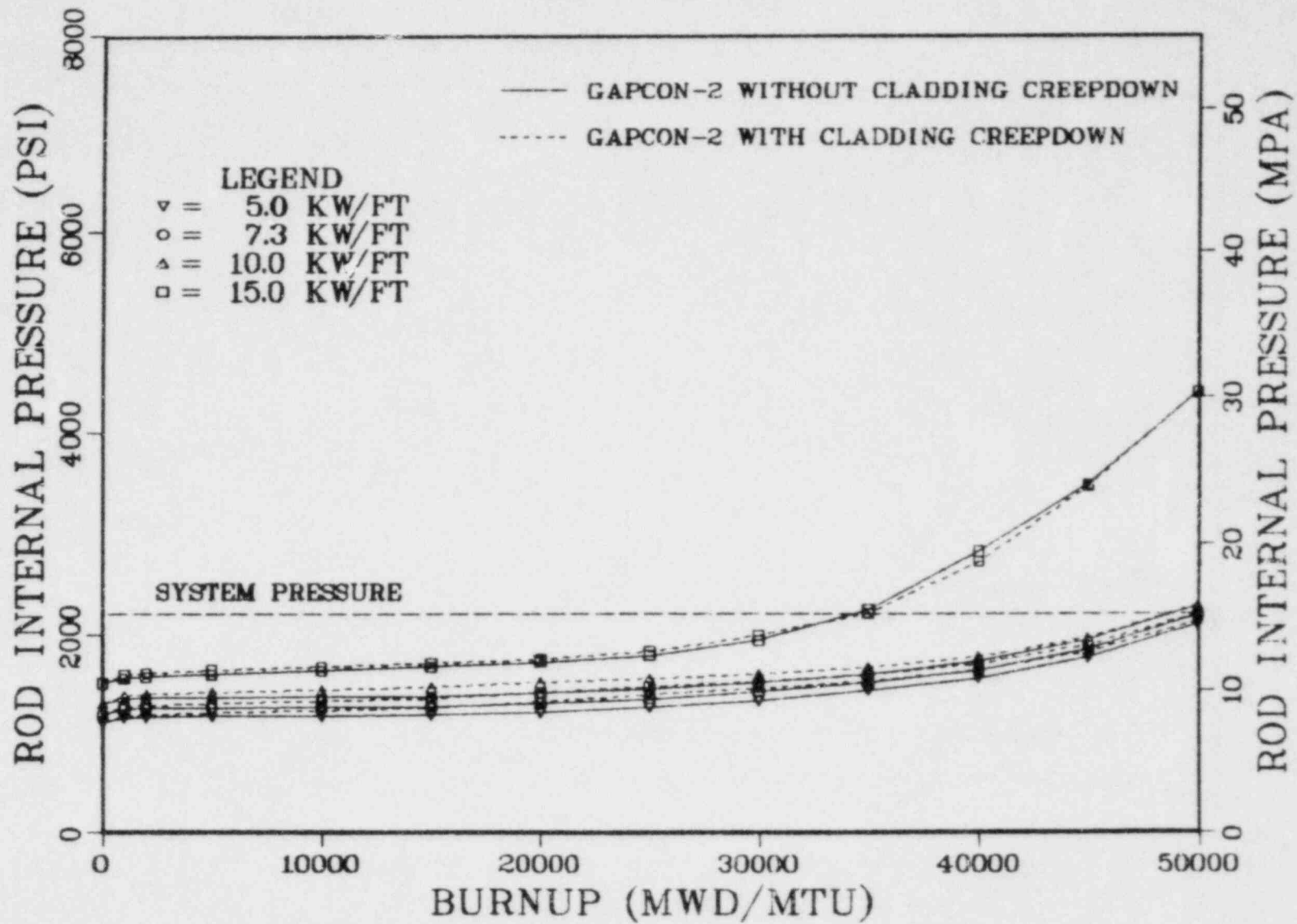


Fig. 23 Rod Internal Pressure with and without Cladding Creepdown.

#### 4. Fuel Restructuring

Fuel restructuring is an effect that was not considered in this study although it can occur in nuclear fuels. The main reason for this omission is that fuel restructuring occurs only at very high temperatures. Very high fuel temperatures, in turn, usually occur only in unstable fuels (i.e., fuels that exhibit a large amount of densification). The GAPCON-THERMAL-2 code has an option that allows restructuring above a given temperature and this value was attained in only a few of the runs (at 15 kW/ft). This confirms the validity of the omission of a fuel restructuring model because the study deals with a very stable fuel type (as specified by the 1% densification parameter). This fuel type is typical of current commercial fuel and is expected to be resistant to restructuring.



#### IV. Summary

During the process of analyzing the various fuel designs, a number of conclusions were reached concerning the computer code used and the resulting predictions. The extensive use of the GAPCON-THERMAL-2 code required by the study, coupled with the use of the ANS-5.4 model, made it possible to determine some of the overall capabilities and deficiencies of the code.

The code itself is somewhat limited by the absence of a self-contained cladding creep model. The addition of a cladding creep model to the GAPCON-THERMAL-2 code did not radically change the overall code predictions. However, runs with the ANS-5.4 model showed larger-than-expected deviation from the NRC model for fission gas release at 15 kW/ft, even though both fission gas release models used a similar data base. This difference is not limited to high burnup conditions. We conclude that the use of more advanced codes may be warranted for modern fuel thermal performance analyses, particularly for high power and burnup conditions.

An examination of the present code predictions at very high power and burnup conditions reveal several fuel thermal performance problems that warrant further regulatory interest. The major findings are: 1) rod pressure may exceed system pressure before 50,000 MWd/MtU, and 2) peak centerline temperature and peak stored energy values do not always occur at beginning of life for constant or nearly constant power conditions.

## References

1. C. E. Beyer, C. R. Hann, D. D. Lanning, F. E. Panisko, and L. J. Parchen, "GAPCON-THERMAL-2; A Computer Program for Calculating the Thermal Behavior of an Oxide Fuel Rod," Battelle Northwest Laboratories Report, BNWL-1898, November 1975. Available for purchase from National Technical Information Service (NTIS), Springfield, Virginia 22161.
2. C. E. Beyer, C. R. Hann, D. D. Lanning, F. E. Panisko, and L. J. Parchen, "User's Guide for GAPCON-THERMAL-2: A Computer Program for Calculating the Thermal Behavior of an Oxide Fuel Rod," Battelle Northwest Laboratories Report, BNWL-1897, November 1975. Available for purchase from National Technical Information Service (NTIS), Springfield, Virginia 22161.
3. Title 10, Code of Federal Regulations, Part 50, Section 46 and Appendices A & F, "Licensing of Production and Utilization Facilities," January 1, 1979. Available from the U.S. Government Printing Office, Washington, D. C. 20402.
4. U.S. Nuclear Regulatory Commission, "Standard Review Plan for the Review of Safety Analysis Reports for Nuclear Power Plants - LWR Edition," USNRC Report NUREG-75/087, Section 4.2 "Fuel System Design." Available for purchase from National Technical Information Service (NTIS), Springfield, Virginia 22161.
5. R. O. Meyer, C. E. Beyer and J. C. Voglewede, "Fission Gas Release From Fuel at High Burnup," Nuclear Regulatory Commission Report, NUREG-0418, March 1978. Available for purchase from National Technical Information Service (NTIS), Springfield, Virginia 22161.
6. "ANS-5.4 Fuel Plenum Gas Activity," to be published by The American Nuclear Society, 555 N. Kensington Avenue La Grange Park, Illinois 60525.
7. "Status Report: ANS-5.4 Fuel Plenum Gas Activity (N218) (Fission Product Release from UO-2 Fuel) April 1977. Available from S. E. Turner, Southern Science Applications, Inc. P. O. Box 10, Dunedin, Fla. 33528.
8. P. J. Pankaskie, "BUCKLE: An analytical Computer Code for Calculating Creep Buckling of an Initially Oval Tube," Battelle Pacific Northwest Laboratories Report BNWL-1784, May 1974. Available for purchase from National Technical Information Service, Springfield, Virginia.

## APPENDIX A

The following is an alphabetical listing of the input parameters required by the GAPCON-THERMAL-2 computer code. Each named variable is defined and an appropriate input value is provided. These values constitute the input parameters used in the fuel design study.

## ATMOS

Initial fill gas pressure  
All PWR fuel designs: 30 ATM  
All BWR fuel designs: 1 ATM  
Additional run of GE 8x3R: 3 ATM

Exact value is not specified in FSARs and representative figures are given here.

## CRUDTH

Initial cladding crud thickness  
Default value of 0.0 inches is assumed for new fuel at beginning of life.

## DBO

Outside diameter of secondary cladding  
Default value of 0.0 inches is assumed because no secondary cladding is present for the designs considered.

## DCI

Cladding inside diameter  
Value is design dependent, see Appendix B.

## DCO

Cladding outside diameter  
Cladding inside diameter plus twice cladding thickness - See Appendix B.

## DE

Equivalent diameter of coolant passage  
Value is design dependent - See Appendix B.

## DFS

Fuel pellet diameter  
Value is design dependent - See Appendix B

## DSINZ

Diameter of restructured fuel zone  
Default value of 0.0 inches is assumed for new fuel at beginning of life.

#### DTEMP

Coolant axial temperature rise

All PWRs: Value is design dependent - see Appendix B

All BWRs: Value in Appendix B (design dependent), is multiplied by an arbitrary factor of eight in order to drive the coolant temperature rapidly to the saturation temperature where it remains constant. The multiplication factor results in an initial rapid increase over the lower 1/8 of the rod, after which GAPCON assumes coolant temperature remains equal to the saturation temperature. (This contrasts to PWRs where the coolant is always subcooled and the temperature increases over the entire rod.)

#### DVOIDZ

Fuel initial central void diameter

Default value of 0.0 inches is assumed for new fuel at beginning of life.

#### EXTP

Coolant pressure

Value is design dependent and is taken as the nominal design system pressure - See Appendix B.

#### FRACAR

Argon fraction of initial fill gas

Argon is a fill gas not ordinarily used in commercial designs, therefore a default value of 0.0 is assumed.

#### FRACH

Hydrogen fraction of initial fill gas

Hydrogen is a minor fill gas contaminant. A default value of 0.0 is assumed for new fuel at beginning of life.

#### FRACHE

Helium fraction of initial fill gas.

The initial fill gas is assumed to be pure helium.

#### FRACN

Nitrogen fraction of initial fill gas

Nitrogen is a minor fill gas contaminant. A default value of 0.0 is assumed for new fuel at beginning of life.

FRACXE

Xenon fraction of initial fill gas  
Xenon is a fission product. A default value of 0.0 is assumed for  
new fuel at beginning of life.

FRDEN

Initial fuel fractional density  
Value is design dependent, see Appendix B

FRDEN2

Final fuel fractional density. Assumed to be  $FRDEN + 1\%$ .  
Typically 1 percent average densification occurs in stable fuel.

FRPU02

PU02 weight fraction  
Default value of 0.0 is utilized to assume new fuel at beginning of  
life.

FRSIN

Restructured fuel fractional density  
 $FRSIN = FRDEN$  to preclude restructuring, which normally does not occur  
in commercial reactor fuel.

FP35

Core average enrichment  $U235/(U235 + U238)$   
Value is design dependent - see Appendix B

FR40

Pu 240 weight fraction  
Default value of 0.0 is assumed for new fuel at beginning of life.

FR41

Pu 241 weight fraction  
Default value of 0.0 is assumed for new fuel at beginning of life.

HBC

Heat transfer coefficient between primary and secondary cladding  
Default value of 0.0 Btu/hr-ft-ft-deg.F utilized as there is no  
secondary cladding.

## ICDF

Value of 1 is utilized in order to calculate cladding elastic deformation  
ICDF=0 No cladding elastic deformation calculated  
ICDF>0 Cladding elastic deformation calculated.

## ICOR

All PWRs: 1  
All BWRs: 4  
ICOR=0 No cladding oxidation calculated  
ICOR<3 PWR cladding oxidation calculated  
ICOR<3 BWR cladding oxidation calculated

## ICREP

Value of 0 is utilized even though plastic deformation occurs because  
GAPCON-2 has no self contained plastic deformation model.  
ICREP=0 No cladding plastic deformation utilized  
ICREP>0 Cladding plastic deformation input by user.

## IDENSF

Value of 1 is utilized in order to calculate densification  
IDENSF=0 No fuel densification calculated  
IDENSF>0 Fuel densification calculated.

## IGAS

Value of 0 is utilized to obtain a best estimate of fission gas  
release  
IGAS=0 Best estimate fission gas release  
IGAS>0 Conservative fission gas release

## IPEAK

Value of 1 is utilized in order to input rod average power  
IPEAK=0 Power input is rod peak power  
IPEAK>0 Power input is rod average

## IRELOC

Value of 1 is utilized to obtain a best estimate of fuel relocation  
IRELOC<0 Conservative fuel relocation  
IRELOC=0 No relocation calculated  
IRELOC>0 Best estimate fuel relocation

## IRELSE

Value of 0 is utilized here for steady state analysis  
IRELSE=0 Fission gas is released during time-step  
IRELSE>0 Fission gas is released after time-step

IRL

Value of 0 is utilized to obtain output at 11 radial fuel nodes.  
IRL=0 Flux depression printed for 11 fuel nodes  
IRL<0 Flux depression printed for IRL fuel nodes

ISTOR

Value of 1 is utilized to obtain stored energy values  
ISTOR=0 Stored energy values not printed  
ISTOR=1 Stored energy values printed

IT

Value of 1 is utilized in order to run an exposure-dependent, rather than time-dependent history.  
IT=0 Time-step input in days  
IT>0 Time-step input in MWD/MTU

KB

Thermal conductivity of secondary cladding  
Default value of 0.0 Btu/hr-ft-deg.F assumed as there is no secondary cladding.

KOOL

Value of 0 is utilized in order to calculate cladding temperature drop  
KOOL=0 Cladding temperature drop calculated  
KOOL>0 Cladding temperature = coolant temperature

LFUEL

Fuel column length  
Value is design dependent - see Appendix B

LVOIDZ

Initial central void length  
Default value of 0.0 inches is assumed for new fuel at beginning of life.

MINI

Value of 0 is utilized to obtain output for peak node.  
MINI<0 Short output for all axial segments  
MINI=0 Long output for hottest axial segment only  
MINI>0 Long output for all axial segments

NCLAD

Value of 0 is utilized as all fuel designs in Appendix B have Zircaloy cladding.  
NCLAD<0 304 SS cladding used  
NCLAD=0 Zircaloy cladding used



#### NFLX

Value of 0 is utilized in order to calculate flux depression

NFLX<0 No flux depression calculated

NFLX=0 Flux depression calculated by GAPCON

NFLX>0 Flux depression input by user

#### NFUEL

Value of 0 is utilized since only  $UO_2$  is present at beginning of life.

NFUEL<0  $UO_2$ - $PuO_2$  thermal conductivity used

NFUEL=0  $UO_2$  thermal conductivity used

NFUEL>0 Fuel thermal conductivity input by user

#### NOH

Value of 0 is utilized to allow  $H_2$  and  $H_2O$  reaction with the cladding although this effect is not expected to be significant.

NOH=0  $H_2$  and  $H_2O$  allowed to react with cladding

NOH>0  $H_2$  and  $H_2O$  not allowed to react with cladding.

#### NPOW

Number of axial fuel segments

Value of 11 is utilized. GAPCON-2 permits a maximum of 20 segments.

An odd value was chosen because an axially symmetric profile results in one of the values being the peak. 11 is also a sufficiently large number to resolve segment differences.

#### NPRFIL

Number of axial power profiles input by user

Value of 1 is utilized. This results in a single stylized axial power profile which is an approximation of the actual time dependent profile.

#### NTIME

Number of time steps input by user

Value of 13 is utilized in order to cover 0 to 50000 MWD/MTU in 5000 MWD/MTU increments plus steps at 1000 and 2000 MWD/MTU

#### PRCDH

Fuel pellets with dish: 2.0

Fuel pellets without dish: 0

2 percent is based on a 1 percent dish volume at each end of the fuel pellet. Actual values are vendor proprietary. A representative value is used.

PROFIL (1,1)

All PWRs: .621, .801, .953, 1.072, 1.153, 1.195, 1.195, 1.153, 1.072,  
.953, .801, .621

All BWRs: .445, .703, .927, 1.105, 1.229, 1.292, 1.292, 1.229, 1.105,  
.927, .703, .455

Normalized axial power profile

Values are segment end-points rather than segment averages. Data based on typical peaking factors of 1.2(PWR) and 1.3(BWR) which were utilized to generate a truncated cosine distribution.

PSEUDO(1)

All PWRs: 4.17, Rod Ave. Power, 8.33, 12.5 \*  
All BWRs: 3.85, Rod Ave. Power, 7.69, 11.54 \*\*  
Rod Power History

\* These average PWR powers correspond to the peak powers of 5, 10, & 15 kW/ft.

\*\* These average BWR powers correspond to the peak powers of 5, 10, & 15 kW/ft.

Core Average = max power (planar)/peaking factor.

RADS

Radius of fuel pellet dish

This information is normally company proprietary However, the following method is used to generate typical values.

$RADS = .80 * (DFS/2)$

KOUC

Arithmetic mean cladding I.D. surface roughness  
A nominal value of 0.00002 inches is utilized

ROUF

Arithmetic mean fuel surface roughness  
A nominal value of 0.000039 inches is utilized

S

Sorbed gas content of the fuel  
Value of 0.0 cc/gram is utilized  
Typical sorbed values are not high enough to effect fuel performance

## SIGHF

Cladding-to-coolant heat transfer correlation value of 0.0 is utilized because the value of the heat transfer coefficient is unknown.

SIGHF=0.0 Film coefficient calculated by GAPCON using Dittus-Boelter and Thom correlations

SIGHF>0.0 SIGHF is heat transfer coefficient (Btu/hr-ft<sup>2</sup>-F)

## TIME (1)

All PWRs = 0.0, 833.22, 1666.67, 4166.67, 8333.33, 12500.0, 16666.67, 20833.33, 25000.0, 29166.67, 33333.33, 37500.0, 41666.67  
MWD/MTU

All BWRs = 0.0, 769.23, 1538.46, 3846.15, 7692.31, 11538.46, 15384.67, 19230.77, 23076.93, 26923.08, 30769.23, 34615.39, 38461.54  
MWD/MTU

These are average MWD/MTU values which correspond to peak values of 0, 1000, 2000, 5000, 10000 MWD/MTU, etc.

## TINLET (1)

Coolant inlet temperature

Value is design dependent, see Appendix B

## TM

Fuel melting temperature

Default value of 2790 DEG. C is utilized.

## TPLAS

Fuel plastic temperature

Default value of 1200 DEG.C is utilized.

## V

Coolant Velocity

Value is design dependent - See Appendix B

## VPLENZ

Rod gas plenum volume

Values are proprietary. The value was approximated by 75 percent of the gross plenum volume. The remaining 25 percent is assumed to be the volume of the spring. Values for plenum length and diameter are design dependent and obtained in Appendix B.

## XCO

CO and CO<sub>2</sub> fraction of sorbed gas

Default value of 0.0 is utilized. Code predictions are not sensitive to small sorbed gas values.

XH

H and H<sub>2</sub> fraction of sorbed gas  
Default value of 0.0 is utilized. Code predictions are not sensitive  
to small sorbed gas values.

XN

N<sub>2</sub> fraction of sorbed gas  
Default value of 0.0 is utilized. Code predictions are not sensitive  
to small sorbed gas values.

ZCLAD

Zircaloy Cladding Option  
All PWRs: 1  
All BWRs: 0  
ZCLAD=0 ZR-2  
ZCLAD>0 ZR-4  
Design dependent, see Appendix B

## APPENDIX B

The following list of fuel assembly parameters is based on a compilation by John T. Maki, an engineering co-op student on assignment to the NRC Core Performance Branch during the summer of 1978. The list presents a number of major design parameters for each of the current light-water-reactor fuels designs. The input data used in this study and shown in Appendix A are a subset of the information given here. The data are taken from publicly-available documents and are non-proprietary.

MAJOR FUEL ASSEMBLY PARAMETERS

VENDOR	B&W	B&W	C-E	C-E	WEST.	WEST.	WEST.	EXXON	EXXON	GE	GE	GE
FUEL ROD ARRAY	15X15	17X17	14X14	16X16	14X14	15X15	17X17	15X15	8X8	7X7	8X8	8X8R
PLANT	3 MILE ISLAND 2	BELLE-FONTE 1	ST. LUCIE 1	ANO UNIT 2	PRAIRIE ISLAND 1	ZION UNIT 1	TROIAN	D.C. COOK 1	OYSTER CREEK	BROWNS FERRY 1	ZIMMER UNIT 1	HATCH UNIT 3
REACTOR TYPE	PWR	PWR	PWR	PWR	PWR	PWR	PWR	PWR	BWR	BWR	BWR	BWR
PLANT COMMERCIAL OPERATION DATE	12-78	9-81	12-76	8-79	12-73	6-73	5-76	8-75	12-69	8-74	1980	7-79
ASSEMBLIES PER CORE	177	205	217	177	121	193	193	193	560	764	560	560
FUEL ROD LOCATIONS PER ASSEMBLY	225	289	196	256	196	225	289	225	64	49	64	64
FUEL RODS PER ASSEMBLY	200	264	176	236	179	204	264	204	60	49	63	62
MAX. BURNABLE POISON RODS PER ASSEMBLY	16	24	12	16	16	20	20	20	4	5	3	3
EMPTY LOCATIONS PER ASSEMBLY	17	25	5	5	17	21	25	21	4	NONE	1	2
ROD PITCH MM (INCH)	14.4 (.568)	12.7 (.501)	14.7 (.580)	12.9 (.5063)	14.1 (.556)	14.3 (.563)	12.6 (.496)	14.3 (.563)	16.3 (.642)	18.7 (.738)	16.3 (.640)	16.3 (.640)
SYSTEM PRESSURE MPA (PSIA)	15.2 (2200)	15.5 (2250)	15.5 (2250)	15.5 (2250)	15.5 (2250)	15.5 (2250)	15.5 (2250)	15.5 (2250)	7.14 (1035)	7.14 (1035)	7.14 (1035)	7.14 (1035)
EQUIVALENT COOLANT PASSAGE DIAMETER MM (INCH)	13.3 (.525)	11.8 (.464)	13.5 (.533)	12.0 (.472)	13.0 (.511)	13.6 (.534)	11.8 (.464)	13.4 (.528)	13.8 (.545)	17.0 (.669)	14.3 (.565)	15.2 (.597)
COOLANT VELOCITY ALONG FUEL RODS M/SEC (FT/SEC)	5.04 (16.52)	4.94 (16.2)	4.33 (14.2)	5.00 (16.4)	4.51 (14.8)	4.66 (15.3)	4.79 (15.7)	4.72 (15.5)	1.89 (6.2)	2.01 (6.6)	2.13 (7.0)	2.01 (6.6)
COOLANT INLET TEMPERATURE C (F)	292 (557.0)	300 (573.7)	284 (544)	290 (553.5)	280 (535.5)	274 (524.2)	289 (552.5)	278 (533)	273 (523.8)	275 (527.8)	278 (532.7)	273 (523.3)
COOLANT AXIAL CORE TEMPERATURE RISE C (F)	29.8 (53.6)	32.9 (59.3)	31.1 (56.0)	33.6 (60.5)	36.9 (66.4)	37.1 (66.8)	37.2 (66.9)	36.5 (65.7)	14 (25)	12 (21)	8.9 (16.1)	14.2 (25.5)

VENDOR	B&W	B&W	C-E	C-E	WEST.	WEST.	WEST.	EXXON	EXXON	GE	GE	GE
FUEL ROD ARRAY	15X15	17X17	14X14	16X16	14X14	15X15	17X17	15X15	8X8	7X7	8X8	8X8
PLANT NET OUTPUT MW (ELECTRIC)	880	1213	802	912	520	1100	1130	1054	620	1067	810	780
CORE THERMAL POWER MW (THERMAL)	2772	3890	2560	2815	1650	3250	3411	3250	1930	3293	2436	2436
CORE AVERAGE POWER DENSITY KW/LITER	90.0	101.6	78.5	96.4	95.6	98.1	104.7	98.1	40.57	50.732	50.51	49.15
AVERAGE LHGR KV/M (KV/FT)	20.0 (6.105)	17.8 (5.43)	20.0 (6.09)	17.5 (5.34)	20.3 (6.20)	22.0 (6.70)	17.8 (5.44)	22.0 (6.70)	15.2 (4.63)	23.1 (7.049)	17.9 (5.45)	17.7 (5.38)
AXIAL PEAK IN AN AVERAGE ROD KV/M (KV/FT)	24.00 (7.33)	21.36 (6.52)	24.00 (7.31)	21.00 (6.41)	24.36 (7.44)	26.40 (8.04)	21.36 (6.53)	26.40 (8.04)	18.24 (6.02)	27.72 (9.16)	21.48 (7.09)	21.24 (6.99)
MAX. PEAK LHGR KV/M (KV/FT)	57.1 (17.4)	48.2 (14.7)	48.2 (14.7)	47.6 (14.5)	55.1 (16.8)	42.3 (12.9)	41.3 (12.6)	43.0 (13.1)	42.3 (12.9)	60.7 (18.5)	44.0 (13.4)	44.0 (13.4)
AXIAL PEAKING FACTOR DESIGN (NOMINAL)	1.46 (1.2)	1.45 (1.2)	1.56 (1.2)	1.47 (1.2)	1.72 (1.2)	1.55 (1.2)	1.74 (1.2)	1.30 (1.2)	1.57 (1.3)	1.50 (1.3)	1.40 (1.3)	1.56 (1.3)
RADIAL PEAKING FACTOR DESIGN (NOMINAL)	1.50 (1.35)	1.34 (1.35)	1.33 (1.35)	1.55 (1.35)	1.58 (1.35)	1.55 (1.35)	1.55 (1.35)	1.42 (1.35)	1.51 (1.4)	1.40 (1.5)	1.40 (1.4)	1.35 (1.4)
MAX. FUEL TEMPERATURE C (F)	2300 (4170)	2020 (3670)	2140 (3890)	1880 (3420)	2200 (4100)	2340 (4250)	1870 (3400)	2200 (3997)	2040 (3700)	2440 (4430)	1830 (3325)	1890 (3436)
CORE AVERAGE ENRICHMENT WT % U-235	2.57	2.96	2.35	2.36	2.90	2.80	2.60	3.02	2.65	2.19	1.80	1.99
MAX. LOCAL EXPOSURE RMB/KG-METAL	55	55	50	55	50	50	50	47.5	35	40	40	45
CLADDING MATERIAL	ZIRC-4	ZIRC-4	ZIRC-4	ZIRC-4	ZIRC-4	ZIRC-4	ZIRC-4	ZIRC-4	ZIRC-2	ZIRC-2	ZIRC-2	ZIRC-2
FUEL ROD LENGTH M (INCH)	3.89 (153.13)	3.86 (152.13)	3.71 (145.9)	4.09 (161.02)	3.87 (152.36)	3.80 (149.7)	3.85 (151.6)	3.86 (152.0)	3.99 (156.92)	4.09 (161.1)	4.09 (161.1)	4.20 (165.4)
ACTIVE FUEL HEIGHT M (INCH)	3.66 (144)	3.63 (143)	3.47 (136.7)	3.81 (150)	3.66 (144)	3.66 (144)	3.65 (143.7)	3.60 (144)	3.66 (144)	3.66 (144)	3.71 (146)	3.81 (150)

VEHENDOR	B&W	B&W	C-E	C-E	WEST.	WEST.	WEST.	EXXON	EXXON	GE	GE	GE
FUEL ROD ARRAY	15X15	17X17	14X14	16X16	14X14	15X15	17X17	15X15	8X8	7X7	8X8	8X8
PLENUM LENGTH IN (INCH)	0.29 (11.27)	0.24 (9.62)	0.22 (8.6)	0.25 (10.0)	0.18 (6.99)	0.21 (8.2)	0.16 (6.3)	0.17 (6.8)	0.27 (10.63)	0.41 (16.0)	0.36 (14.0)	0.25 (10.0)
FUEL ROD O.D. MM (INCH)	10.92 (.430)	9.63 (.379)	11.18 (.440)	9.70 (.382)	10.72 (.422)	10.72 (.422)	9.50 (.374)	10.77 (.424)	12.74 (.5015)	14.30 (.563)	12.52 (.493)	12.27 (.483)
CLADDING I.D. MM (INCH)	9.58 (.377)	8.43 (.332)	9.86 (.388)	8.43 (.332)	9.48 (.3734)	9.48 (.3734)	8.36 (.329)	9.25 (.364)	10.91 (.4295)	12.68 (.499)	10.80 (.425)	10.64 (.419)
CLADDING THICKNESS MM (INCH)	.673 (.0265)	.597 (.0235)	.660 (.026)	.635 (.025)	.617 (.0243)	.617 (.0243)	.572 (.0225)	.762 (.030)	.914 (.036)	.813 (.032)	.864 (.034)	.813 (.032)
DIAMETRAL GAP MICRON (P'L)	178 (7.0)	203 (8.0)	216 (8.5)	178 (7.0)	190 (7.5)	190 (7.5)	165 (6.5)	190 (7.5)	254 (10.0)	305 (12.0)	229 (9.0)	229 (9.0)
FUEL PELLETT DIAMETER MM (INCH)	9.40 (.370)	8.23 (.324)	9.64 (.3795)	8.26 (.325)	9.29 (.3659)	9.29 (.3659)	8.19 (.3225)	9.06 (.3565)	10.66 (.4195)	12.37 (.487)	10.57 (.416)	10.41 (.410)
FUEL PELLETT LENGTH MM (INCH)	17.78 (.700)	9.53 (.375)	16.51 (.650)	9.91 (.390)	15.24 (.600)	15.24 (.600)	13.46 (.530)	6.93 (.273)	8.13 (.320)	12.70 (.500)	10.67 (.420)	10.41 (.410)
FUEL PELLETT DENSITY % T.D.	94	94	94.75	95	94	95	95	94	95	95	95	95
FUEL PELLETT CHAMFER	YES	YES	YES	YES	NO	NO	NO	NO	YES	YES	YES	YES
FUEL PELLETT DISH	YES	YES	YES	YES	YES	YES	YES	YES	YES	YES	NO	NO
FILL GAS	HELIUM	HELIUM	HELIUM	HELIUM	HELIUM	HELIUM	HELIUM	HELIUM	HELIUM	HELIUM	HELIUM	HELIUM
FUEL ROD PREPRESSURIZATION	YES	YES	YES	YES	YES	YES	YES	YES	NO	NO	NO	NO
BURNABLE POISON PELLETT COMPOSITION	AL203- B4C	AL203- B4C	AL203- B4C	AL203- B4C	SI02- B203-M20	SI02- B203-M20	SI02- B203-M20	AL203- B4C	U02- GD203	U02- GD203	U02- GD203	U02- GD203
POISON IN COOLANT	BORON	BORON	BORON	BORON	BORON	BORON	BORON	BORON	NONE	NONE	NONE	NONE



## APPENDIX B References

1. Babcock and Wilcox 15x15, "Final Safety Analysis Report, Three Mile Island, Unit 2," Docket 50-320, February 1974. Available in NRC PDR for inspection and copying for a fee.
2. Babcock & Wilcox 17x17, "Preliminary Safety Analysis Report, Bellefonte Unit 1," Docket 50-438, June 1973. Available in NRC PDR for inspection and copying for a fee.
3. Combustion Engineering 14x14, "Final Safety Analysis Report, St. Lucie Unit 1," Docket No. 50-335, February 1973. Available in NRC PDR for inspection and copying for a fee.
4. Combustion Engineering 16x16, "Final Safety Analysis Report, Anco Unit 2," Docket No. 50-368, March 1974. Available in NRC PDR for inspection and copying for a fee.
5. Westinghouse Electric 14x14, "Final Safety Analysis Report, Prairie Island Unit 1," Docket 50-252, January 1971. Available in NRC PDR for inspection and copying for a fee.
6. Westinghouse Electric 15x15, "Final Safety Analysis Report, Zion Unit 1," Docket No. 50-295, August 1971. Available in NRC PDR for inspection and copying for a fee.
7. Westinghouse Electric 17x17, "Final Safety Analysis Report, Trojan," Docket 50-344, February 1973. Available in NRC PDR for inspection and copying for a fee.
8. Exxon 15x15, "D. C. Cook, Unit 1 Cycle 2 Reload Fuel Licensing Data Submittal," XN-76-25, July 1976. Available in NRC PDR as Topical Report X-76, for inspection and copying for a fee.
9. Exxon 8x8, "Oyster Creek Nuclear Generating Station Facility Change Request No. 6," Docket No. 50-219, April 1974. Available in NRC PDR for inspection and copying for a fee.
10. General Electric 7x7, "Final Safety Analysis Report, Browns Ferry Unit 1," Docket 50-259 rev. November 1978. Available in NRC PDR for inspection and copying for a fee.
11. General Electric 8x8, "Final Safety Analysis Report, Zimmer Unit 1," Docket No. 50-358, September 1975. Available in NRC PDR for inspection and copying for a fee.
12. General Electric 8x8R, "Final Safety Analysis Report, E. Hatch Unit 2," Docket 50-366, October 1975. Available in NRC PDR for inspection and copying for a fee.

## APPENDIX C

The following legend presents an identification of the symbols used in Figures 15 through 18 of Appendices D-I. Each symbol represents a different LWR fuel design as described previously. The legend is presented here to avoid a redundant presentation of this information on each of the graphs that follow.

### LEGEND

- ◻ = B&W 15X15 (THREE MILE ISLAND-UNIT 2)
- = B&W 17X17 (BELLEFONTE-UNIT 1)
- ▲ = C-E 14X14 (ST. LUCIE-UNIT 1)
- + = C-E 16X16 (ANO-UNIT 2)
- x = WEST. 14X14 (PRAIRIE ISLAND-UNIT 1)
- = WEST. 15X15 (ZION-UNIT 1)
- ▼ = WEST. 17X17 (TROJAN)
- = EXXON 15X15 (D.C. COOK-UNIT 1)
- ✕ = EXXON 8X8 (OYSTER CREEK)
- = G.E. 7X7 (BROWNS FERRY-UNIT 1)
- = G.E. 8X8 (ZIMMER-UNIT 1)
- = G.E. 8X8R (HATCH-UNIT 2)
- = G.E. 8X8R PREP. (HATCH-UNIT 2)

## APPENDIX D

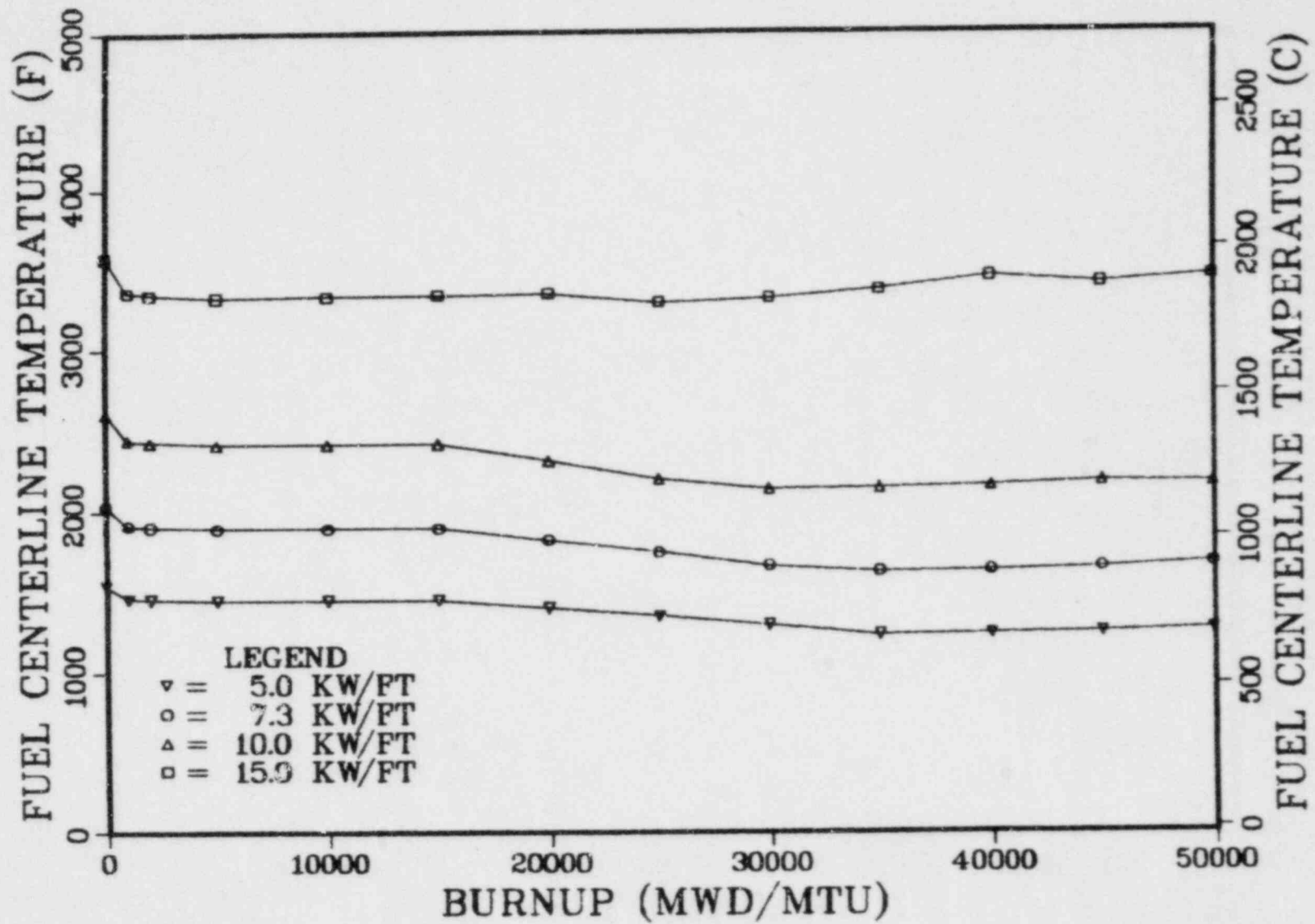
### FUEL CENTERLINE TEMPERATURE

The following graphs are of fuel centerline temperature vs. burnup, and the data are given for the peak axial node at specified peak burnups. In general, the peak centerline temperature occurs at beginning of life or soon thereafter for PWR's, while the peak centerline temperature occurs at midlife or late in life for BWR's. There are a few exception with the BWR's, for example at low power, where peak temperatures are also attained at beginning of life.

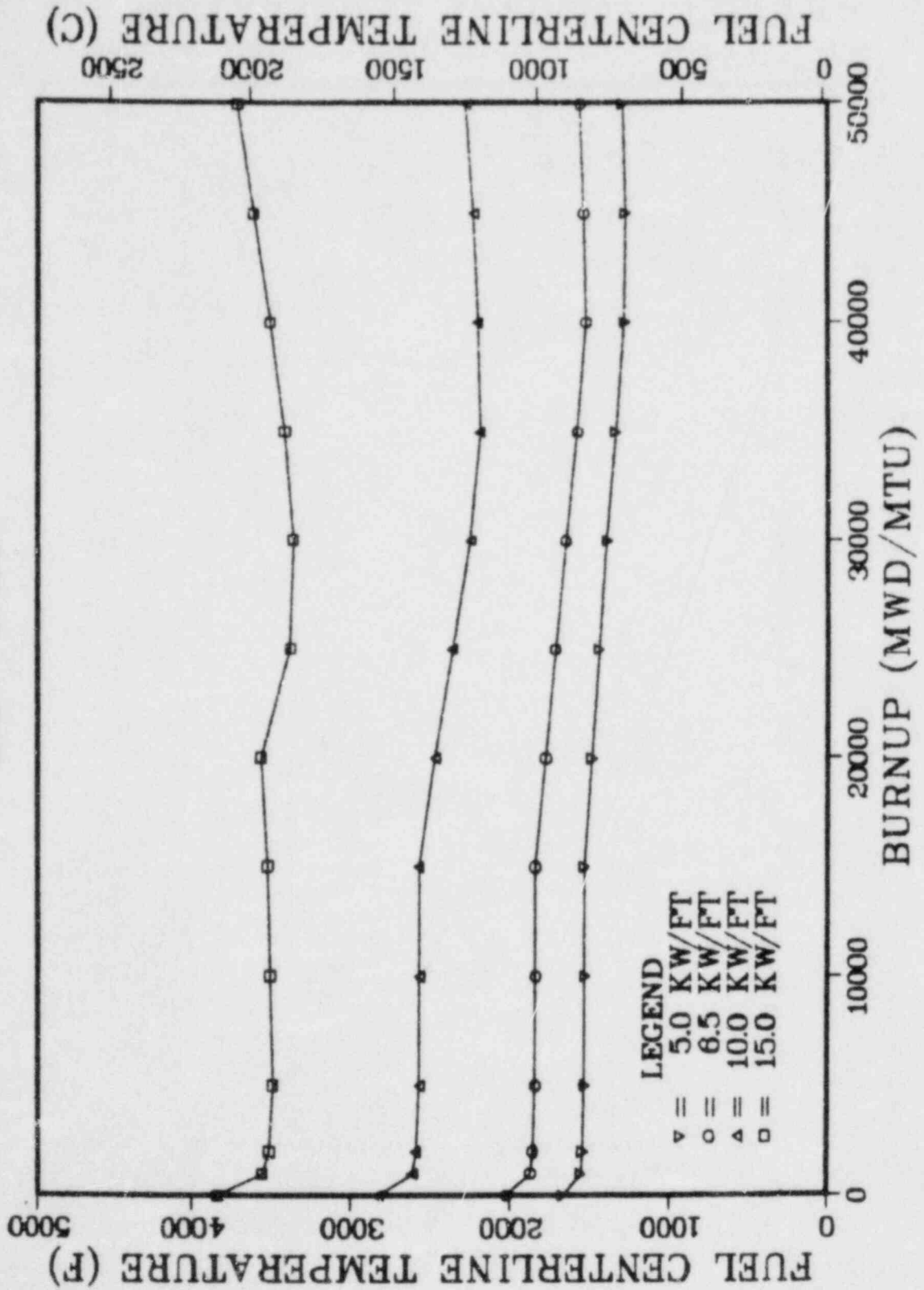
In all the cases considered, the fuel did not reach temperatures above 5080°F (the melting point of  $UO_2$ ).

The multi-design plots reveal some additional results of interest. For power levels between 5 and 10 kW/ft, there is little difference between the values for each of the 13 designs, but at 15 kW/ft, the BWRs demonstrate higher centerline temperatures compared with the PWRs. The difference can be related to the values for gap conductivity at 15 kW/ft; these values are much lower for the unpressurized BWRs and result in higher fuel temperatures.

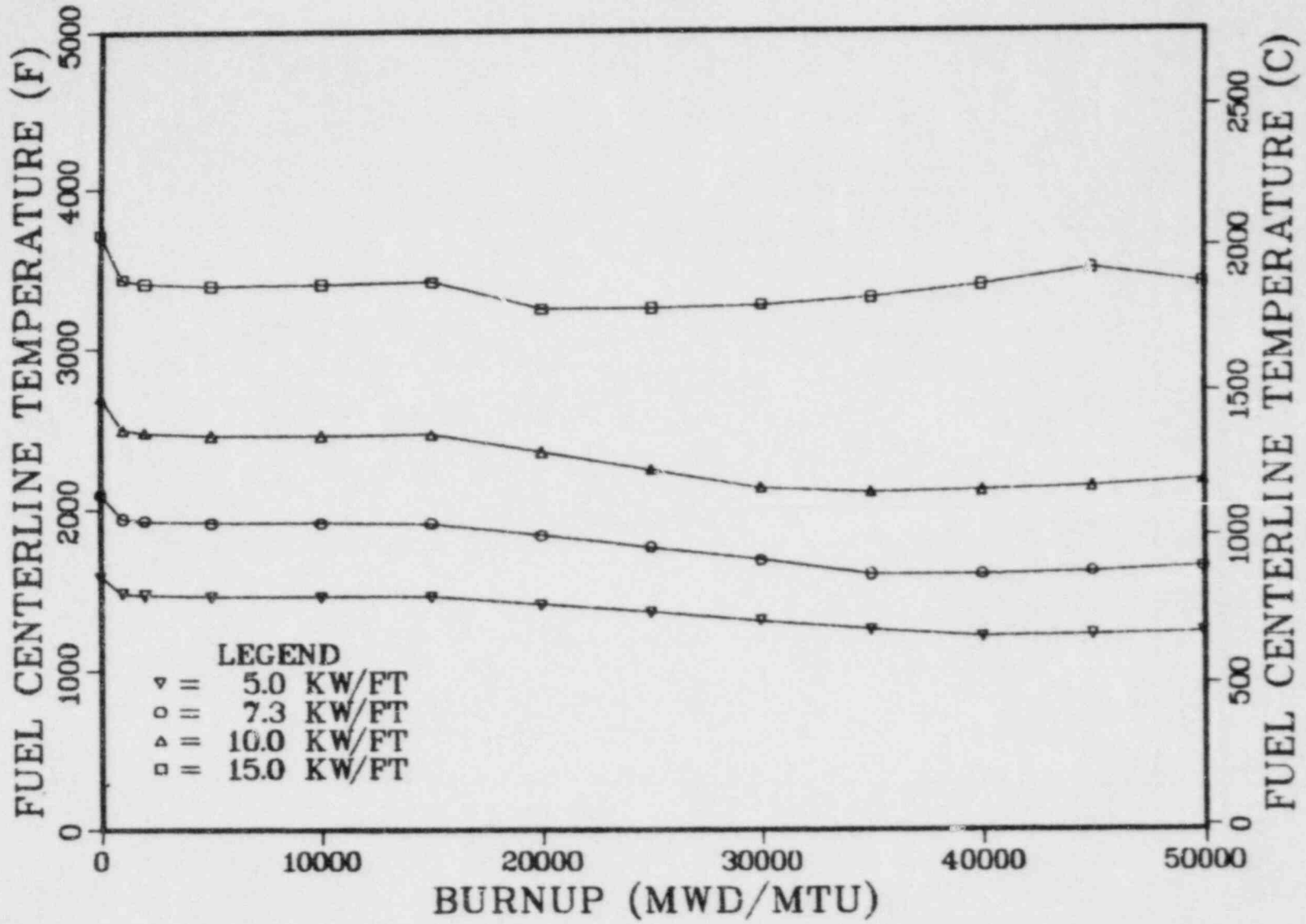
## B&amp;W 15X15



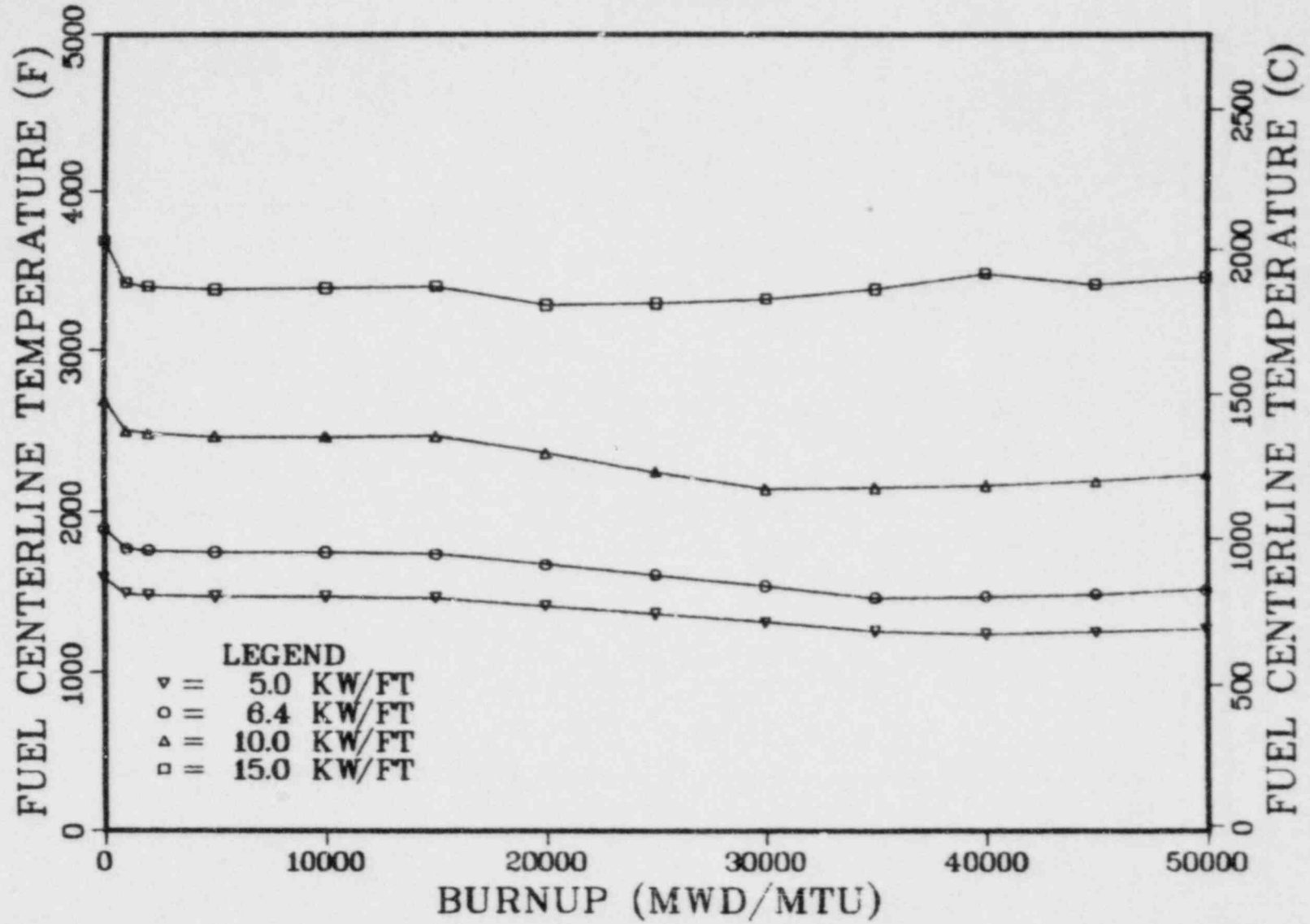
B&W 17X17



## C-E 14X14

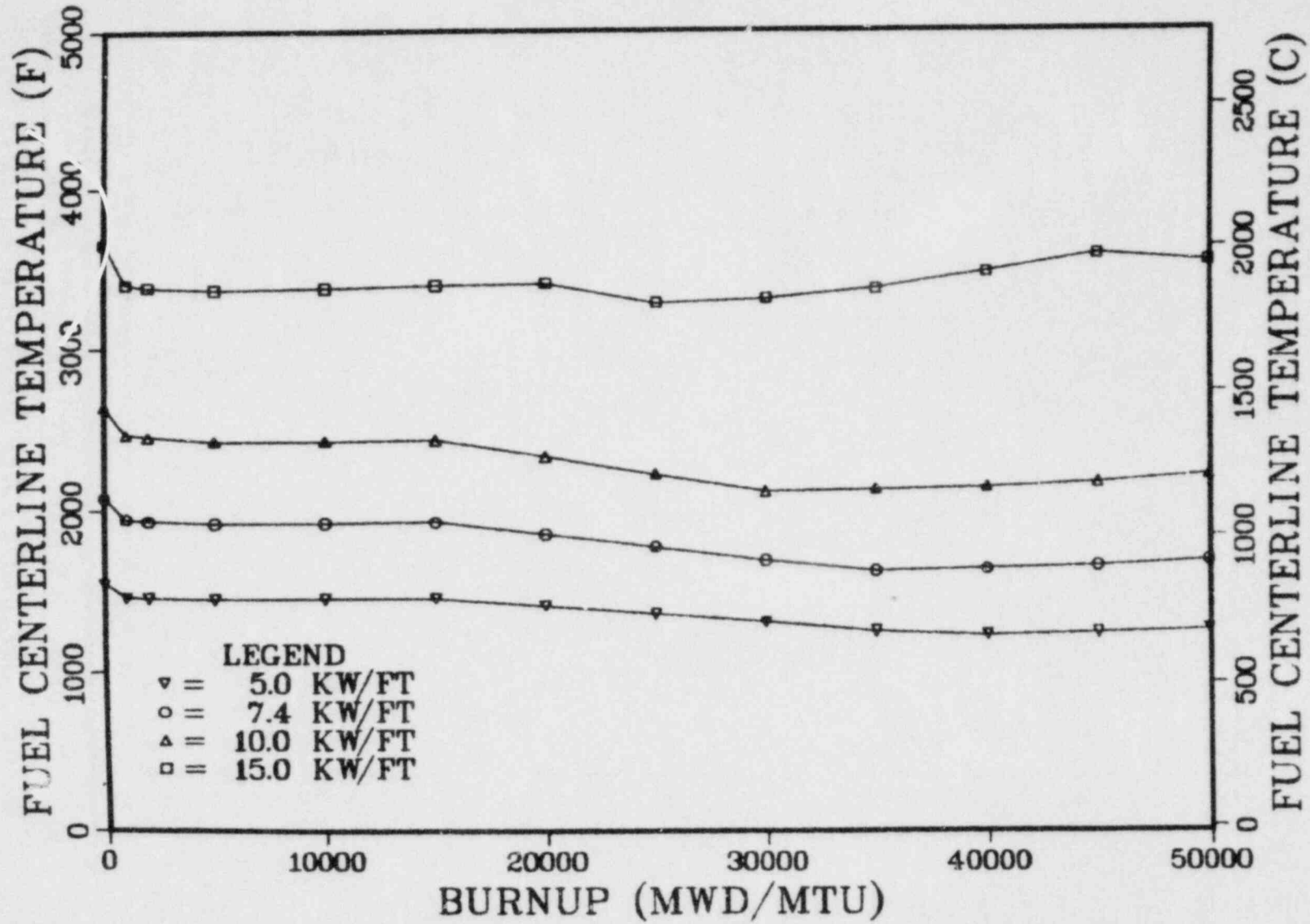


### C-E 16X16

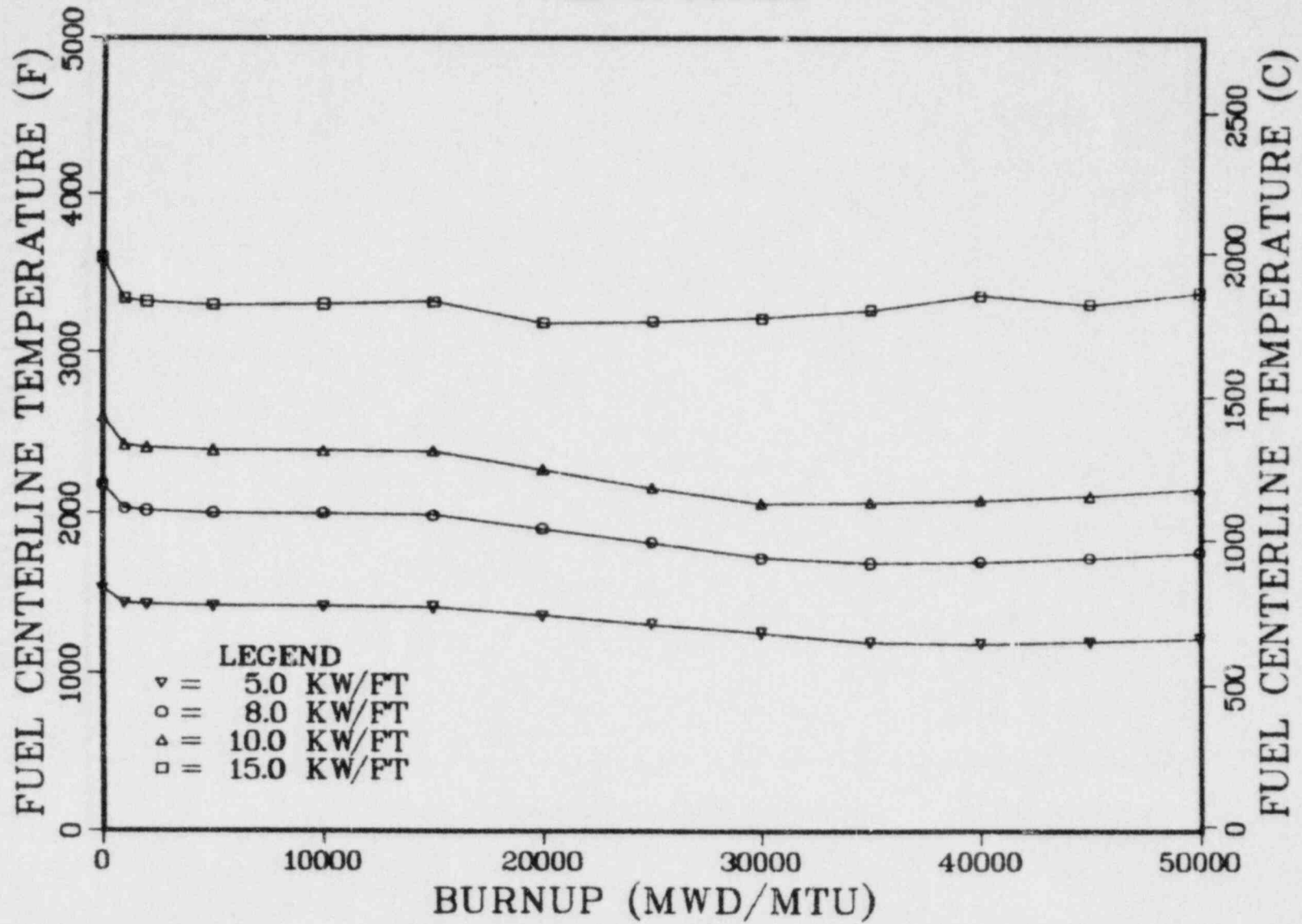




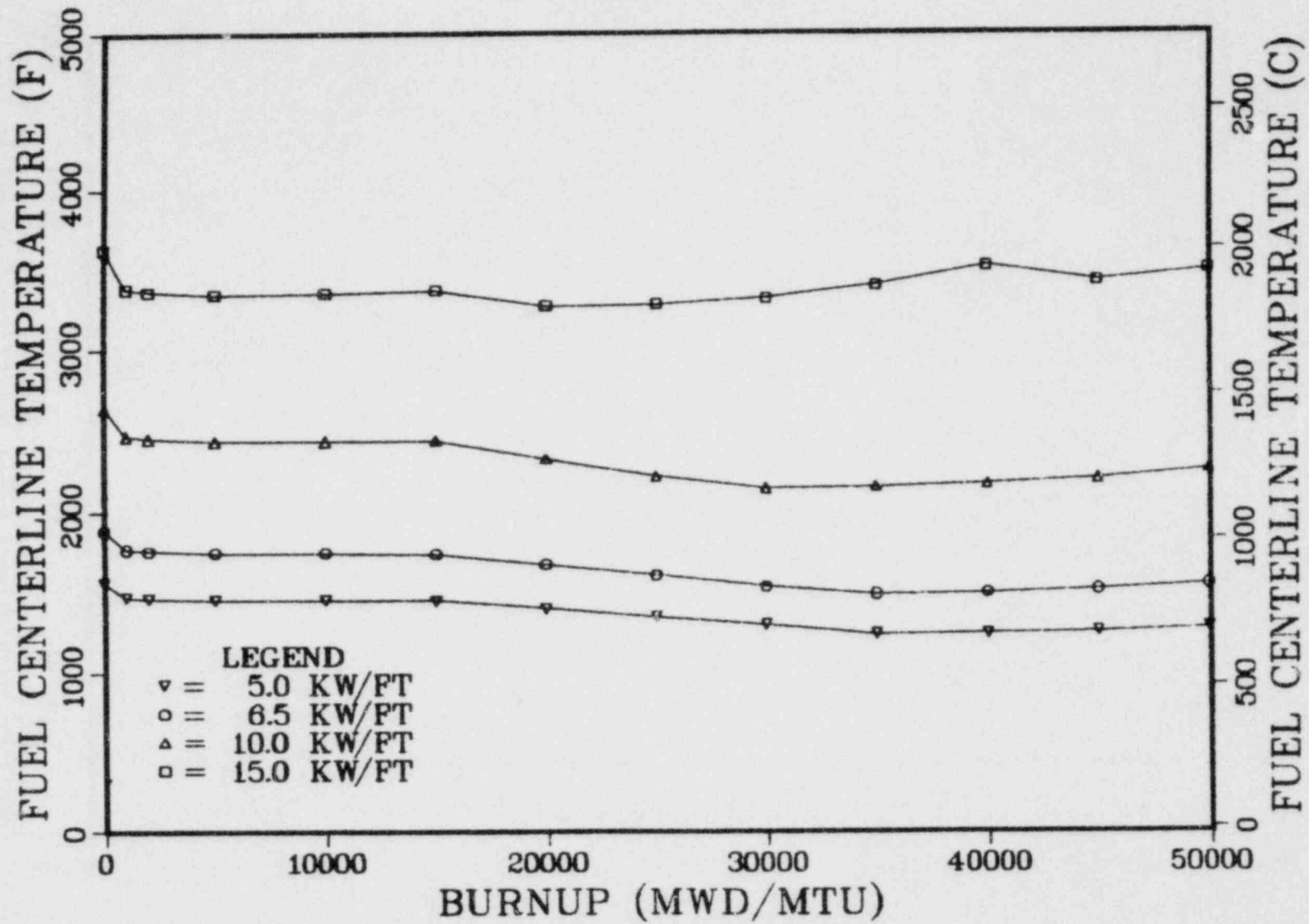
## WEST 14X14



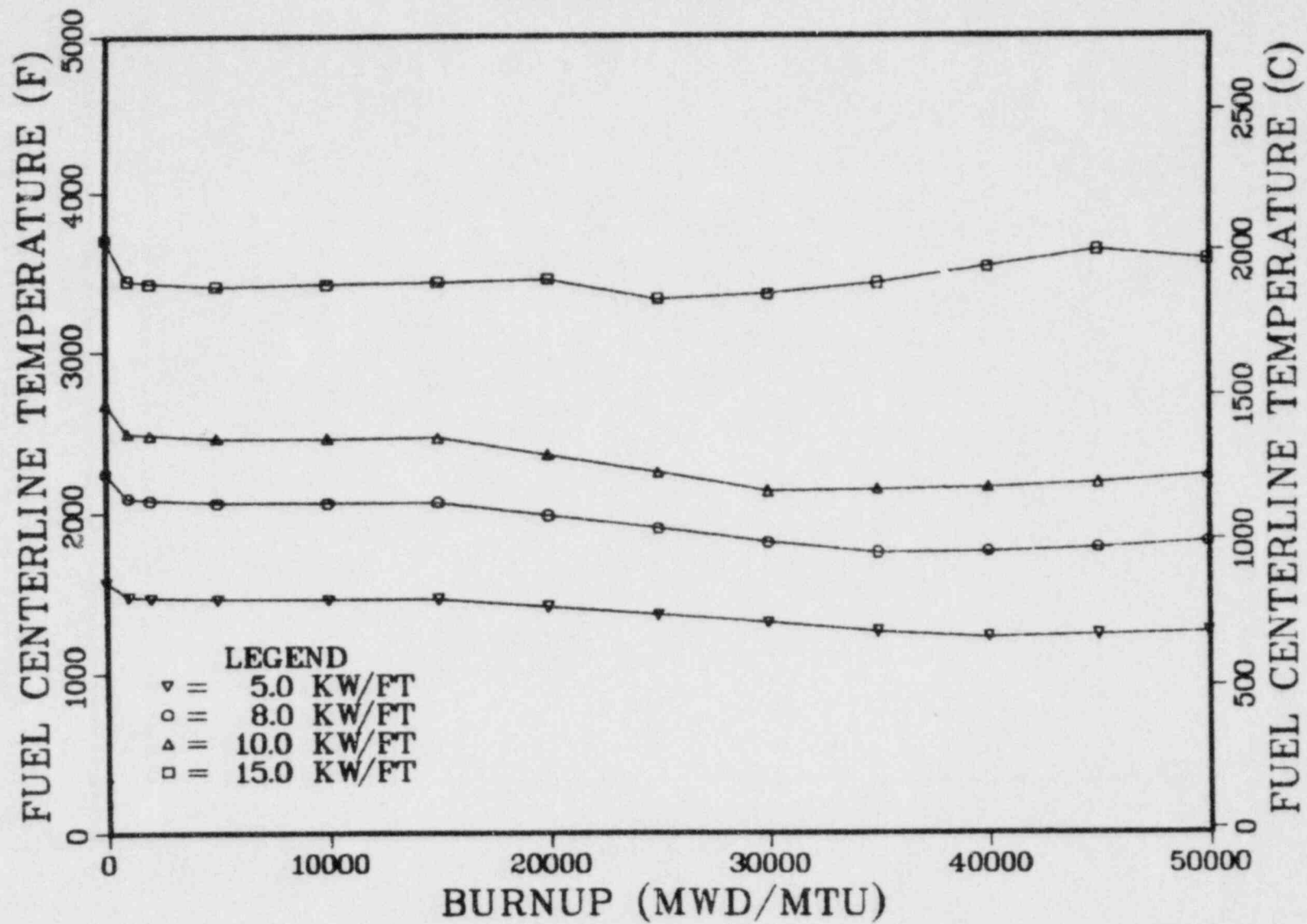
# WEST 15X15



## WEST 17X17

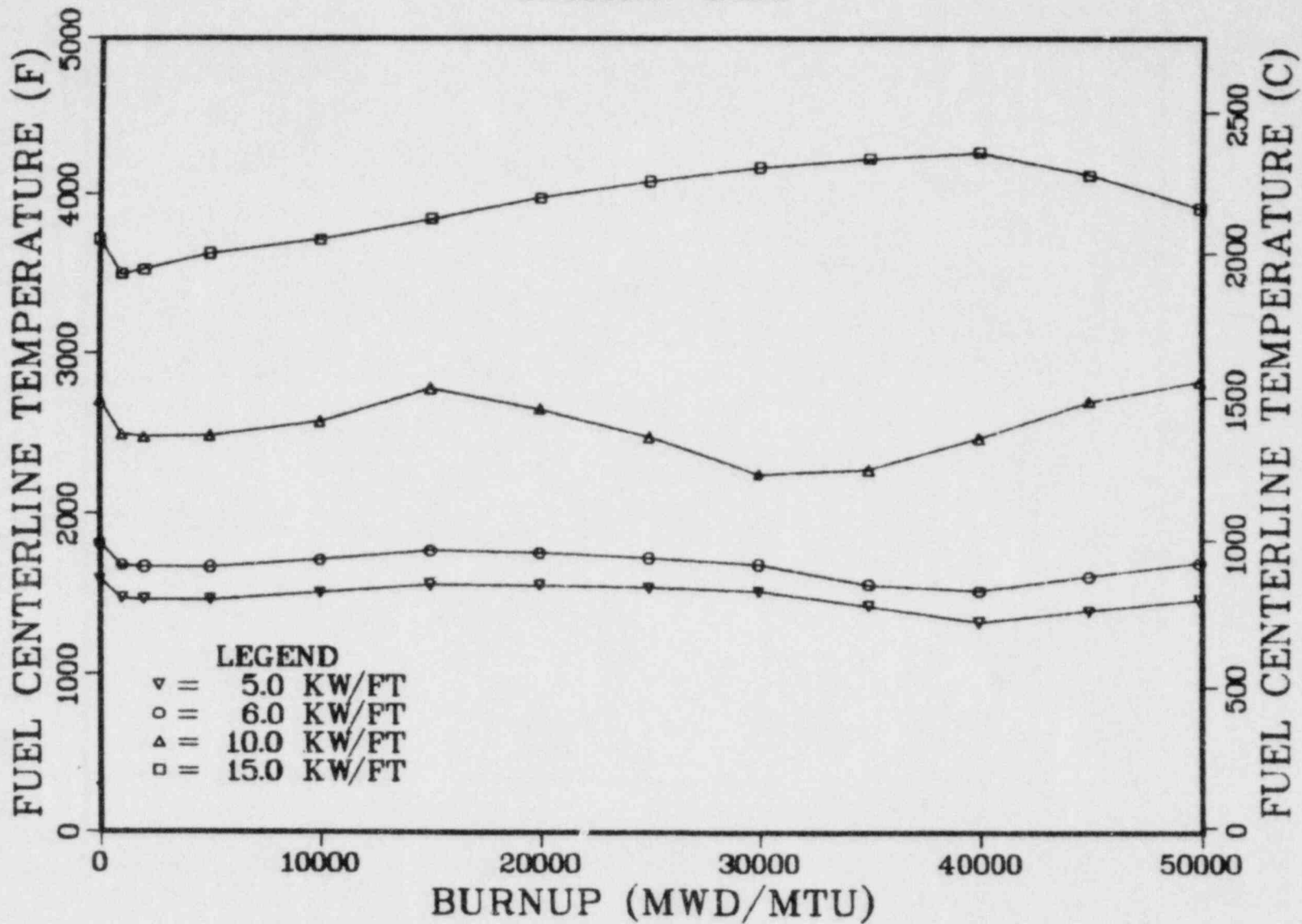


## EXXON 15X15



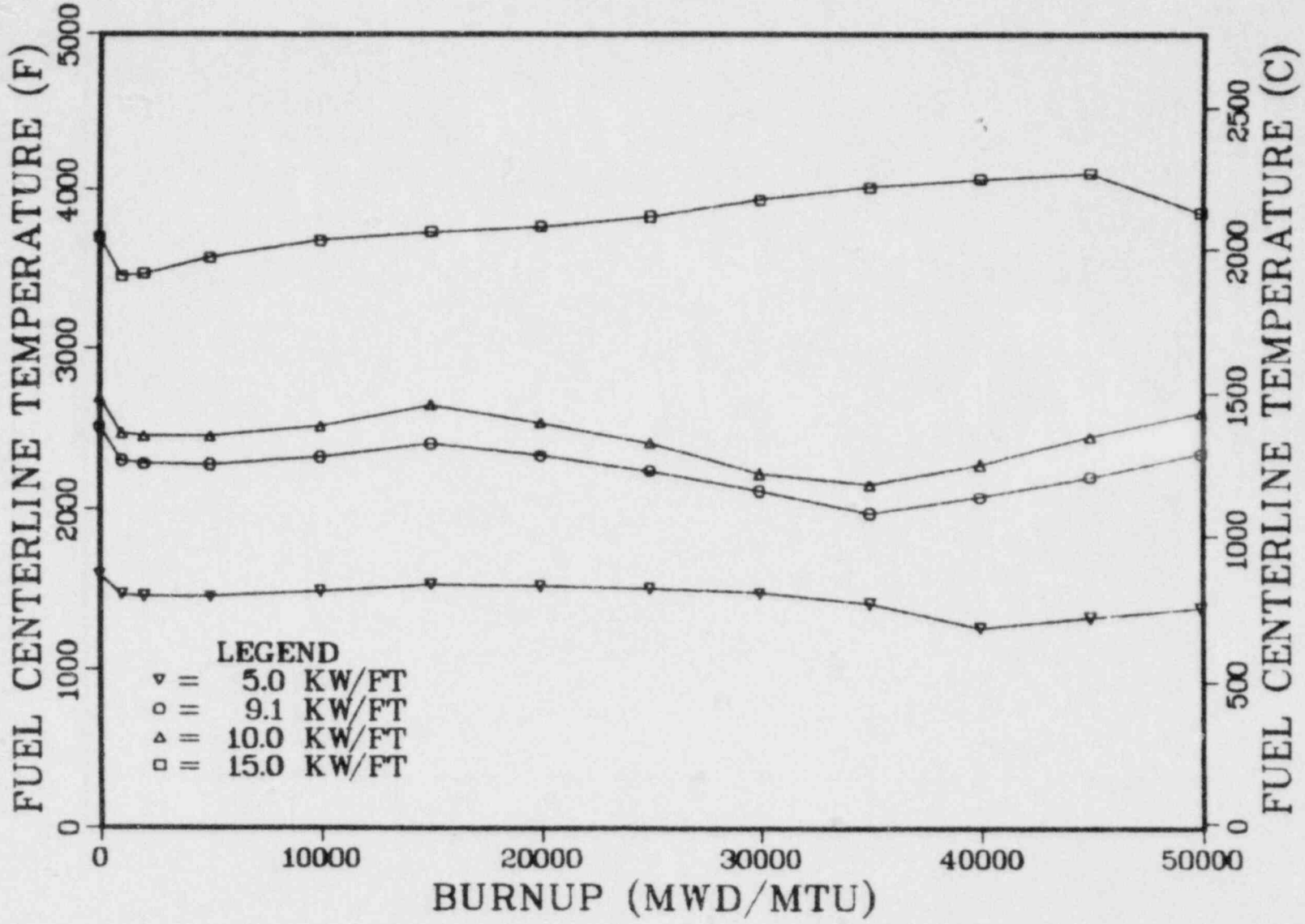
# EXXON 8X8

01-0

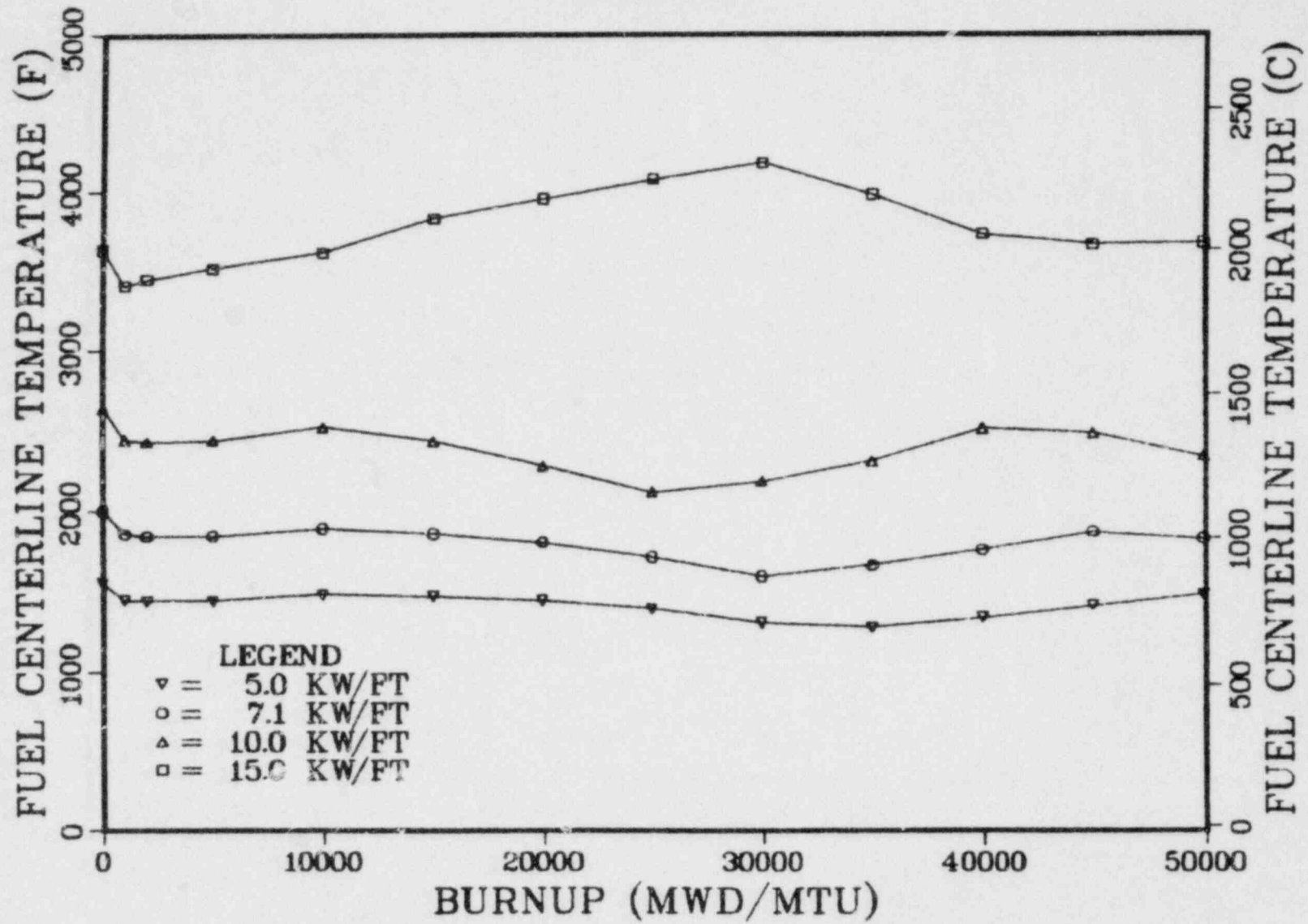


# G.E. 7X7

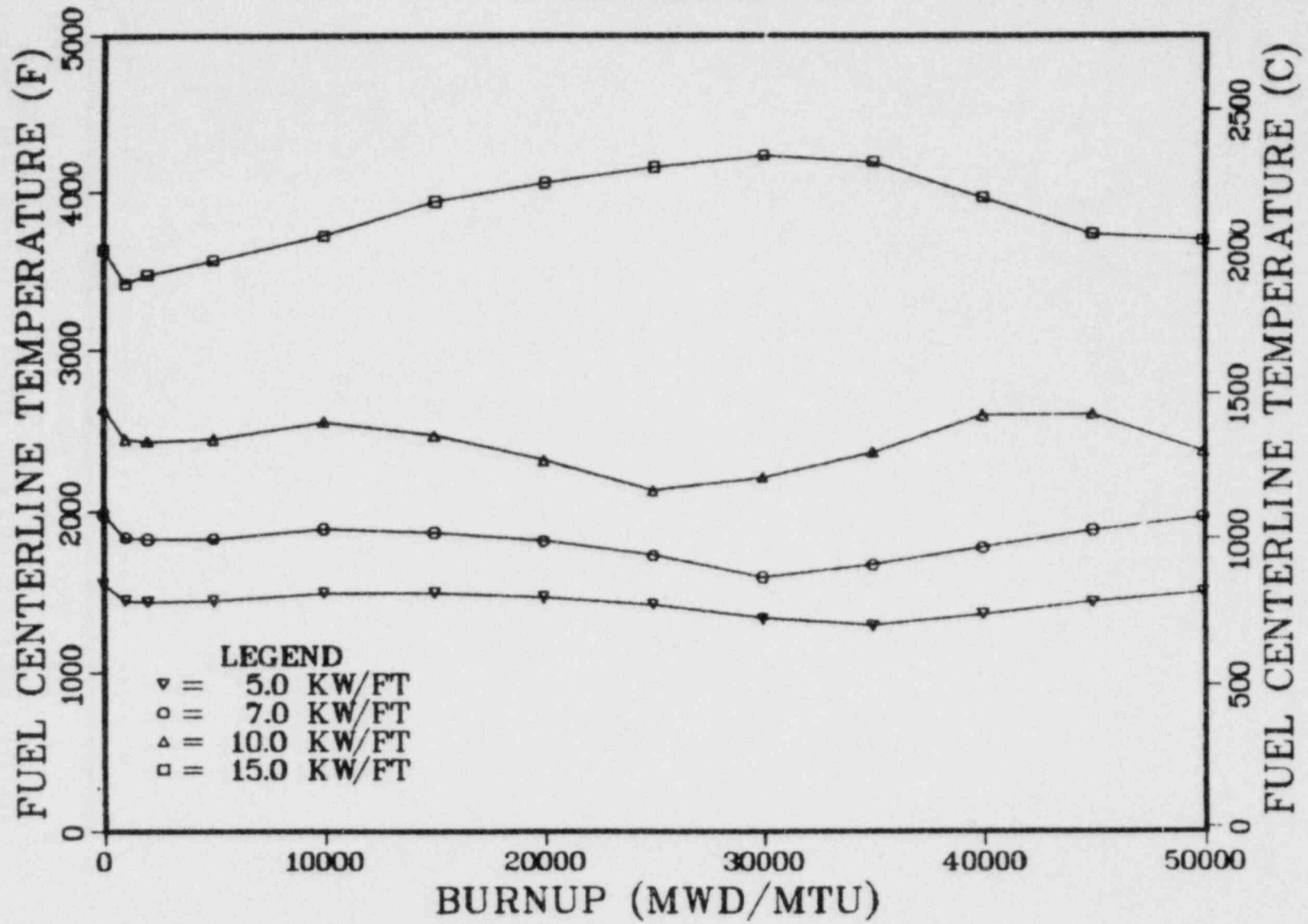
11-0



## G.E. 8X8



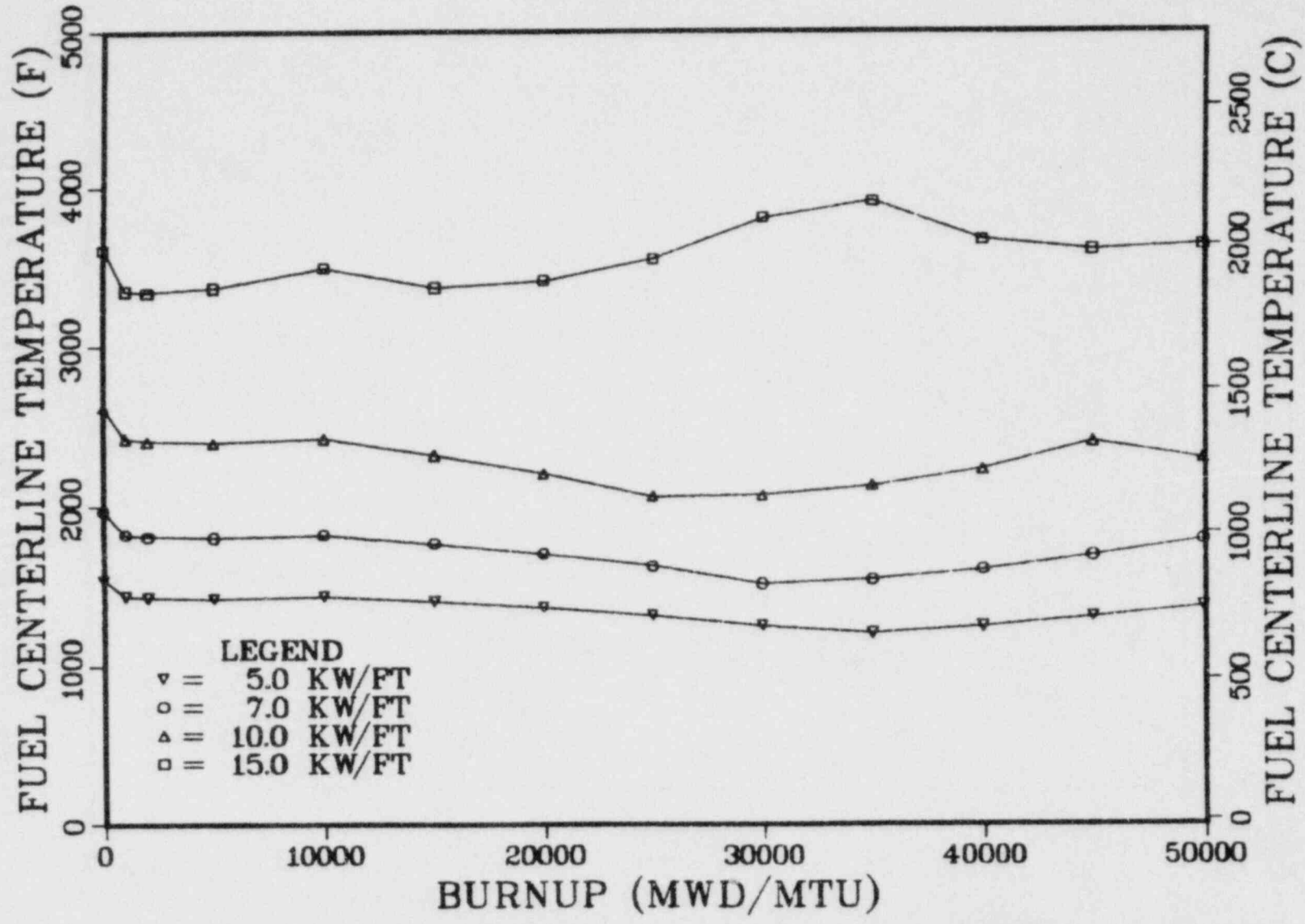
## G.E. 8X8R

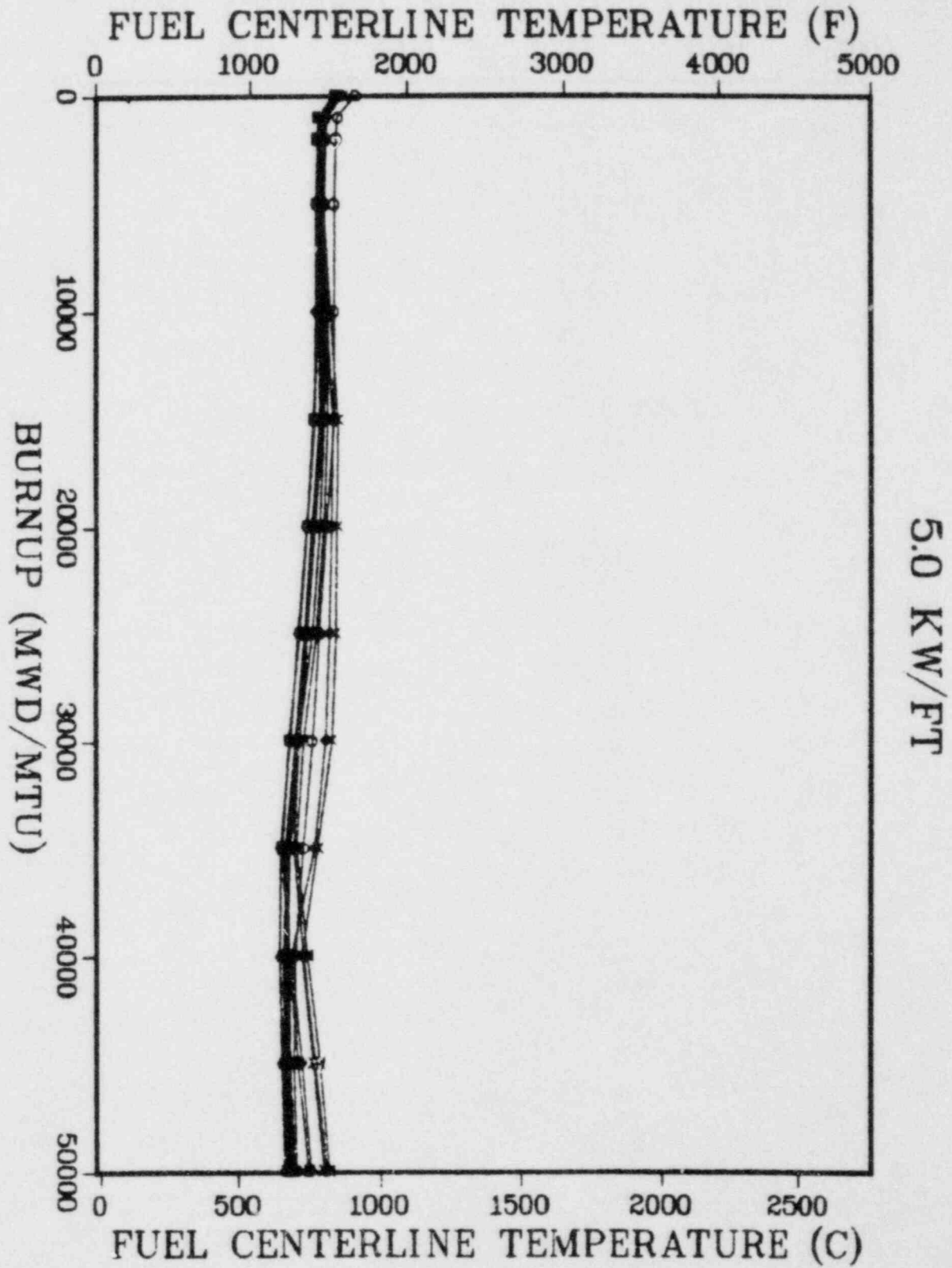


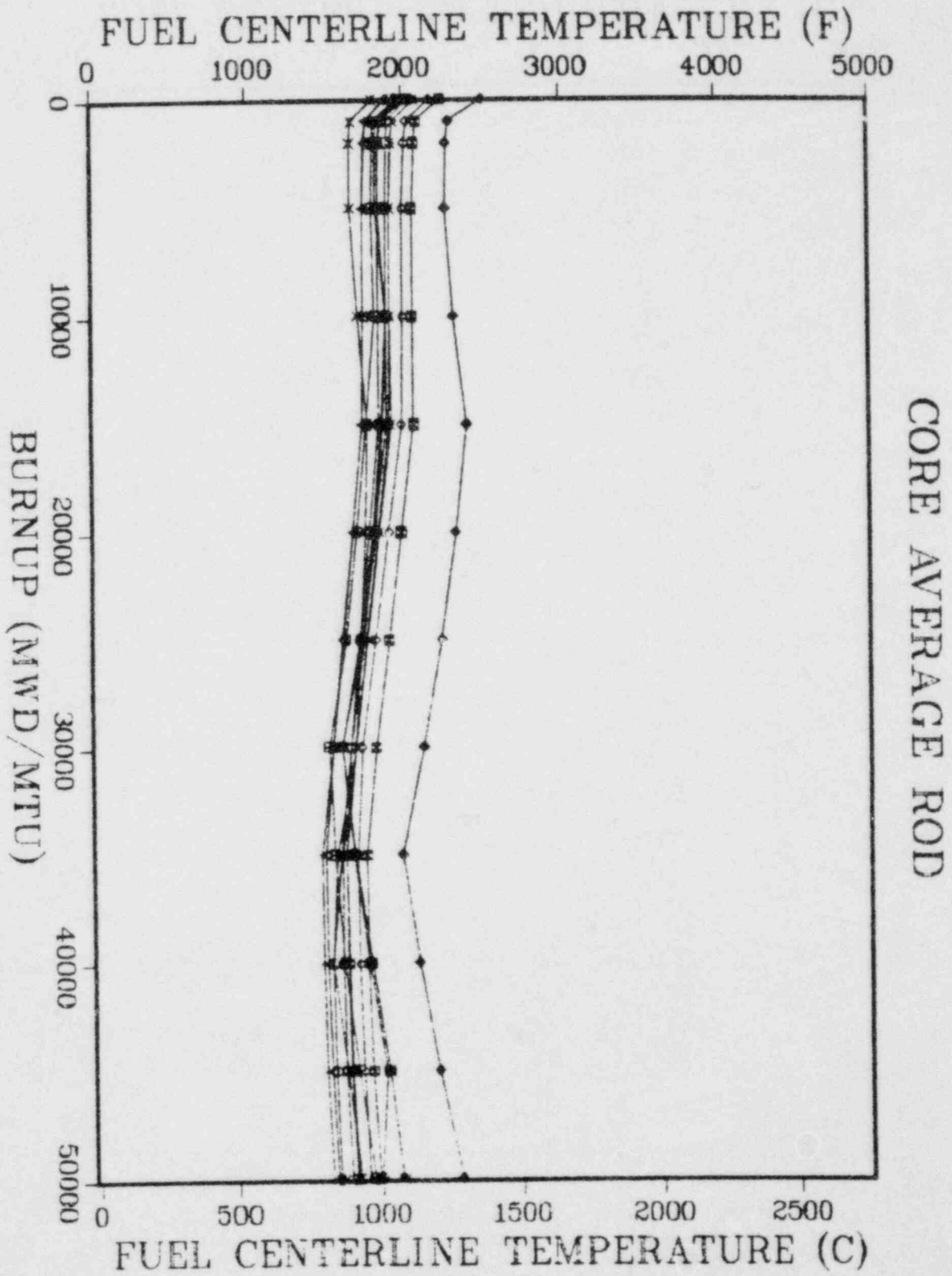


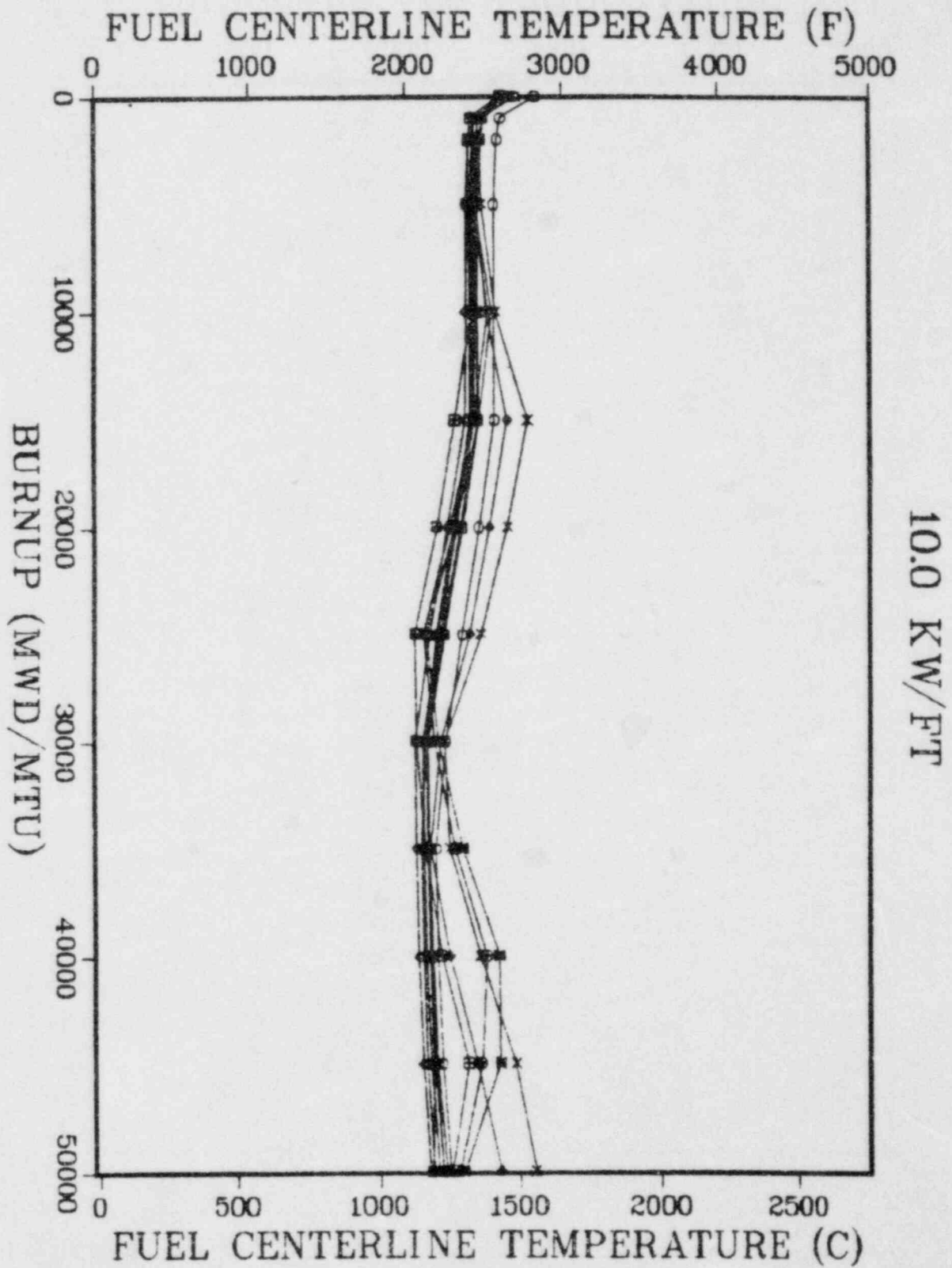
# G.E. 8X8R-P

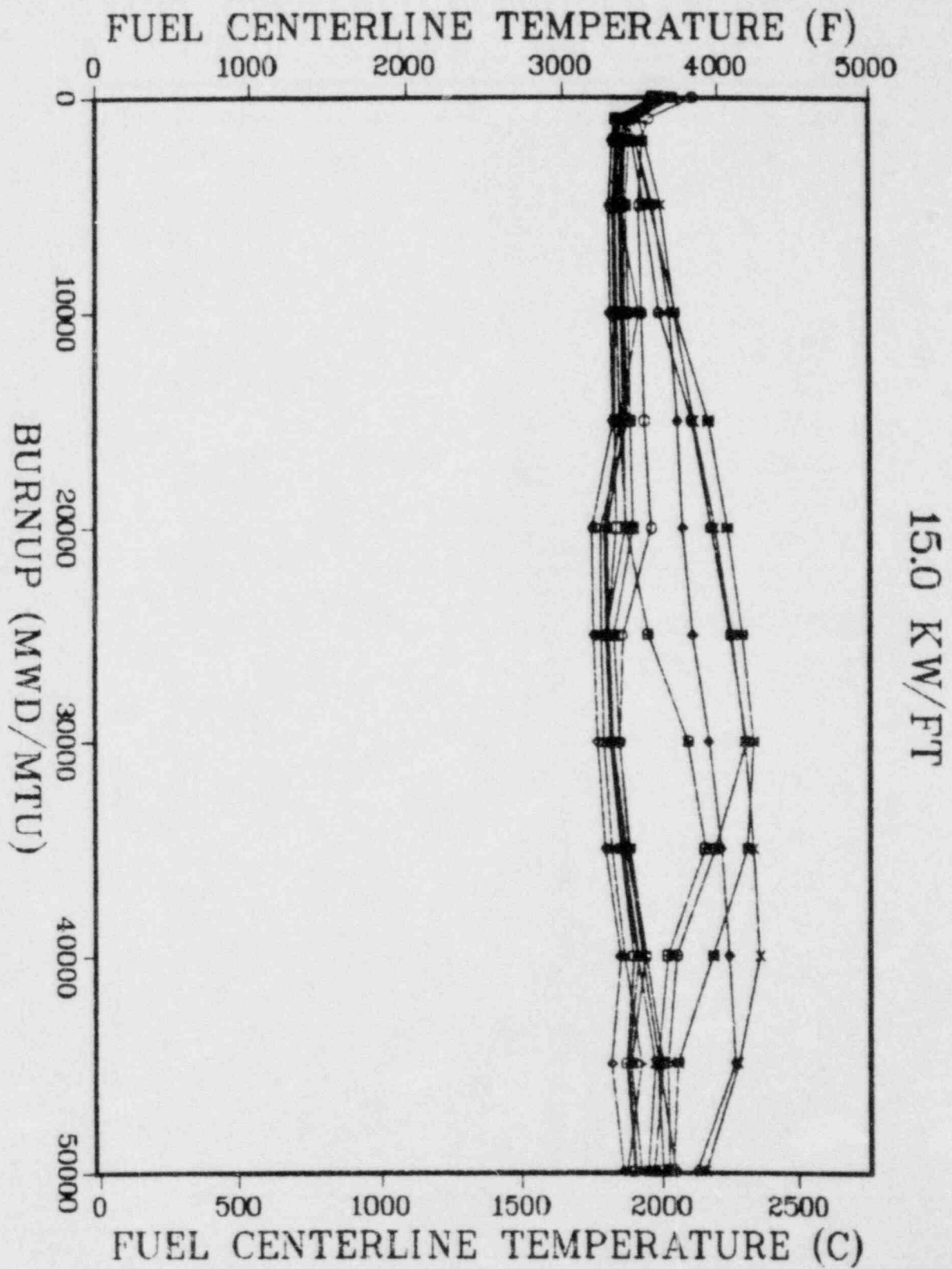
D-14











## APPENDIX E

### RADIAL TEMPERATURE

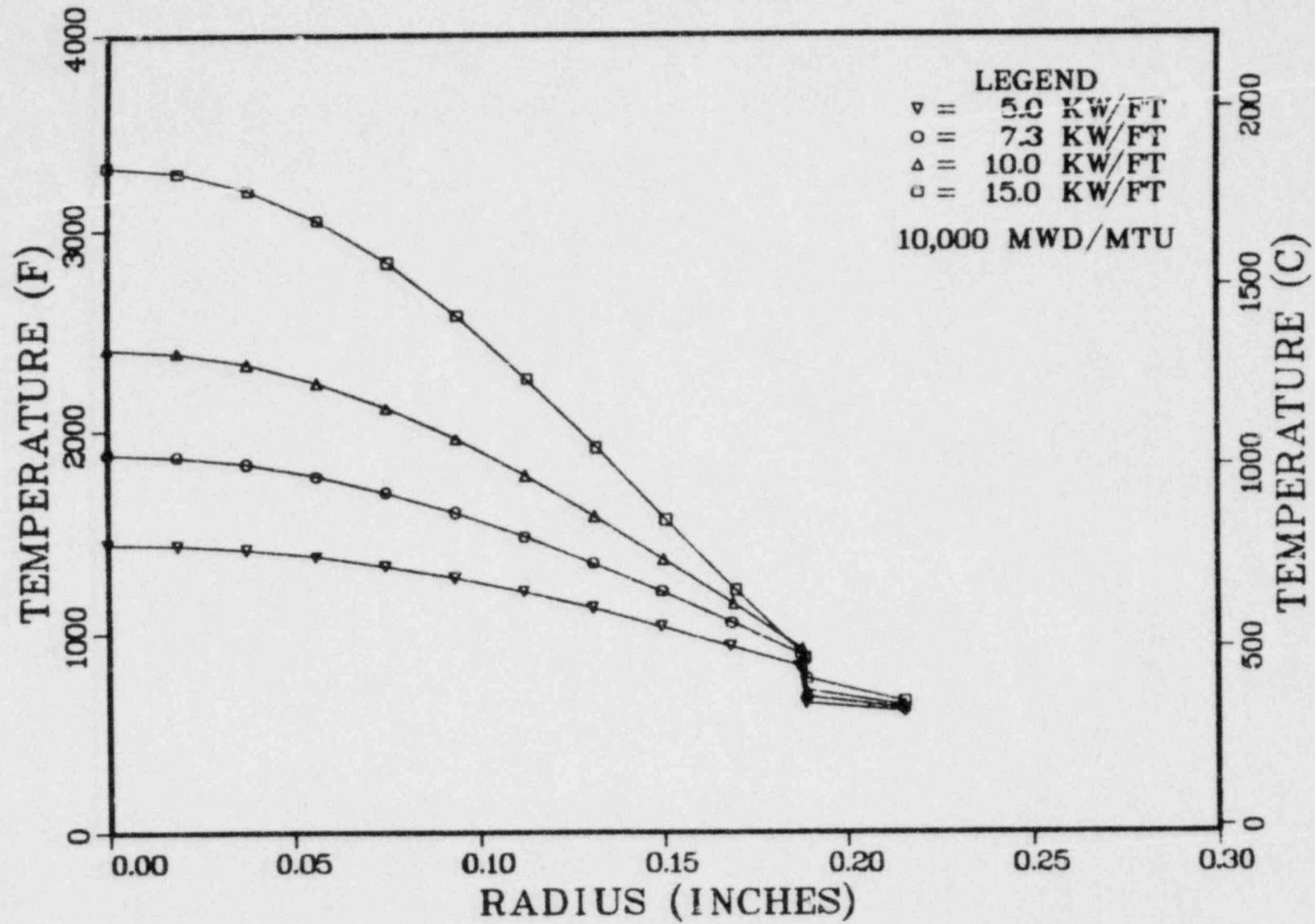
The following graphs present fuel rod temperature as a function of radius, and the data are given for the peak axial node at a rod peak burnup of 10,000 MWd/tU.

The graphs demonstrate the traditional parabolic temperature profile that is associated with cylindrical fuel, while the sharp increases in temperature at the foot of the graphs are due to the drop across the gap from the fuel surface to the inside cladding surface. The flat segments of the graphs represent the nearly uniform temperatures across the cladding.

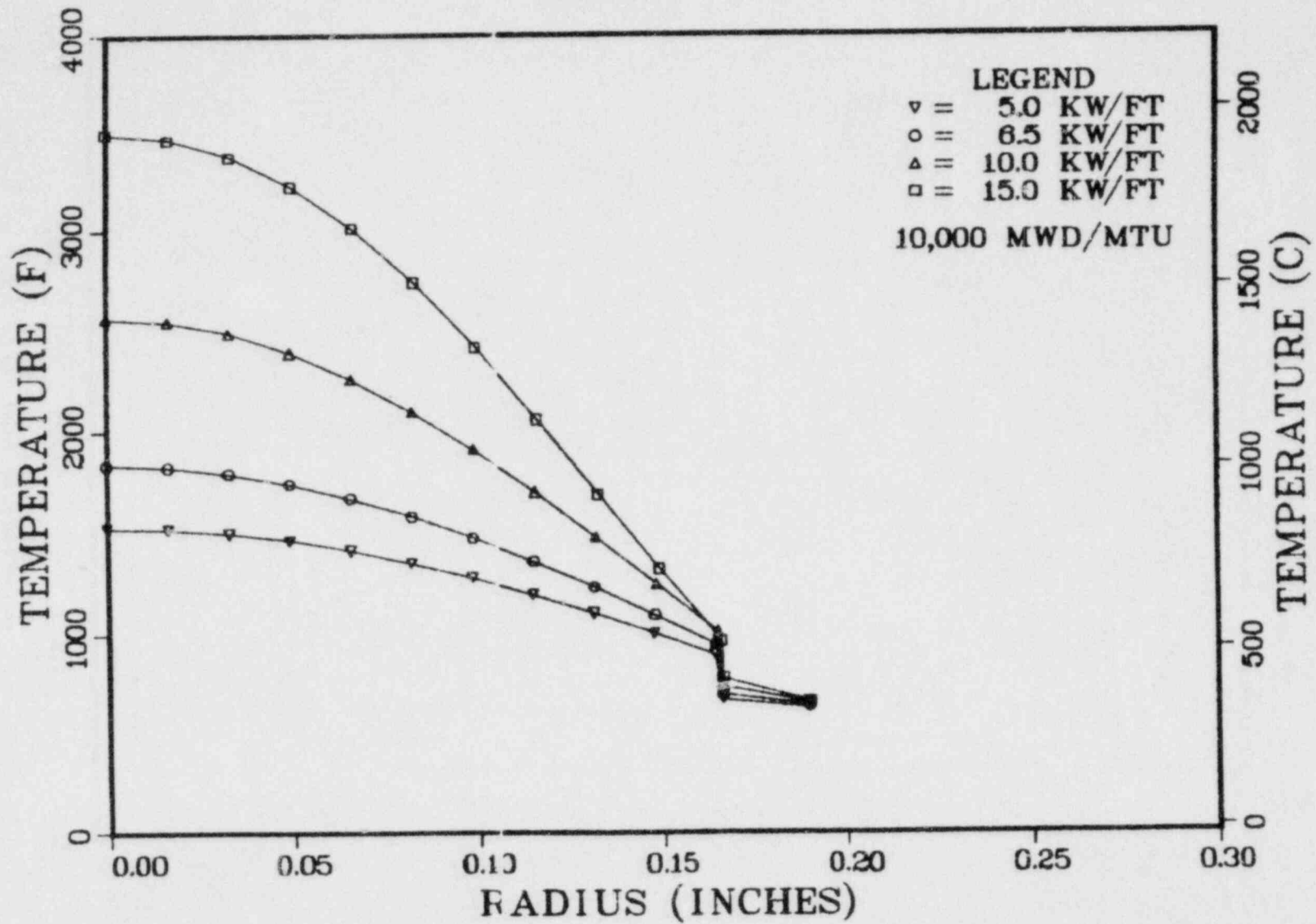
All the graphs are drawn on the same scale, and the large and small diameter fuel rods can be easily differentiated. Differences in cladding thickness are also apparent as the BWR's have thicker claddings than PWRs.

The remaining graphs show a remarkable similarity in fuel centerline temperature even though a 50% differential in pellet diameter exists between the largest and the smallest diameter fuel rods. This result is expected for the 5, 10 and 15 kW/ft plots as a constant linear power is utilized for each design, regardless of diameter. An analysis of the radial temperature distribution in the rod shows this quantity can be related to the linear power and thermal conductivity of the fuel and is independent of the diameter if the flux depression is small.

# B&W 15X15

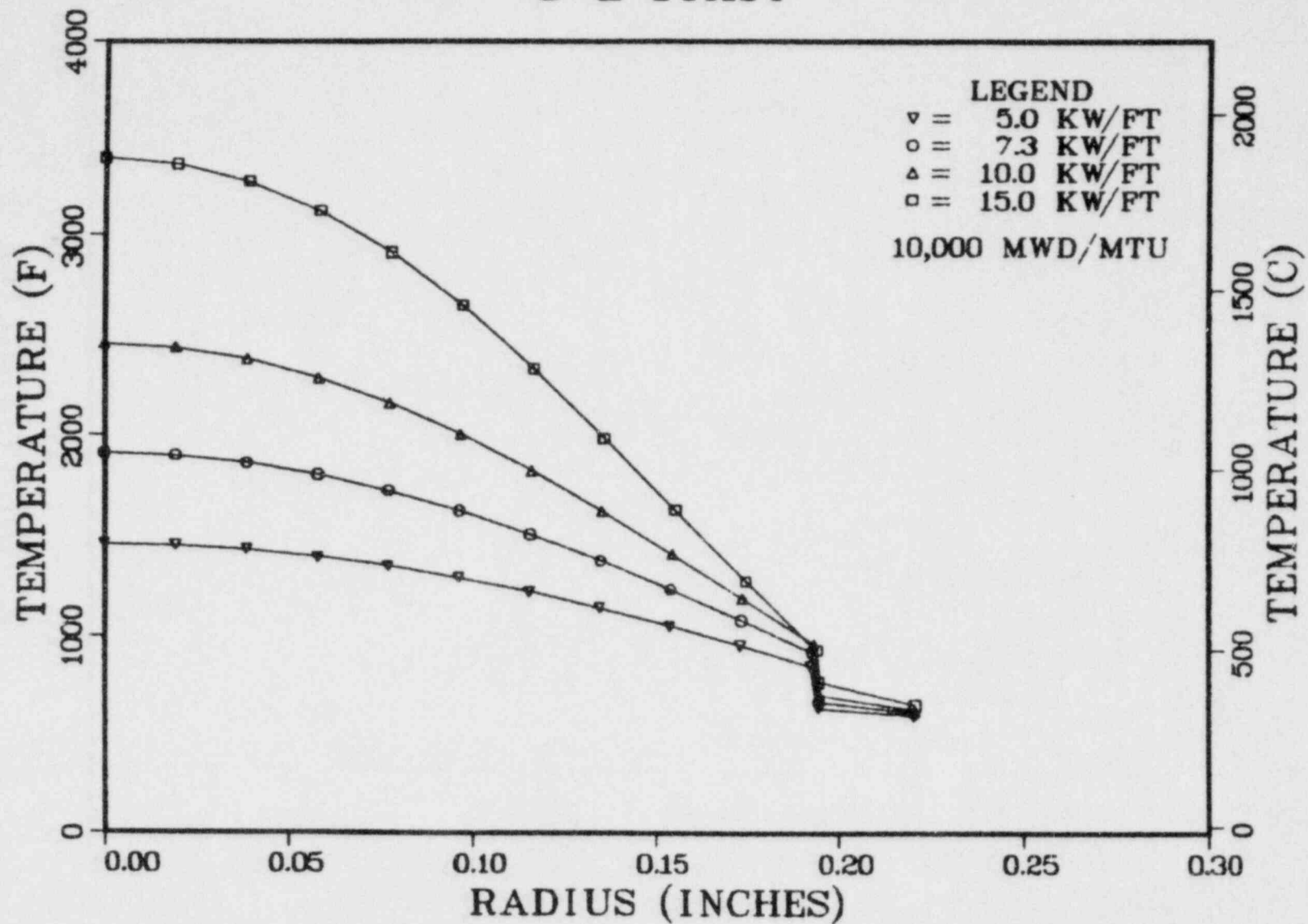


# B&W 17X17

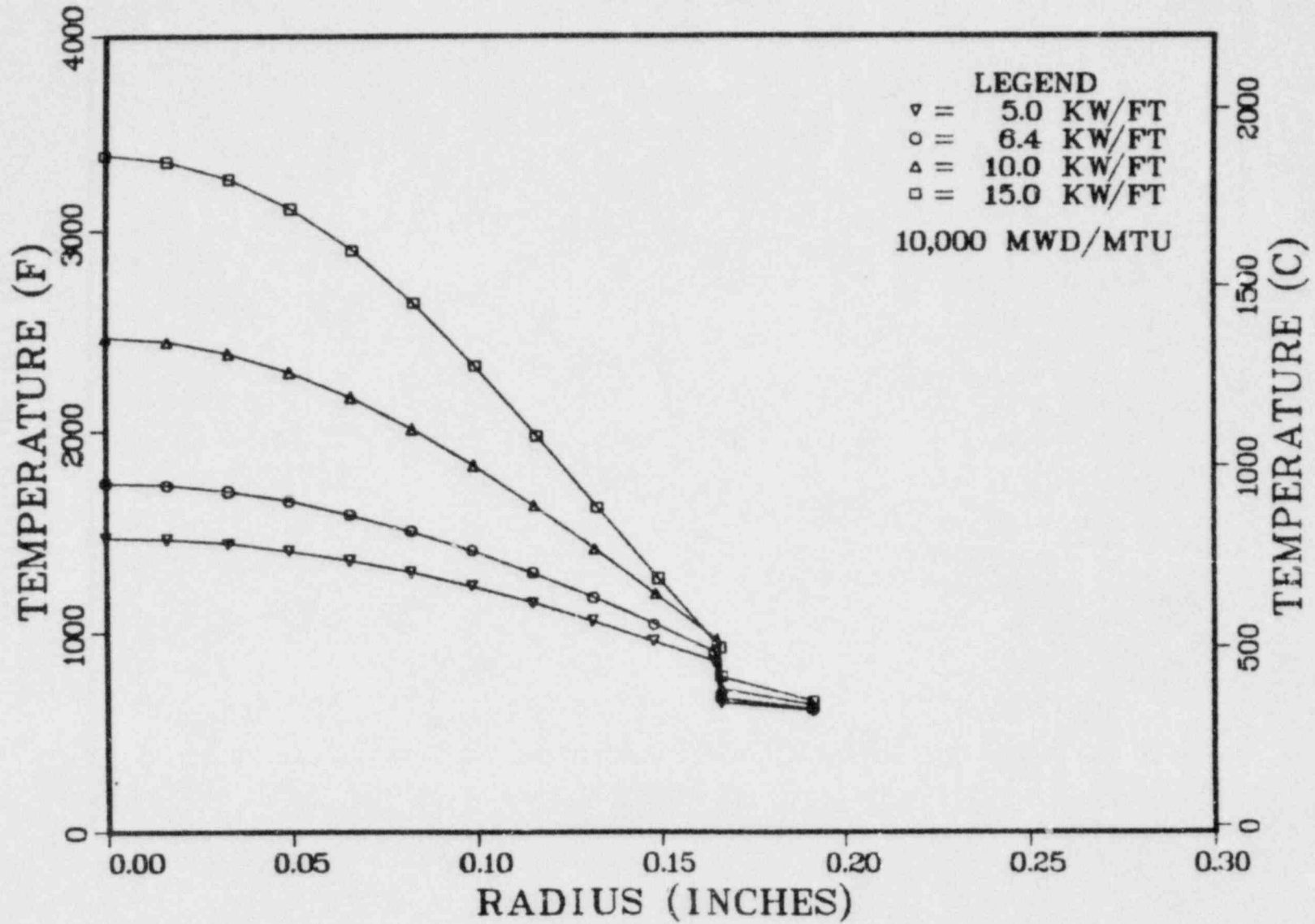




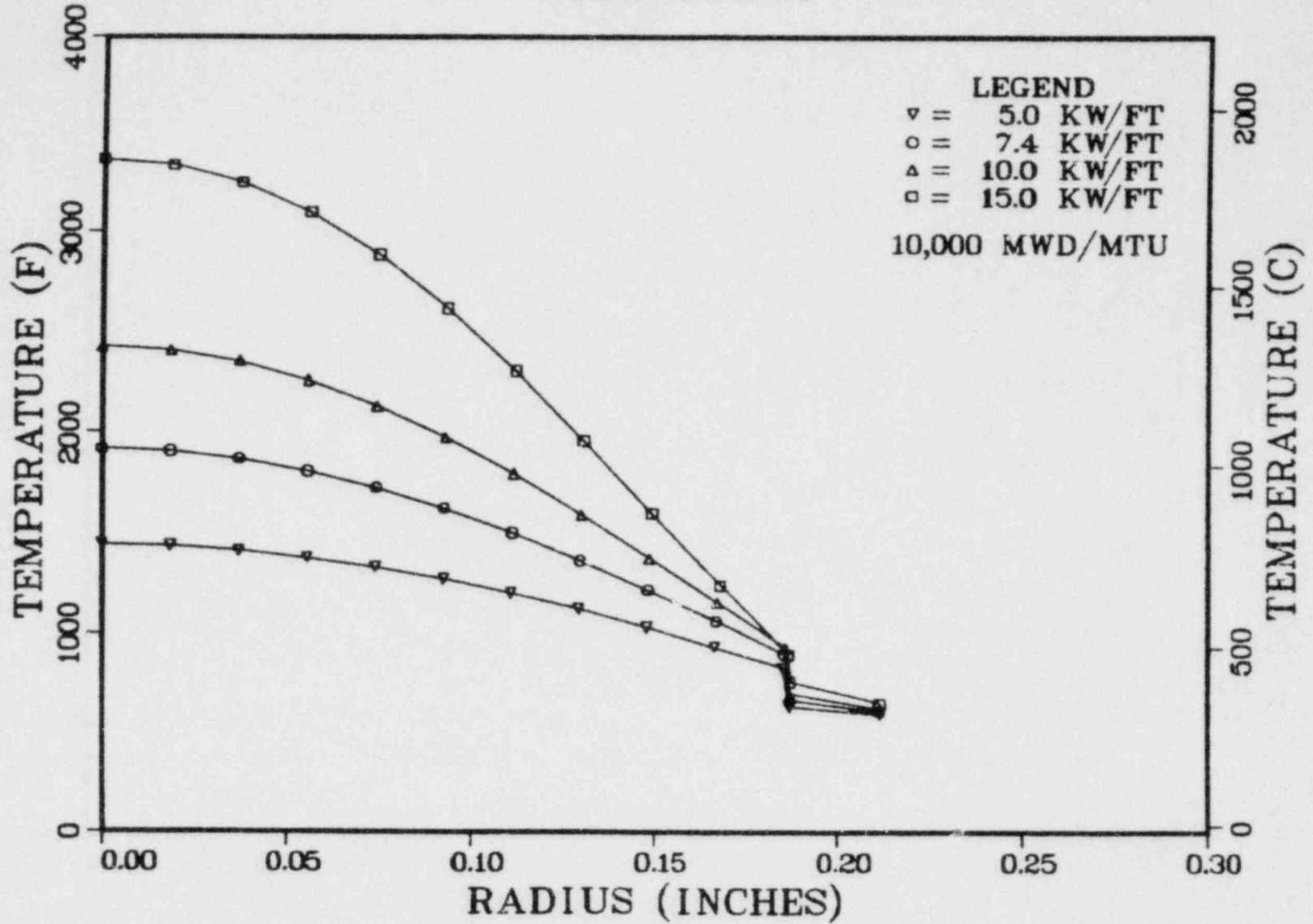
# C-E 14X14



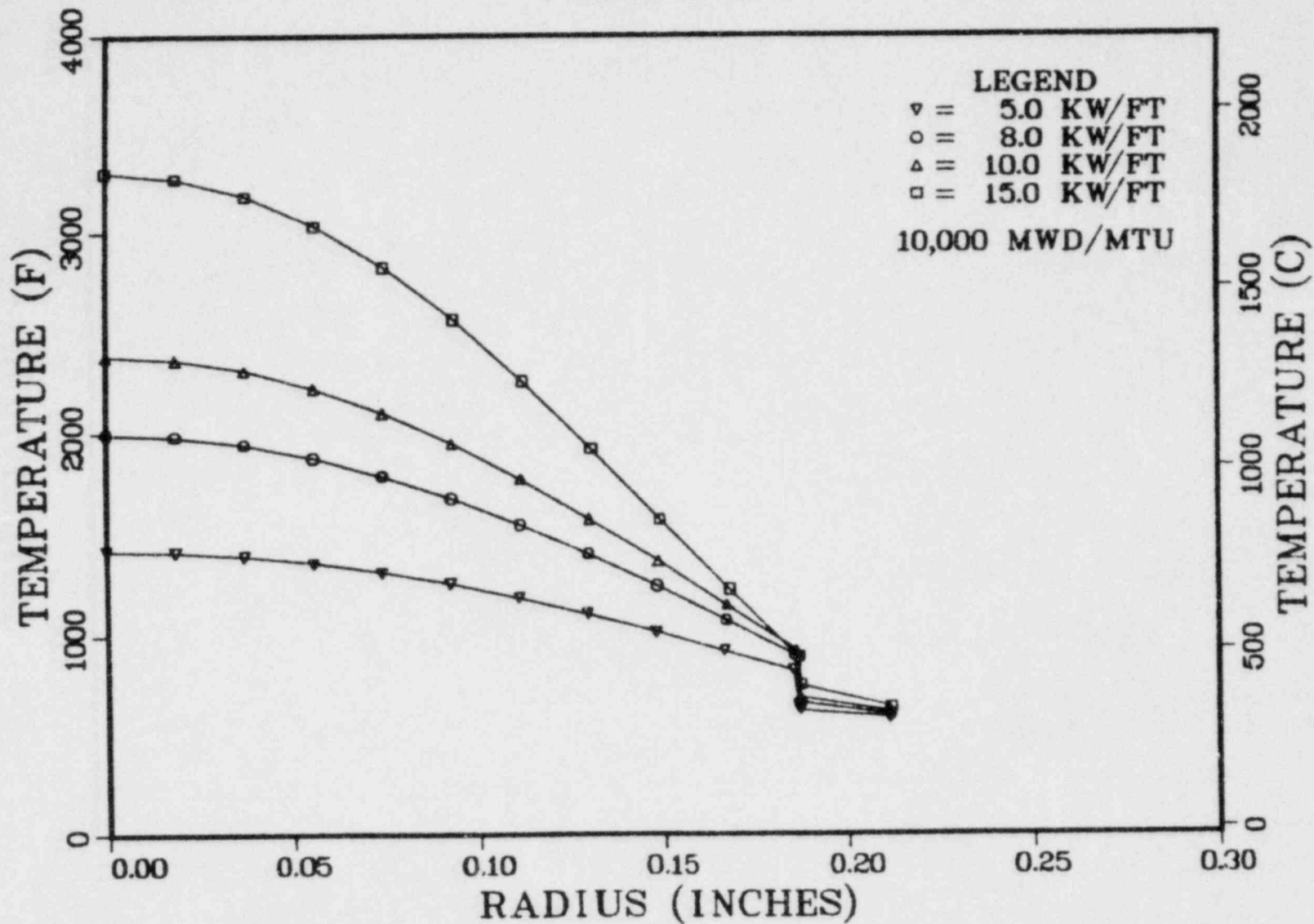
# C-E 16X16



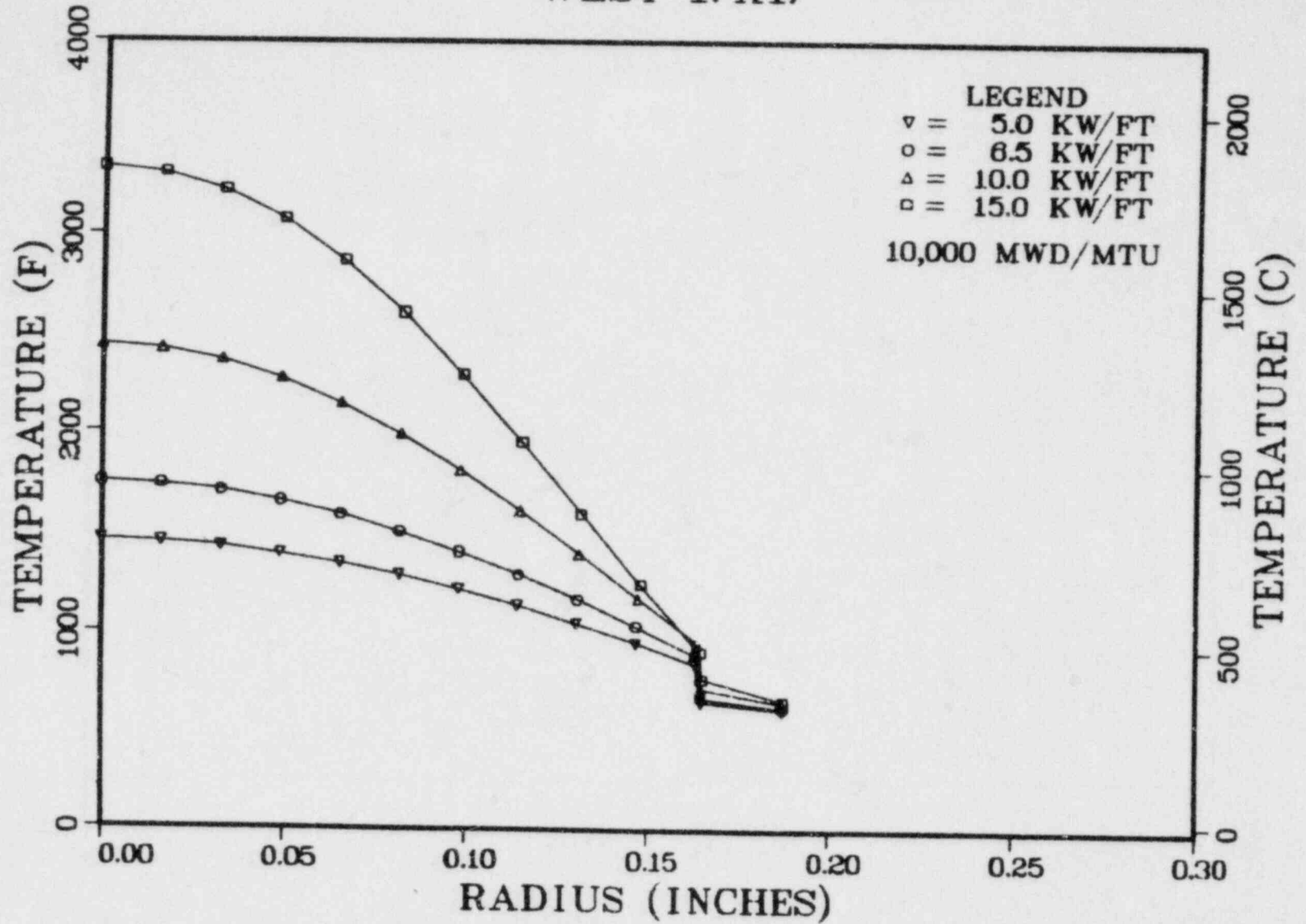
# WEST 14 X14



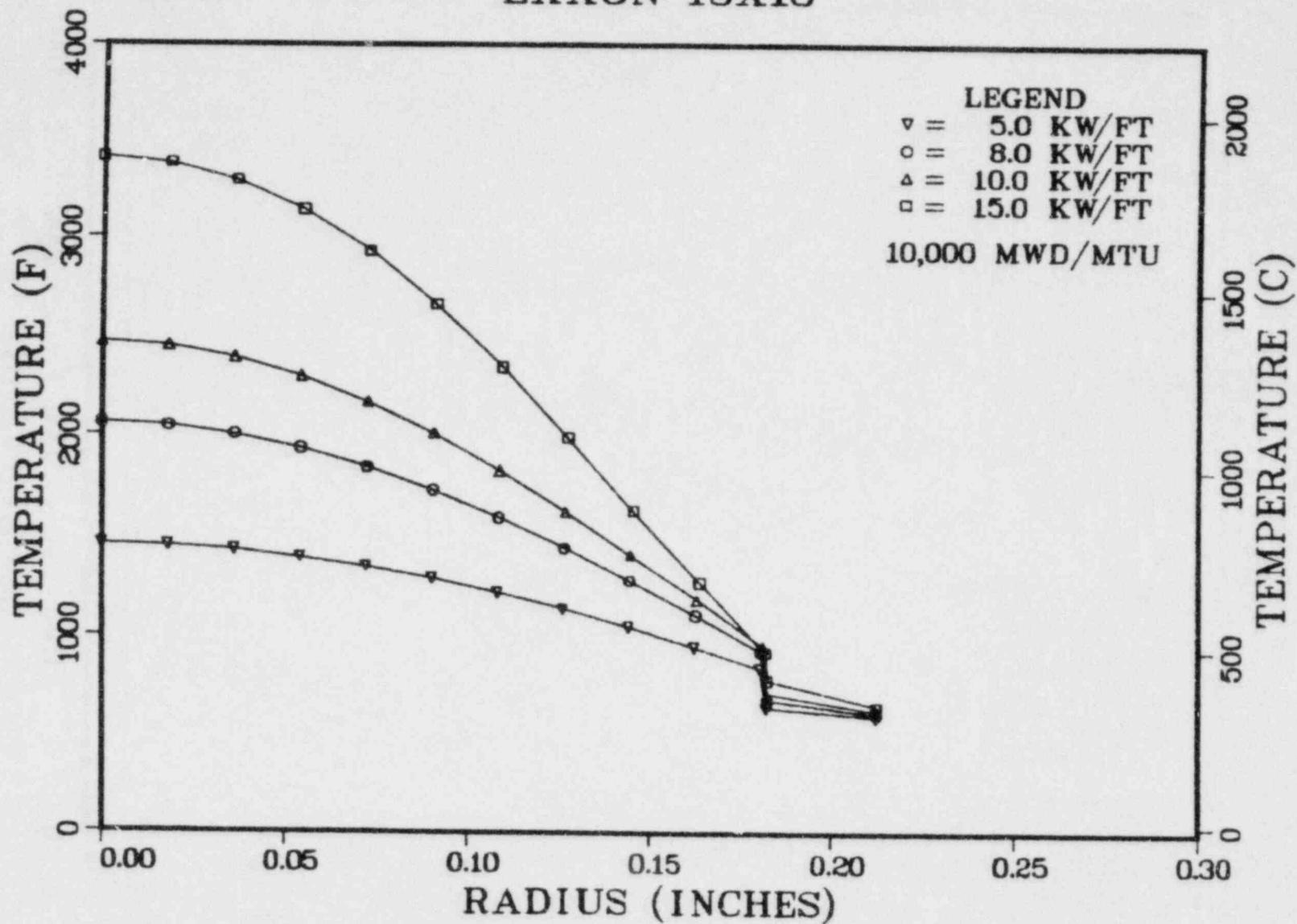
# WEST 15X15



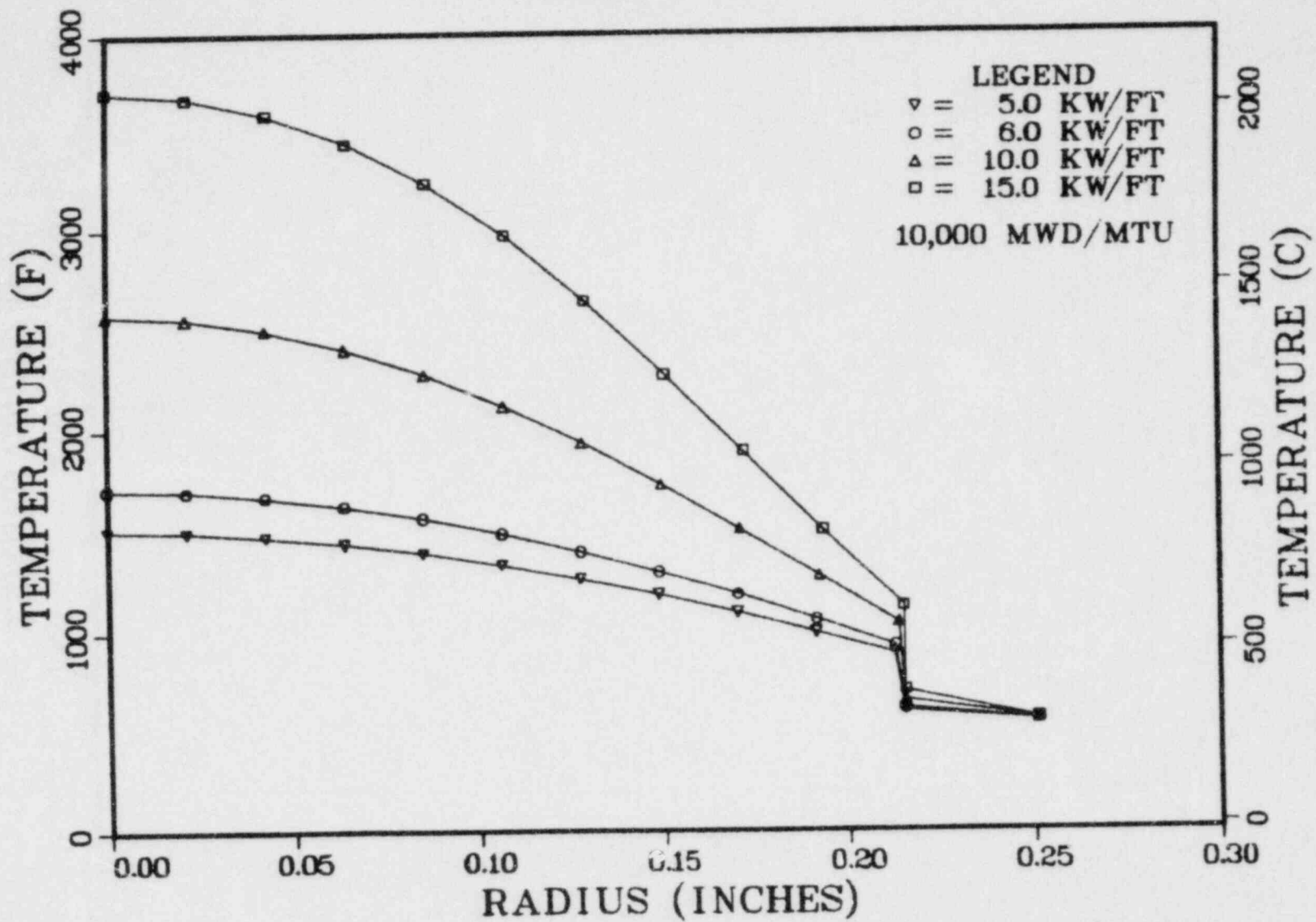
# WEST 17X17



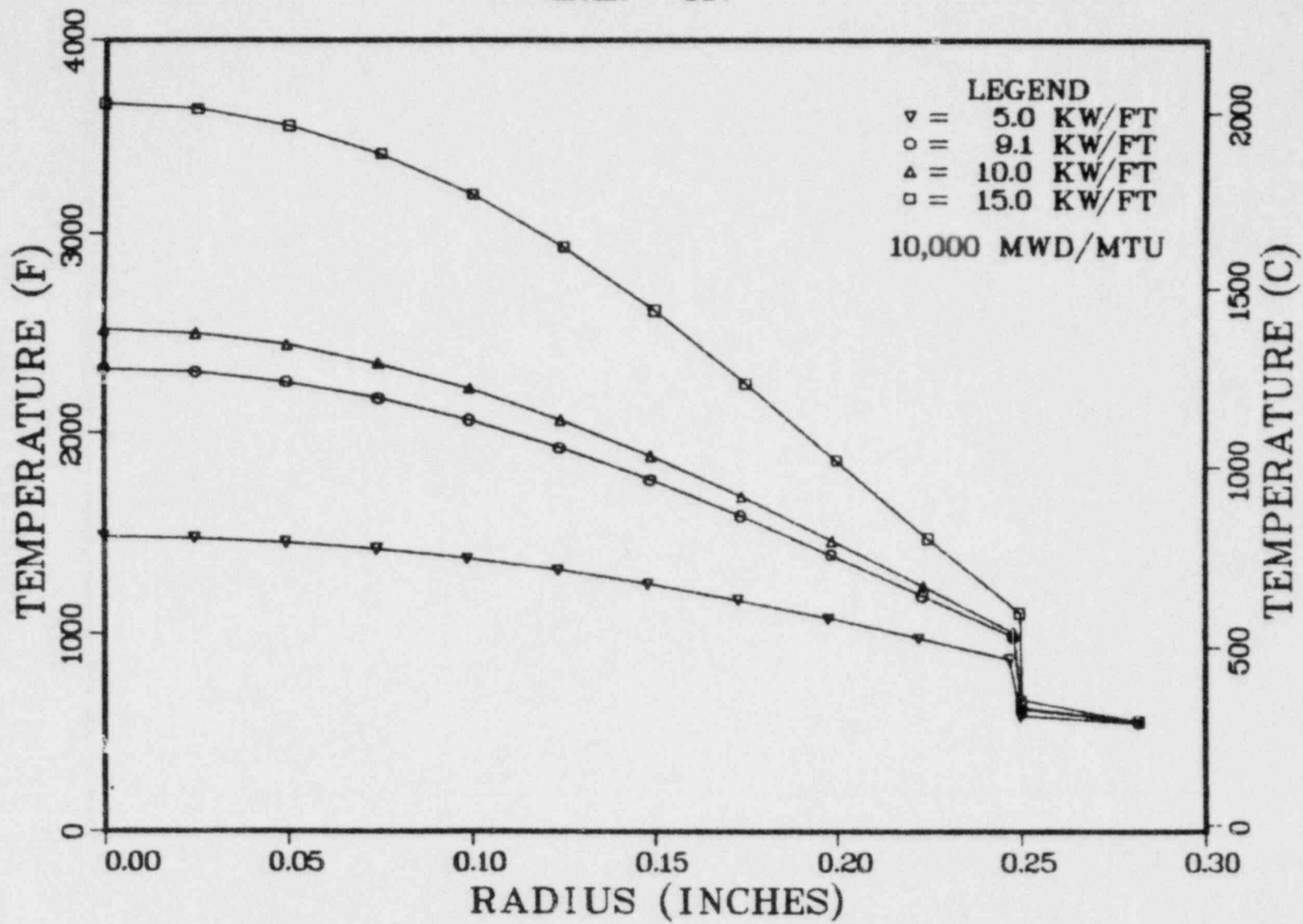
# EXXON 15X15



# EXXON 8X8

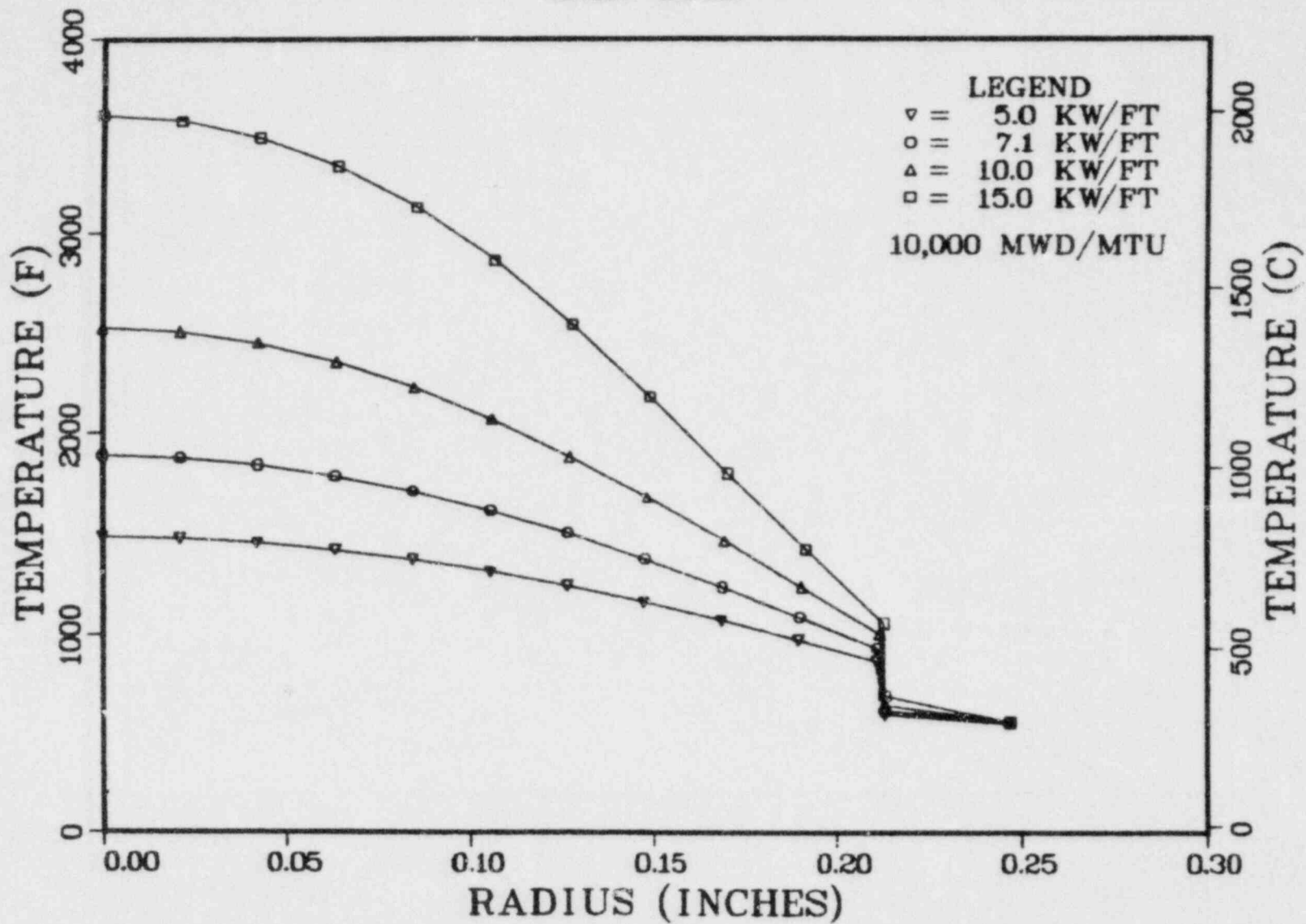


# G.E. 7X7

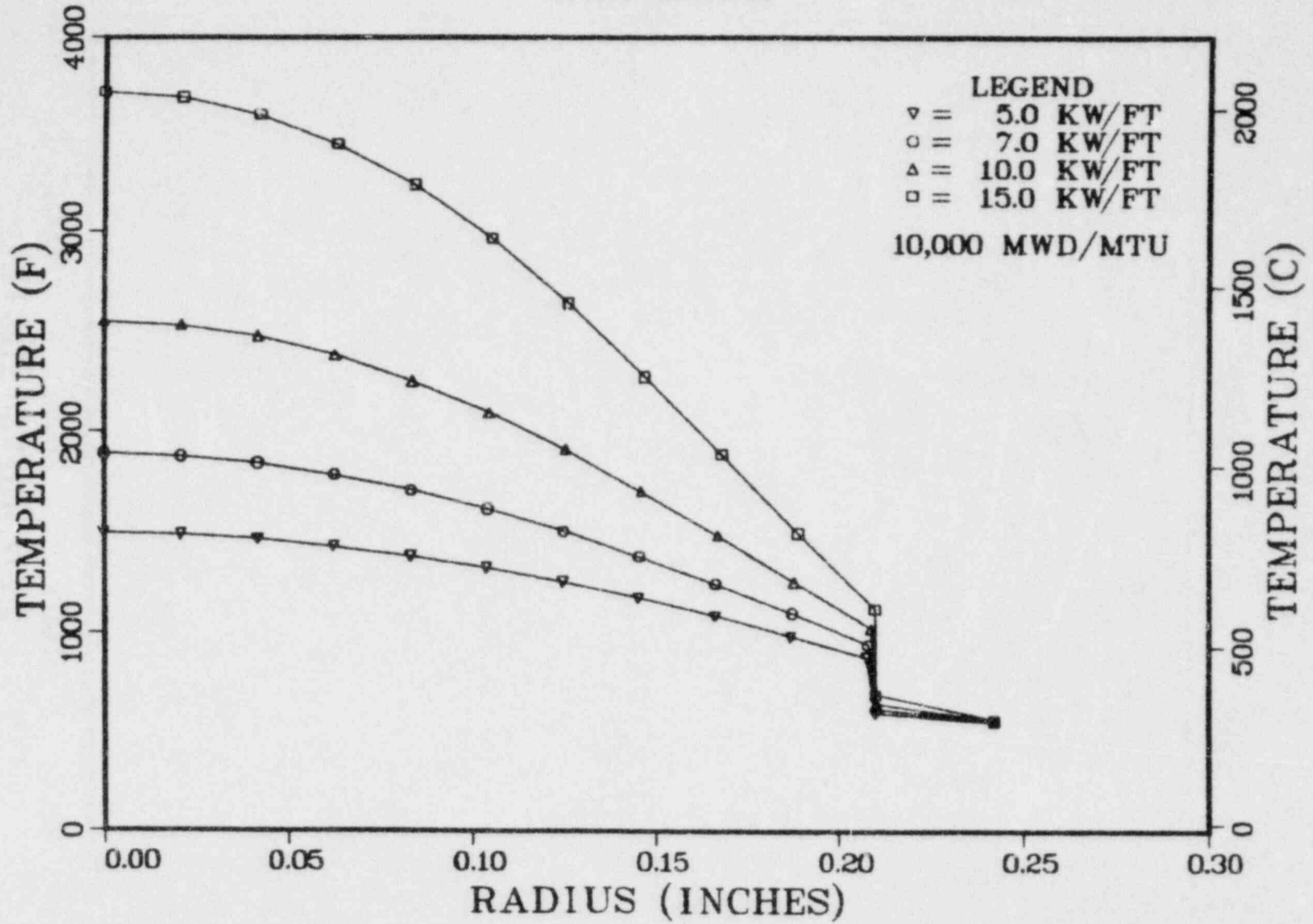


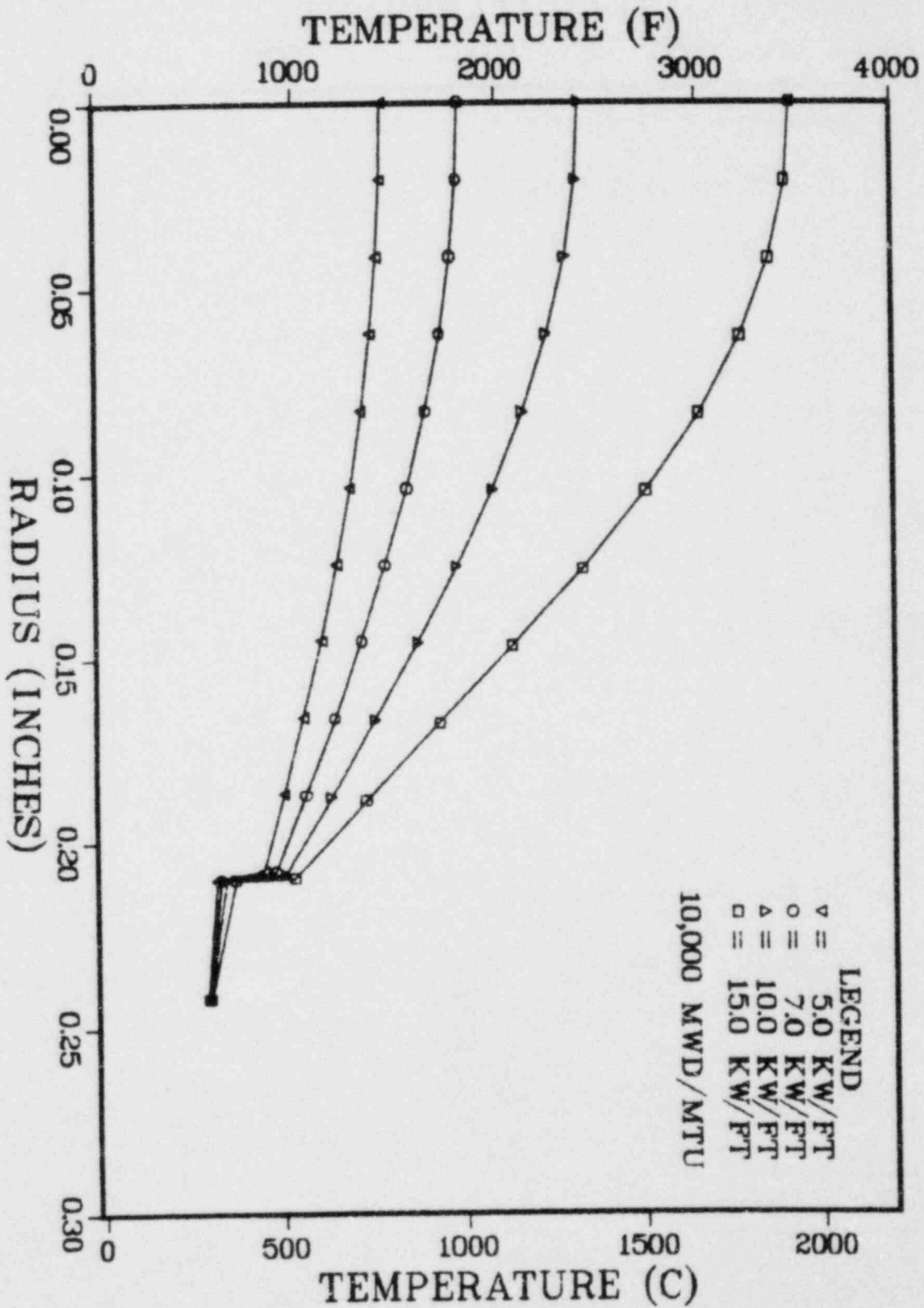


# G.E. 8X8

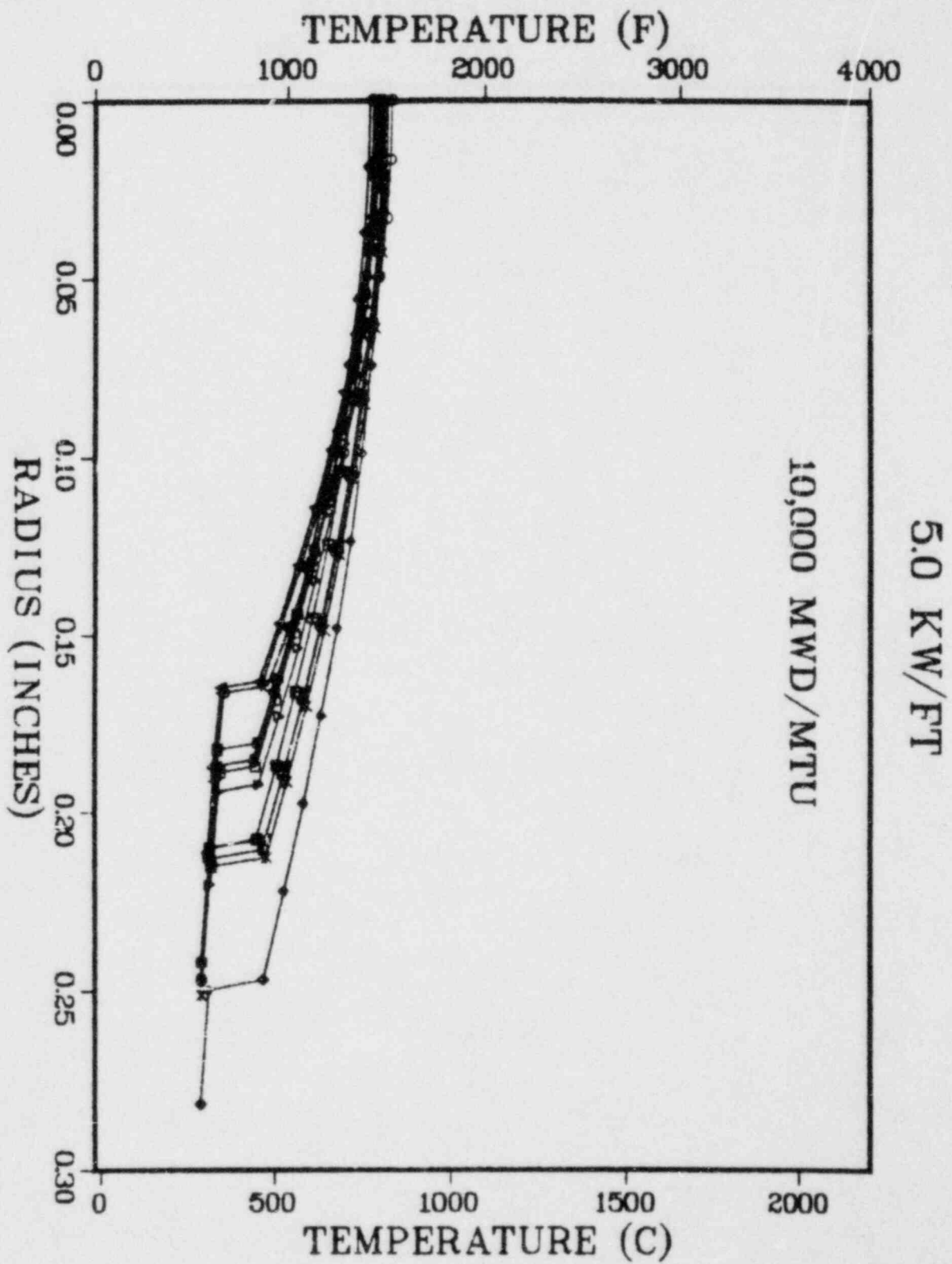


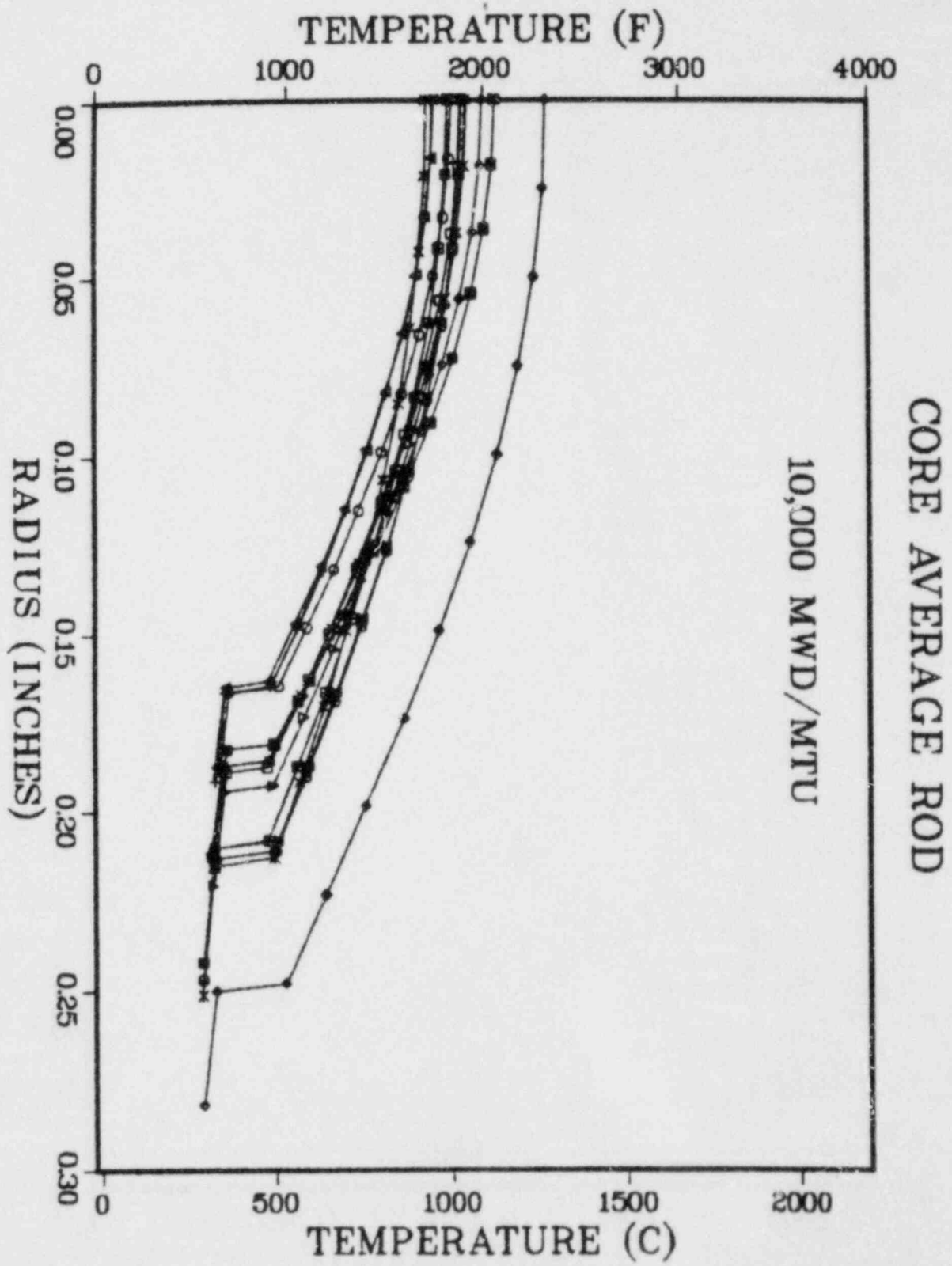
# G.E. 8X8R

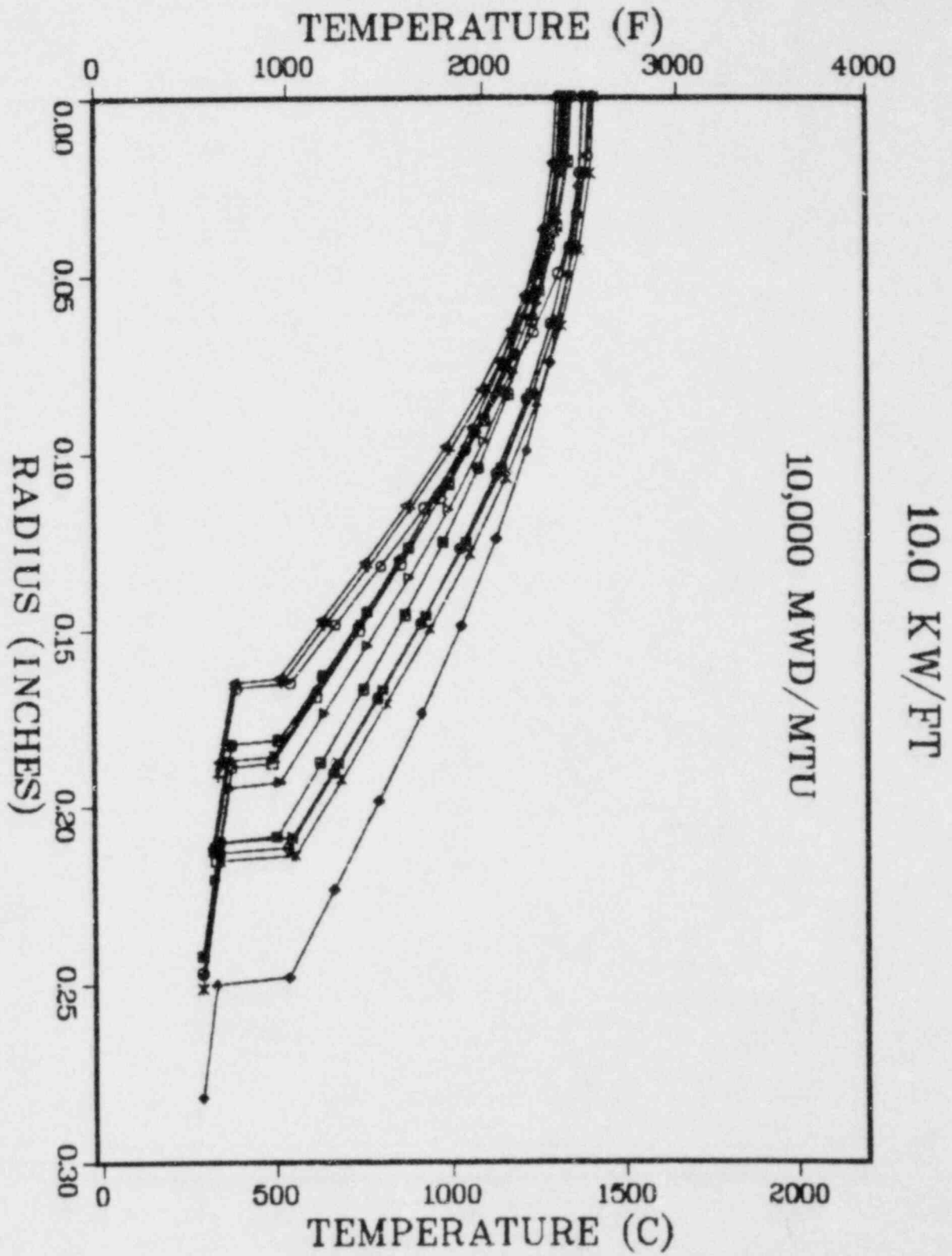




G.E. 8X8R-P

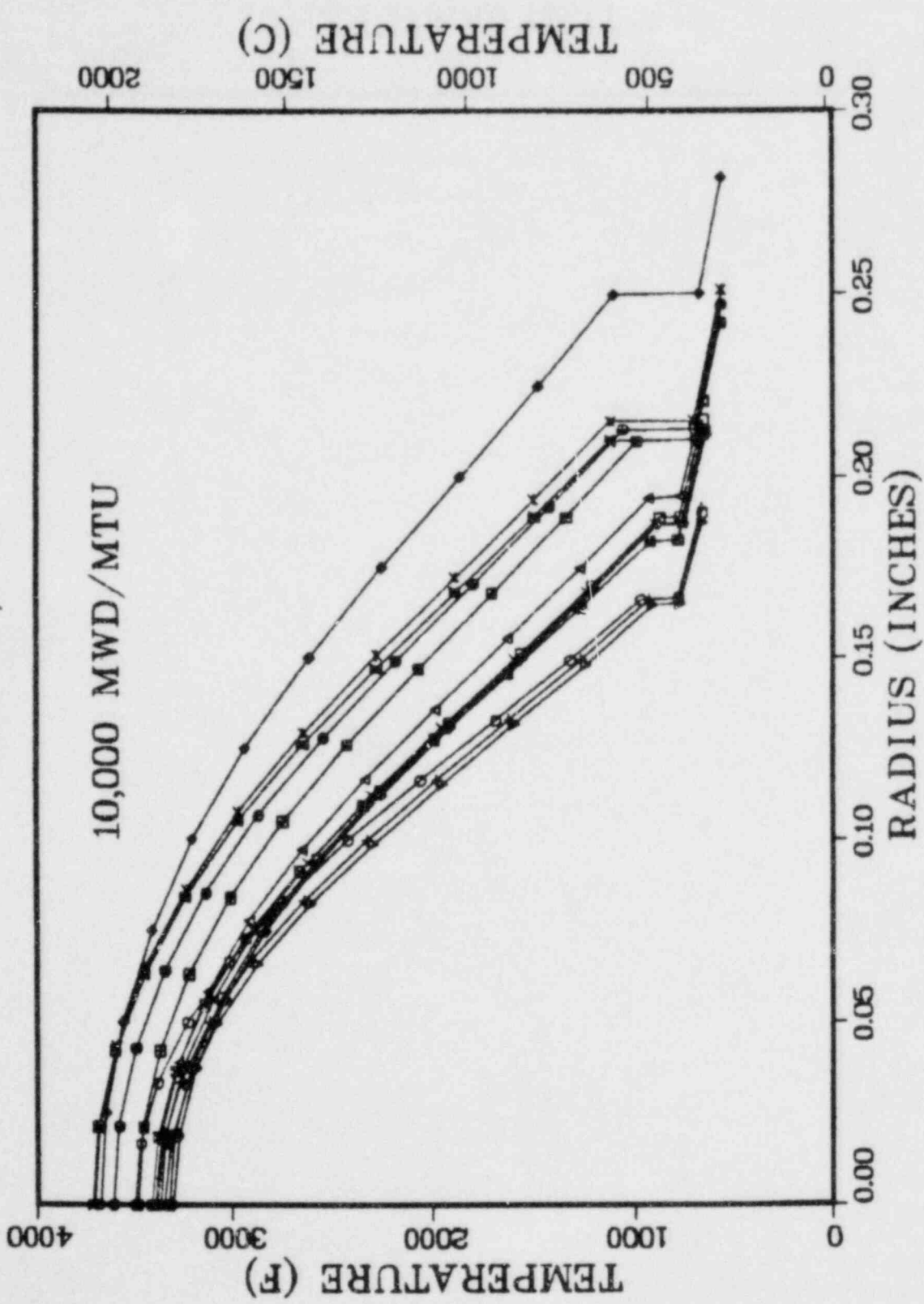






15.0 KW/FT

10,000 MWD/MTU



## APPENDIX F

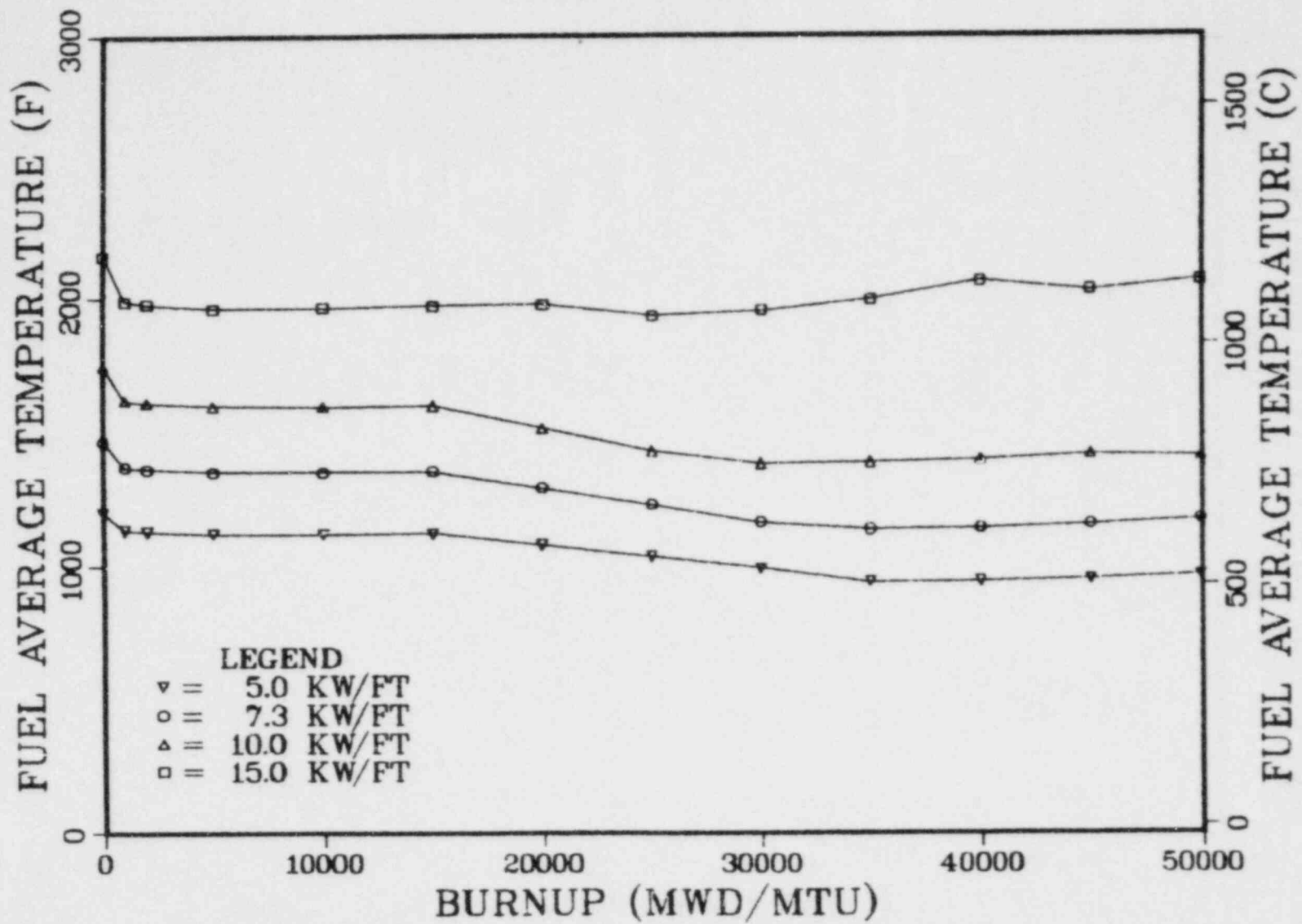
### FUEL AVERAGE TEMPERATURE

The following graphs are of fuel volume-averaged temperature vs. burnup, and the data are given for the peak axial node at specified peak burnups. In general, the peak volume-averaged temperature occurs at beginning of life or soon thereafter for PWR's, while the peak volume-averaged temperature occurs at midlife or late in life for BWR's. There are a few exceptions with the BWR's, for example at low power, where peak volume-averaged temperatures are also attained at beginning of life.

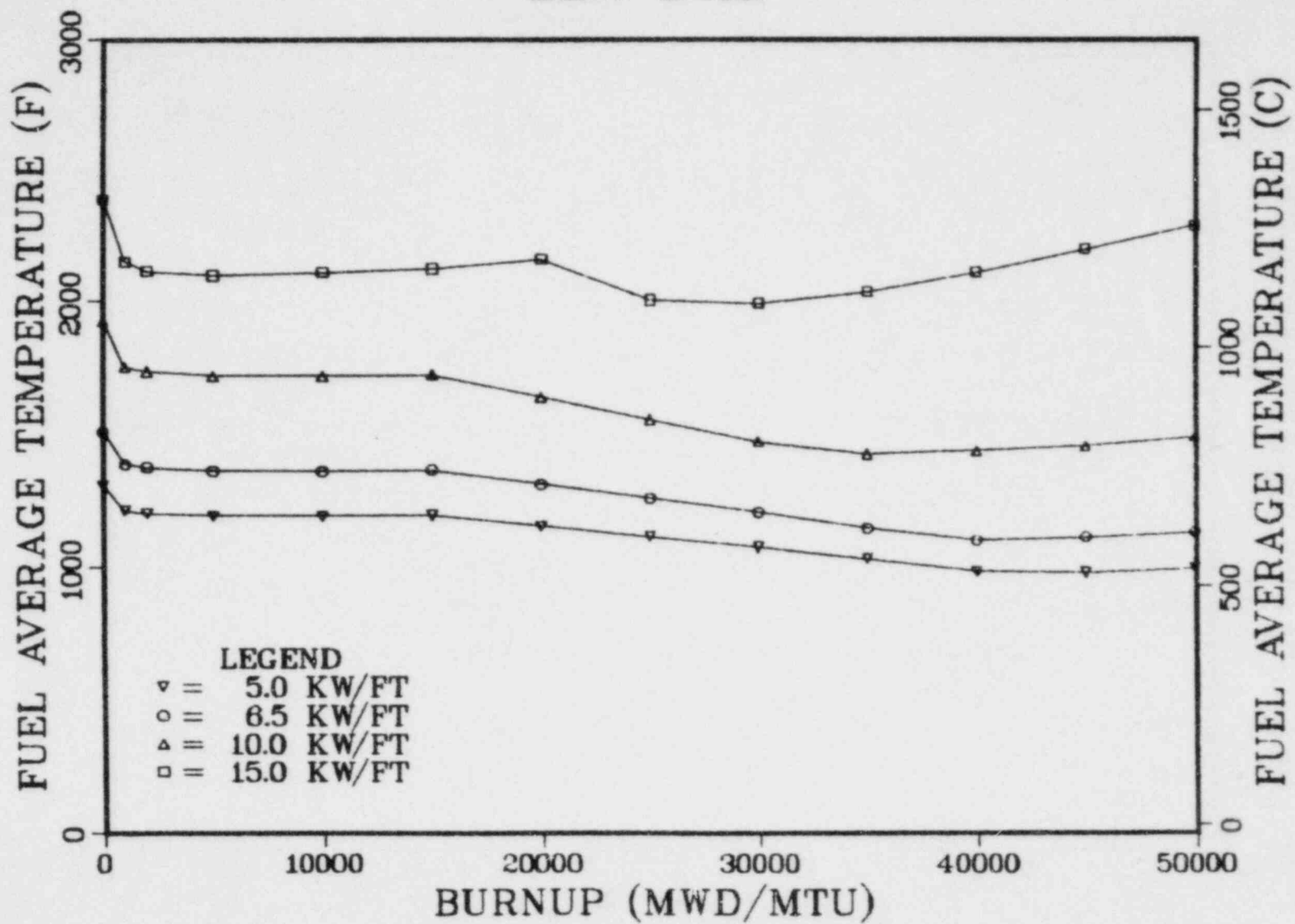
The multi-design plots reveal some additional results of interest. For power levels between 5 and 10 kW/ft, there is little difference between the values for each of the 13 designs, but at 15 kW/ft, the BWR's demonstrate higher volume-averaged temperatures compared with the PWRs. The difference can be related to the values for gap conductivity at 15 kW/ft; these values are much lower for the unpressurized BWRs and result in higher fuel temperatures.



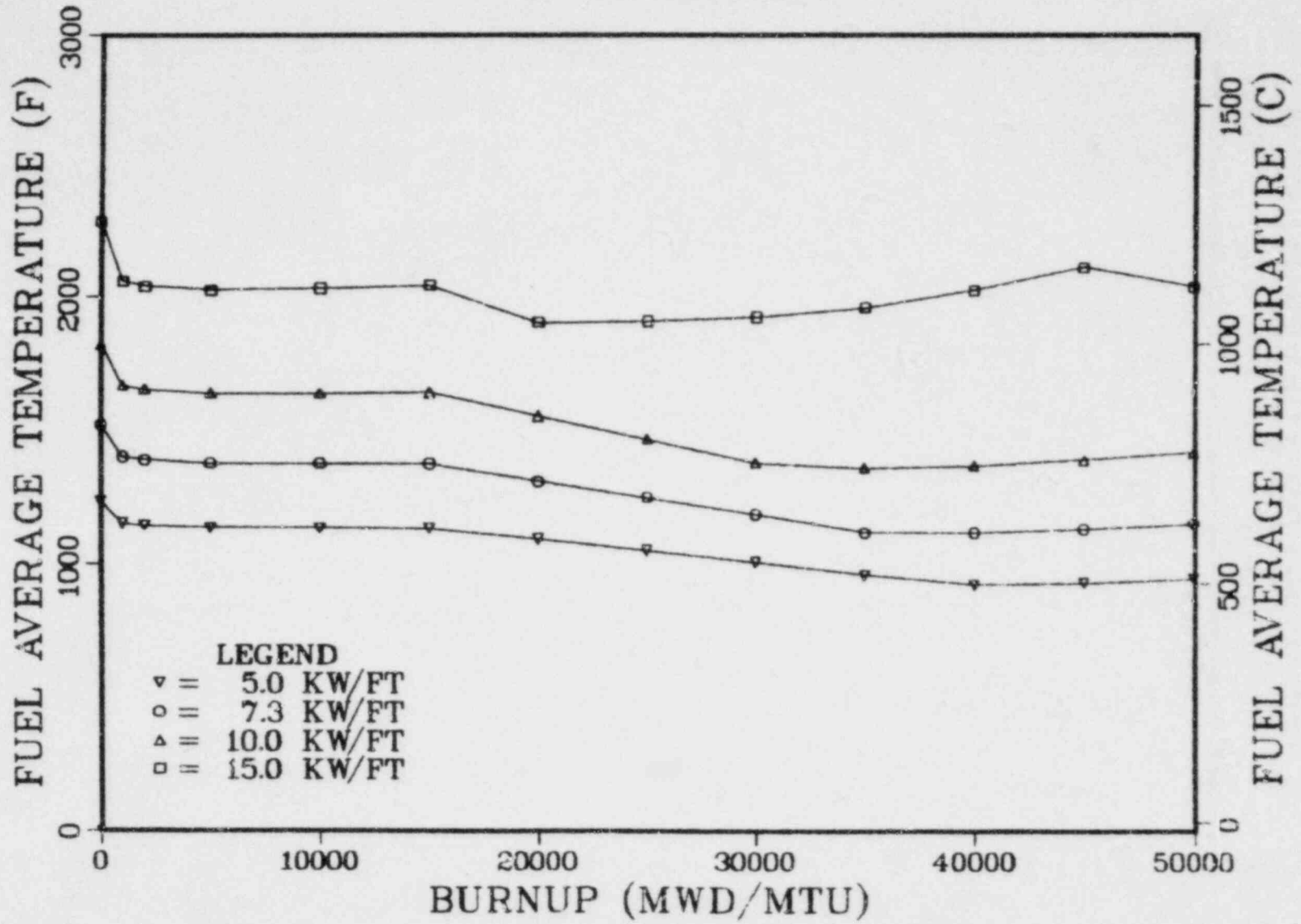
# B&W 15X15



# B&W 17X17



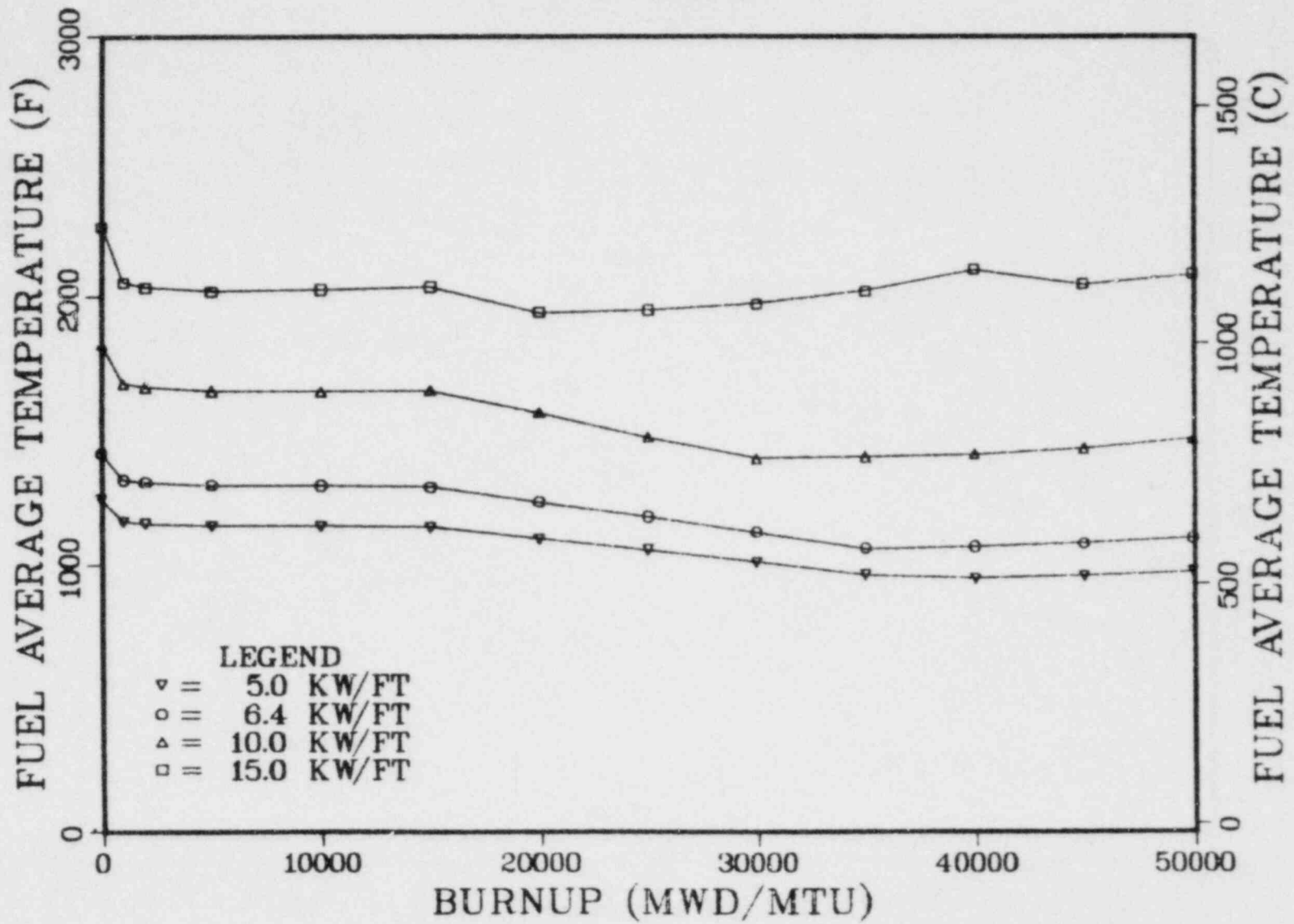
# C-E 14X14



F-4

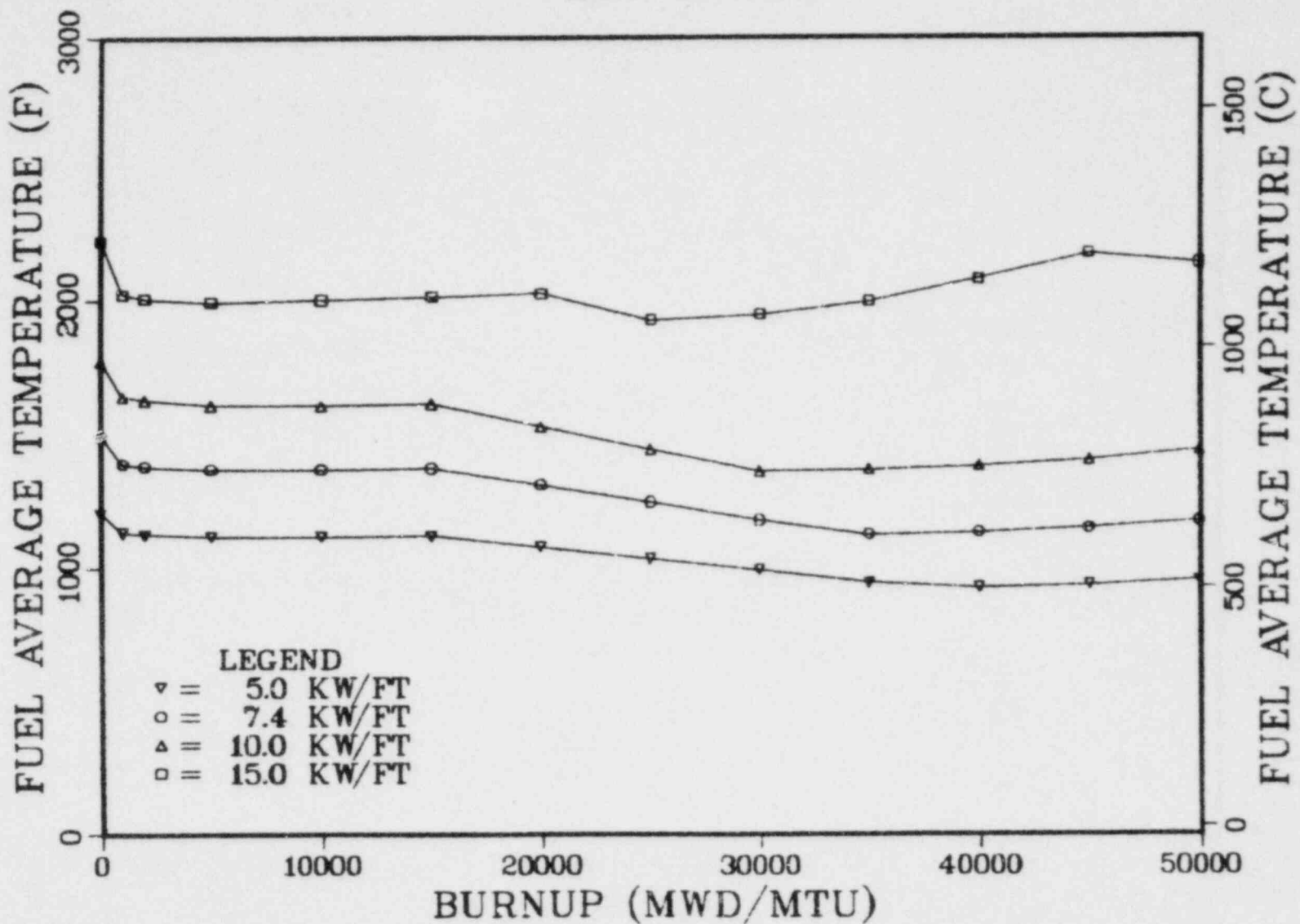
# C-E 16X16

F-5

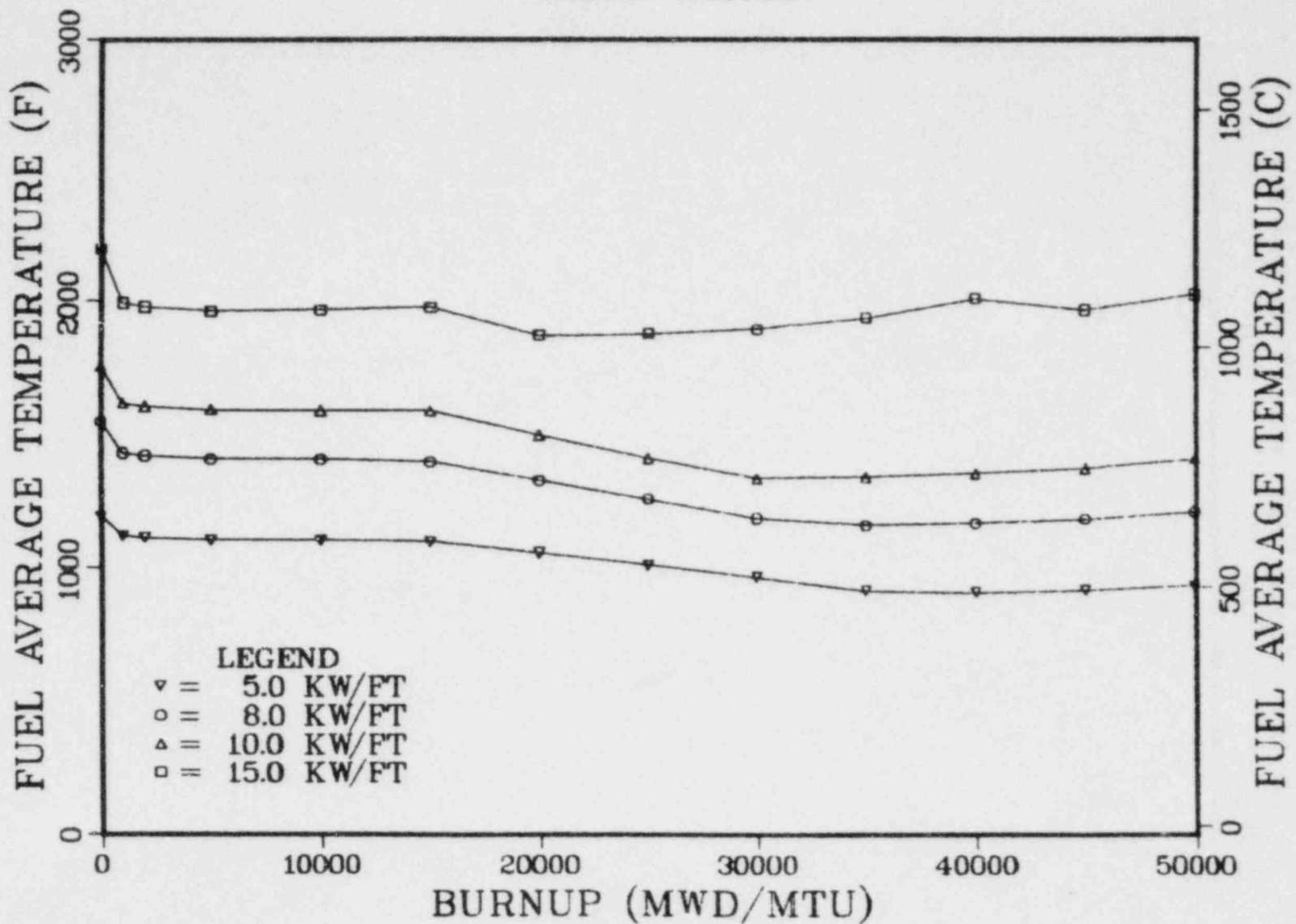


# WEST 14X14

F-6

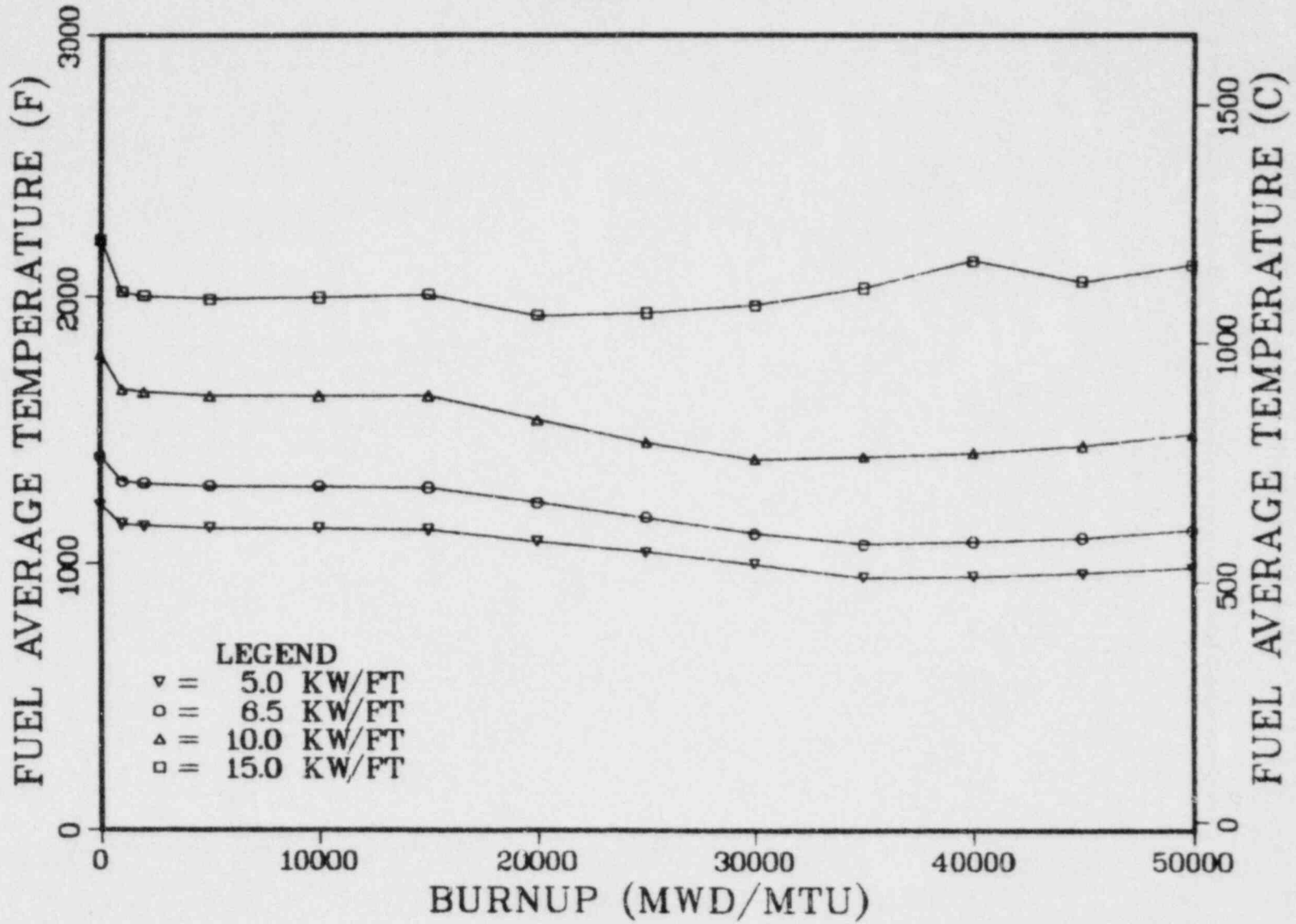


# WEST 15X15



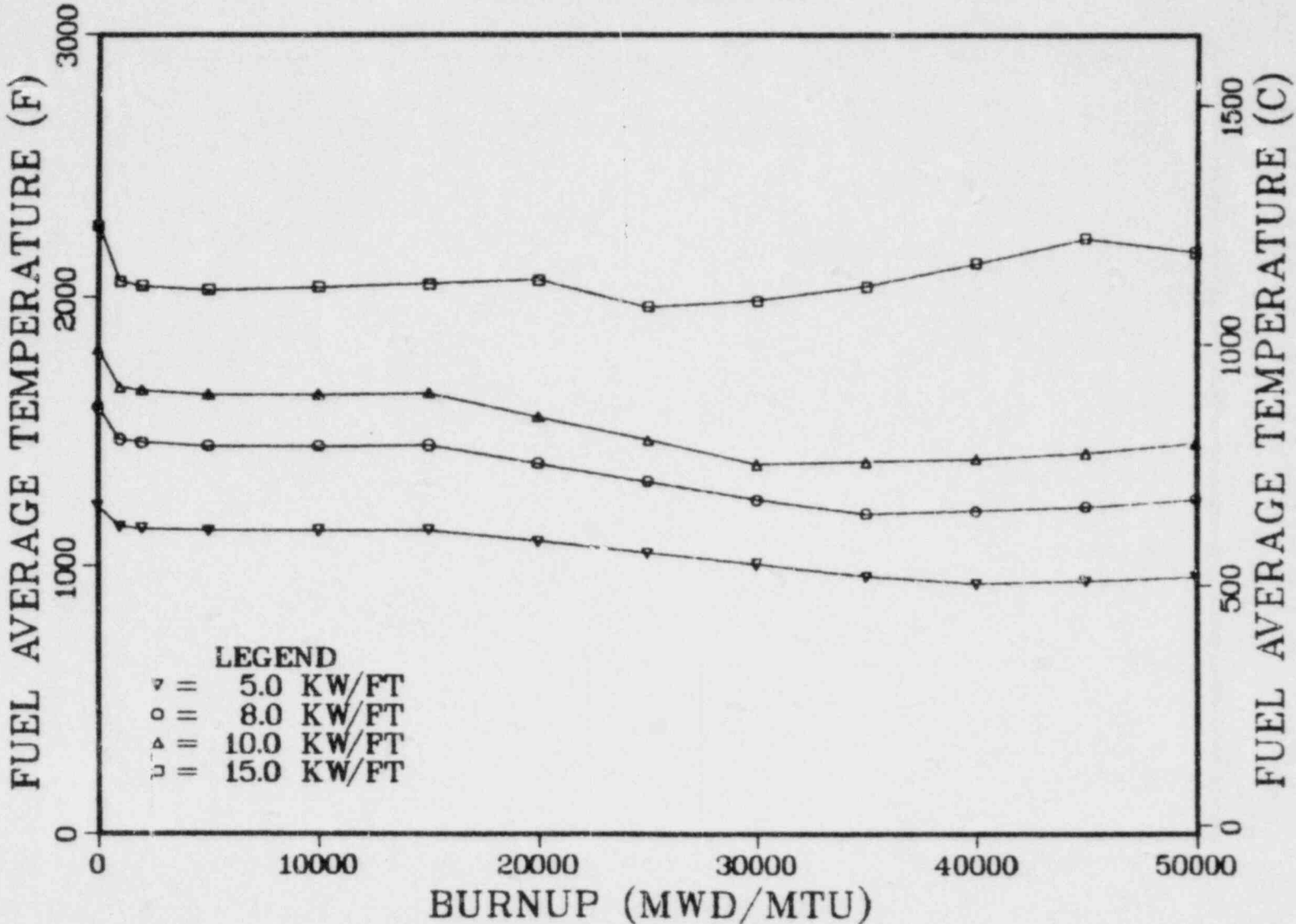
# WEST 17X17

F-8



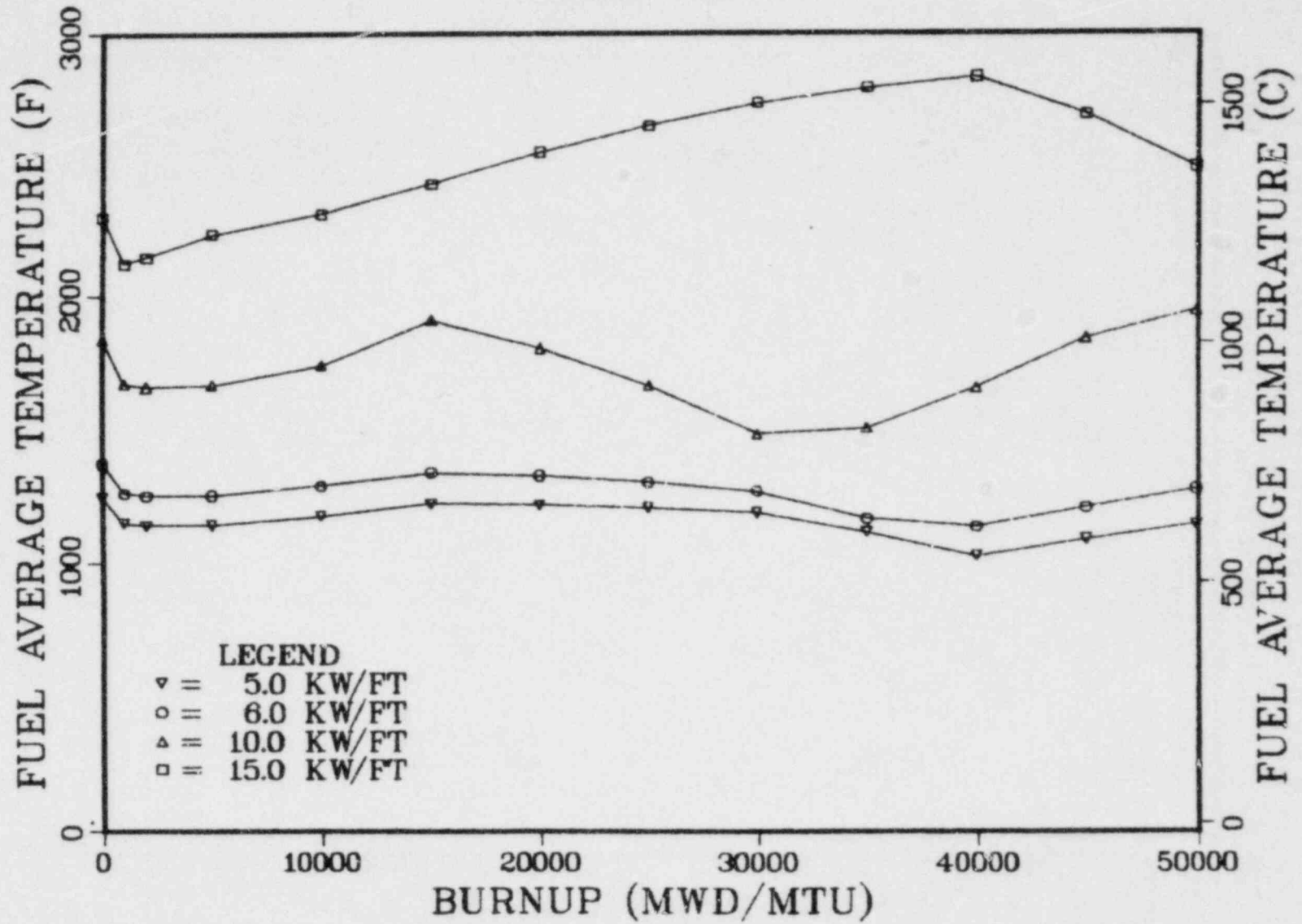
# EXXON 15X15

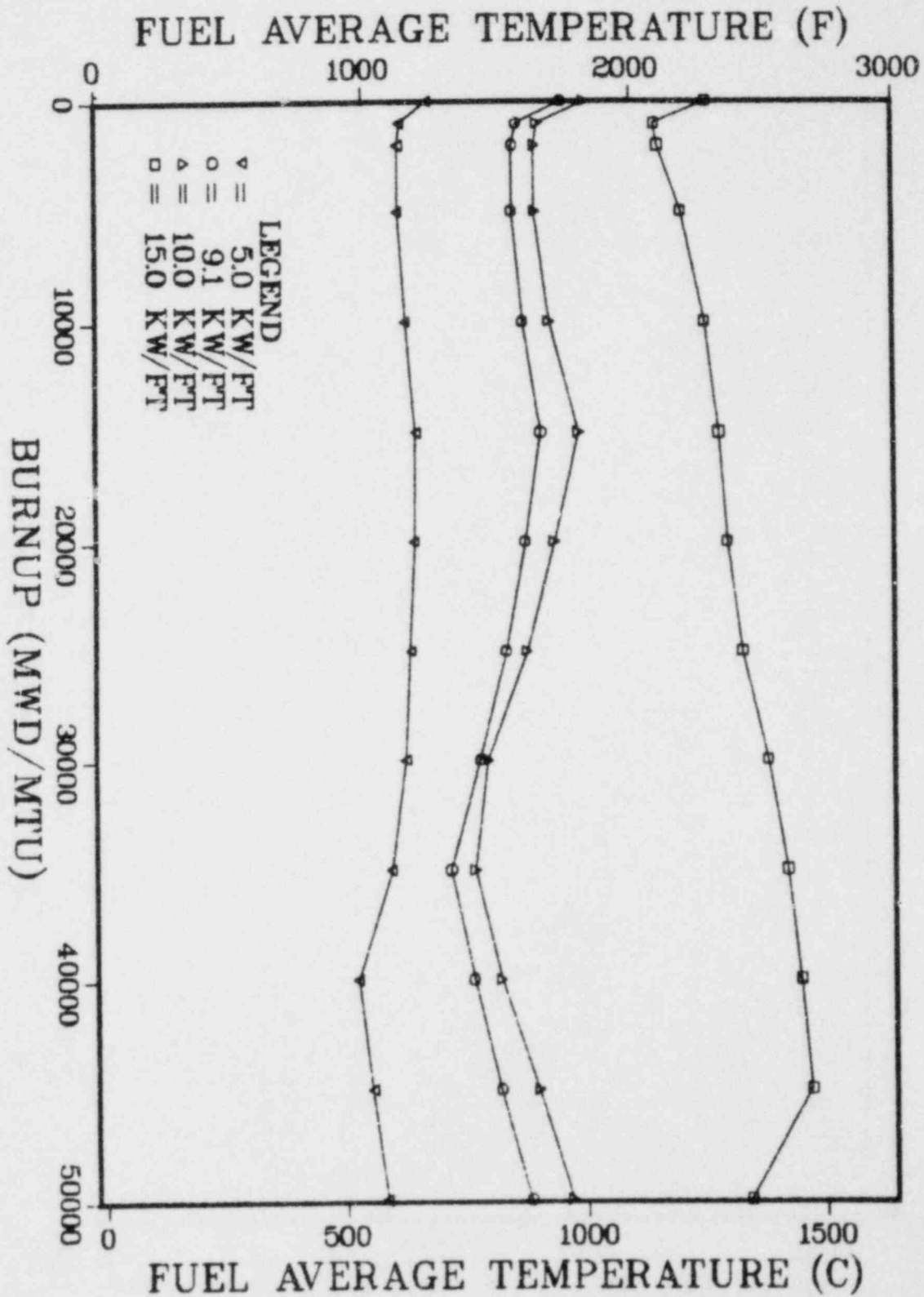
F-9





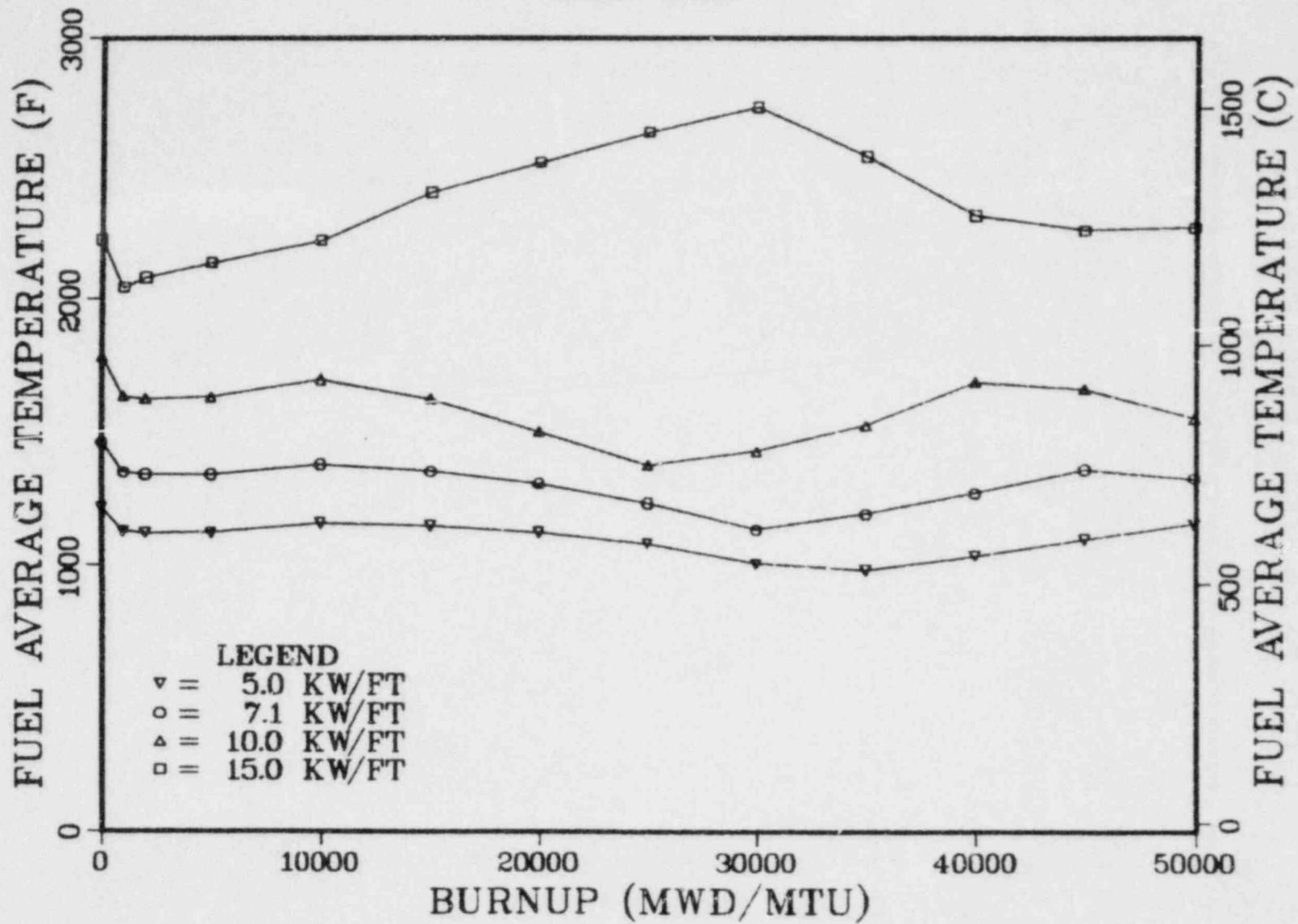
# EXXON 8X8



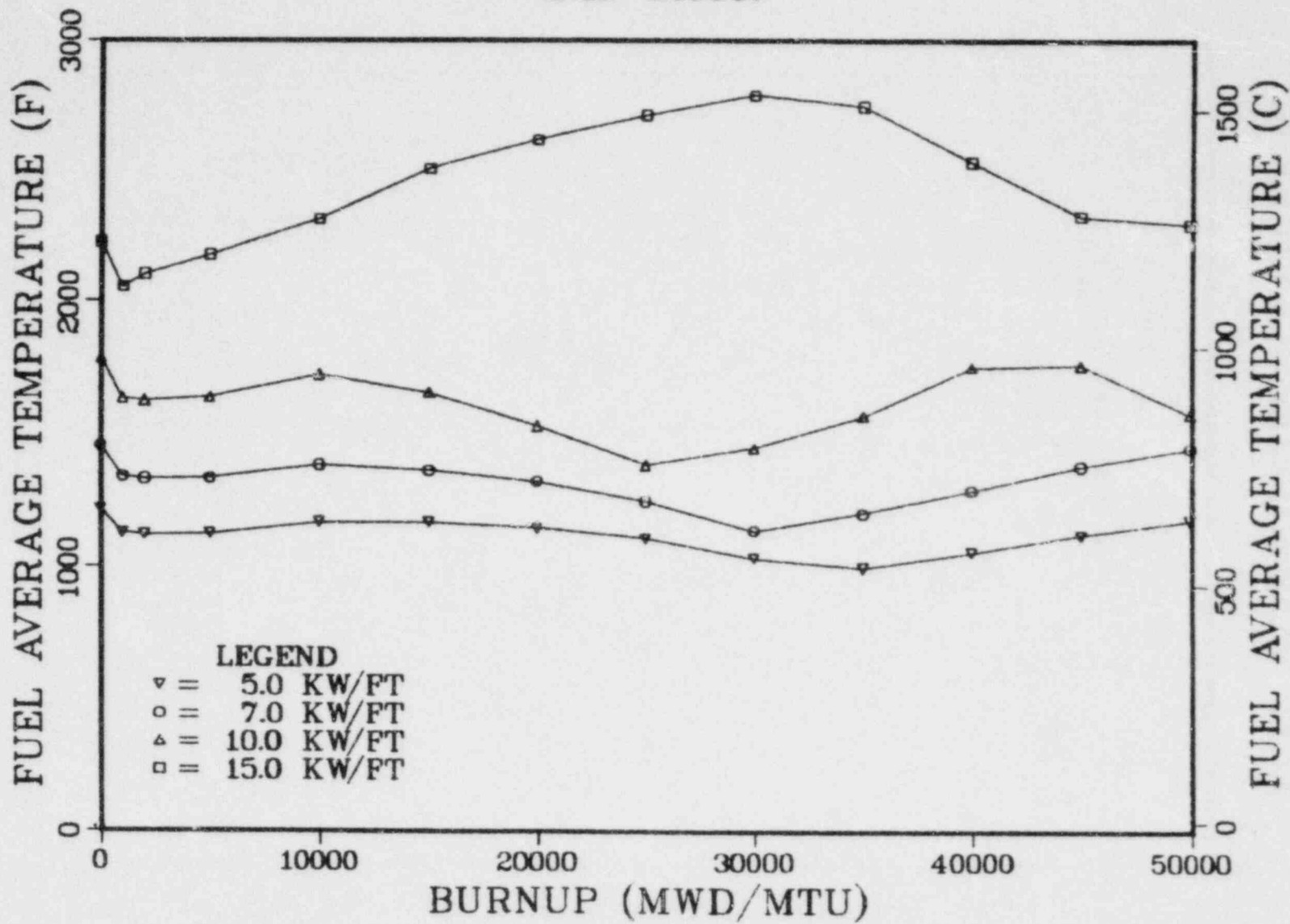


G.E. 7X7

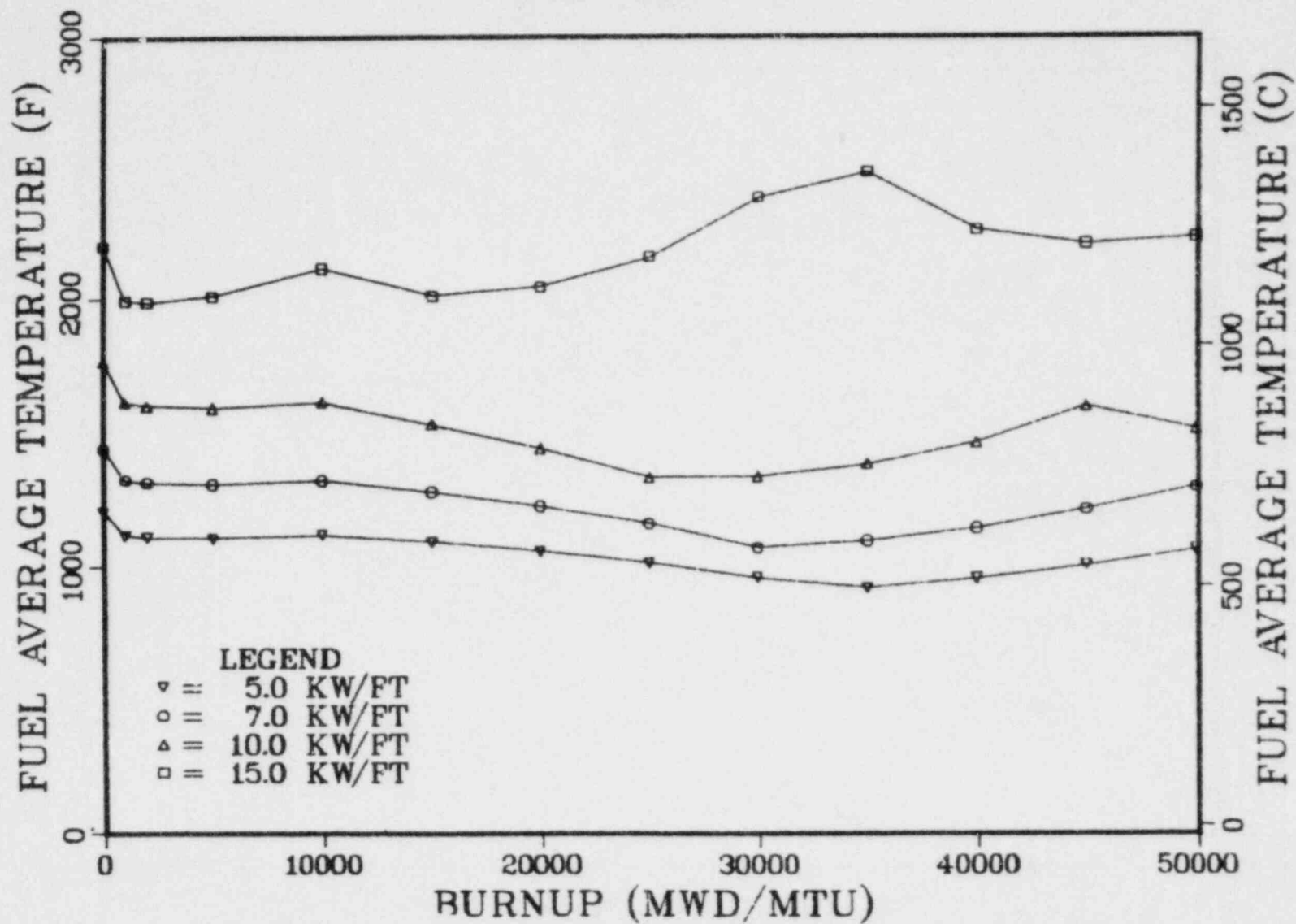
# G.E. 8X8

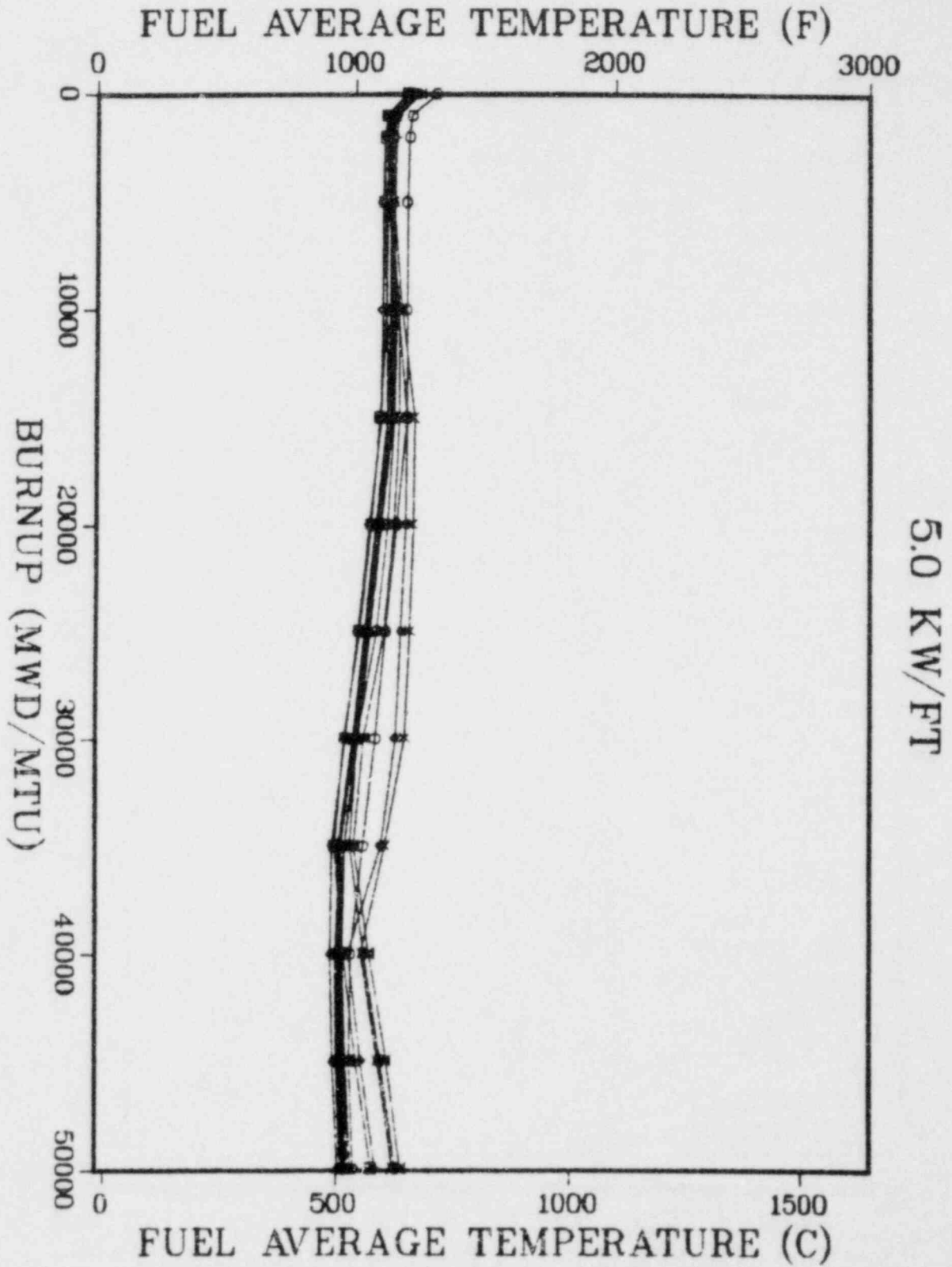


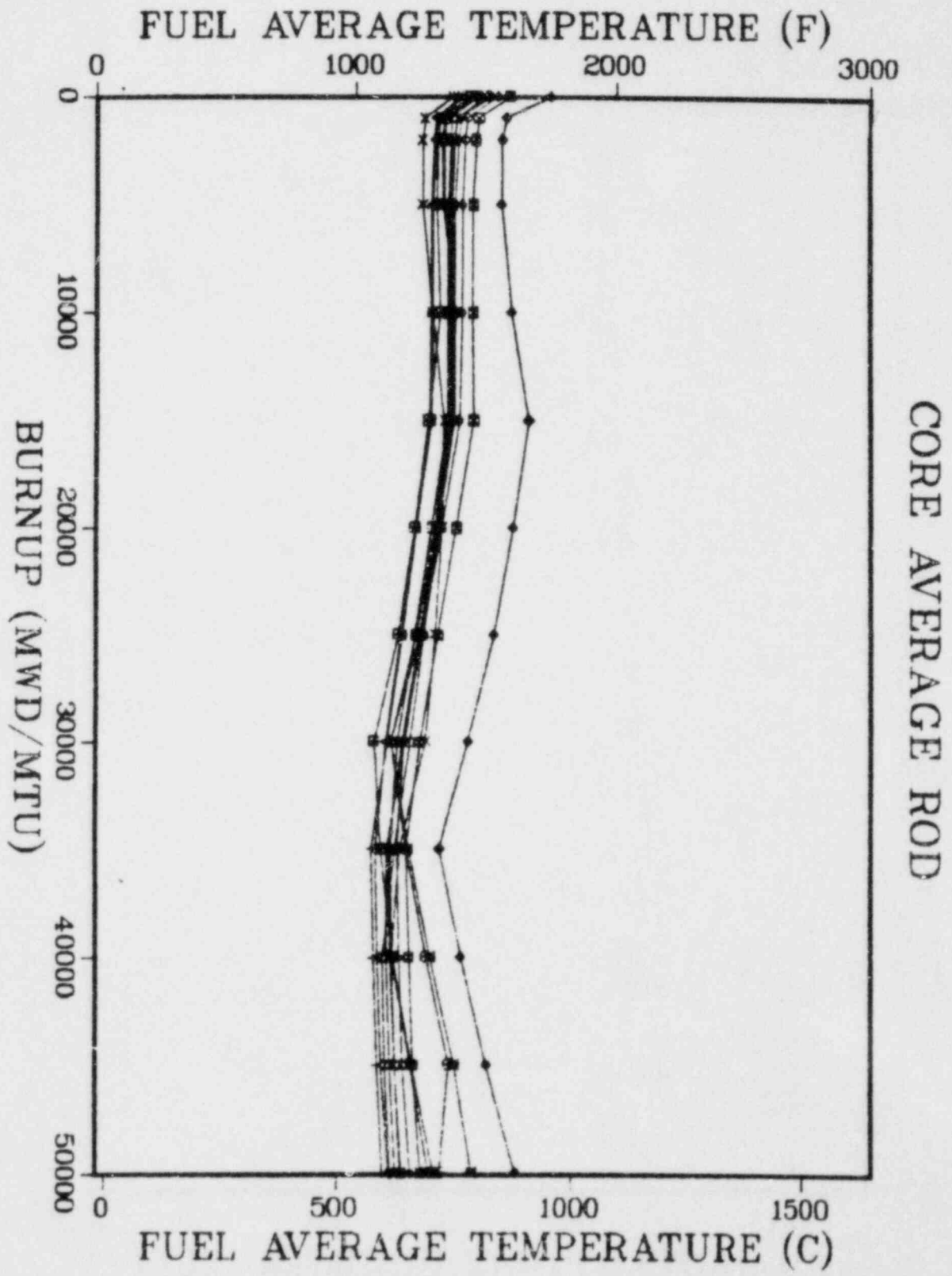
# G.E. 8X8R

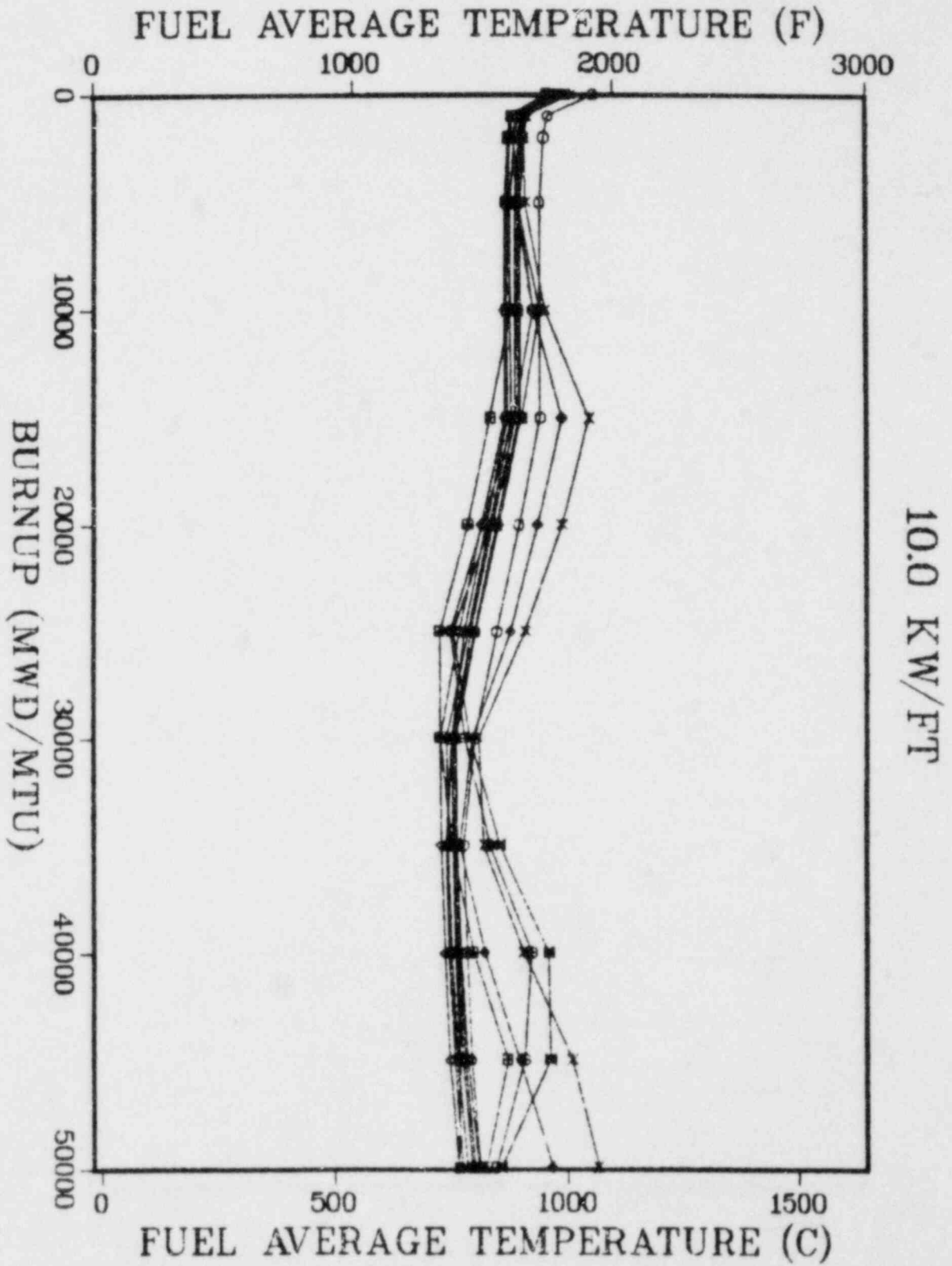


# G.E. 8X8R-P

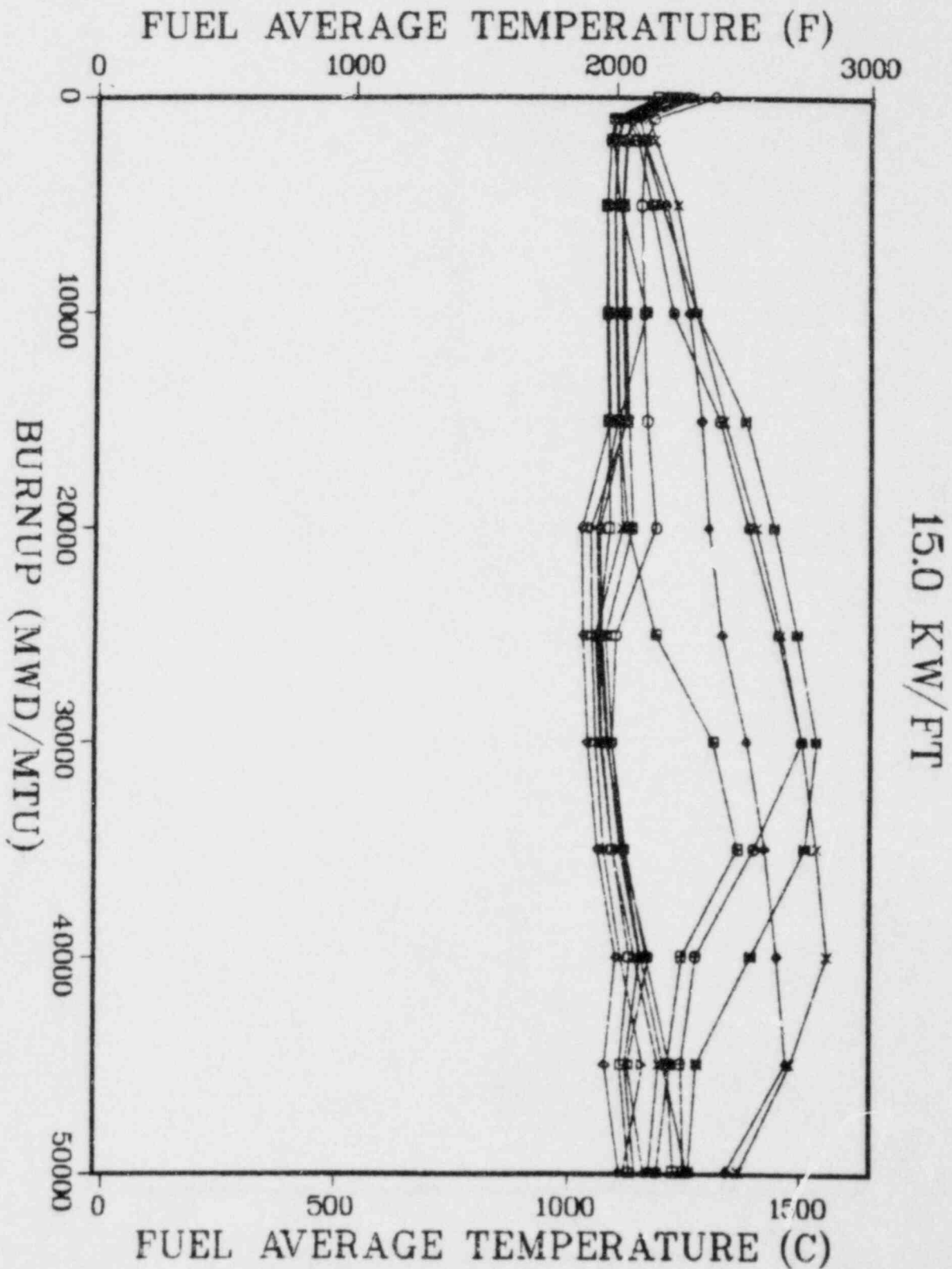










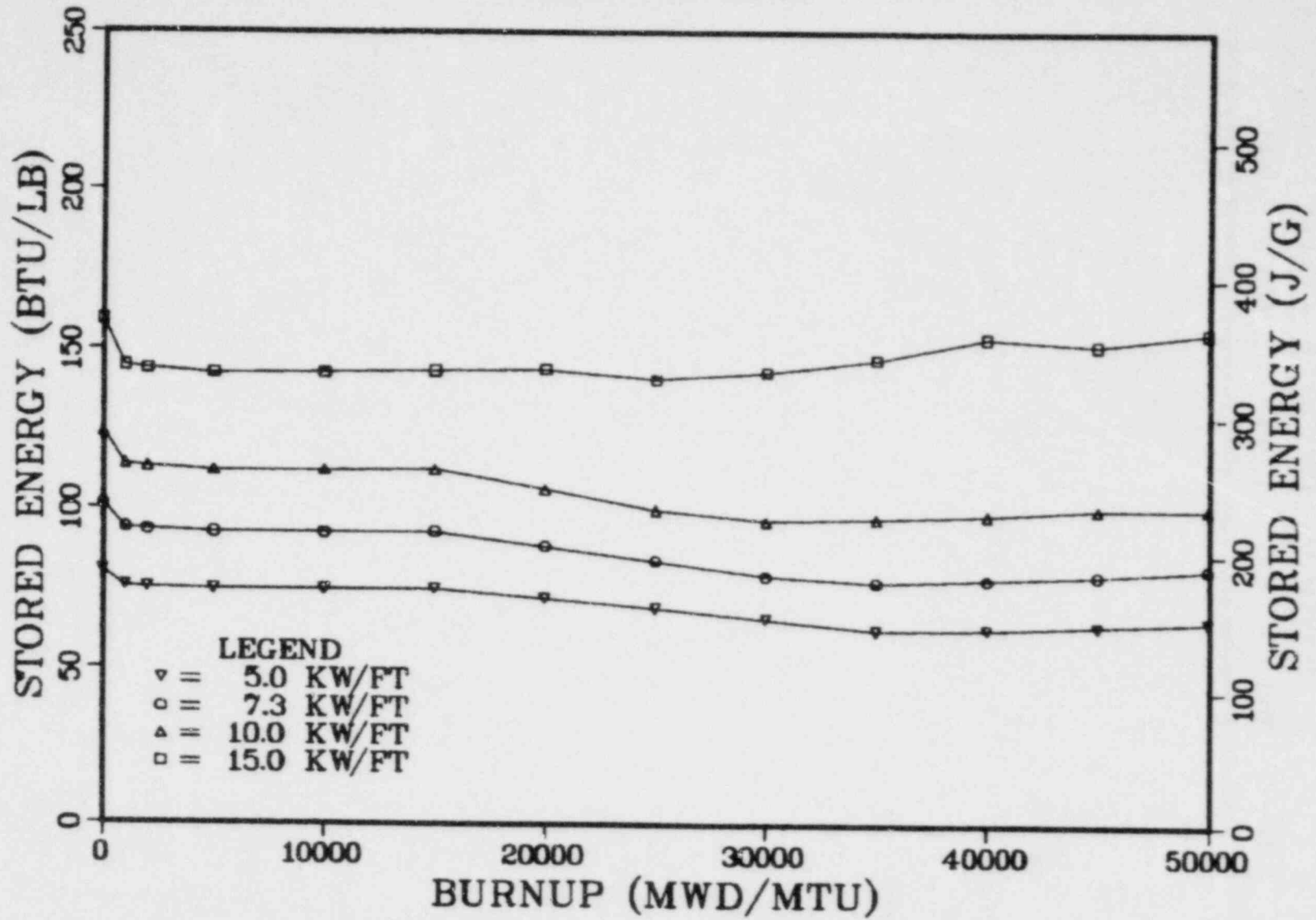


## APPENDIX G

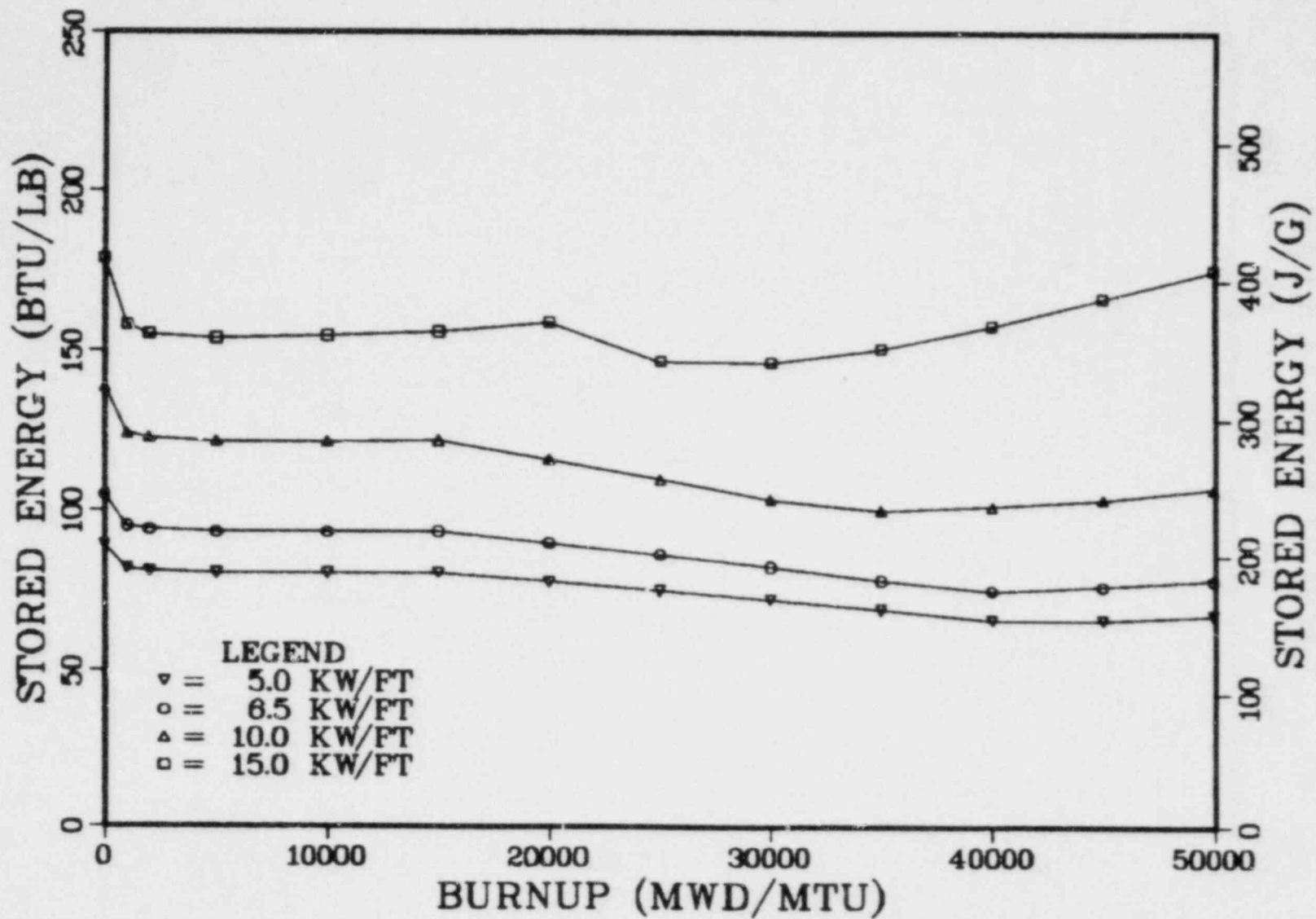
### STORED ENERGY

The following graphs show the stored energy of the peak axial node as a function of local burnup at that location. The results are similar to those shown for fuel volume-averaged temperature. In general, the peak stored energy occurs at beginning of life for PWR's, but may occur later at high power levels. The general case for BWR's is that the peak stored energy occurs late-in-life. Values are presented in units of stored energy per unit mass of the fuel.

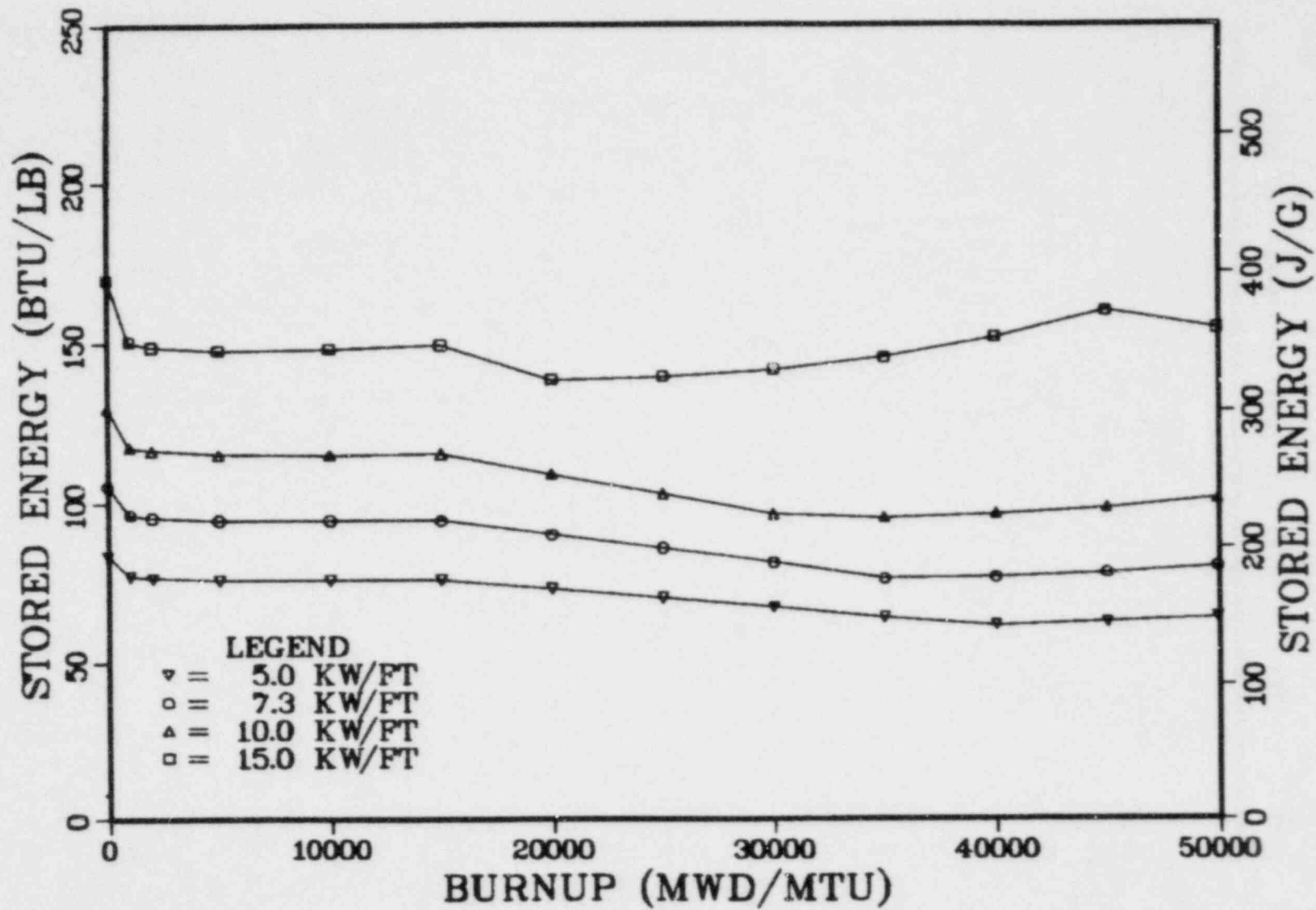
### B&W 15X15



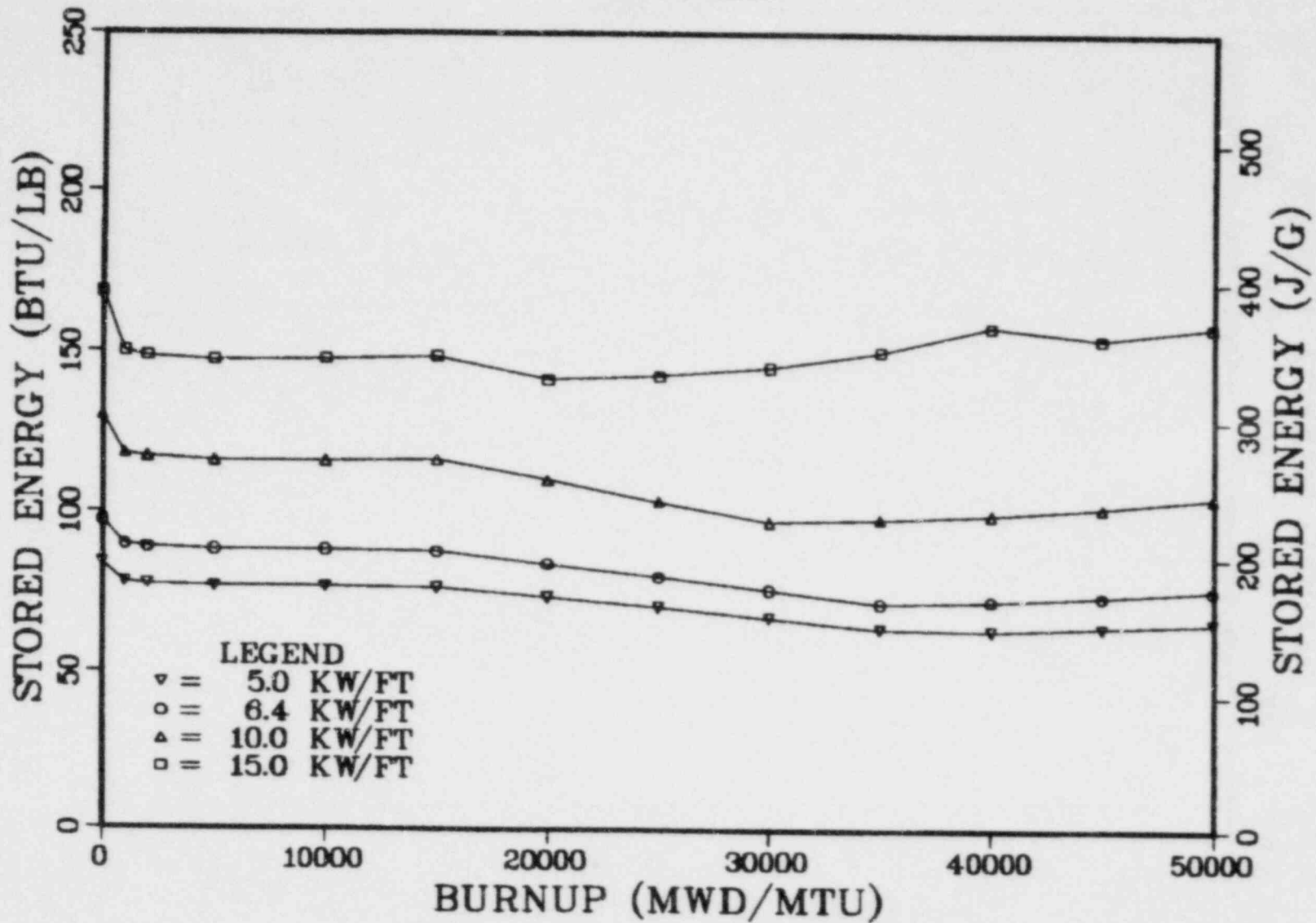
## B&amp;W 17X17



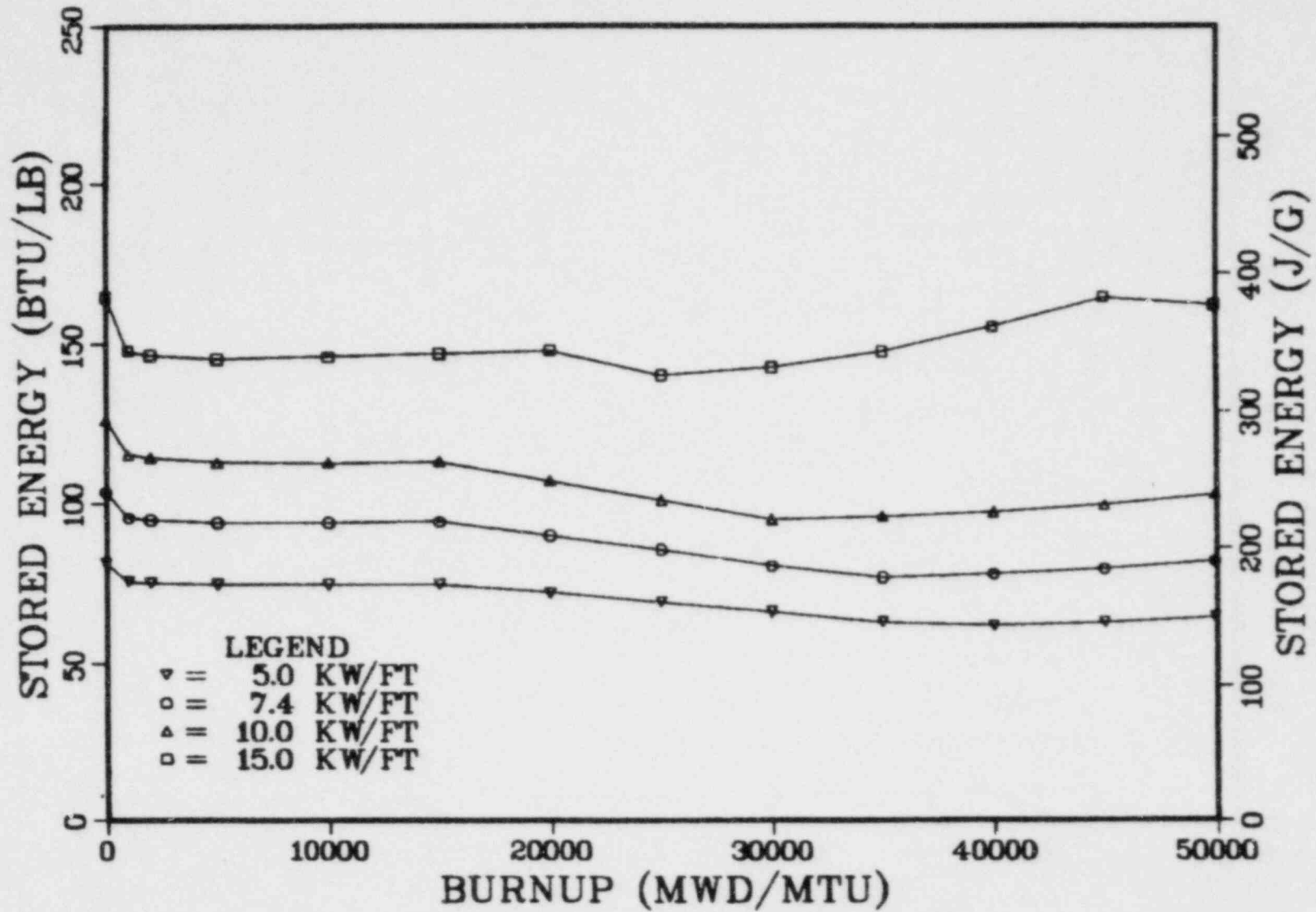
# C-E 14X14



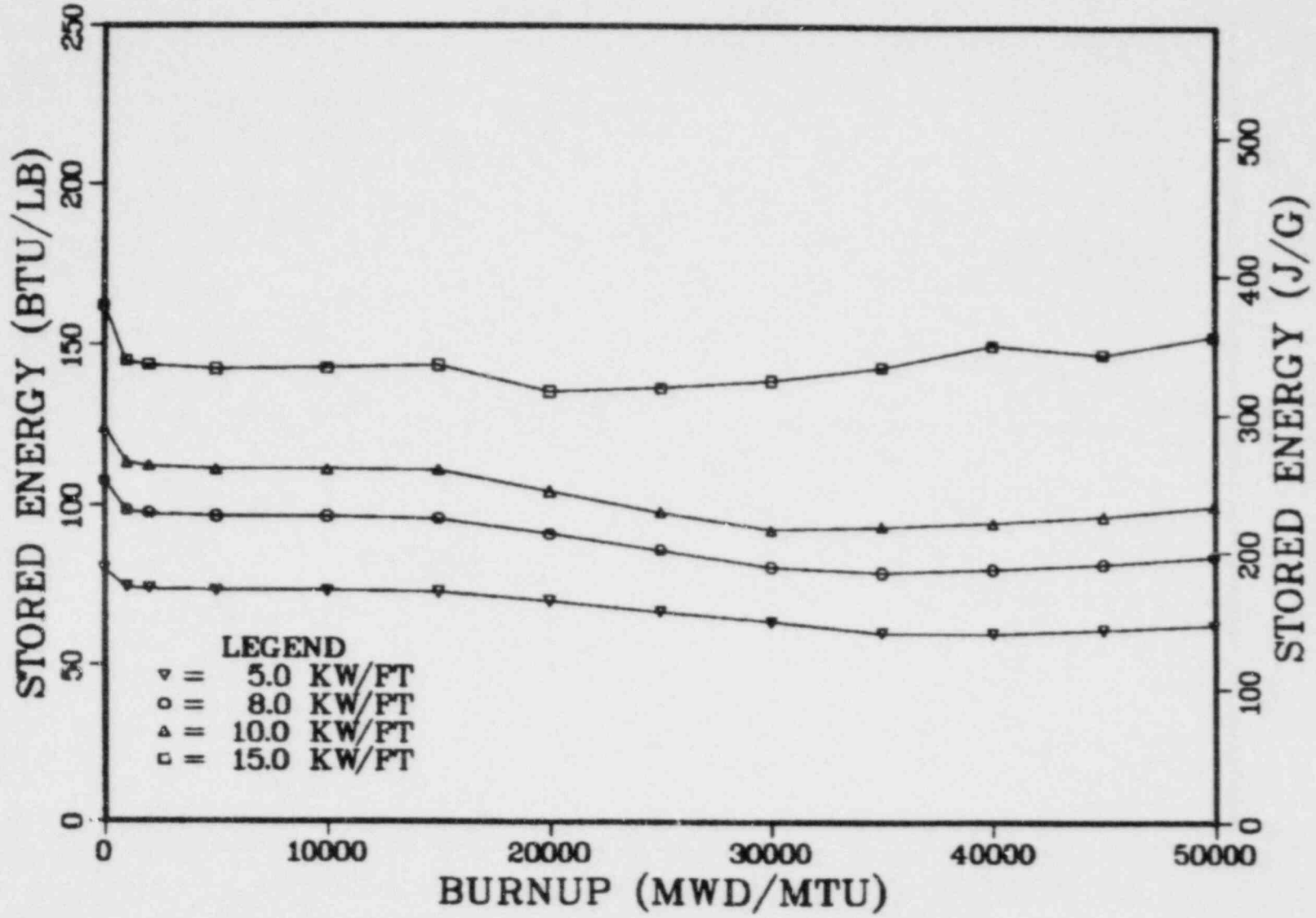
C-E 16X16



## WEST 14X14

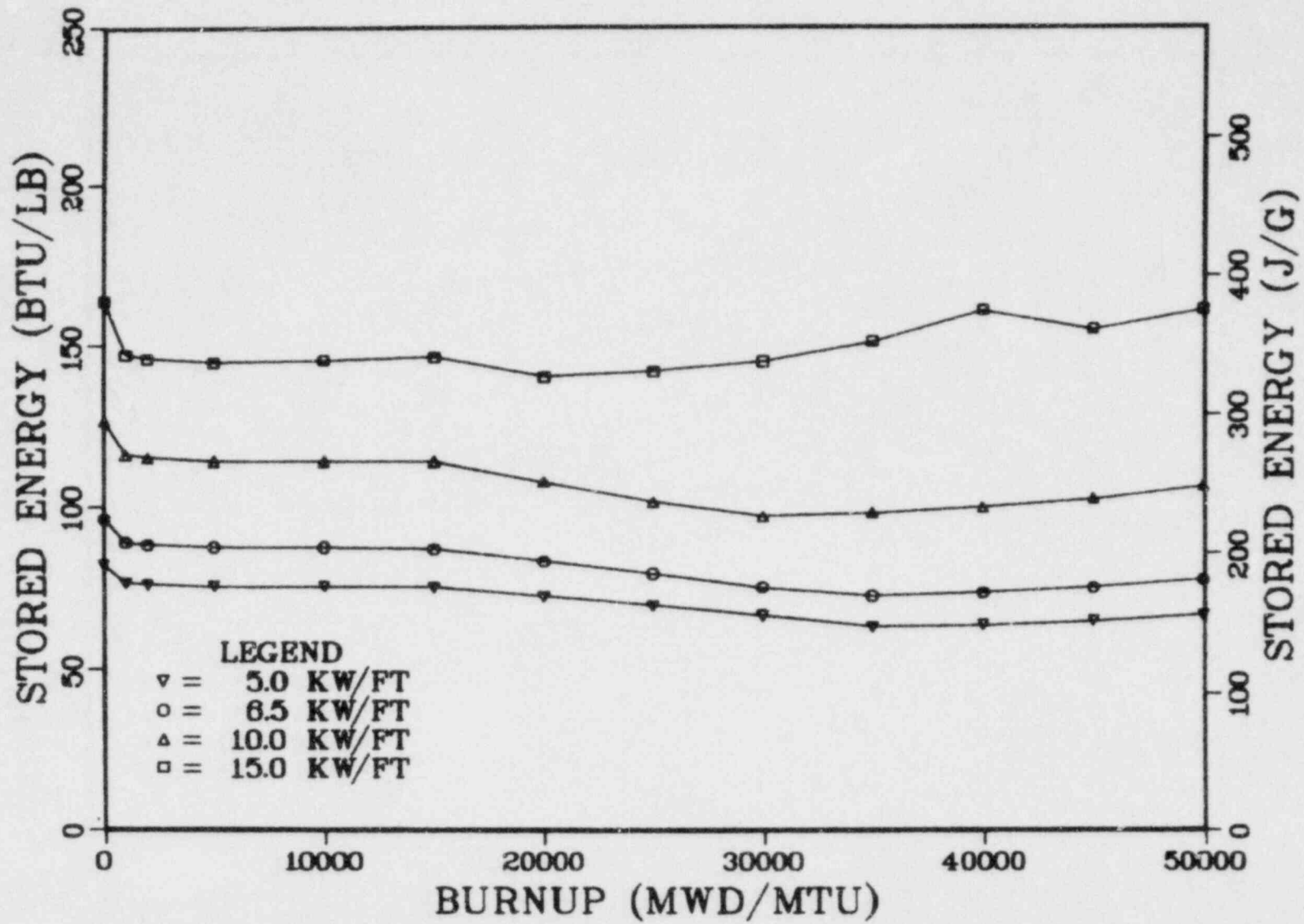


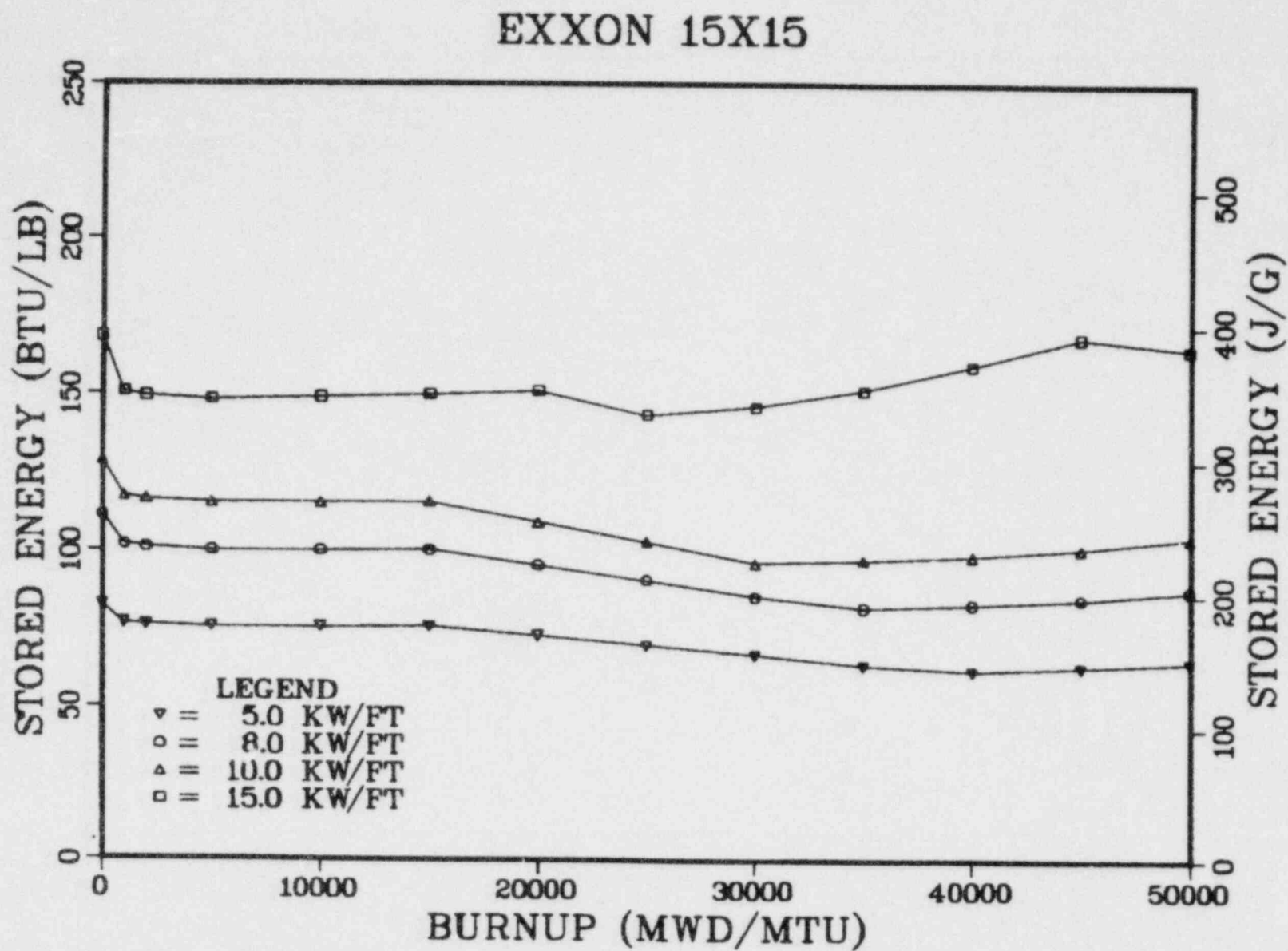
### WEST 15X15

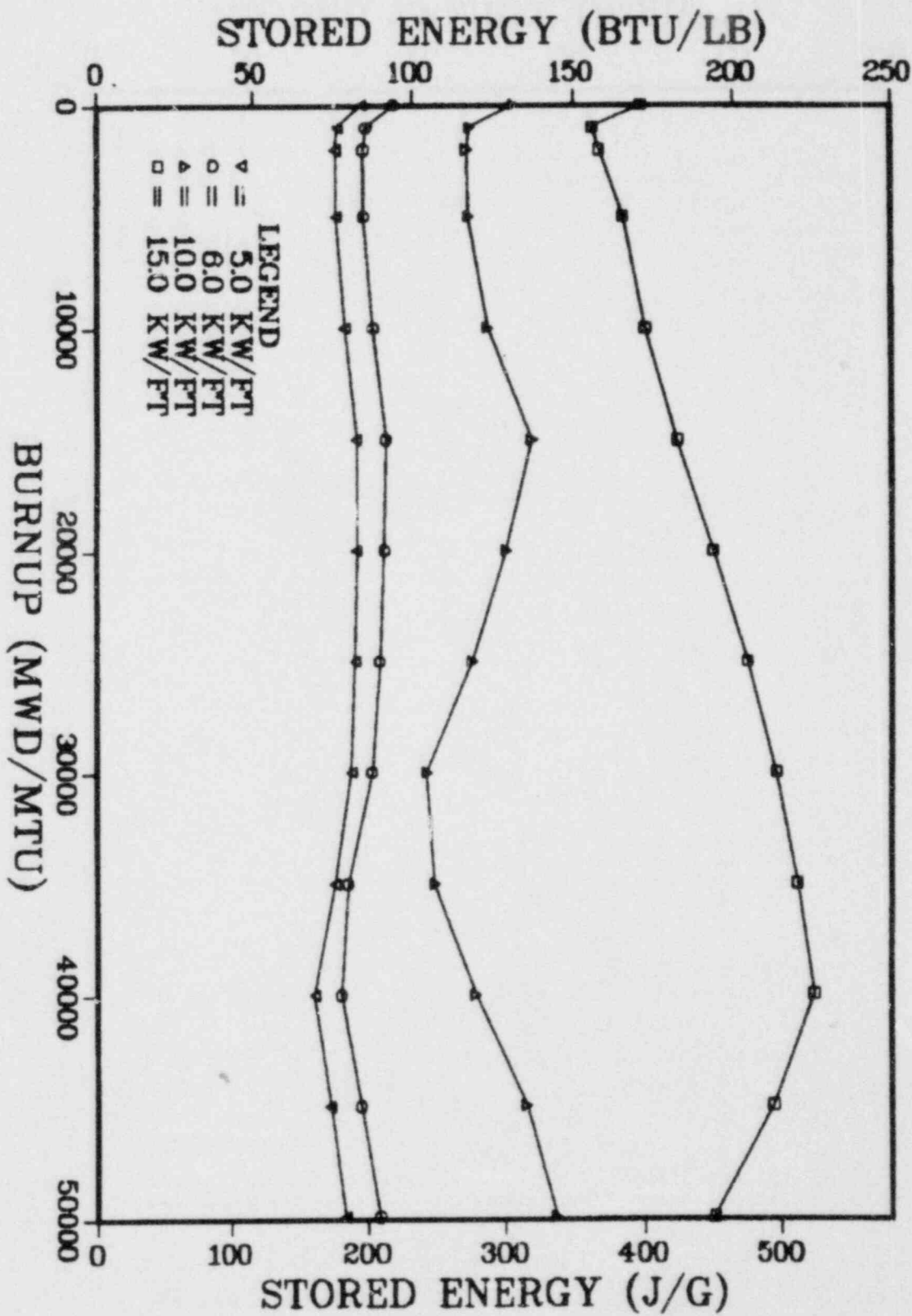




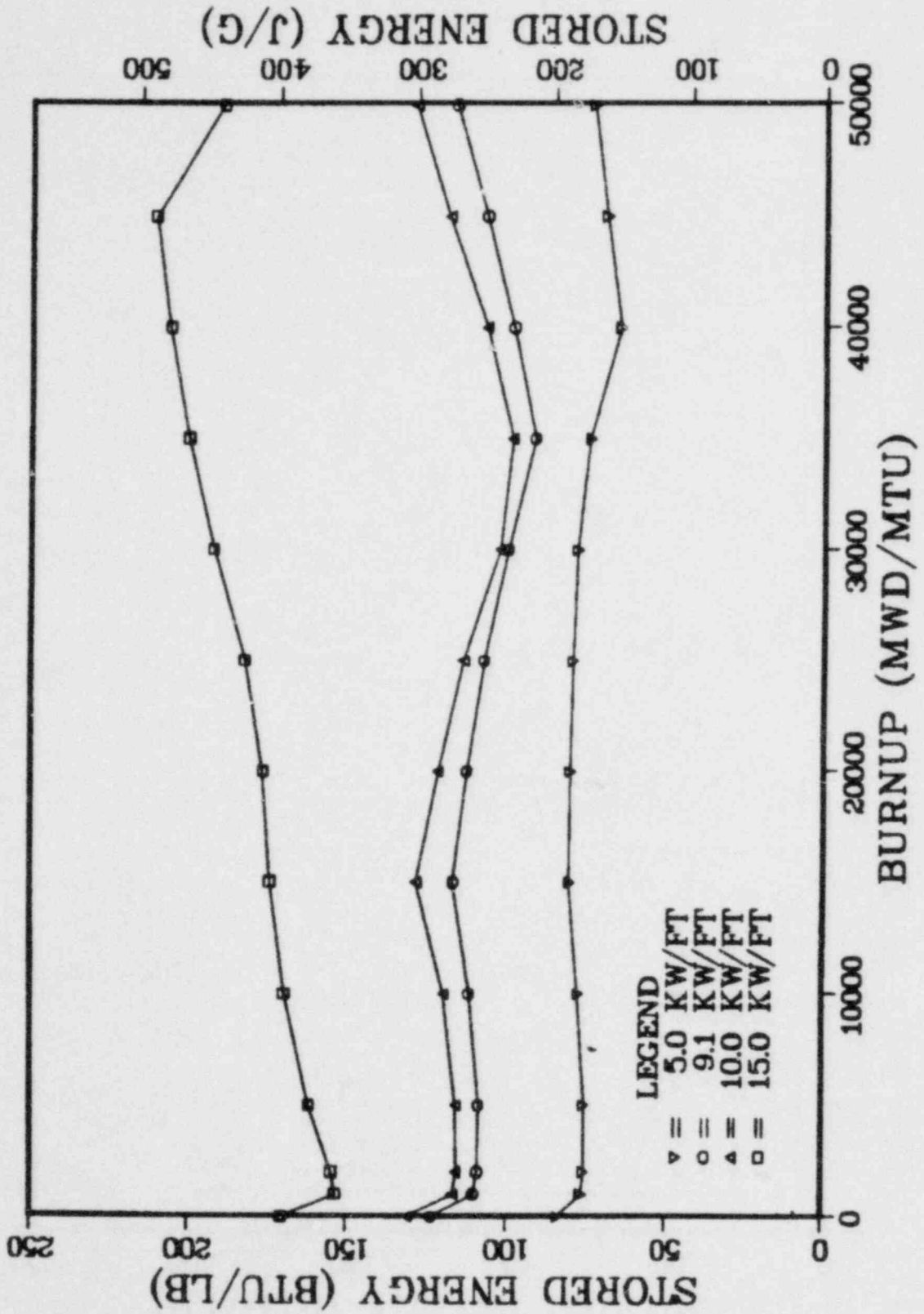
## WEST 17X17

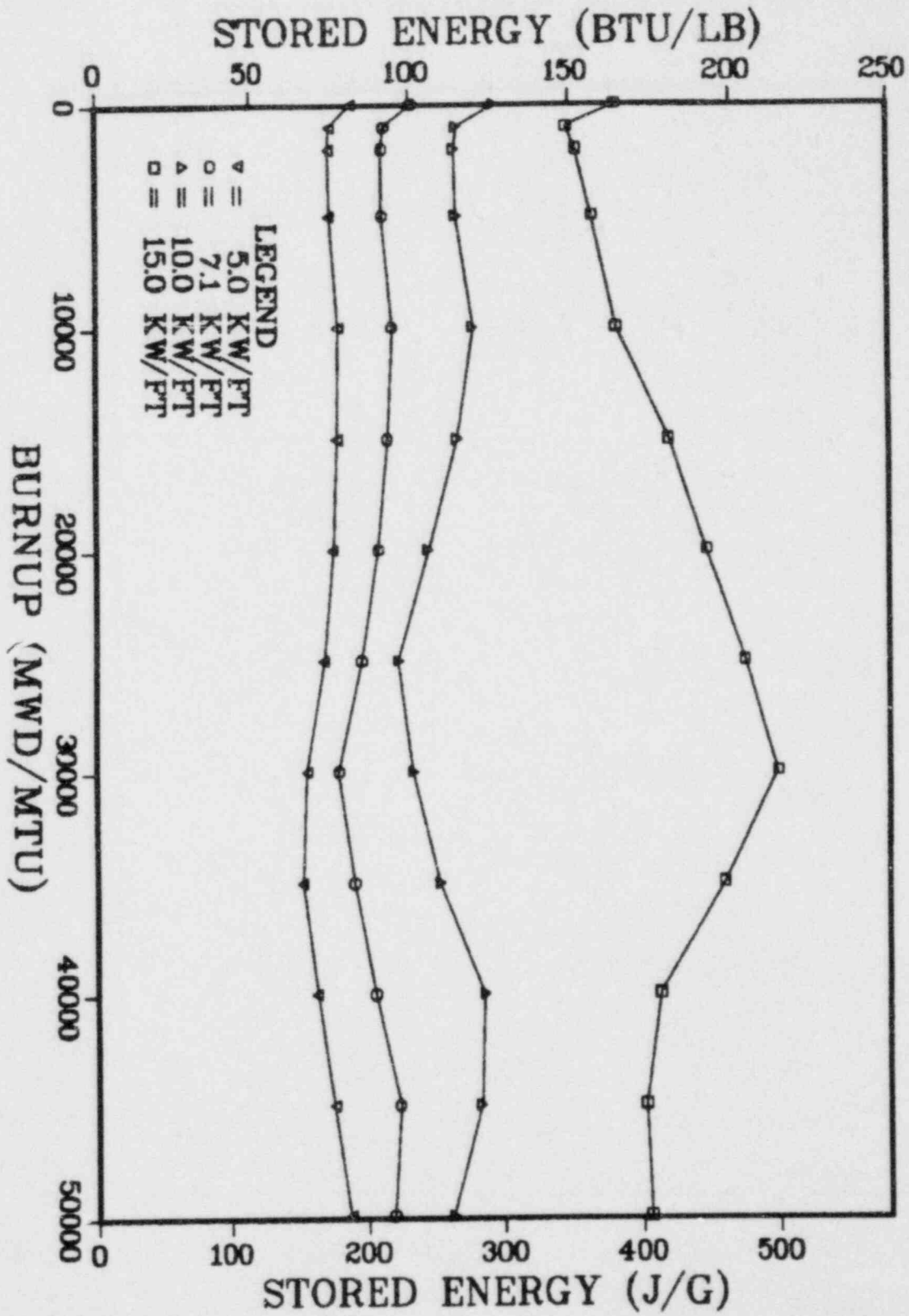






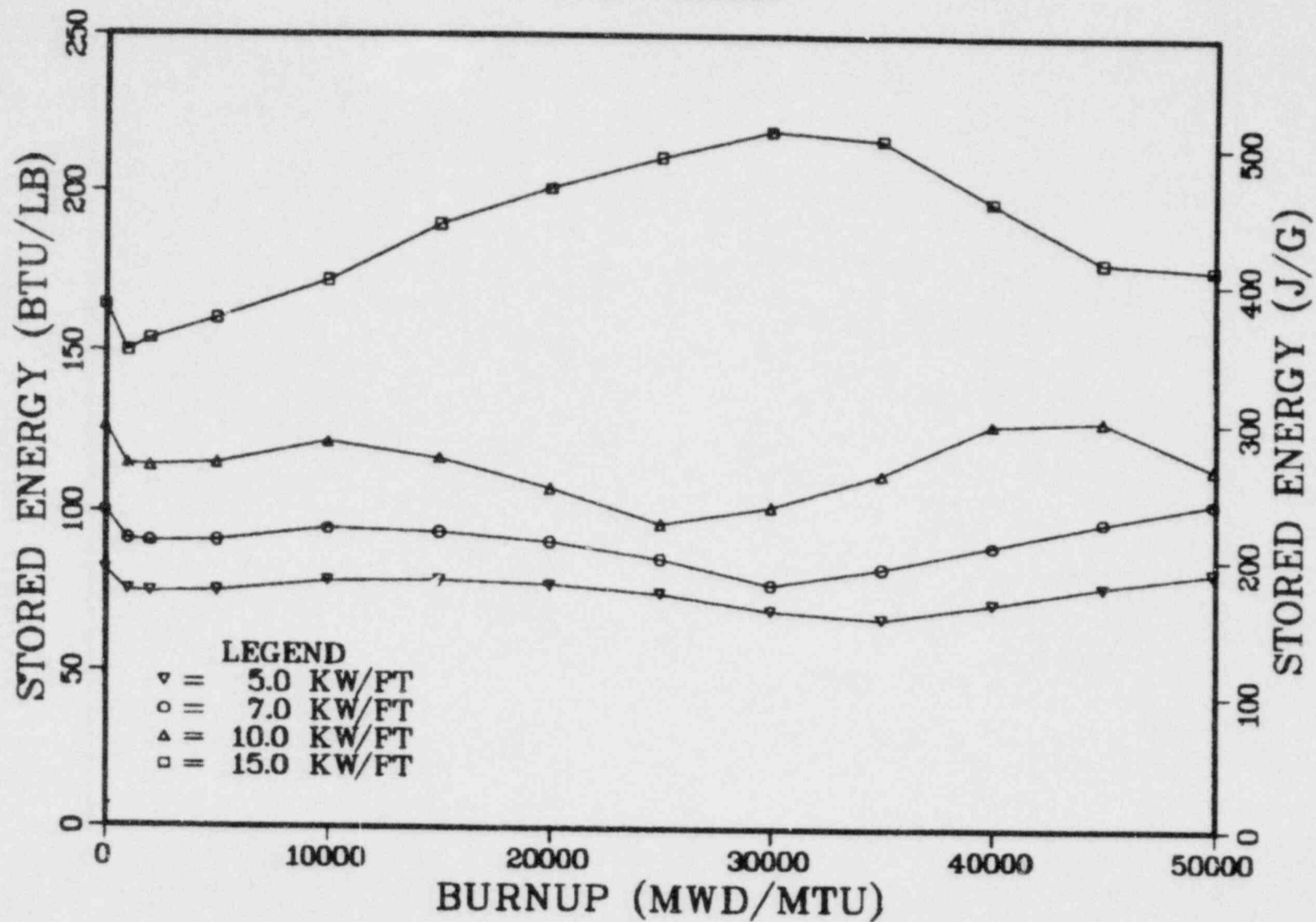
G.E. 7X7

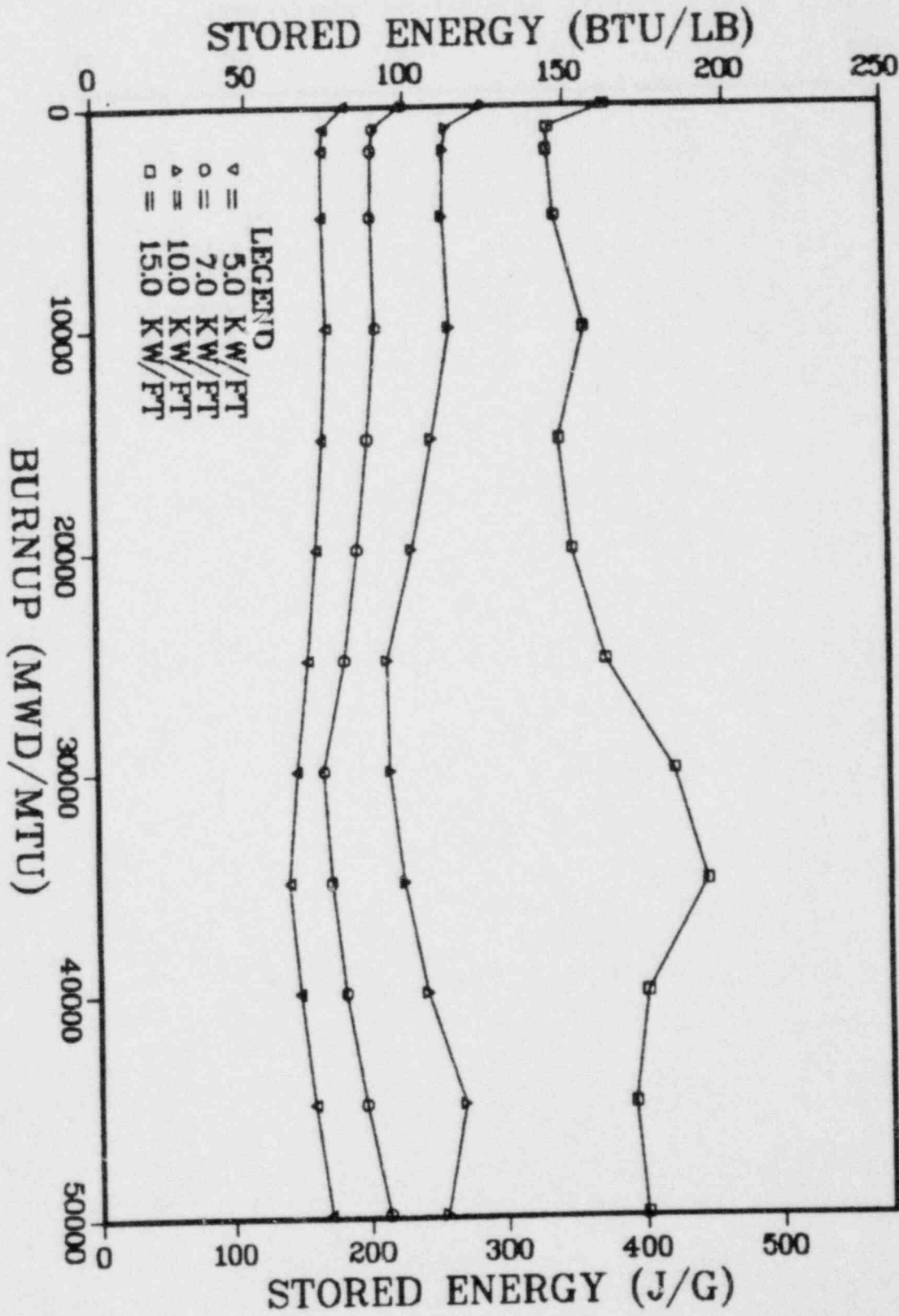




G.E. 8X8

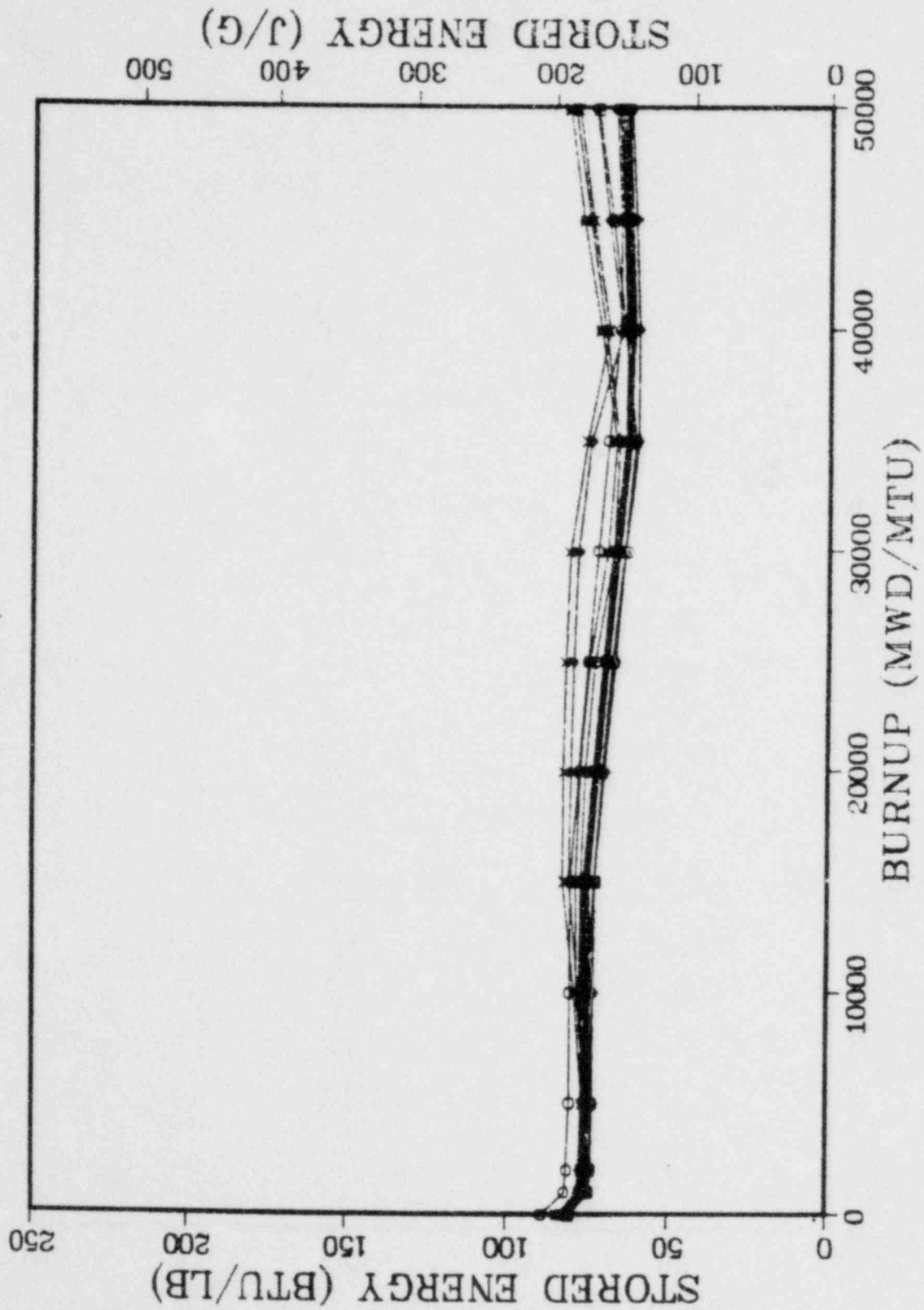
## G.E. 8X8R



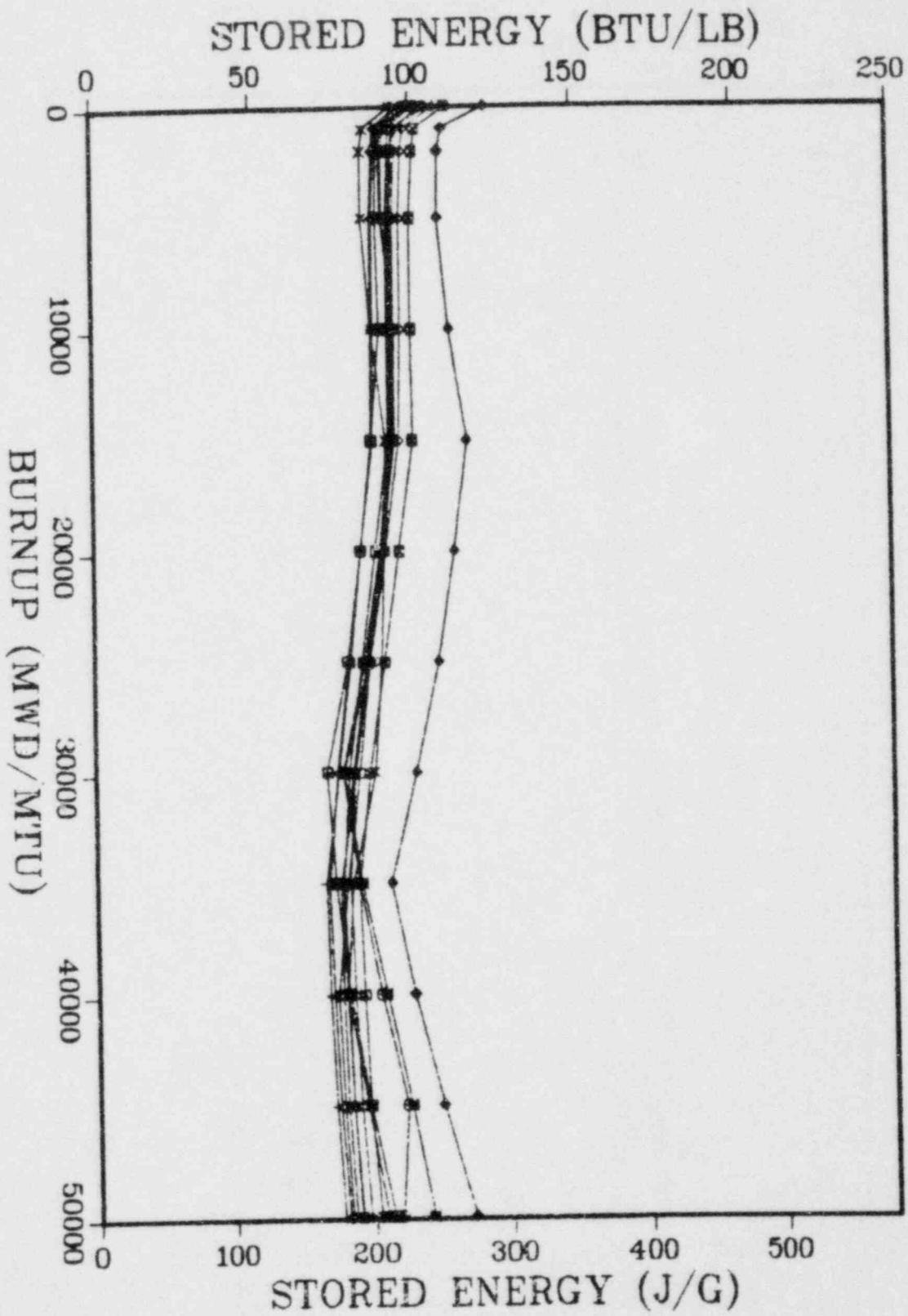


G.E. 8X8R-P

5.0 KW/FT









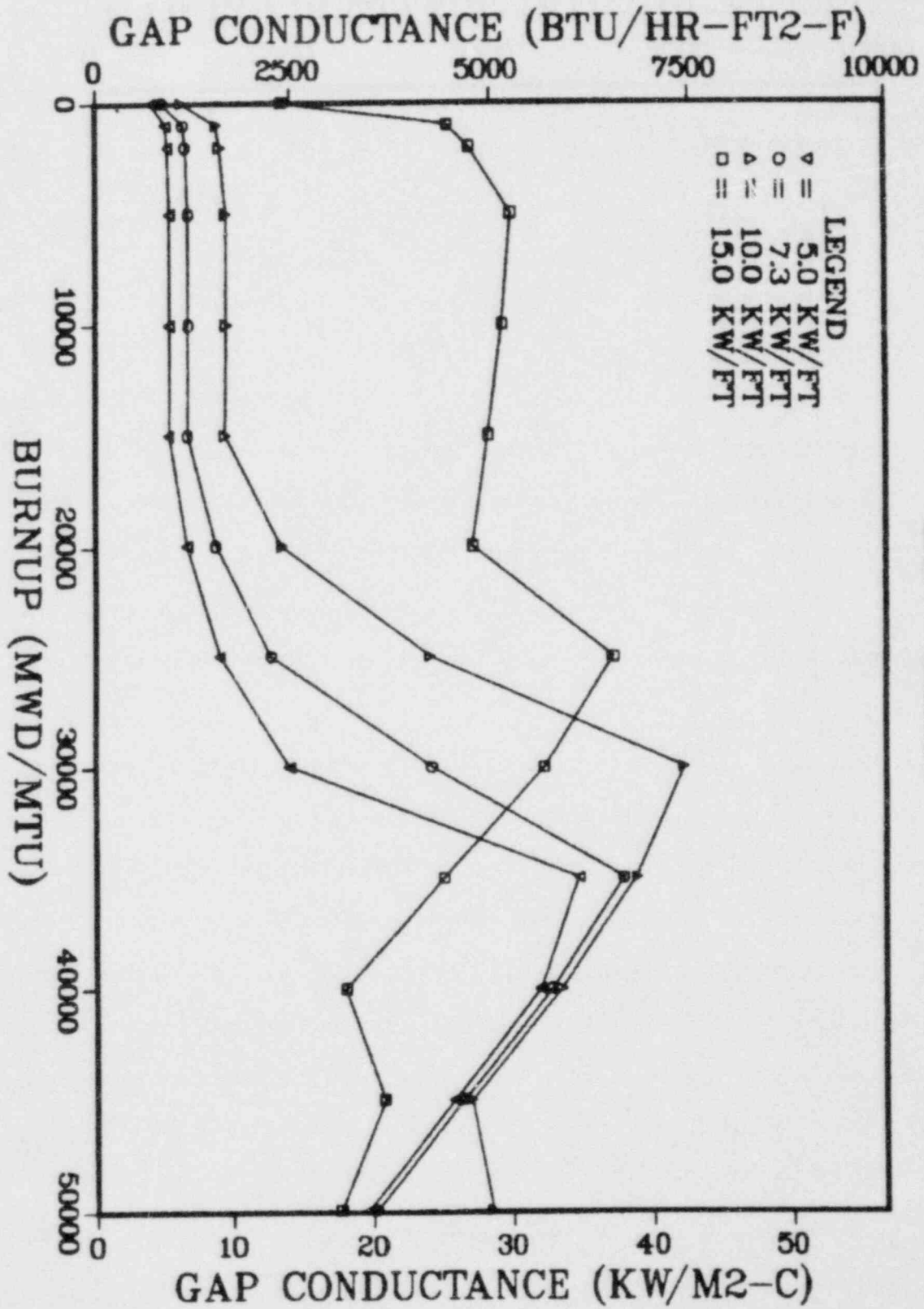


## APPENDIX H

### GAP CONDUCTANCE

The following graphs show the variation of gap conductance with burnup, and the data are given for the peak axial node at specified rod peak burnups. The graphs of PWR gap conductance show a wide variation in values (due to gap closure) with the differences increasing as a function of increased linear power rating. Also, the gap conductivity for a PWR tends to demonstrate a pronounced peak at mid-life burnup when gap closure occurs. The value of gap conductance decreases thereafter due to fill gas dilution with fission gases.

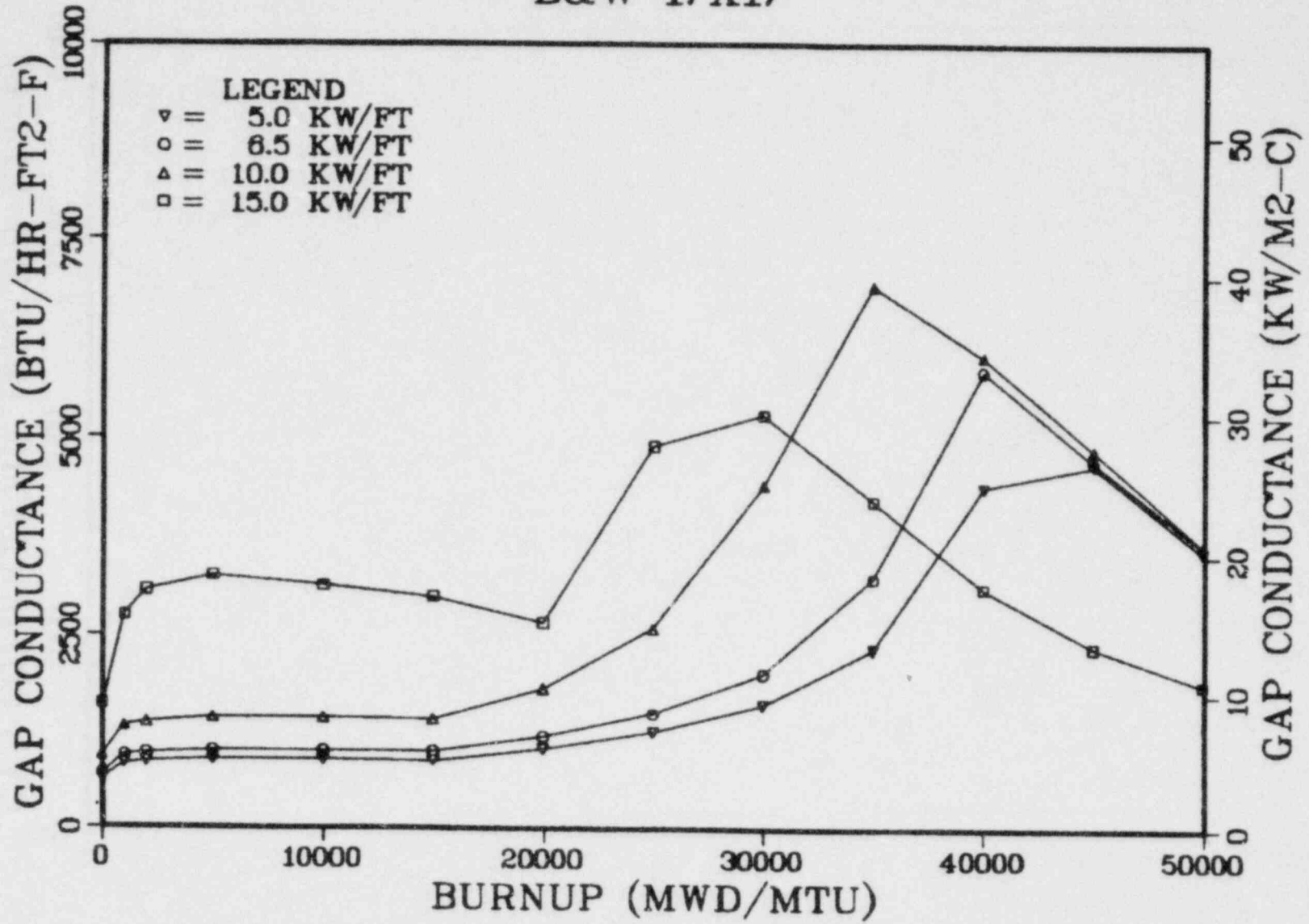
In general, gap conductivity is greater for a PWR than a BWR, which can be attributed to prepressurization. This is also shown for the prepressurized GE 8x8R design which has gap conductivity values larger than those for the unpressurized GE 8x8R design. The BWR designs also show less variation in gap conductance due to thicker cladding, which is more resistant to the cladding creepdown and gap closure.



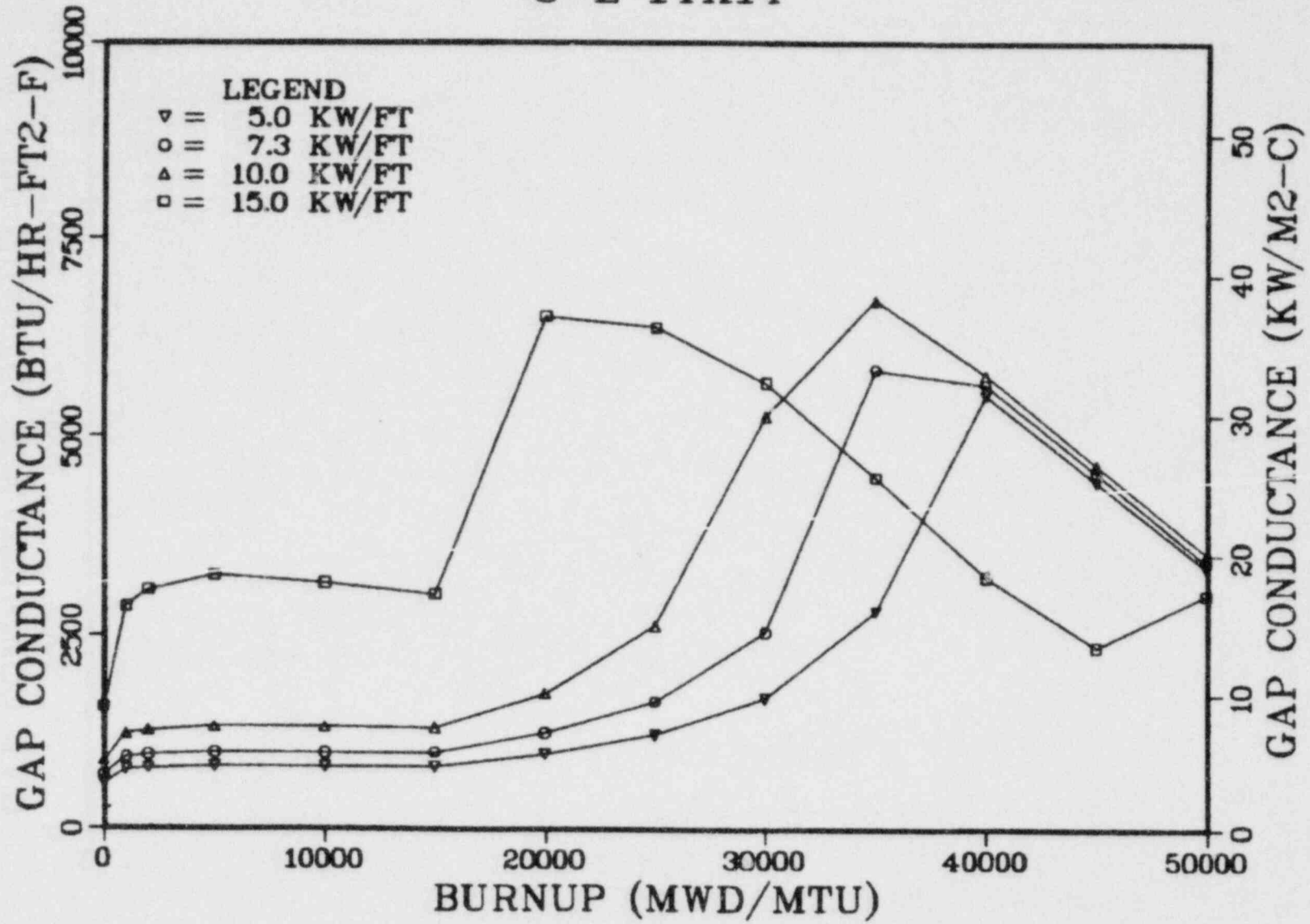
B&W 15X15

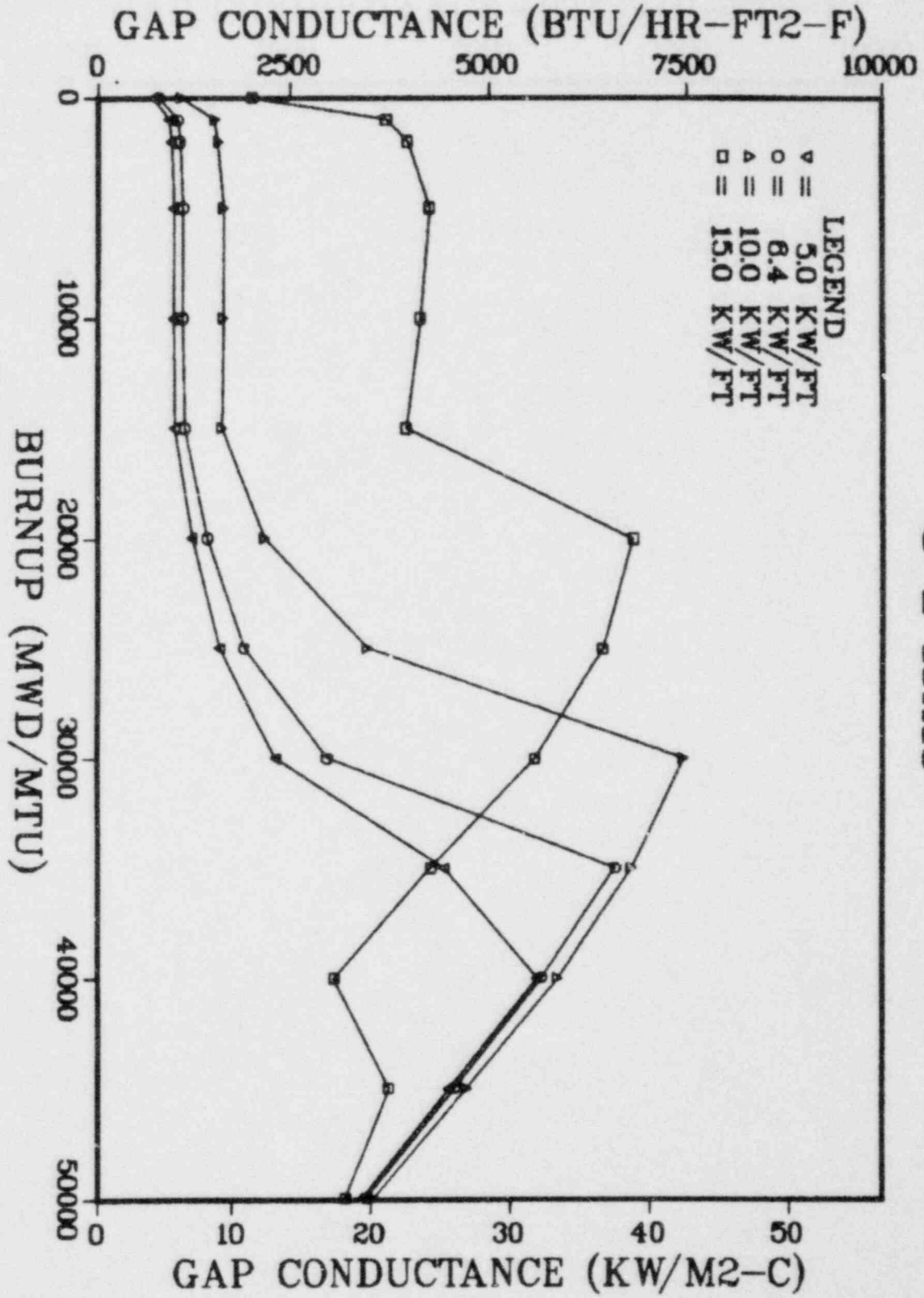
B&W 17X17

H-3



# C-E 14X14

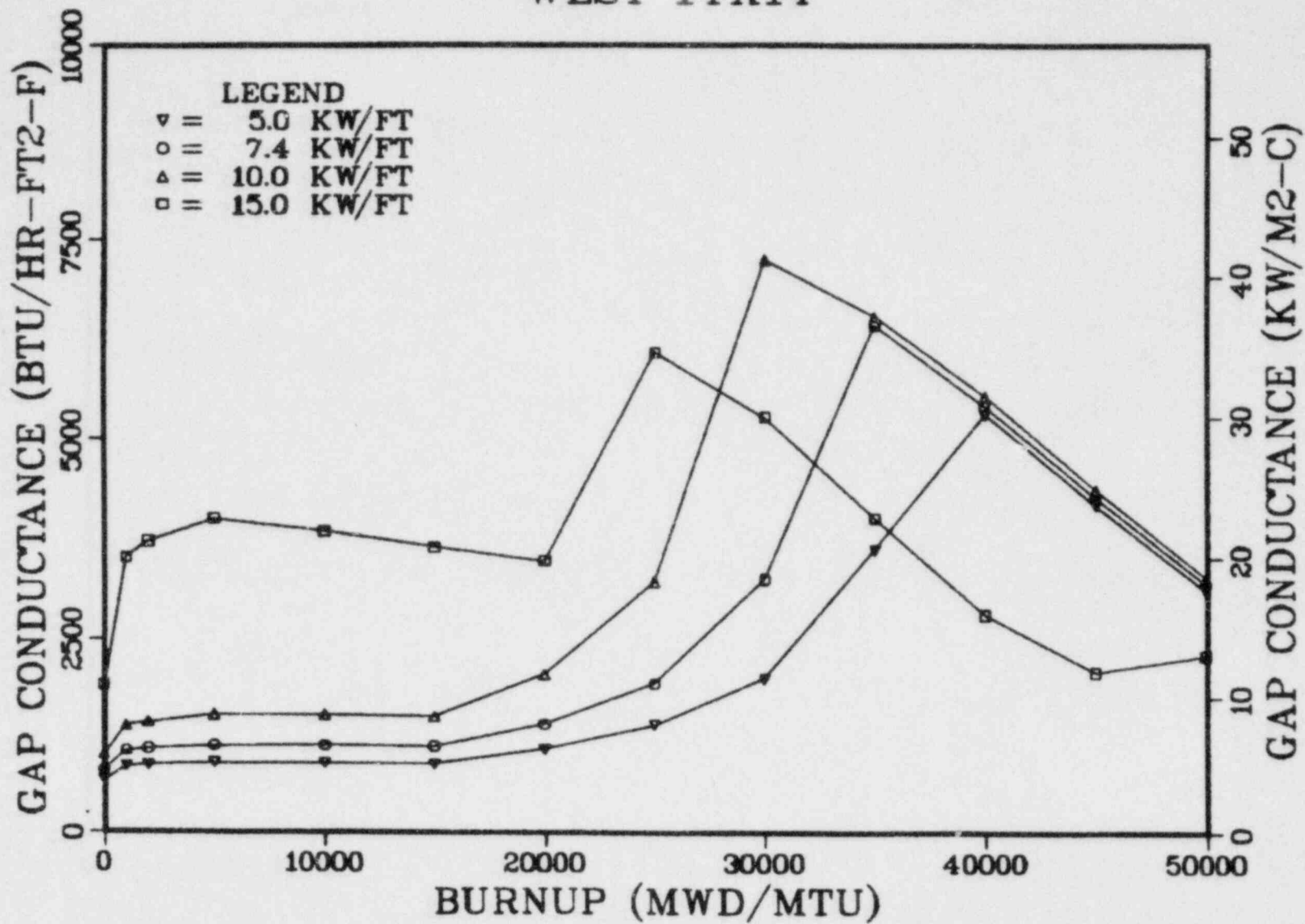


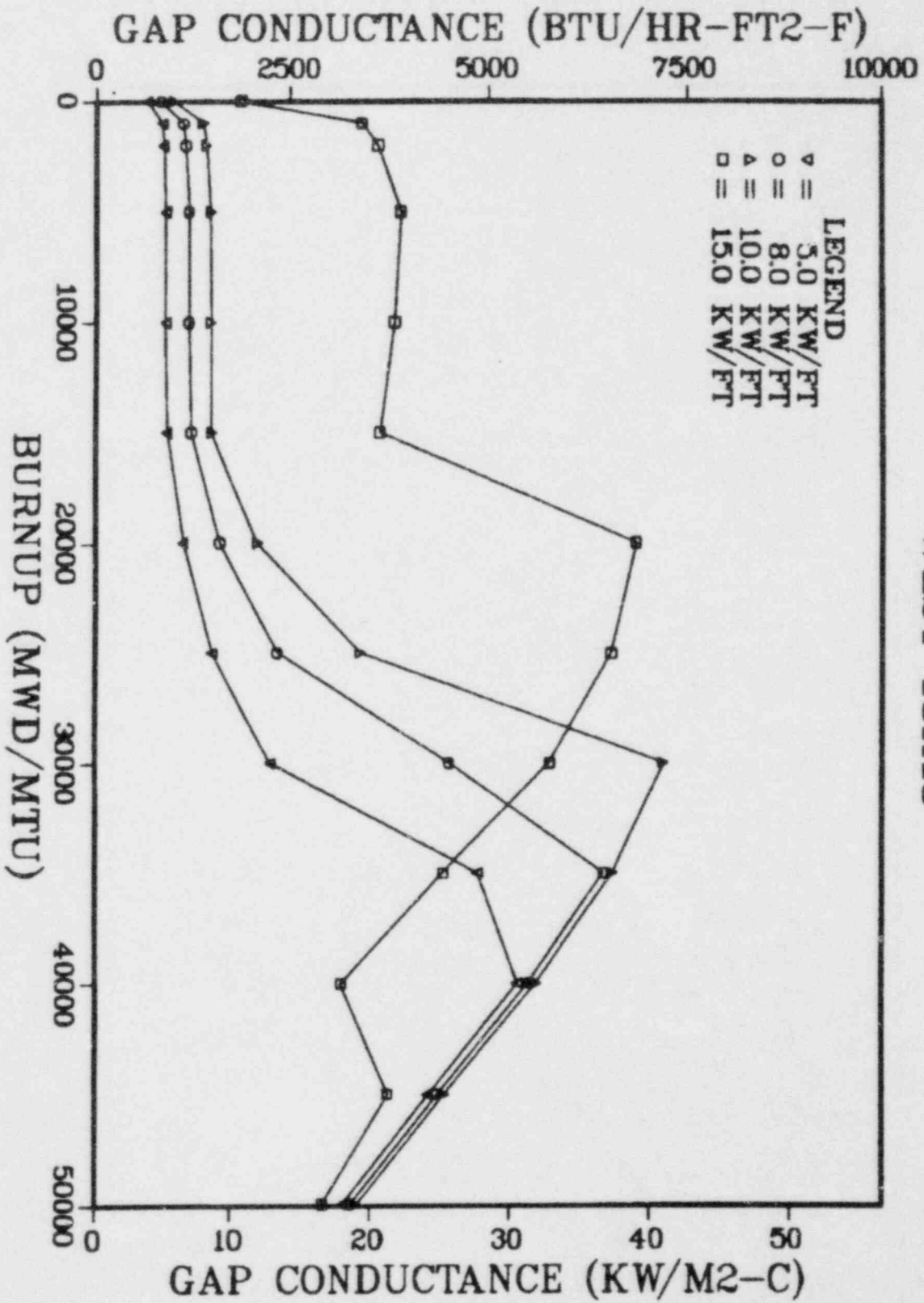


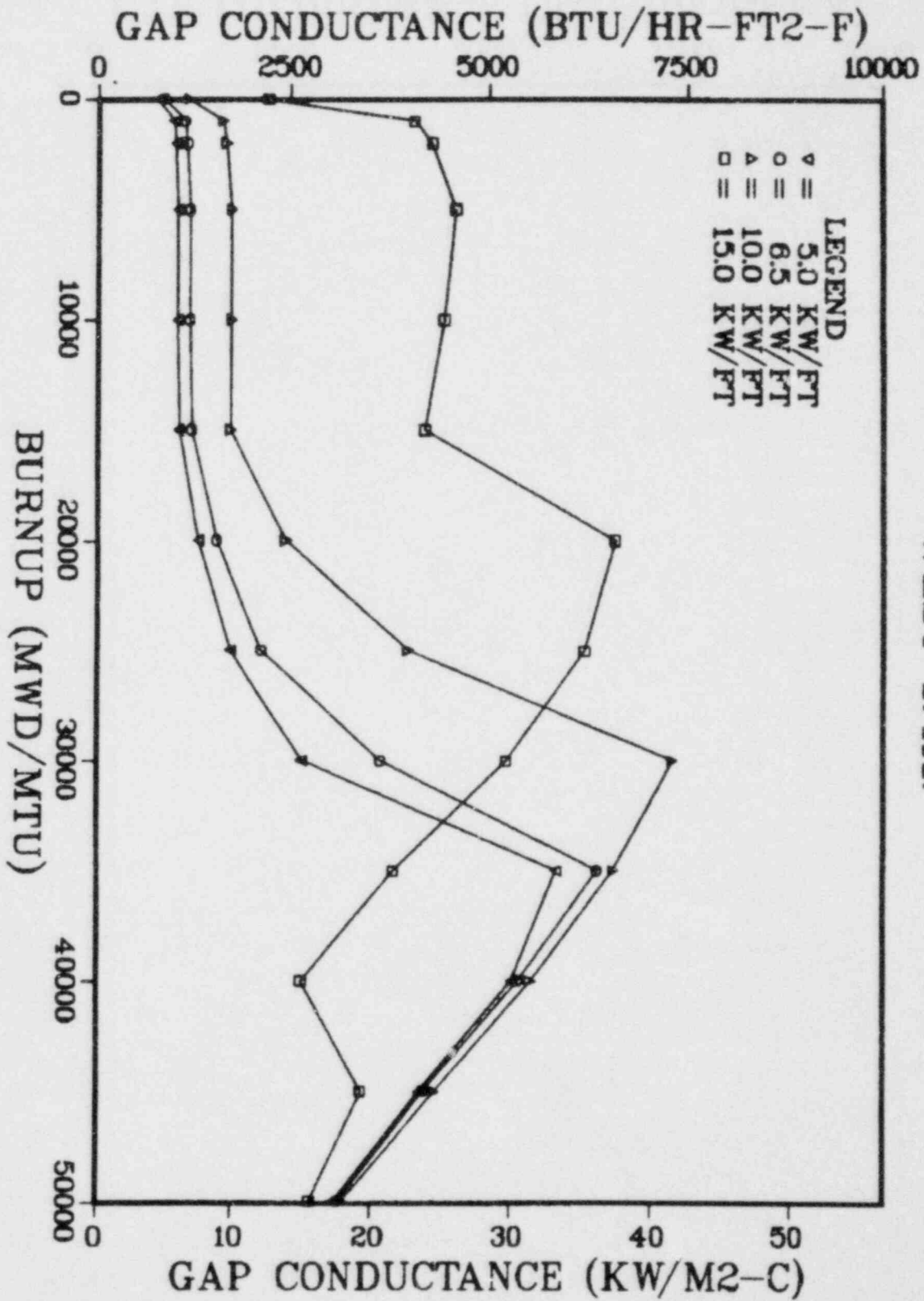
C-E 16X16



# WEST 14X14

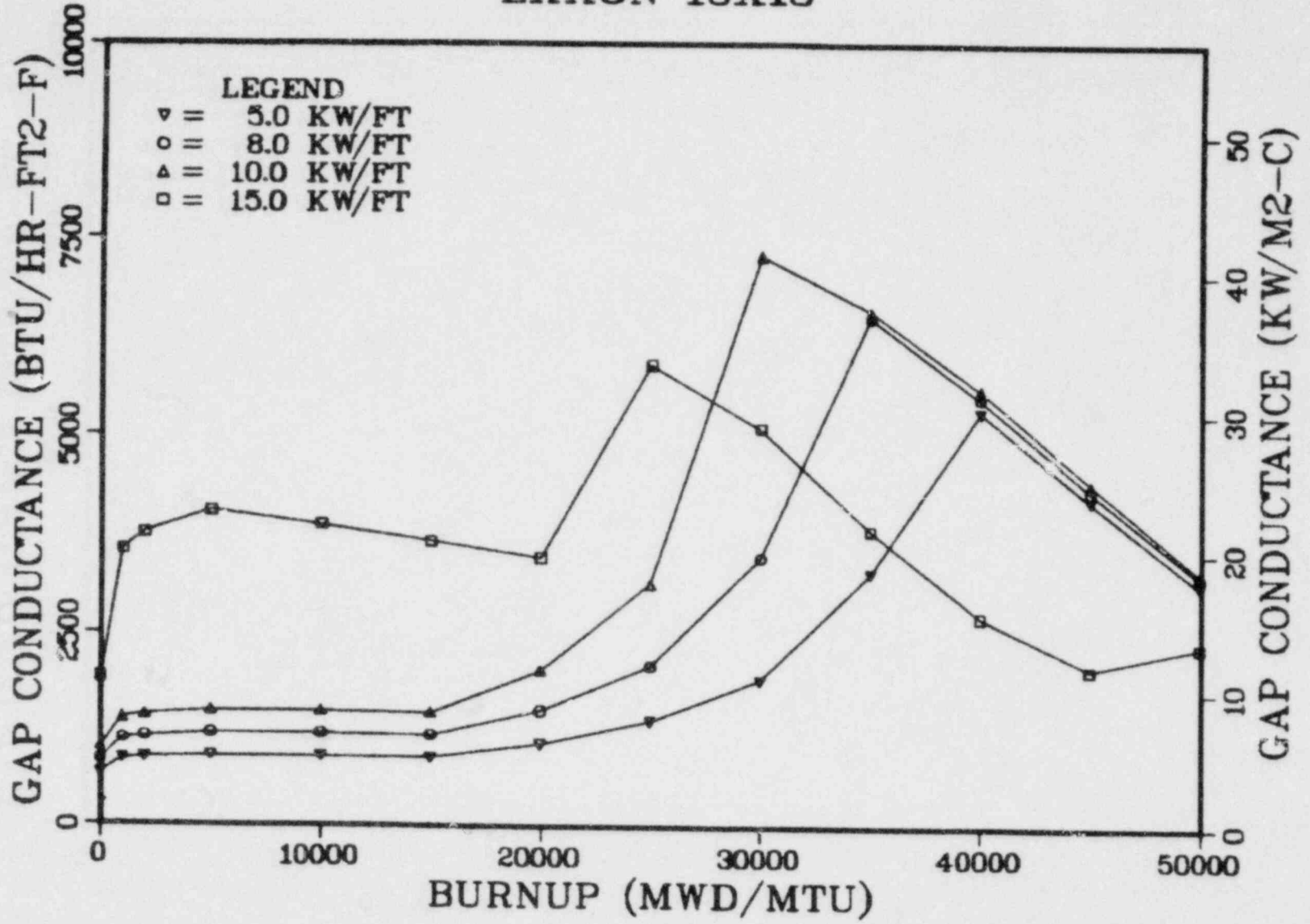




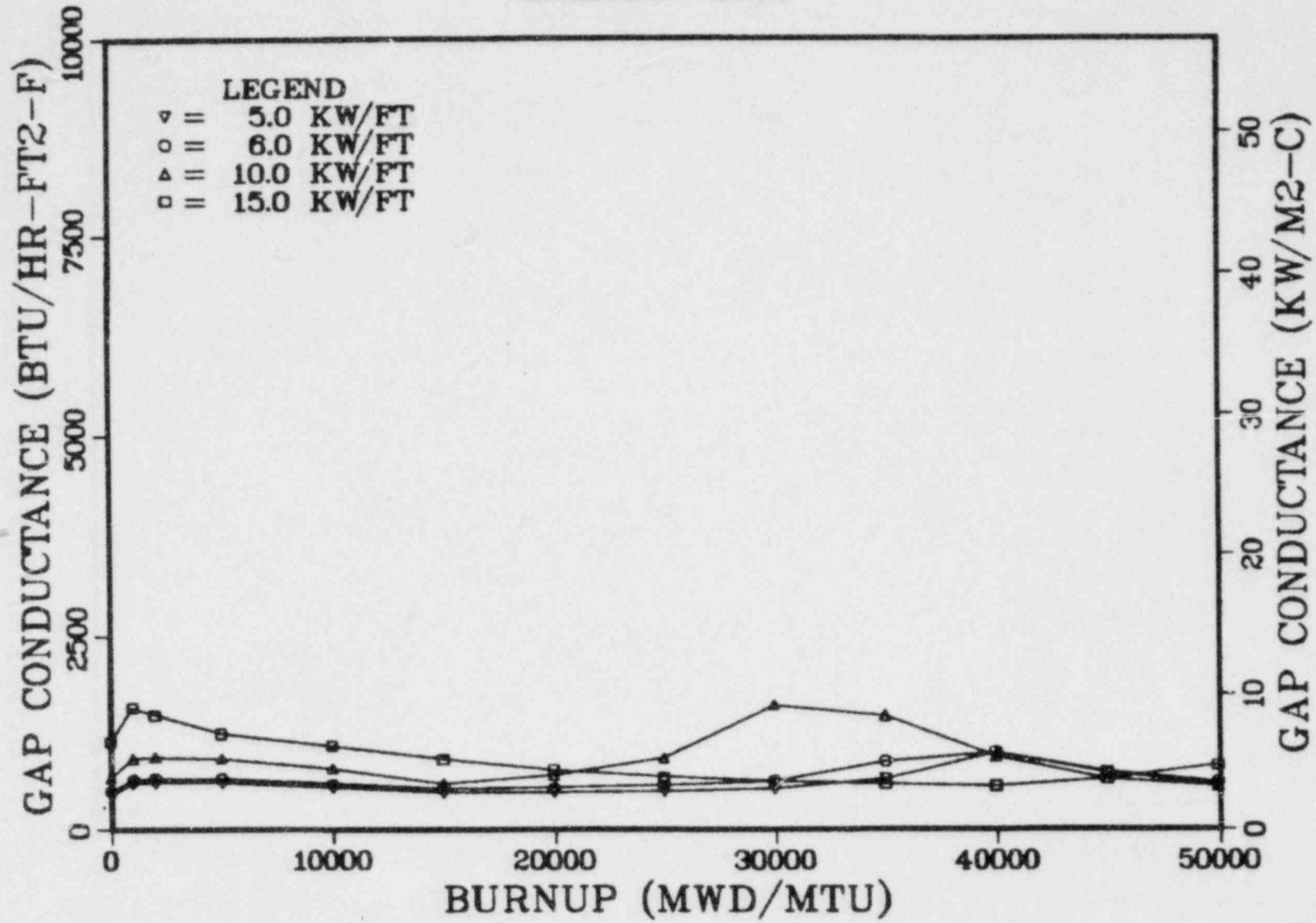


WEST 17X17

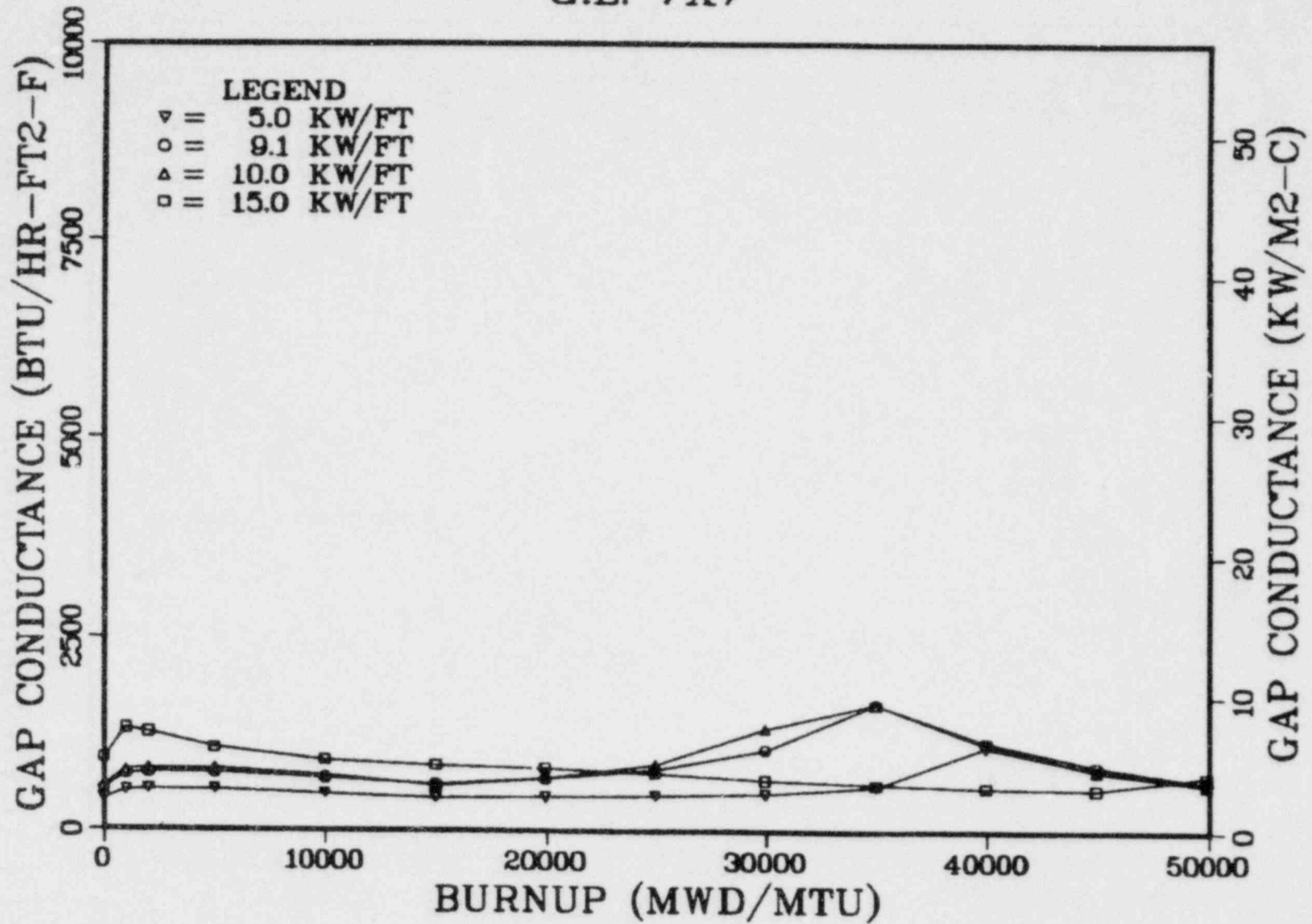
# EXXON 15X15



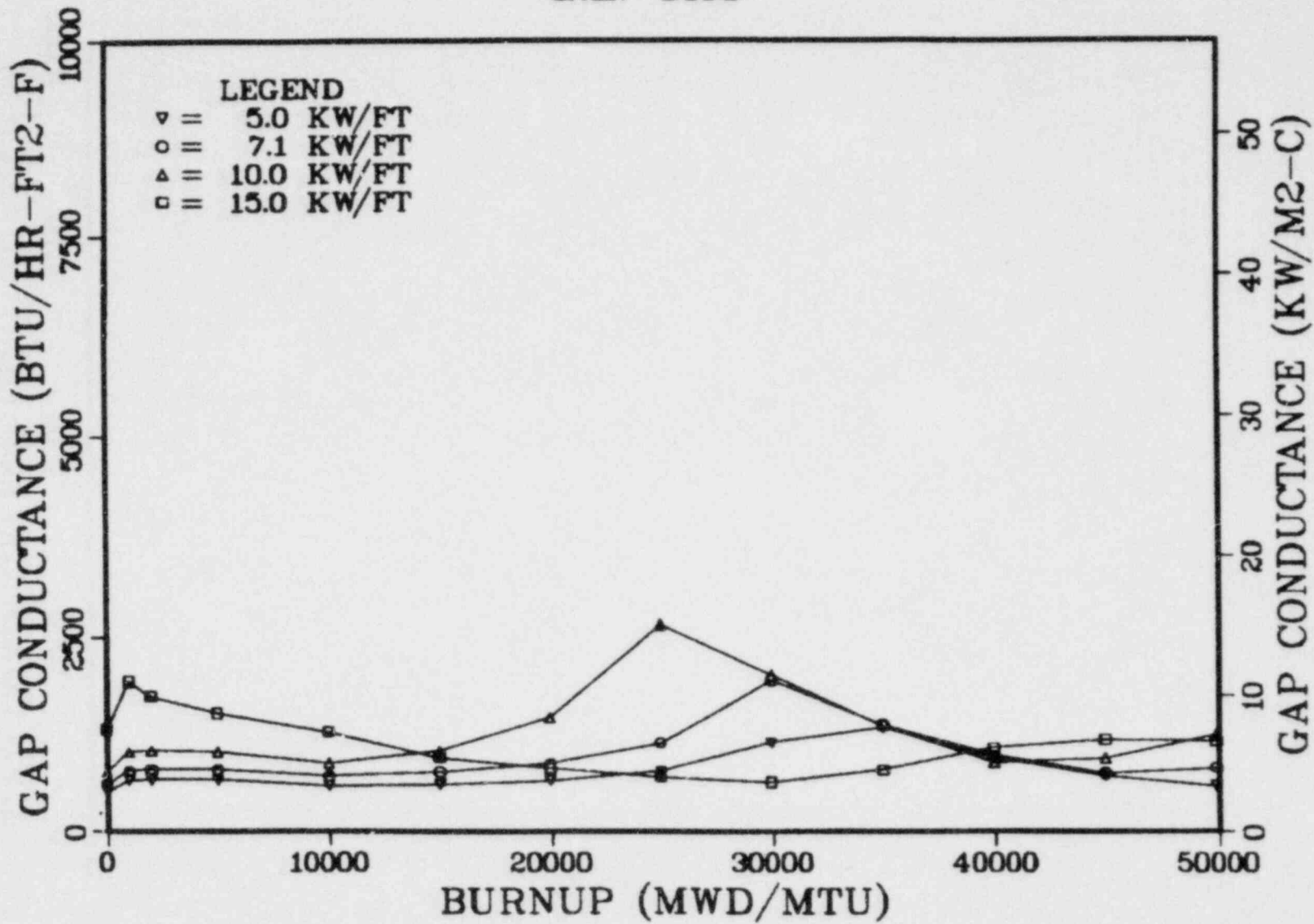
## EXXON 8X8



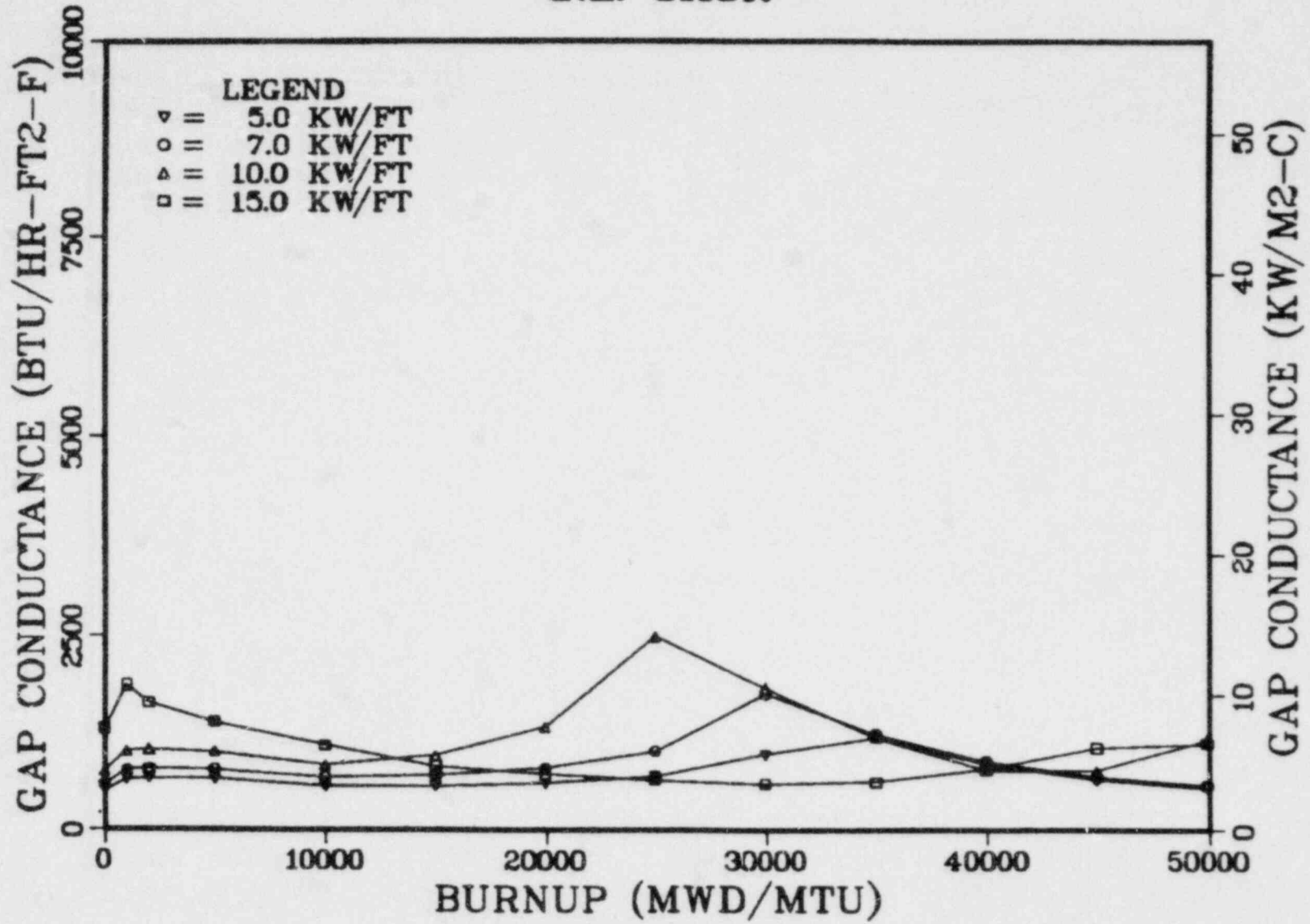
G.E. 7X7



# G.E. 3X8

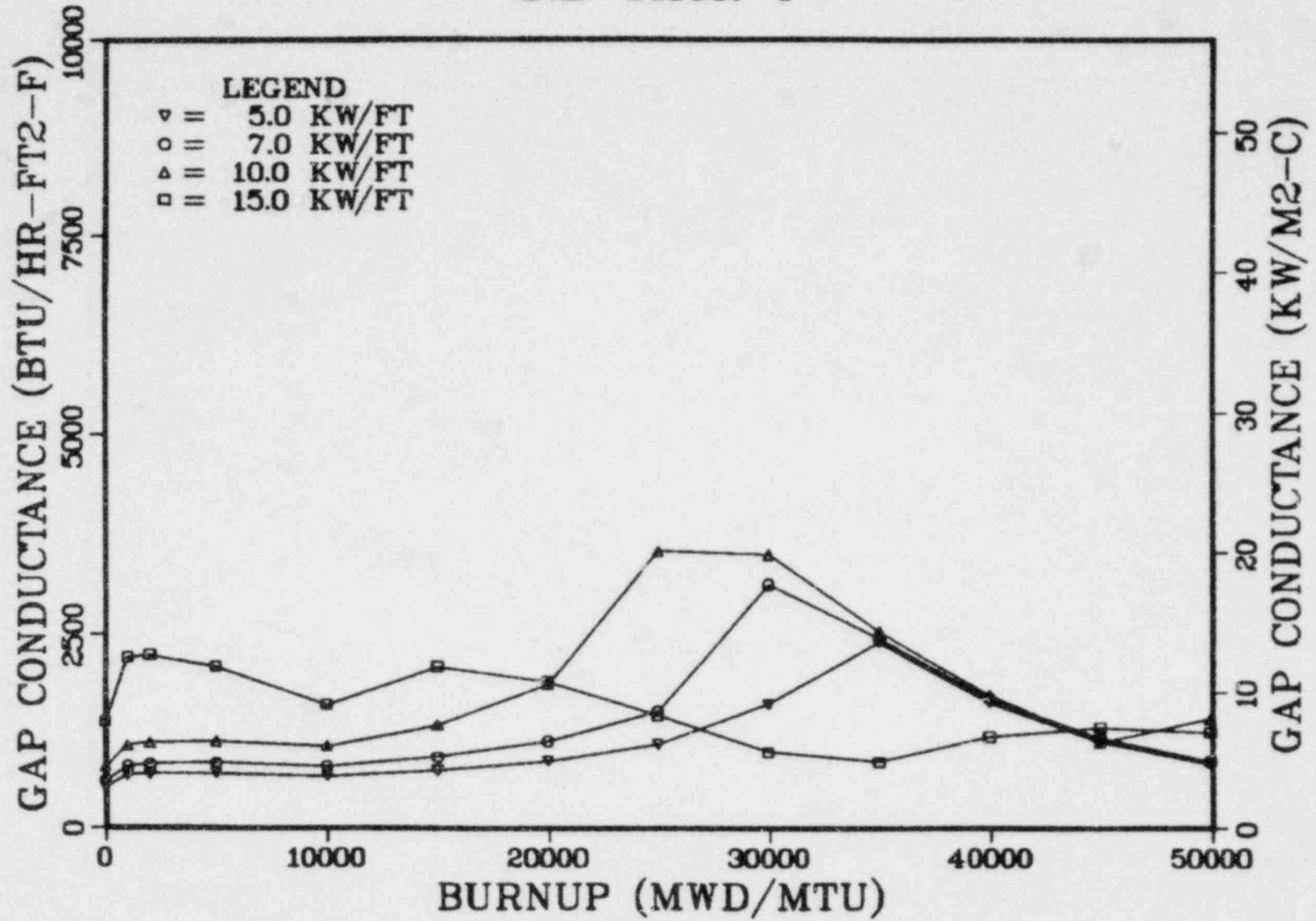


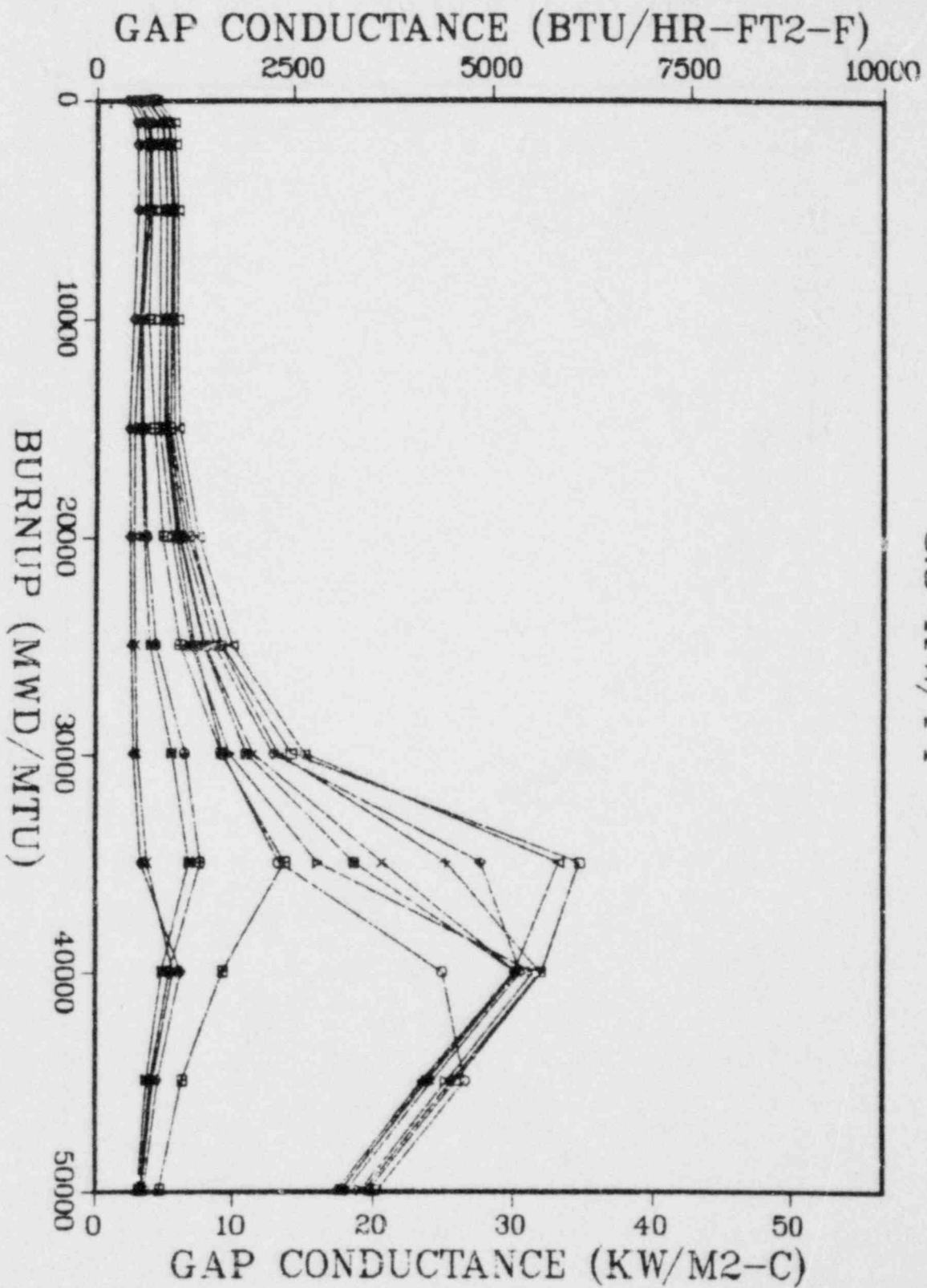
G.E. 8X8R





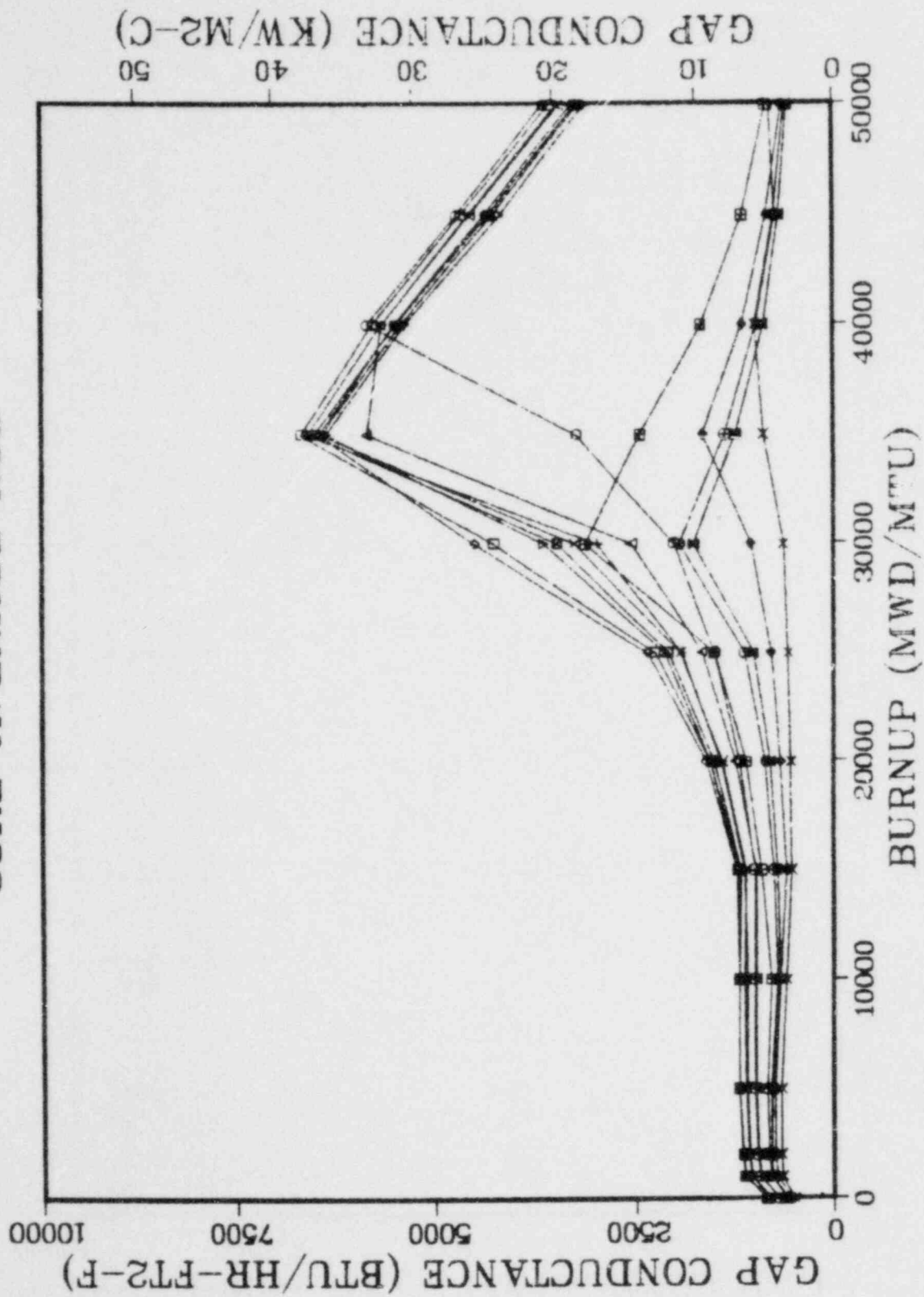
### G.E. 8X8R-P

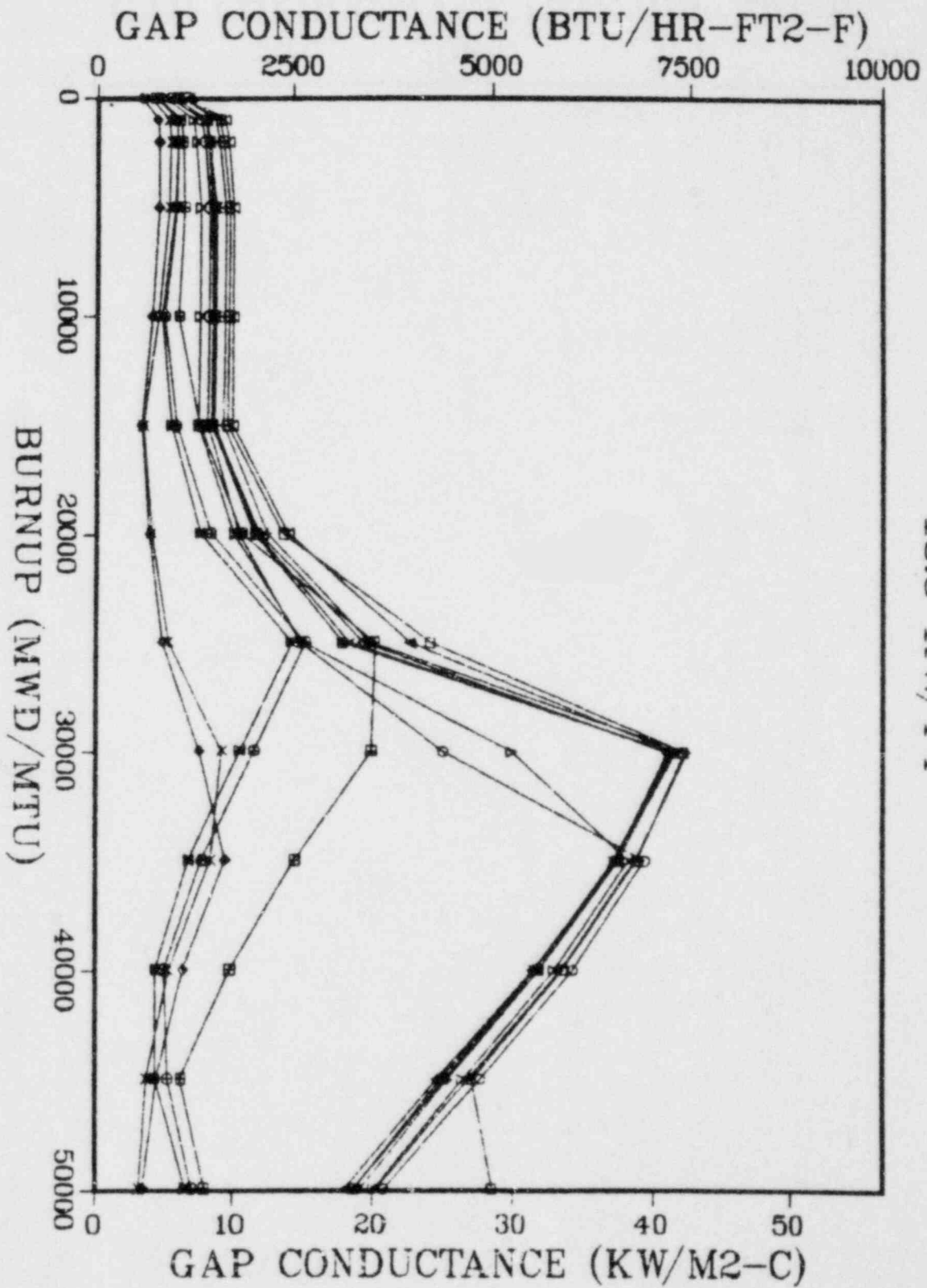


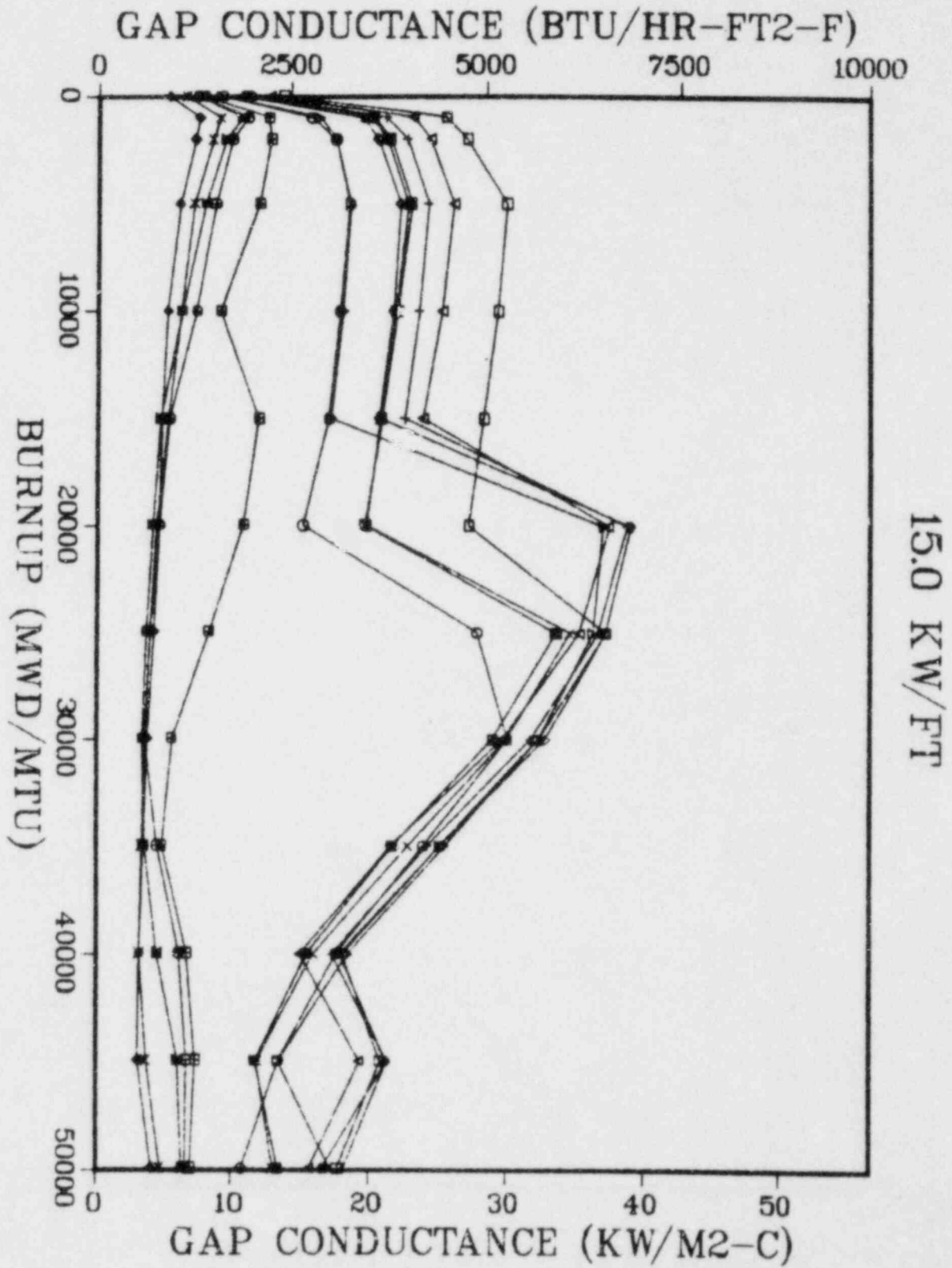


5.0 KW/FT

CORE AVERAGE ROD







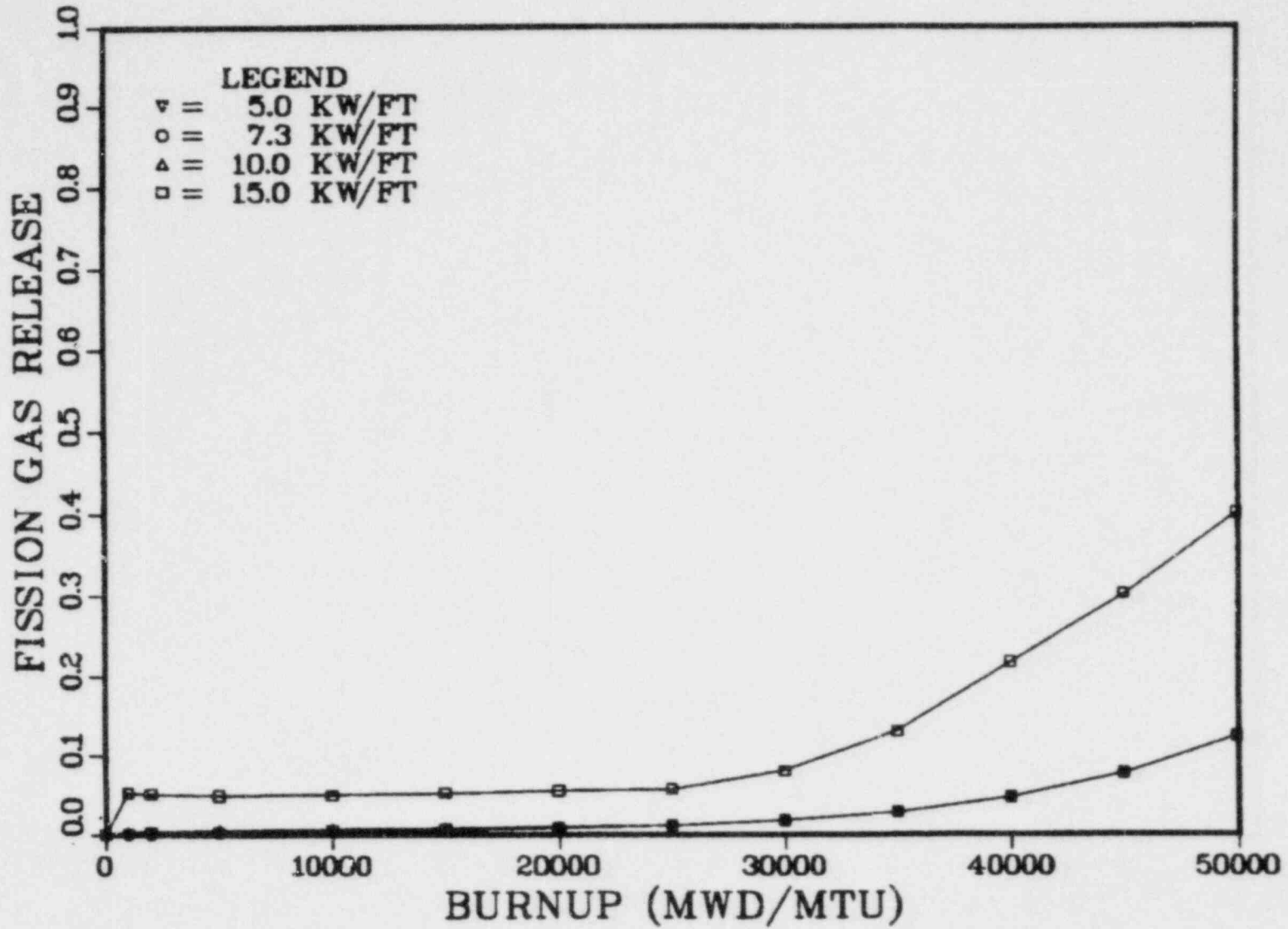
## APPENDIX I

### FISSION GAS RELEASE

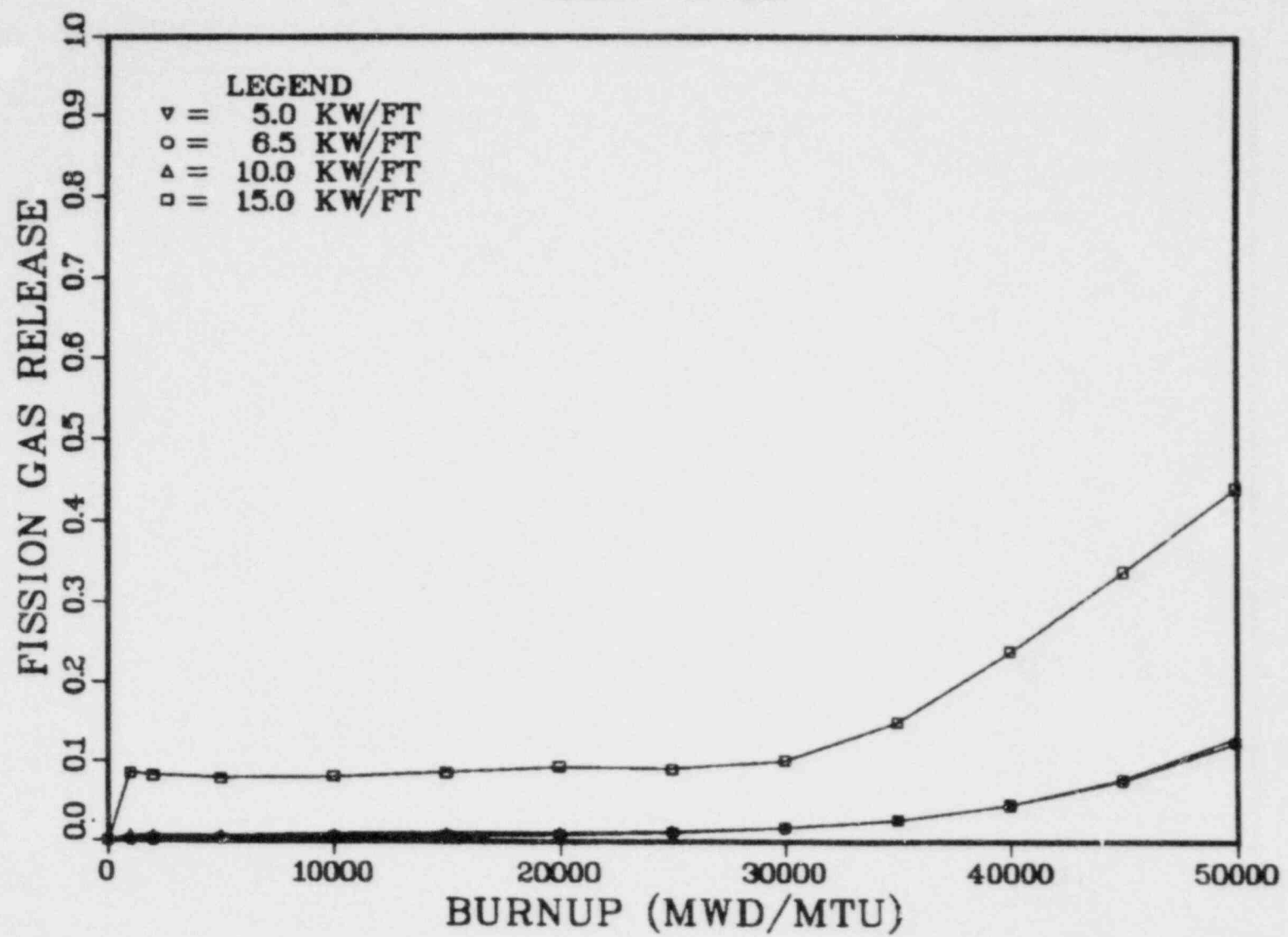
The following graphs show the effects of burnup on fission gas release, and the data are rod average fission gas release at specified rod peak burnups. Examination of the graphs shows that high fission gas release is directly related to high burnups and power ratings.

In general, the curves for the first three power levels coincide, showing little effect of rod power, while there is a noticeable increase in the amount of fission gas released at 15 kW/ft. The effect at lower power levels is due to the minimum values predicted at the NRC-corrected Beyer-Hann fission gas release model. Burnup considerations are predominant for the 10 kW/ft and lower power levels, while it is not until 15 kW/ft that temperature considerations also play an important role. At 15 kW/ft fission gas release is greater for the BWRs than for the PWRs. This is attributed to the lower gap conductivity of unpressurized BWR fuel design which results in higher fuel temperatures.

# B&W 15X15

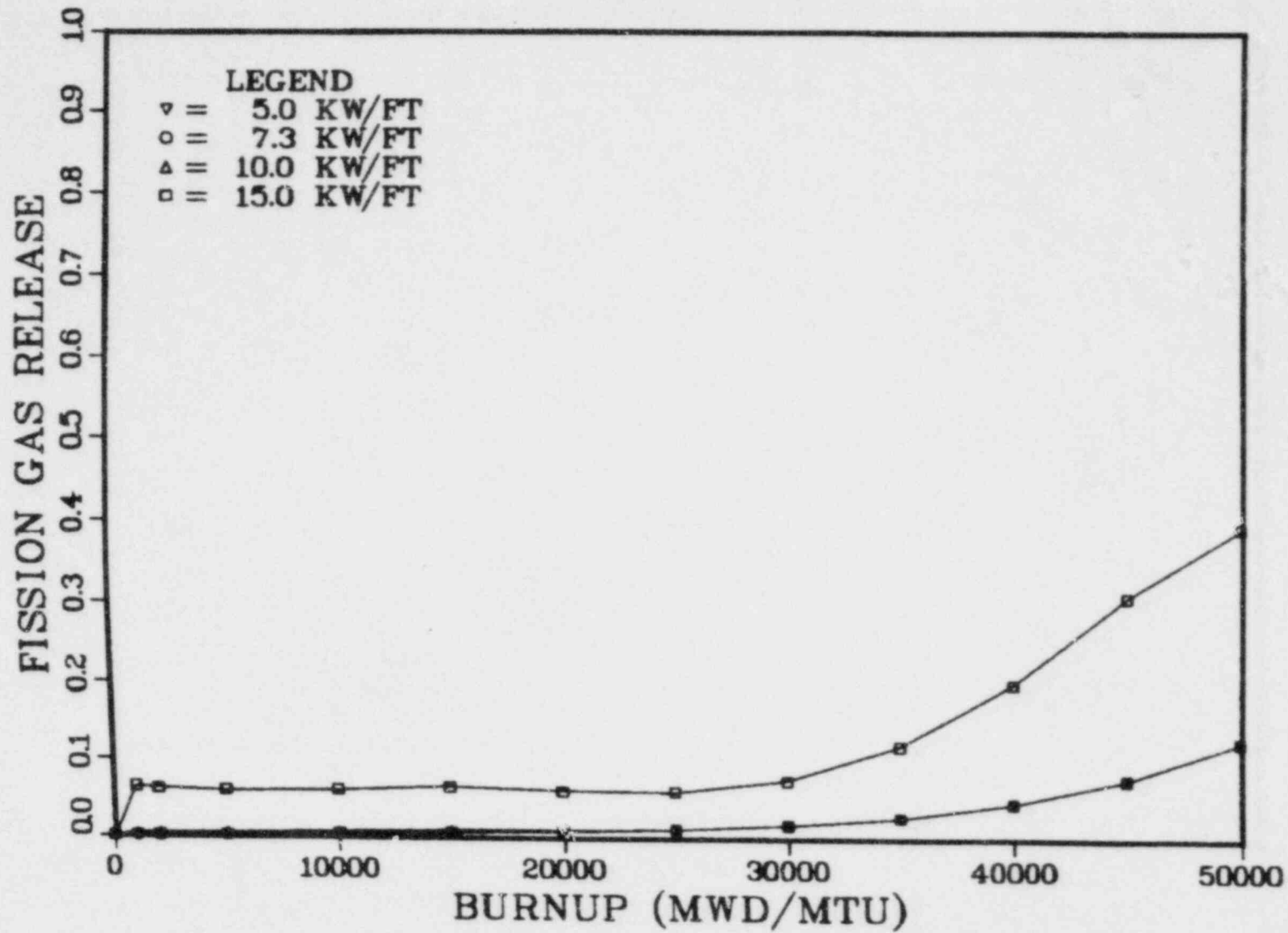


# B&W 17X17

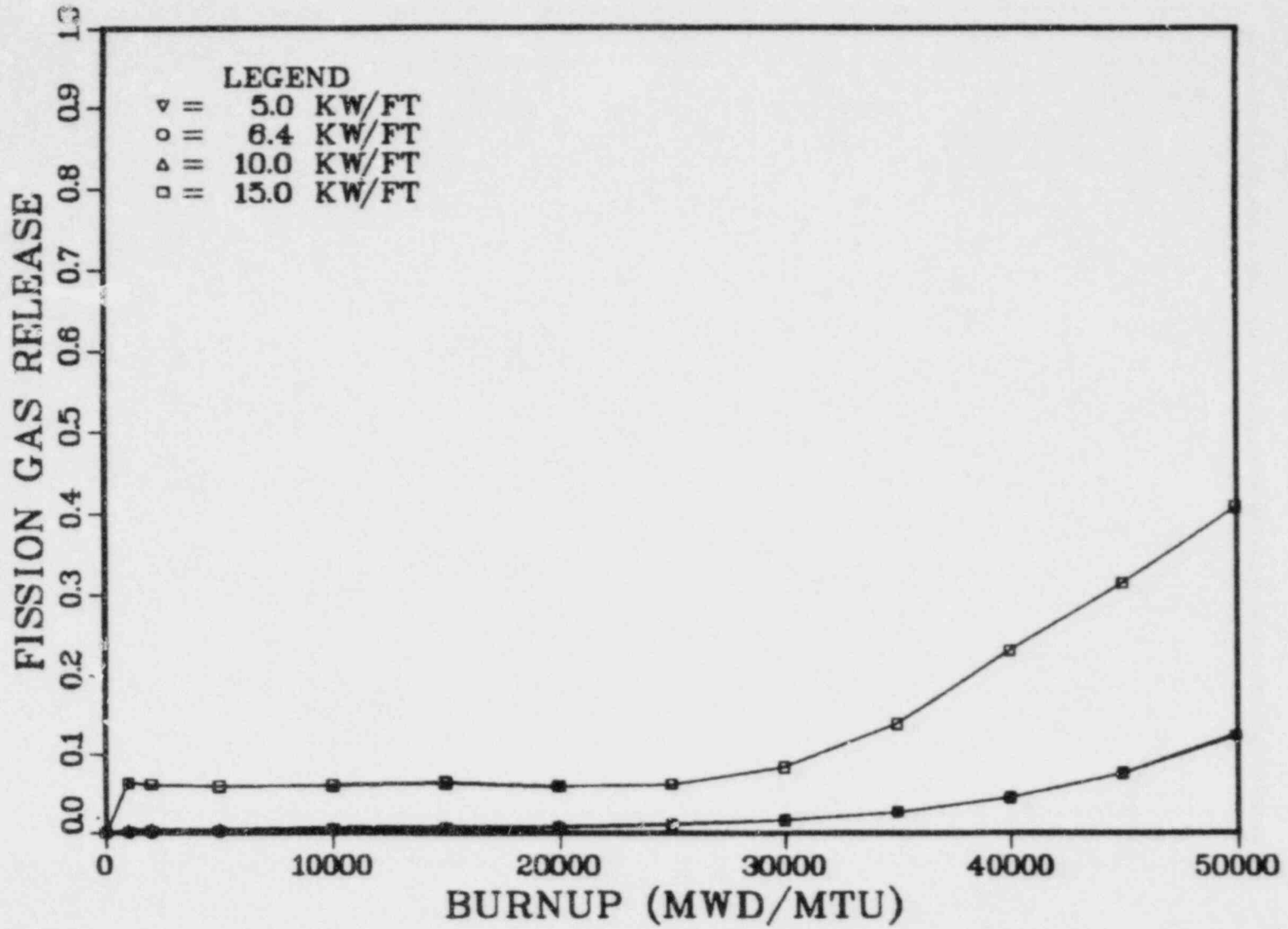




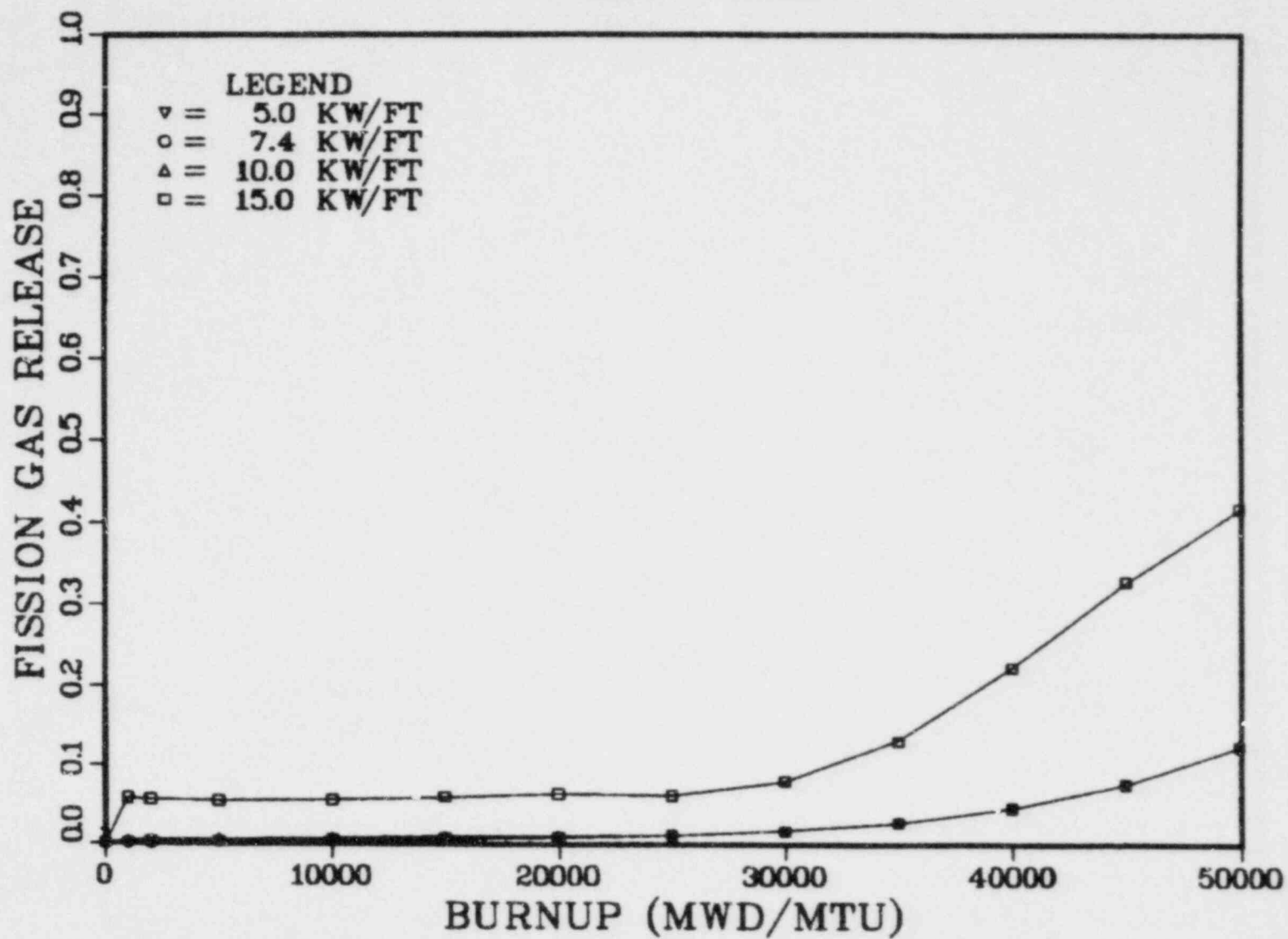
# C-E 14X14



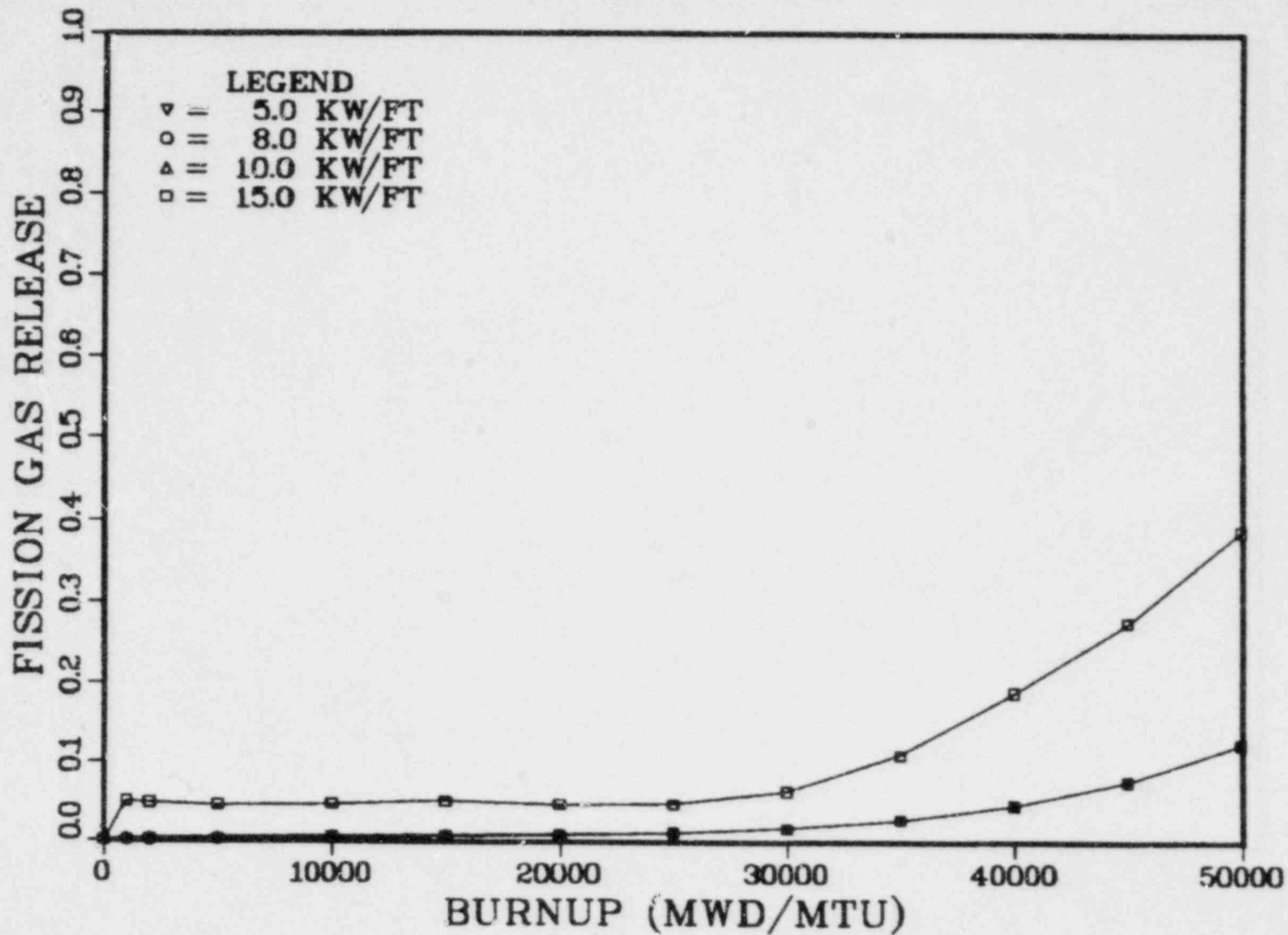
# C-E 16X16



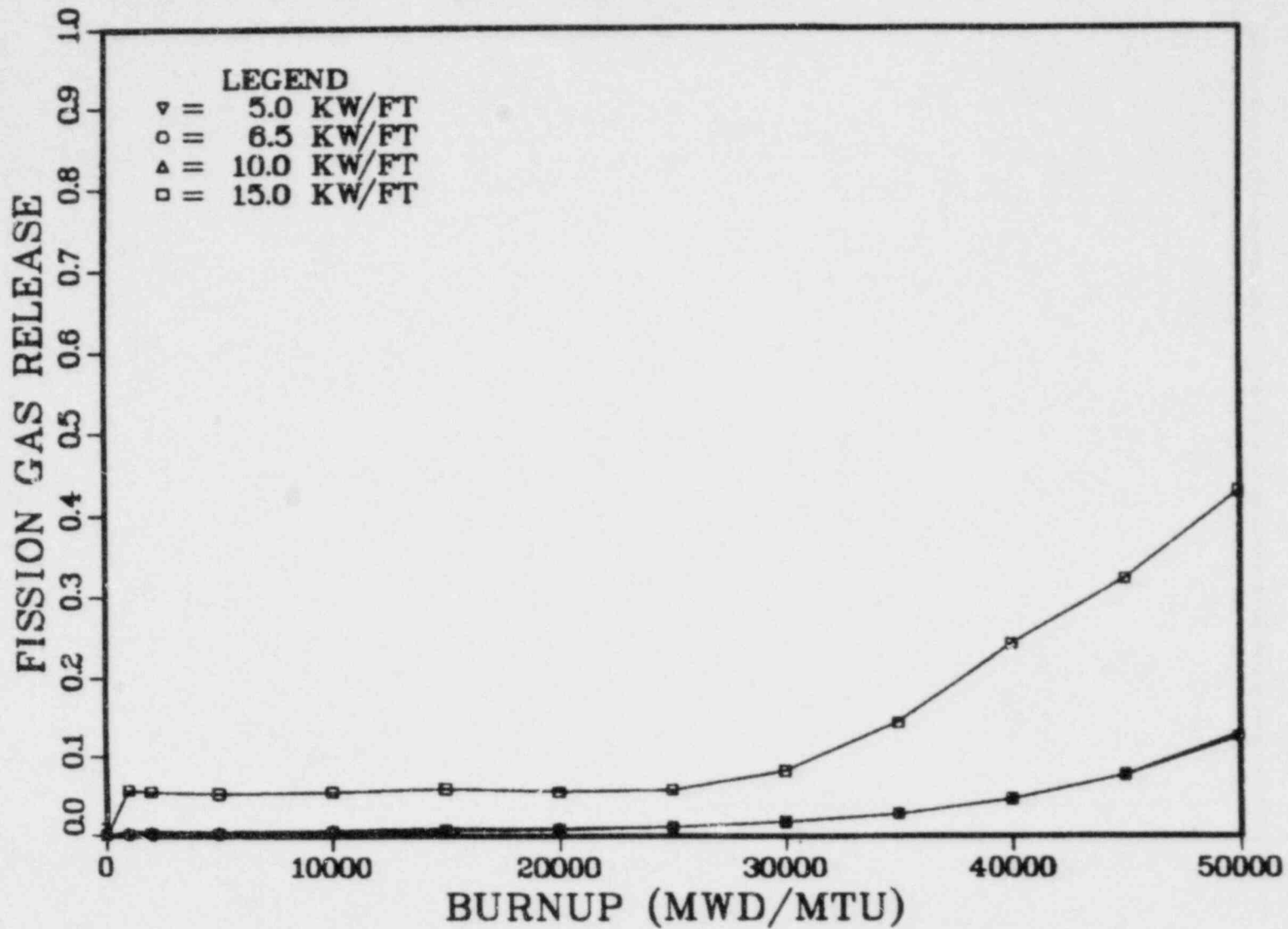
# WEST 14X14



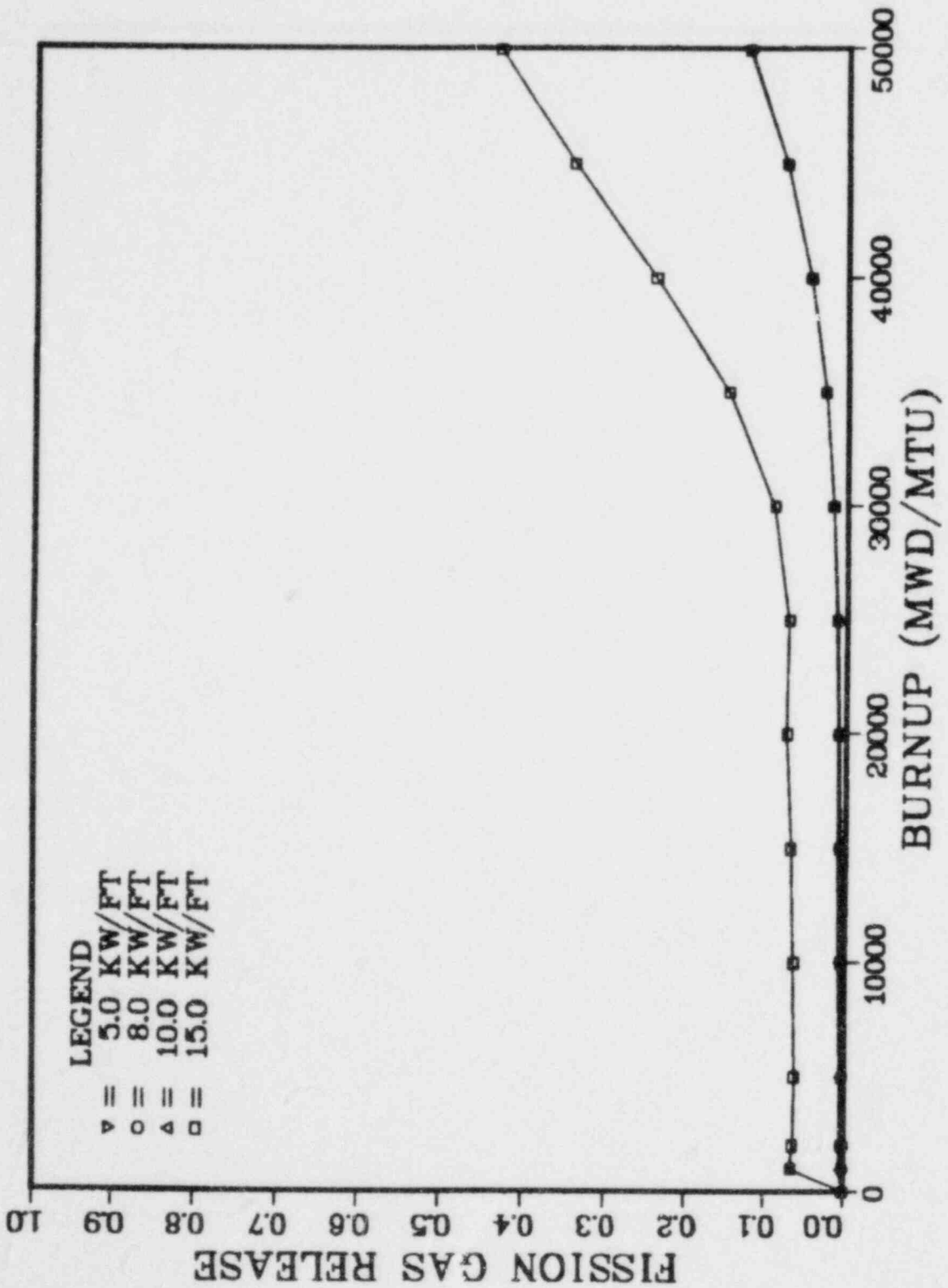
# WEST 15X15



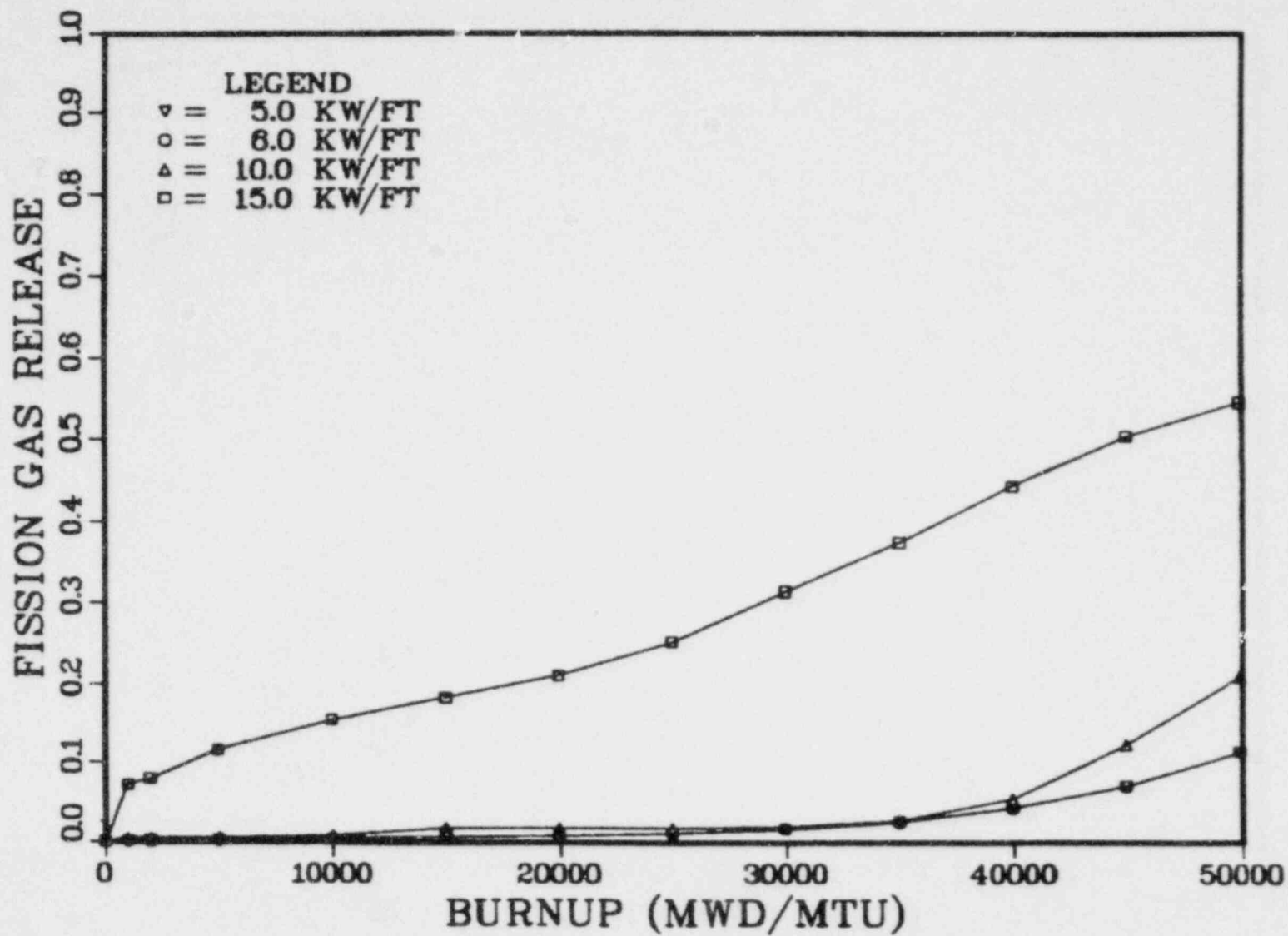
# WEST 17X17



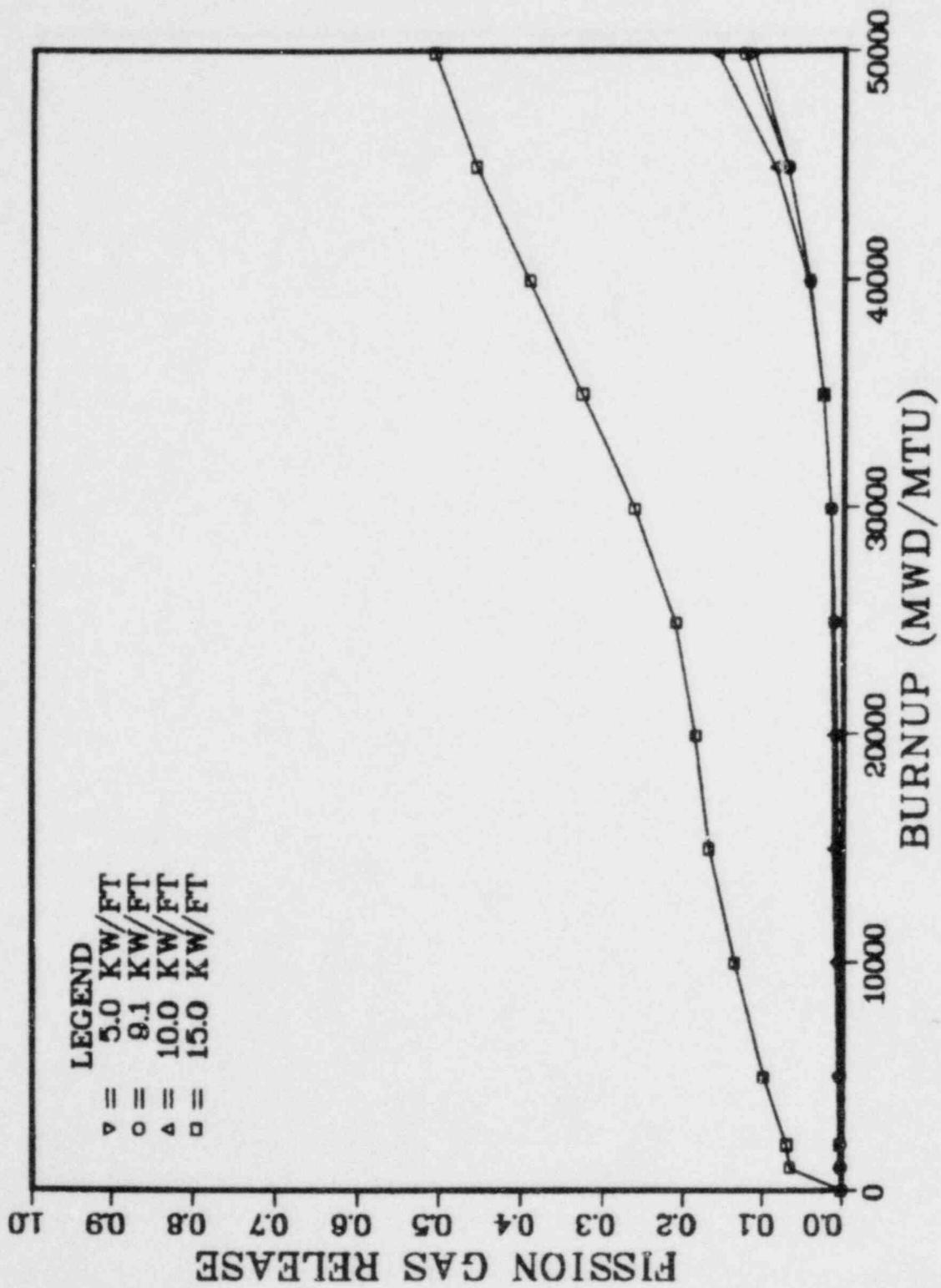
# EXXON 15X15



## EXXON 8X8

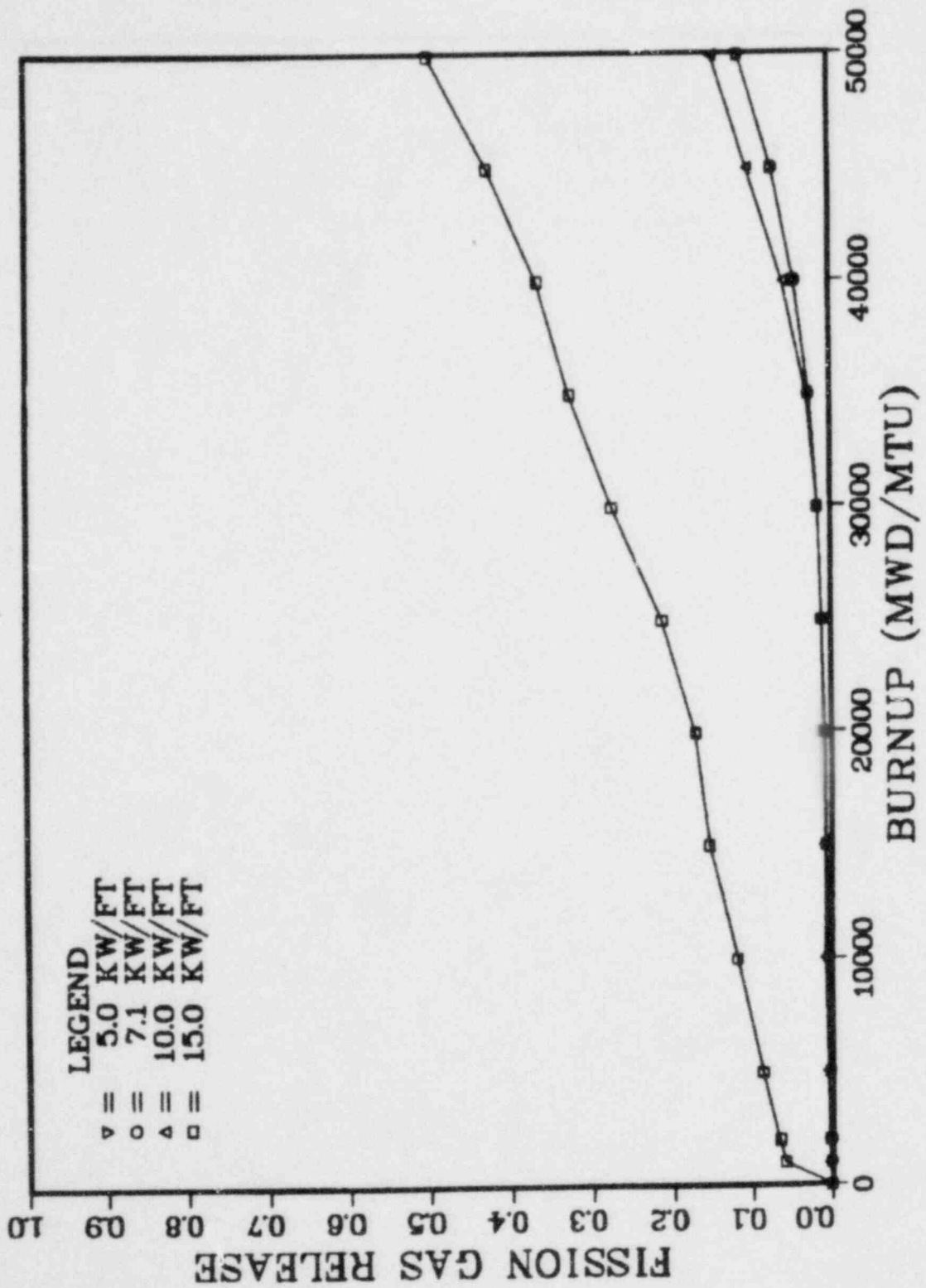


G.E. 7X7

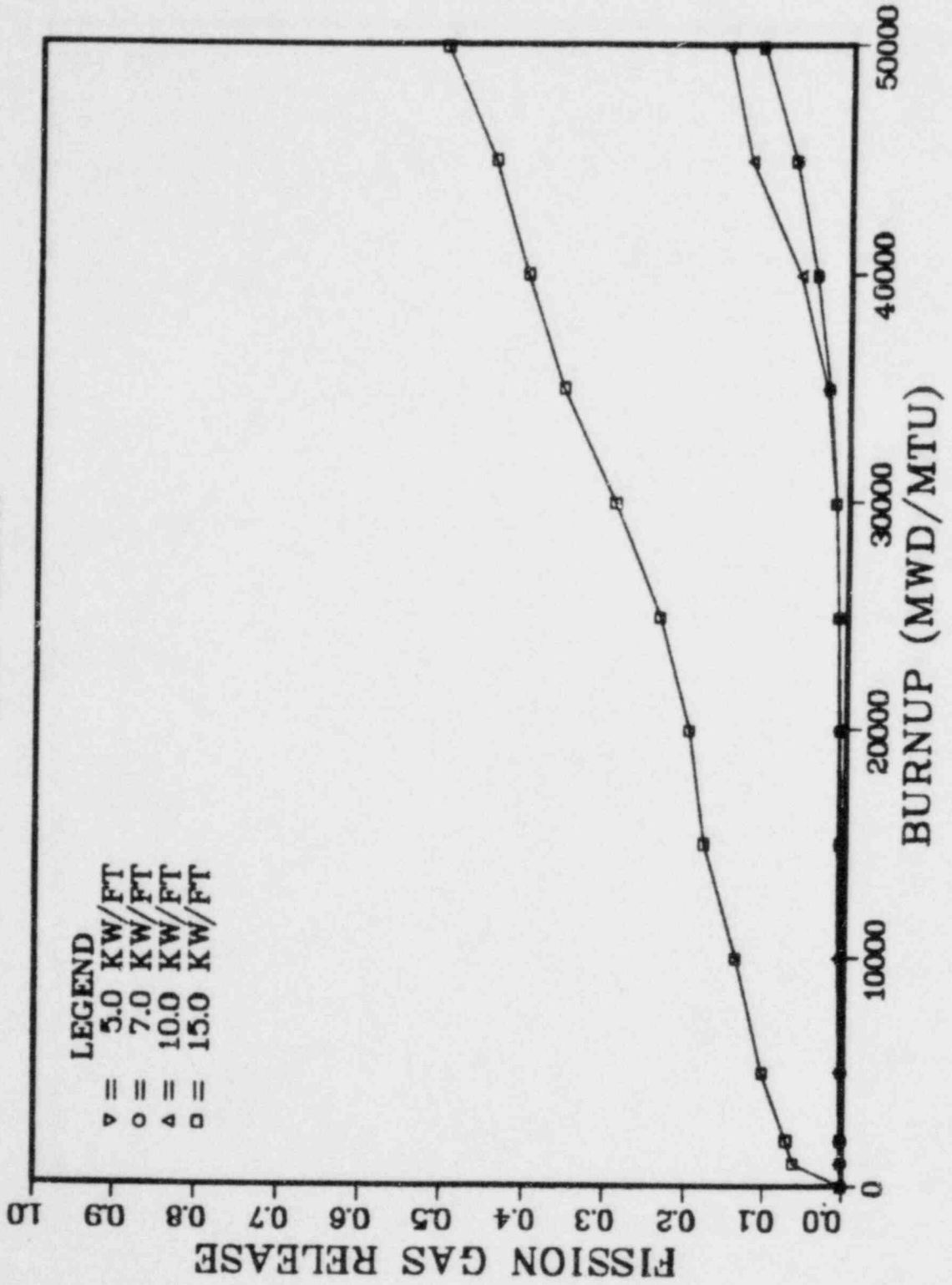




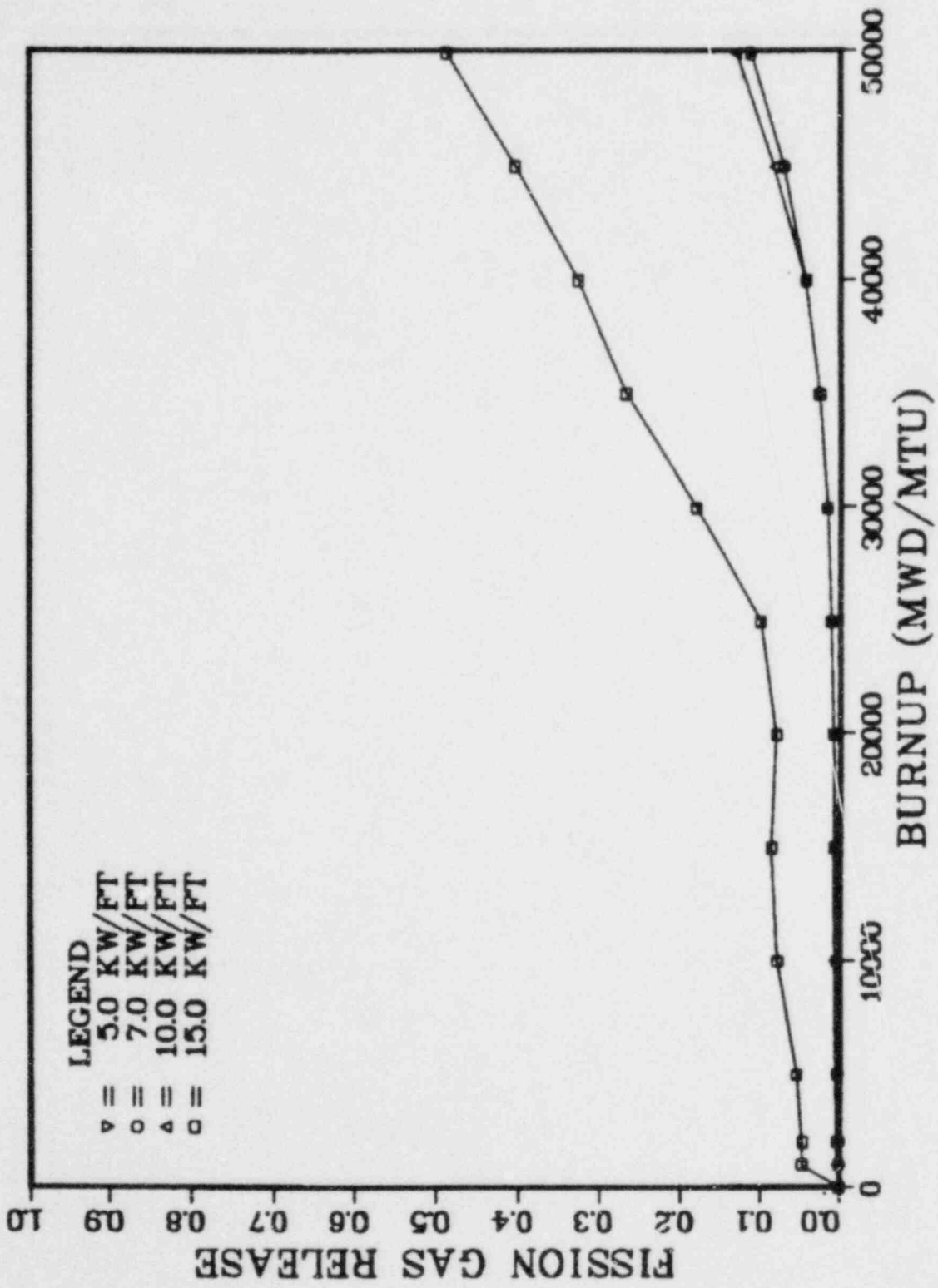
# G.E. 8X8



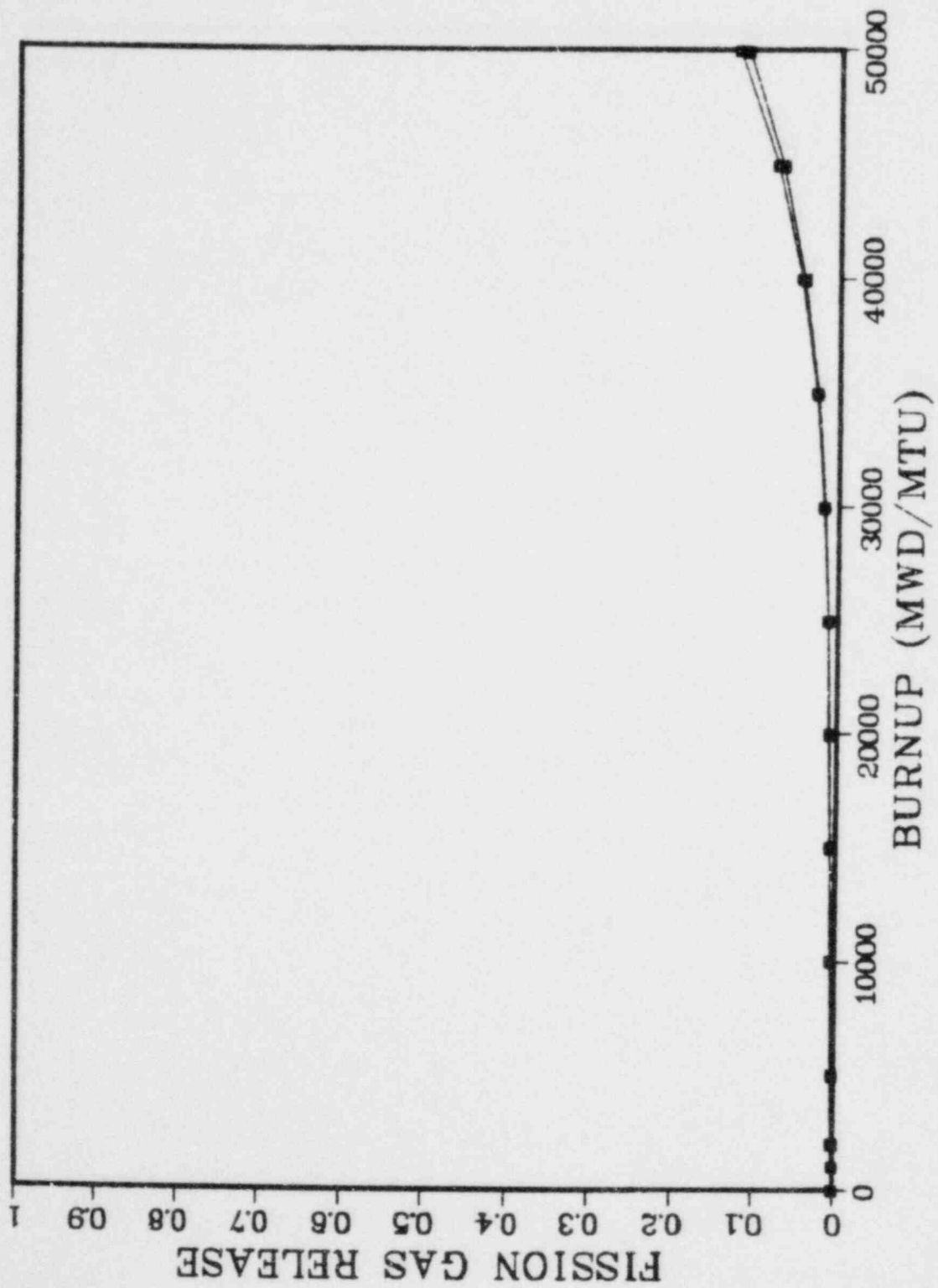
# G.E. 8X8R



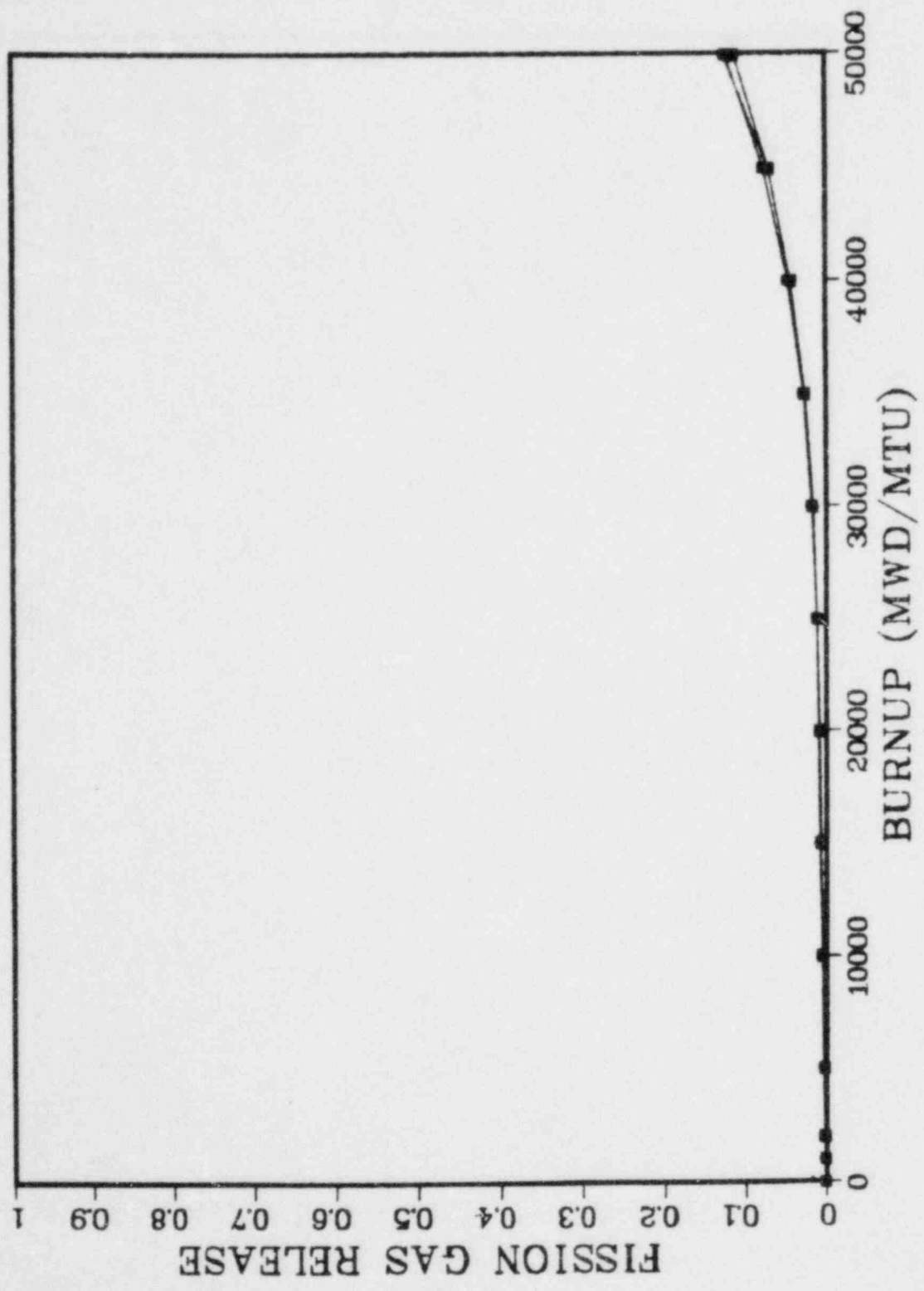
G.E. 8X8R-P



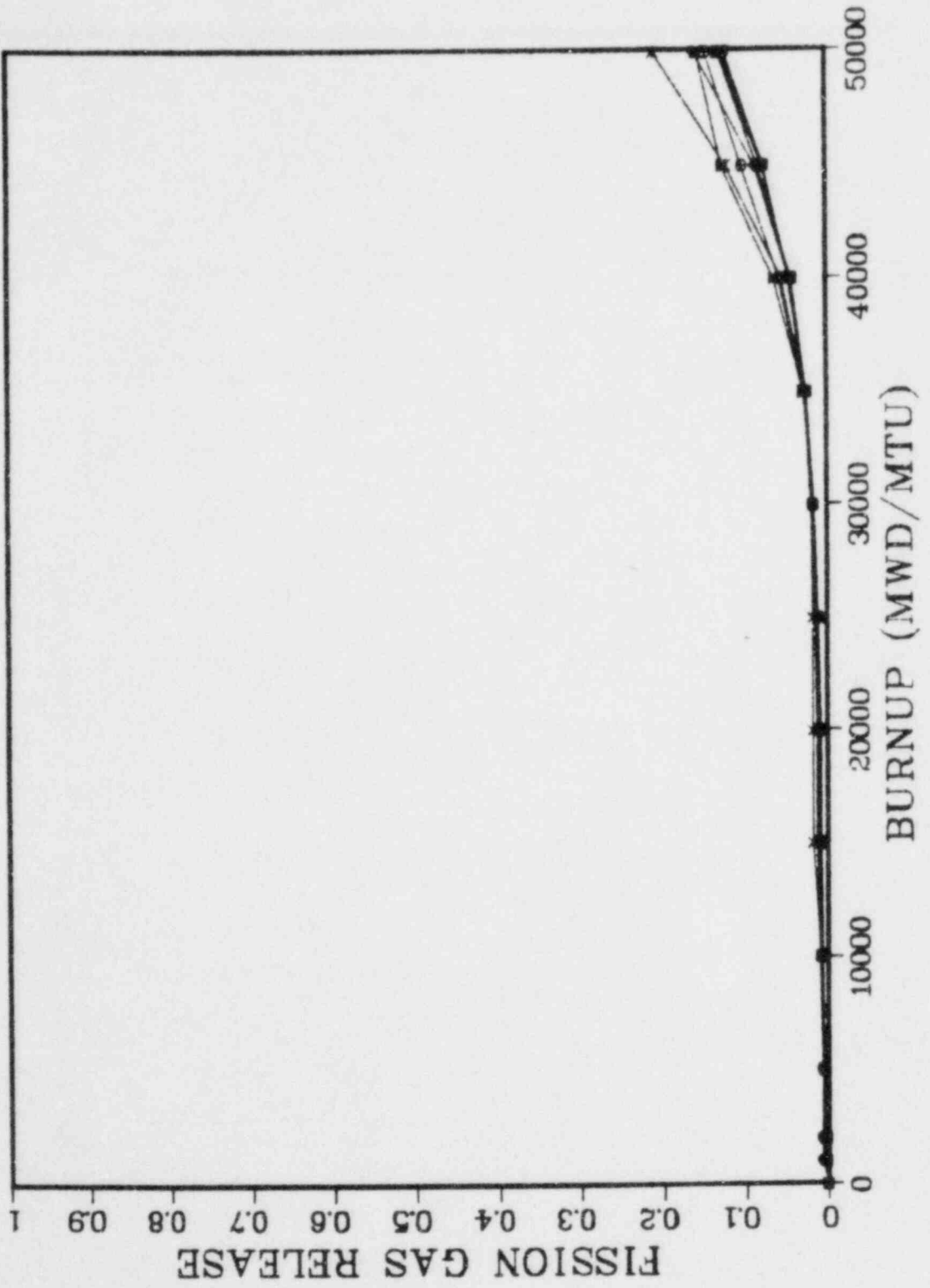
5.0 KW/FT



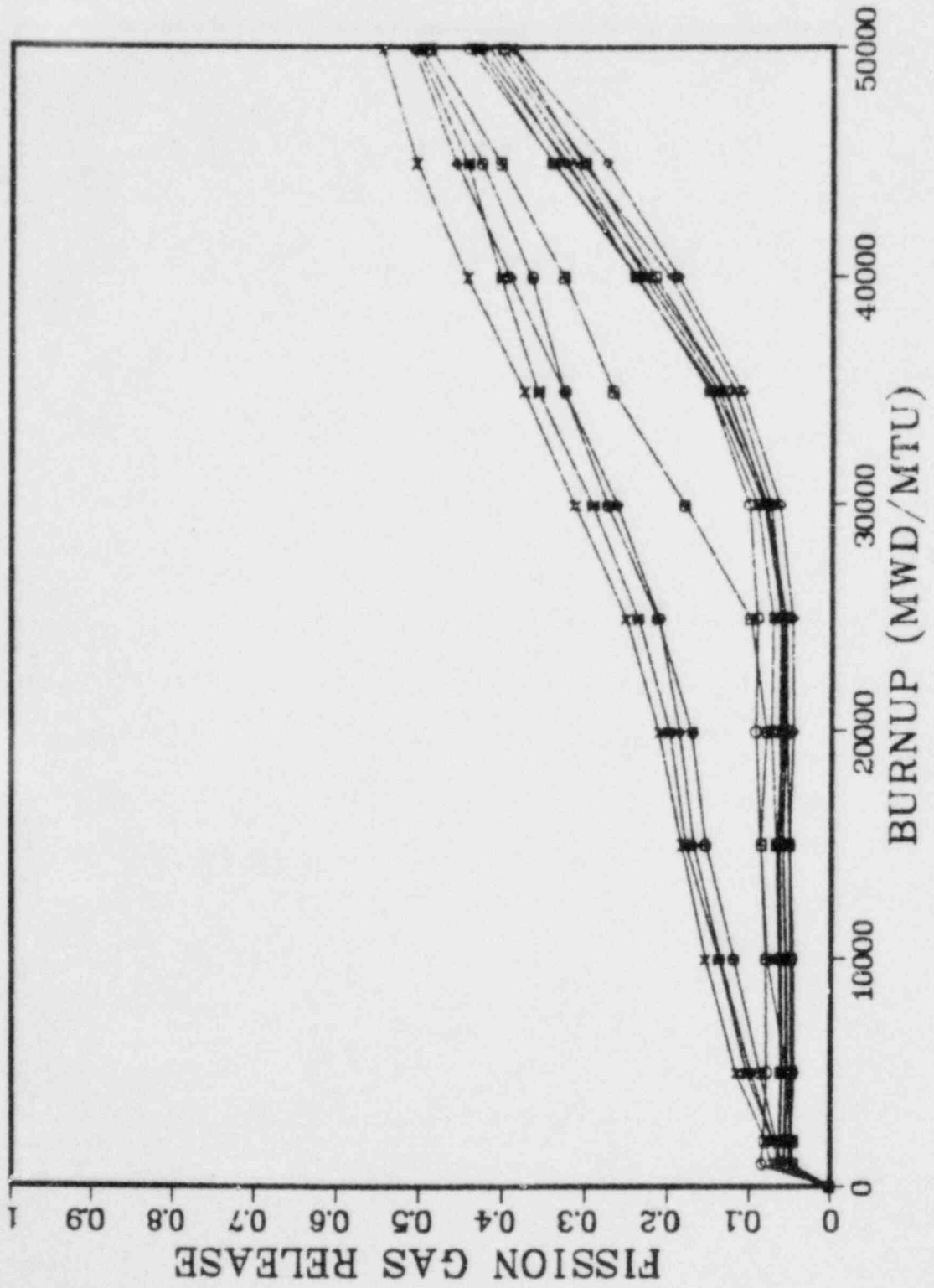
# CORE AVERAGE ROD



10.0 KW/FT



15.0 KW/FT



## APPENDIX J

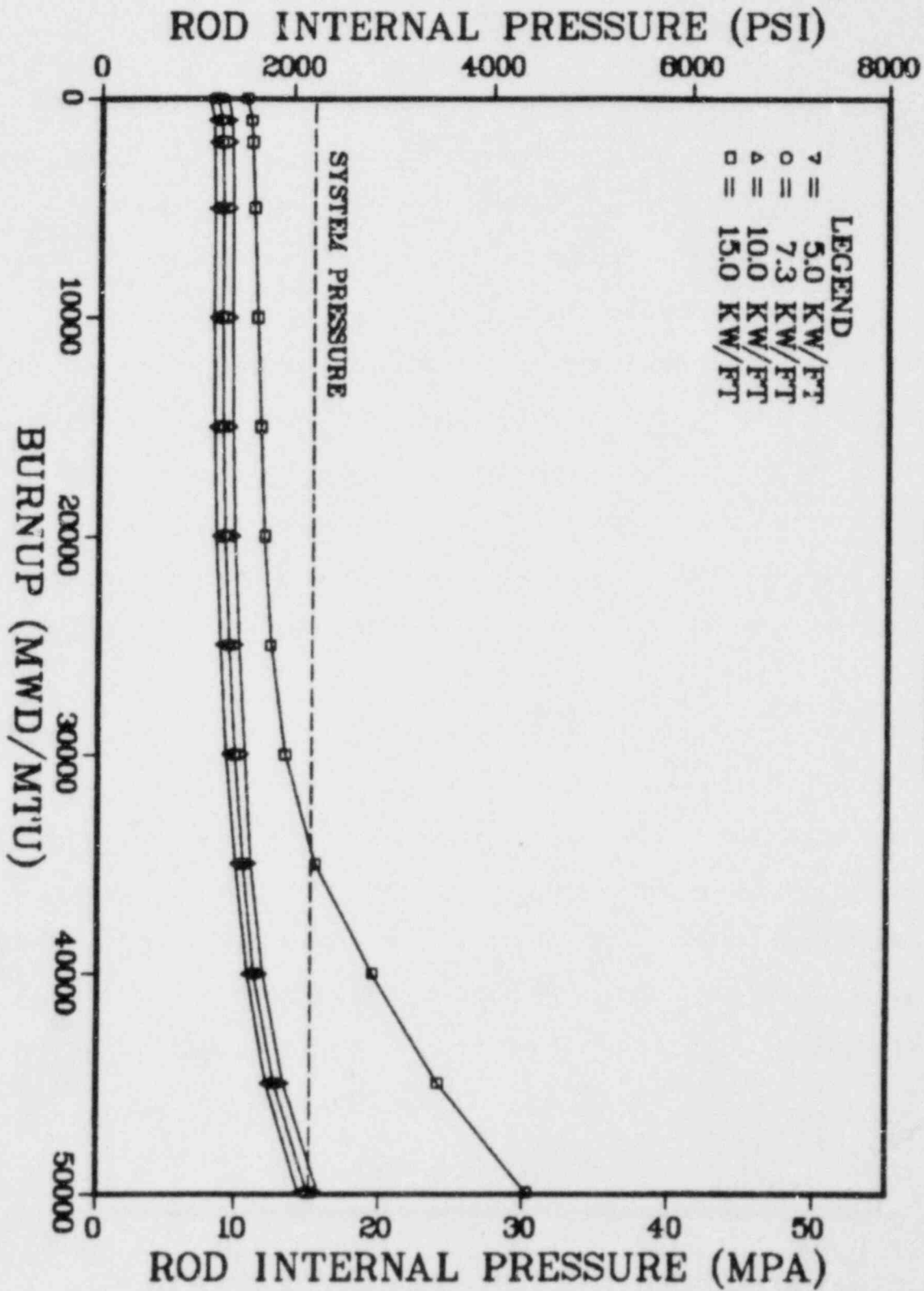
### ROD INTERNAL PRESSURE

The following graphs show the effects of burnup on rod internal pressure, and the data are rod average internal pressure at specified rod peak burnups. In all the cases studied, the rod internal pressure eventually exceeded the system pressure at some burnup level. These values normally exceed current discharge burnup. At 5 and 10 kW/ft and for the rod power associated with core average power, system pressure was not exceeded until 50,000 Mwd/MtU. At 15 kW/ft, system pressure was exceeded somewhat earlier.

Although the time in life at which the rod internal pressure exceeds system pressure is dependent on the power history of the rod, the code predicts that all fuel designs will eventually reach this condition at any power level. The power histories selected in this study are bounding. That is, the rod pressure criteria would be violated more quickly for these constant power histories than for those which only occasionally reach peak values.

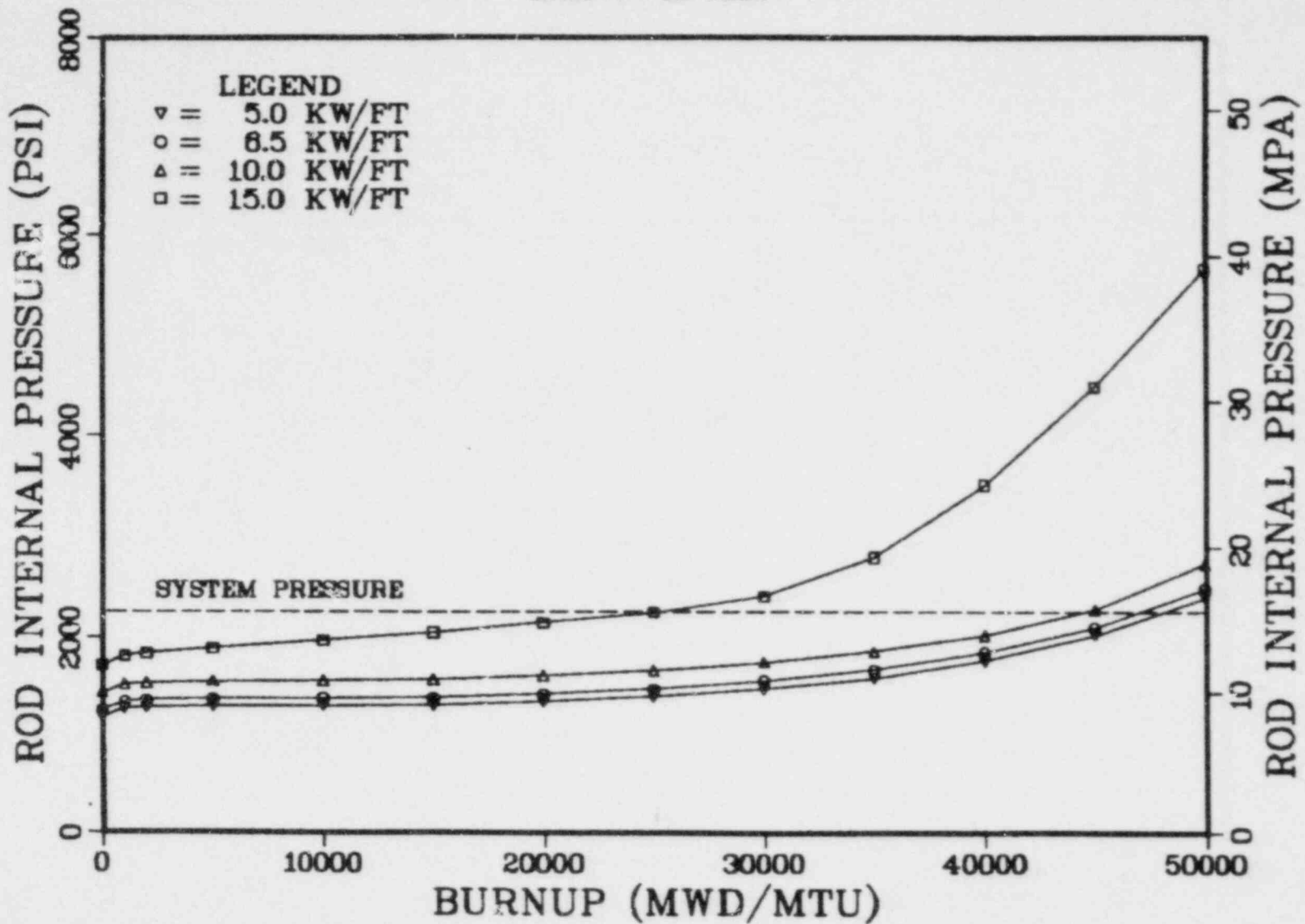
There is a substantial pressure difference between PWR and BWR designs at beginning of life due to the difference in initial prepressurization values. The BWR GE 7x7 fuel design has the lowest rod internal pressure value which is attributed to the large plenum volume.



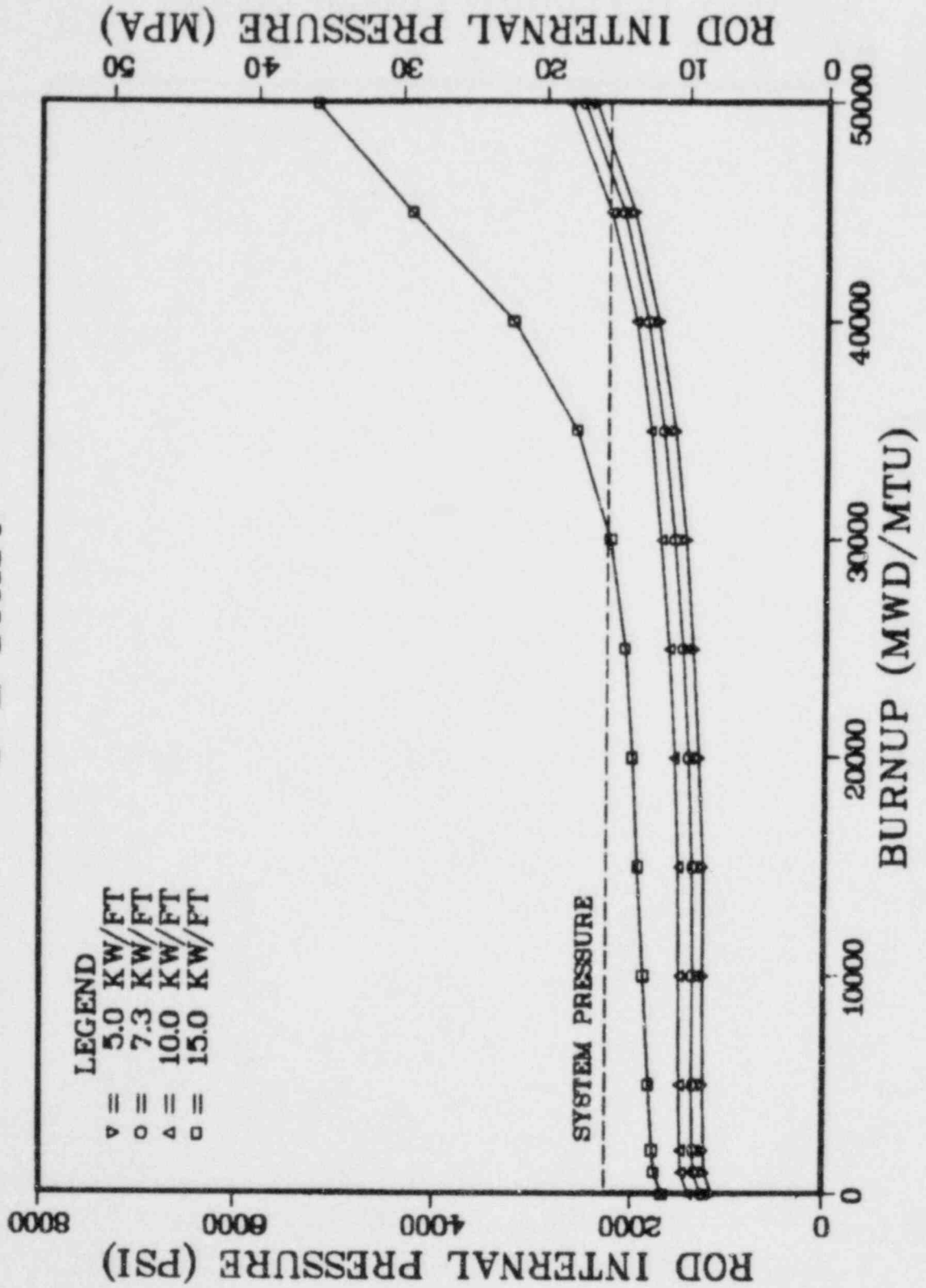


B&W 15X15

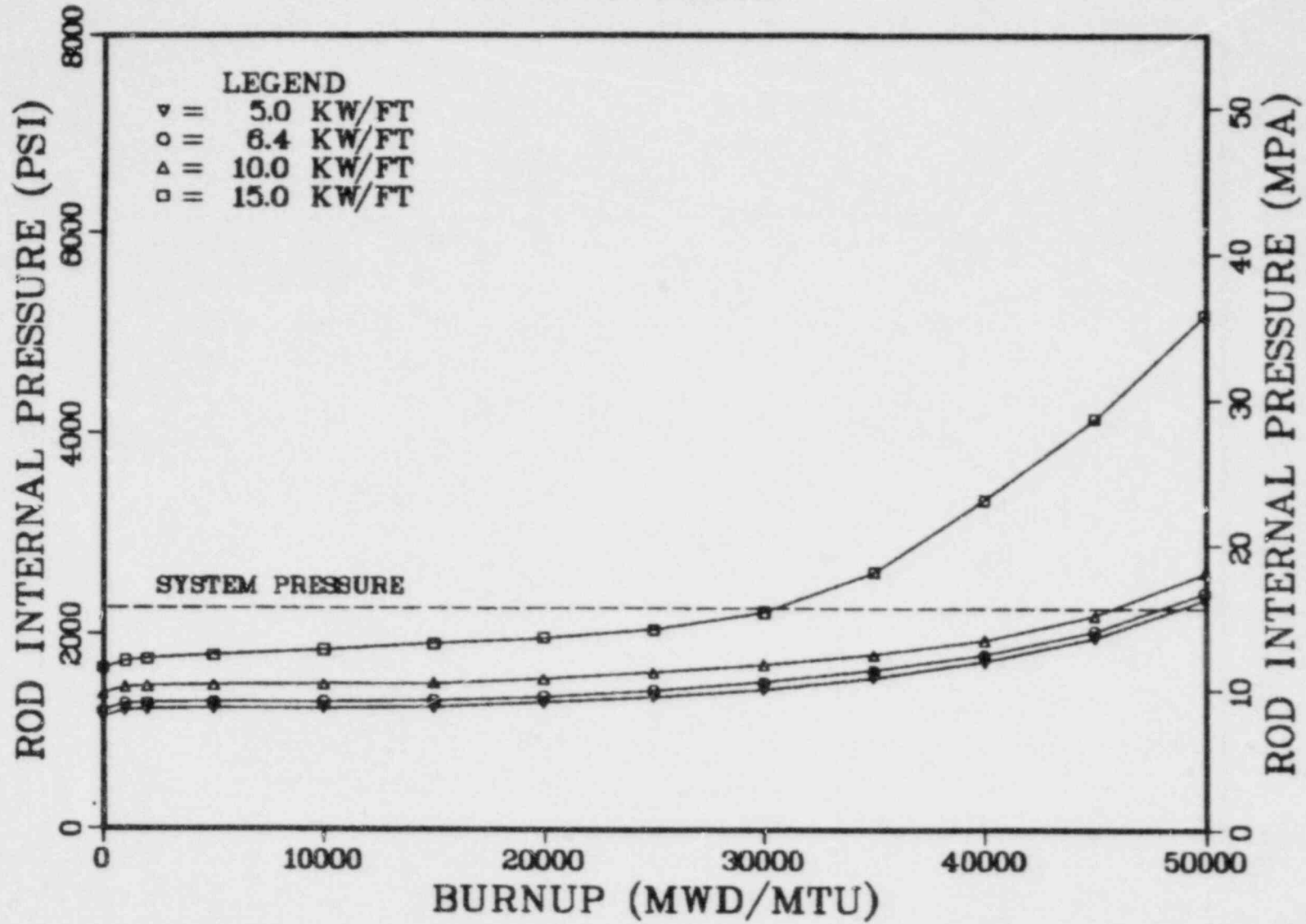
### B&W 17X17

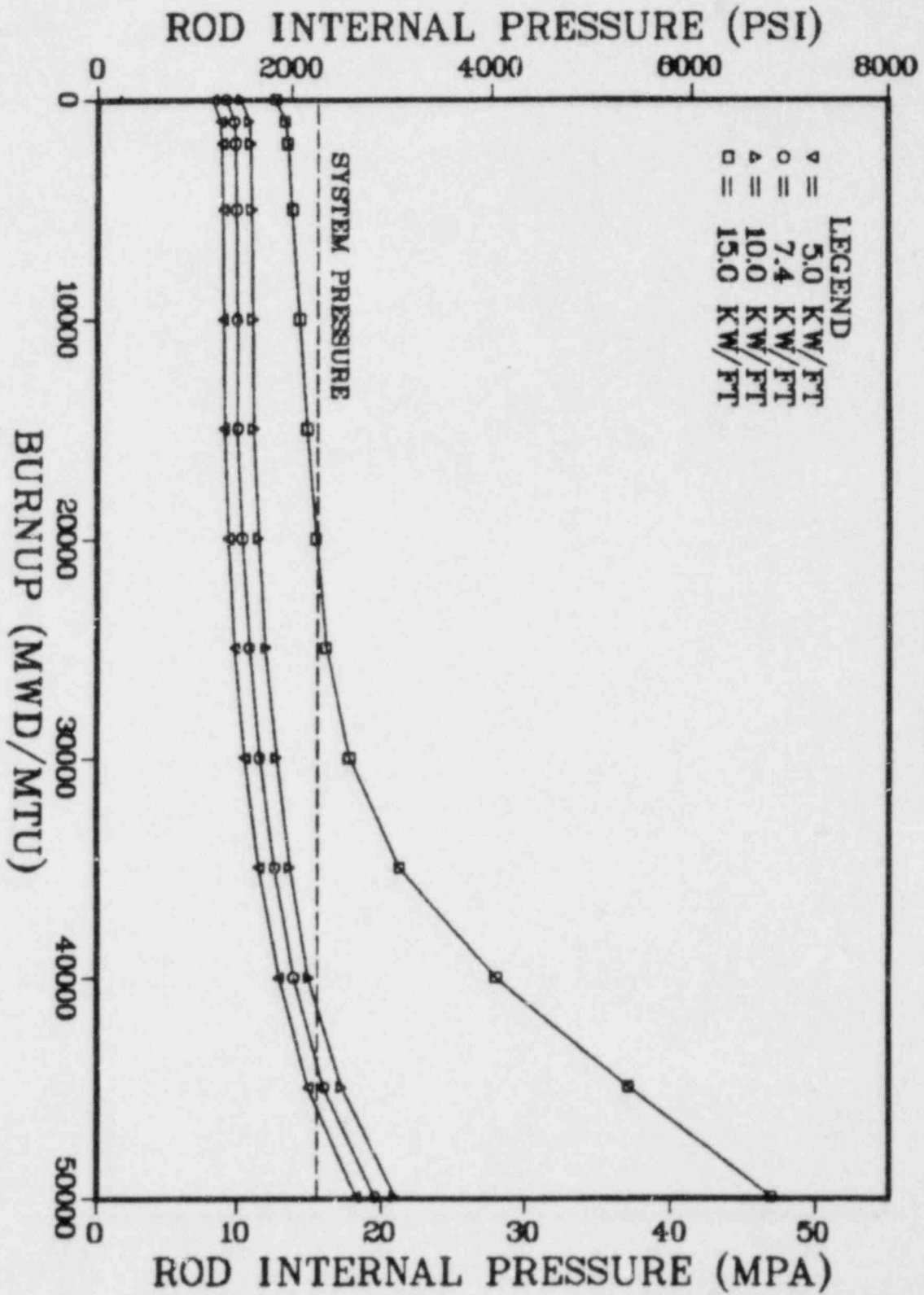


C-E 14X14



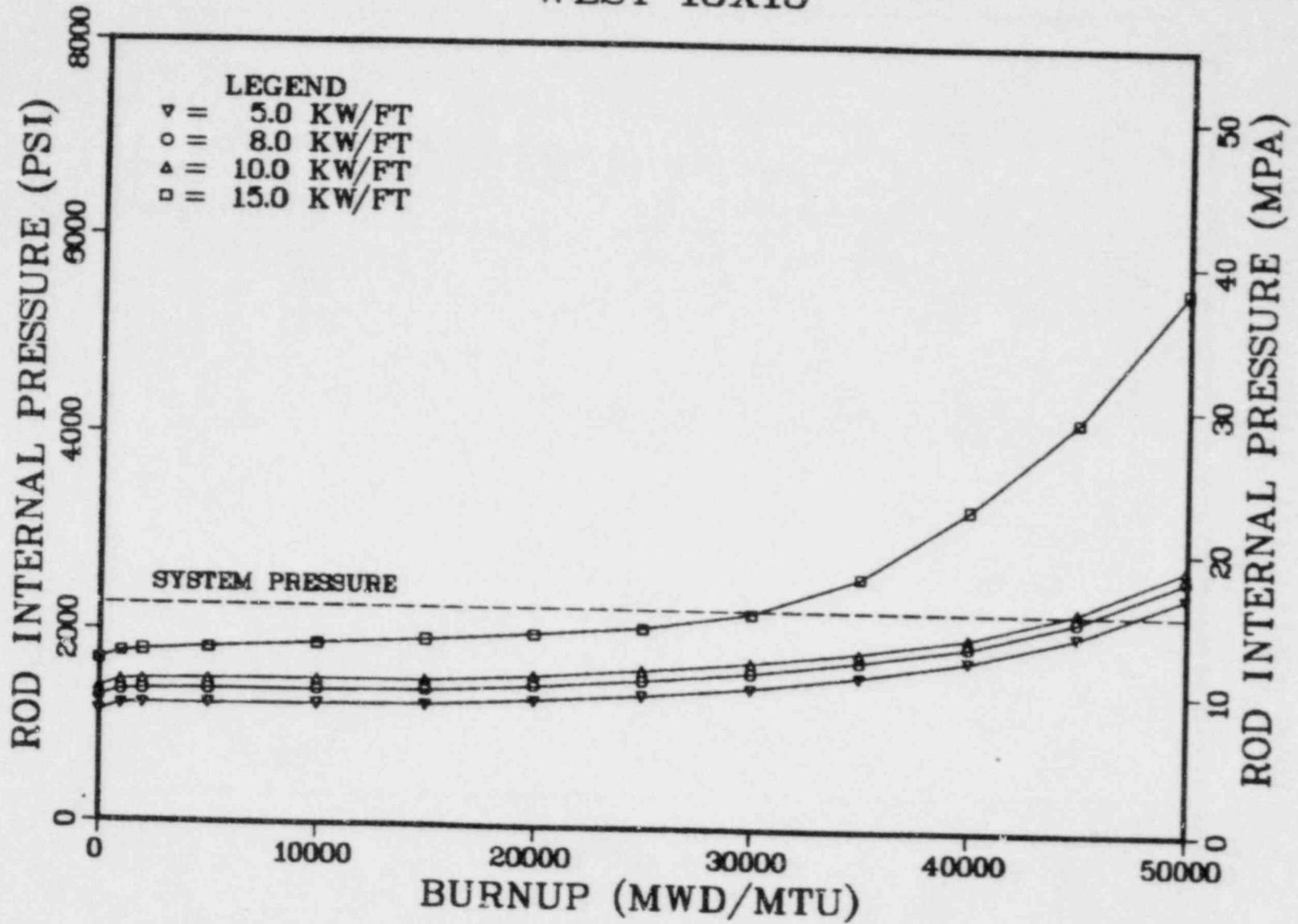
C-E 16X16



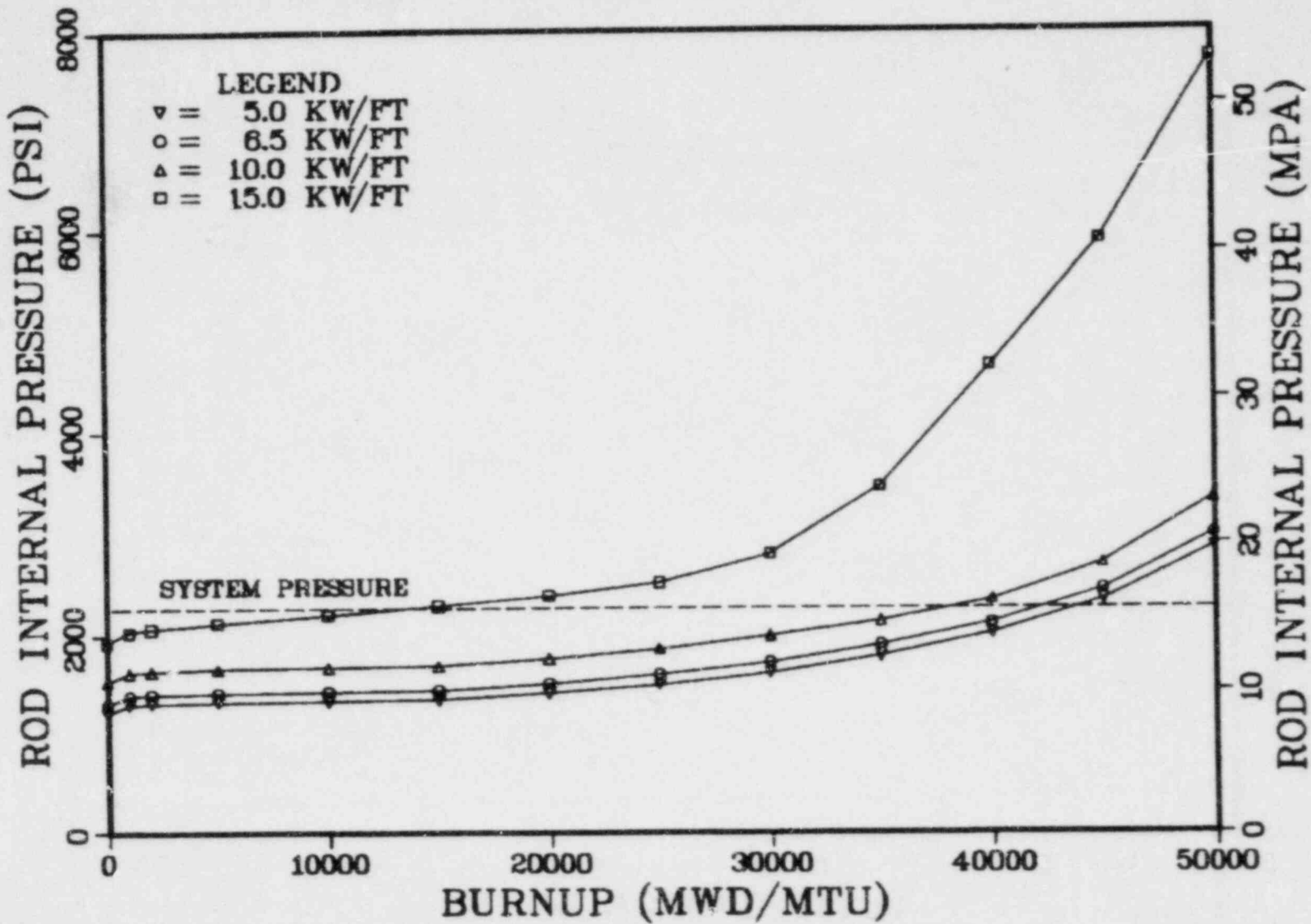


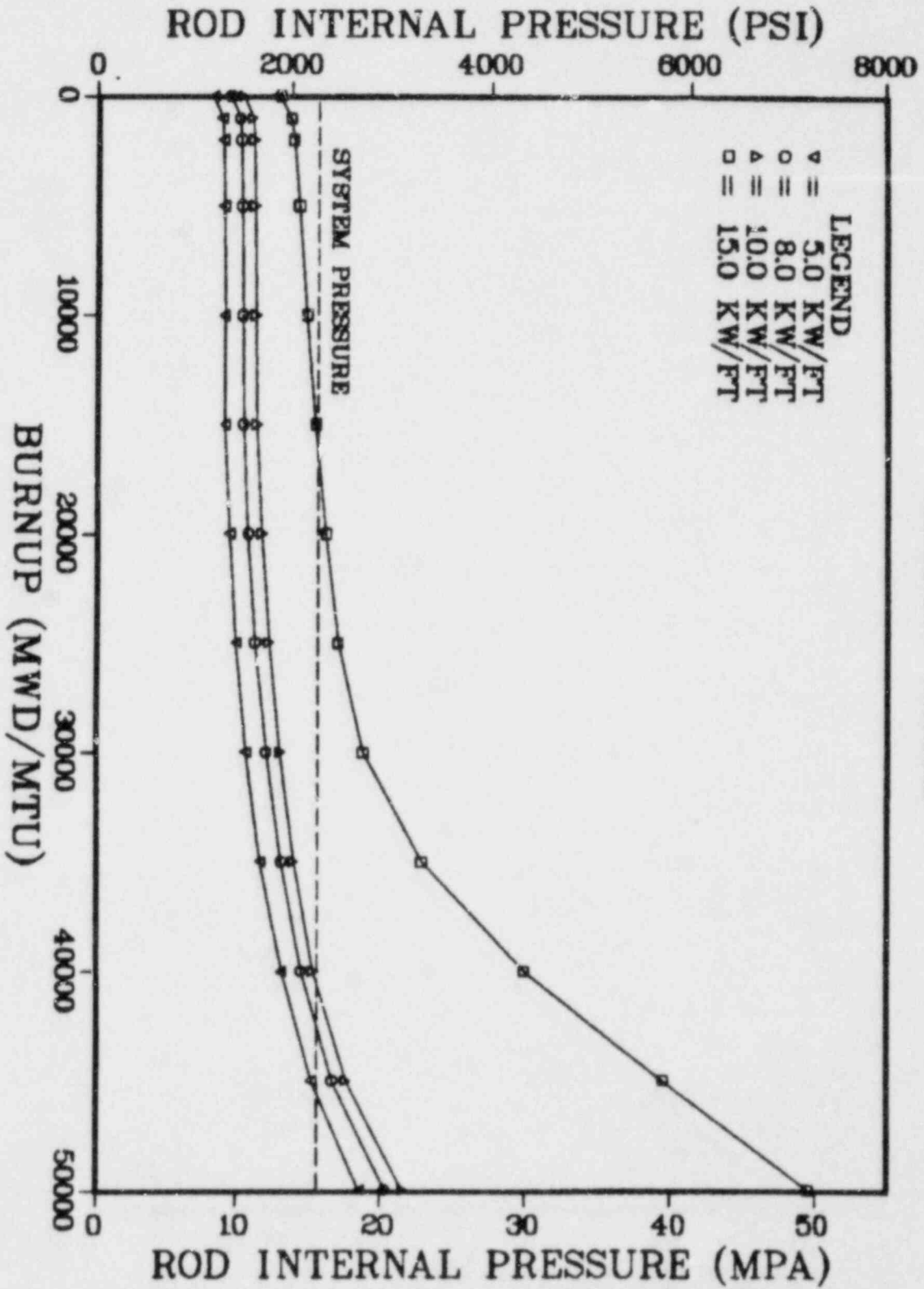
WEST 14X14

# WEST 15X15

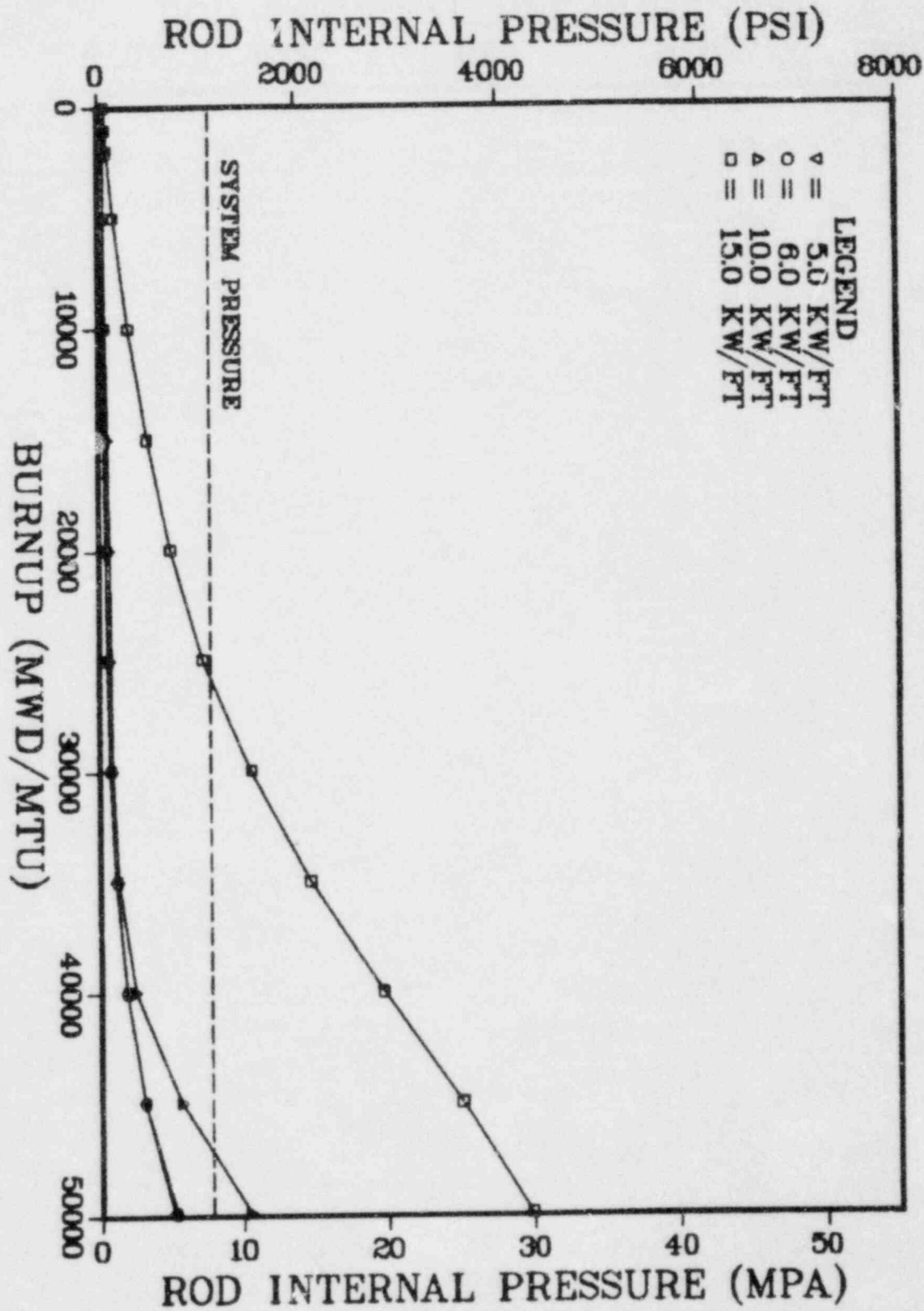


# WEST 17X17



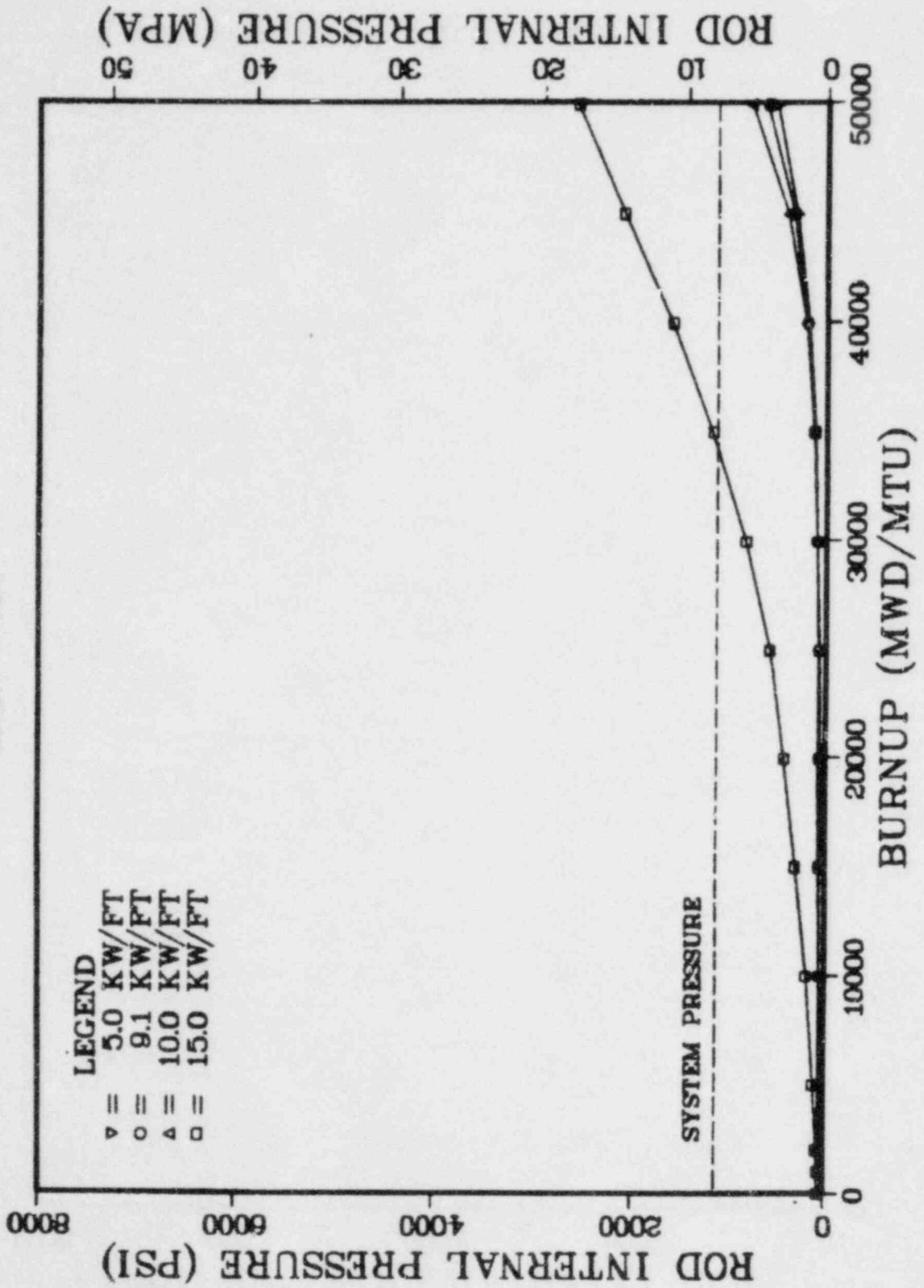




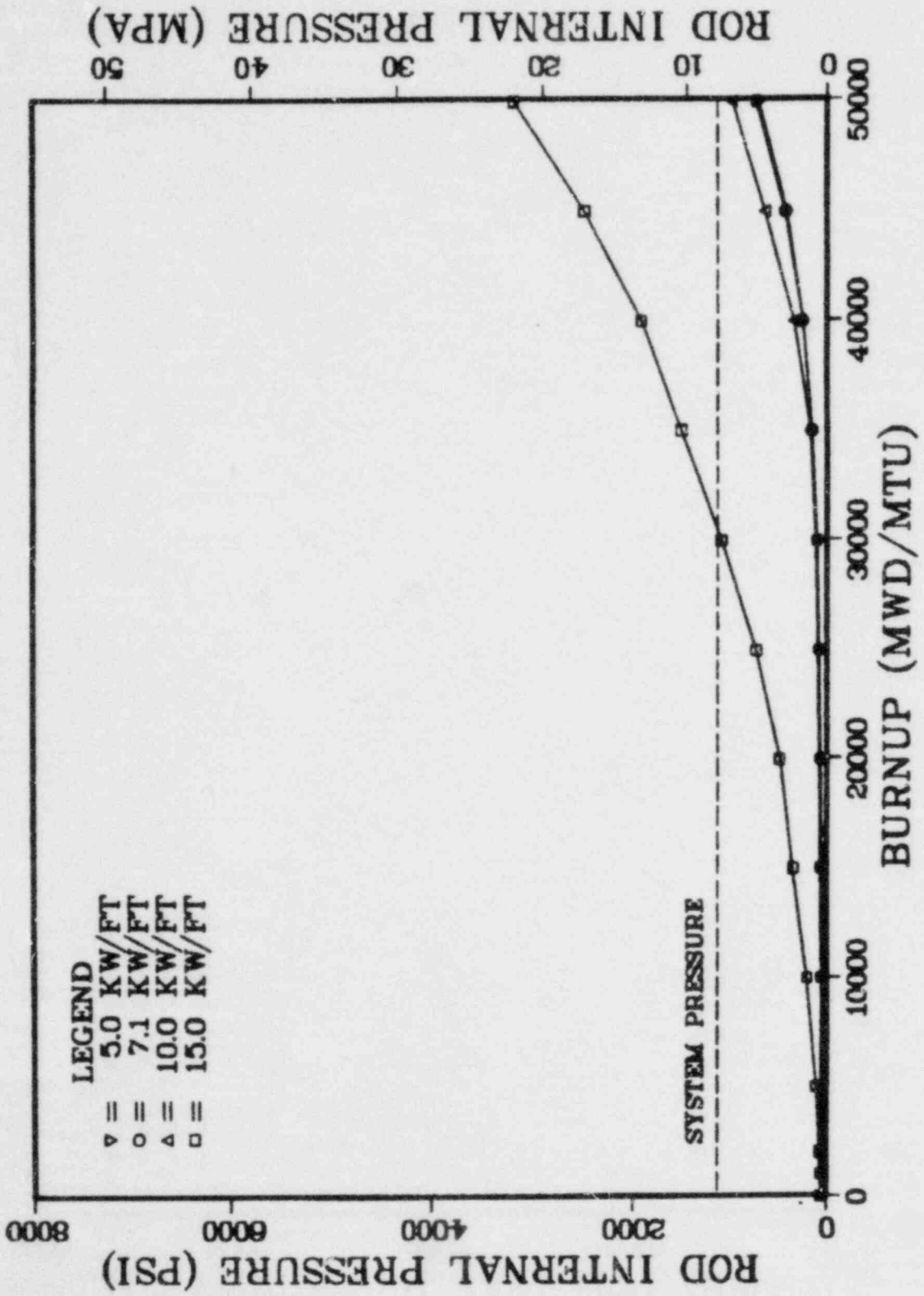


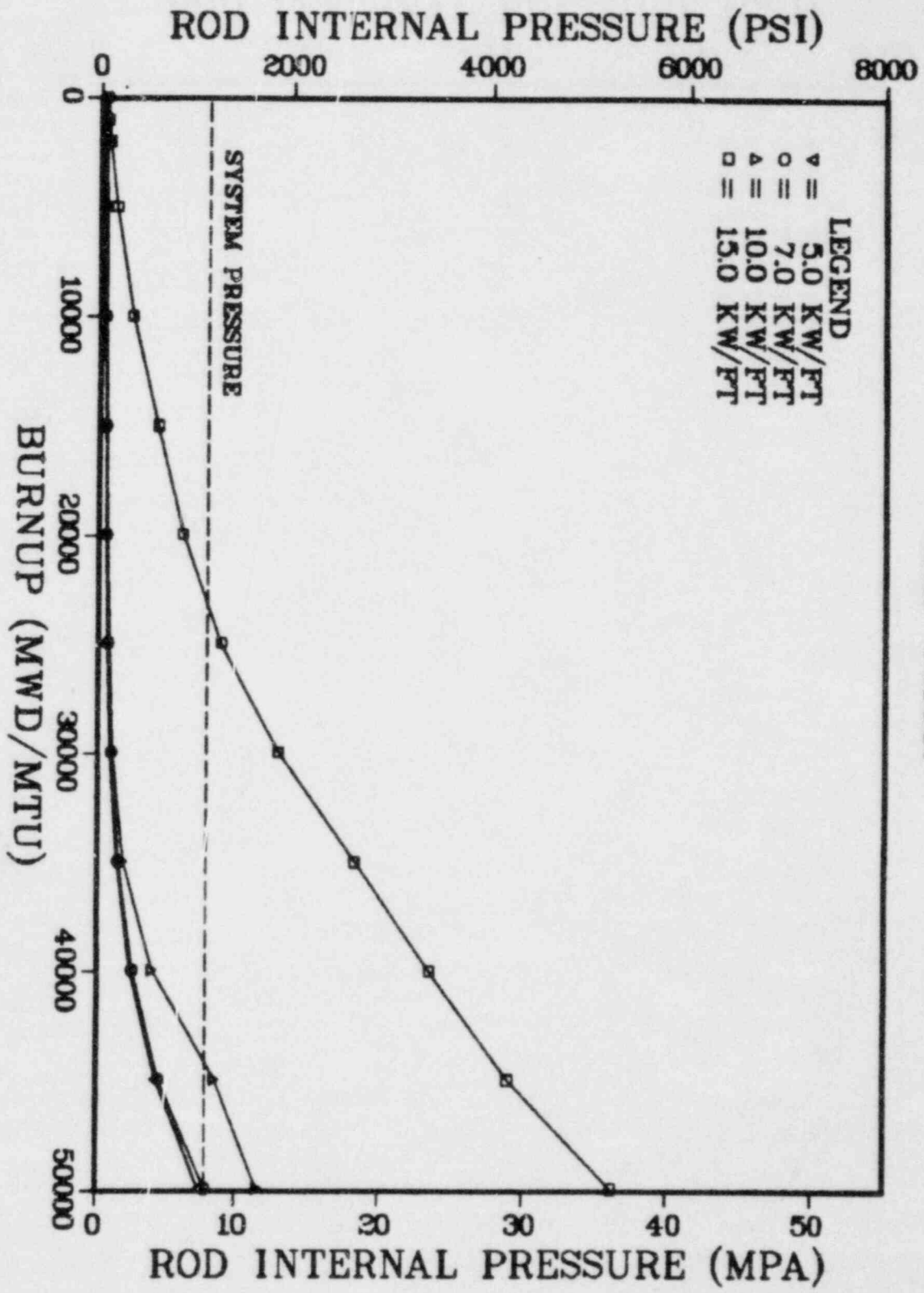
EXXON 8X8

G.E. 7X7

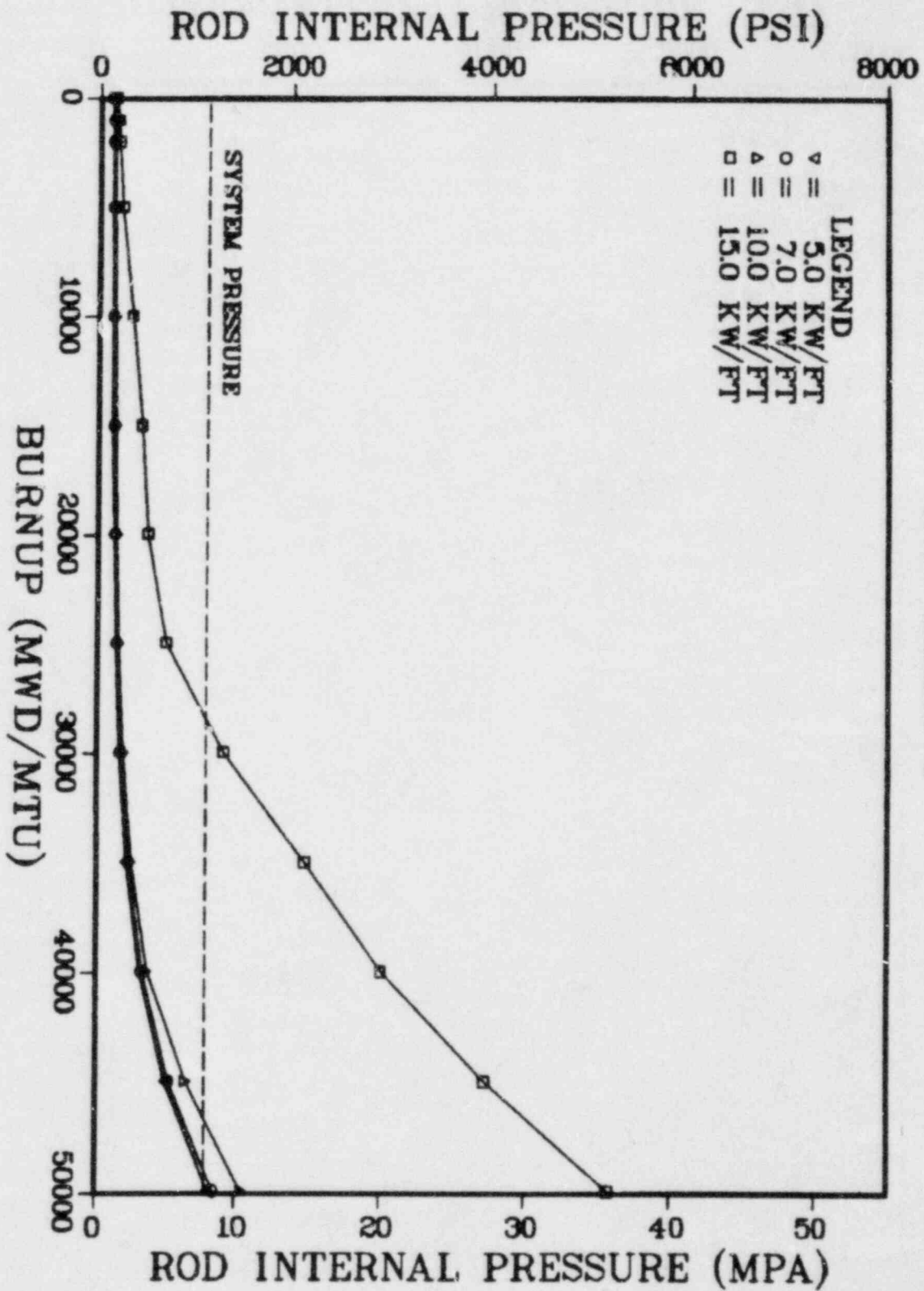


# G.E. 8X8

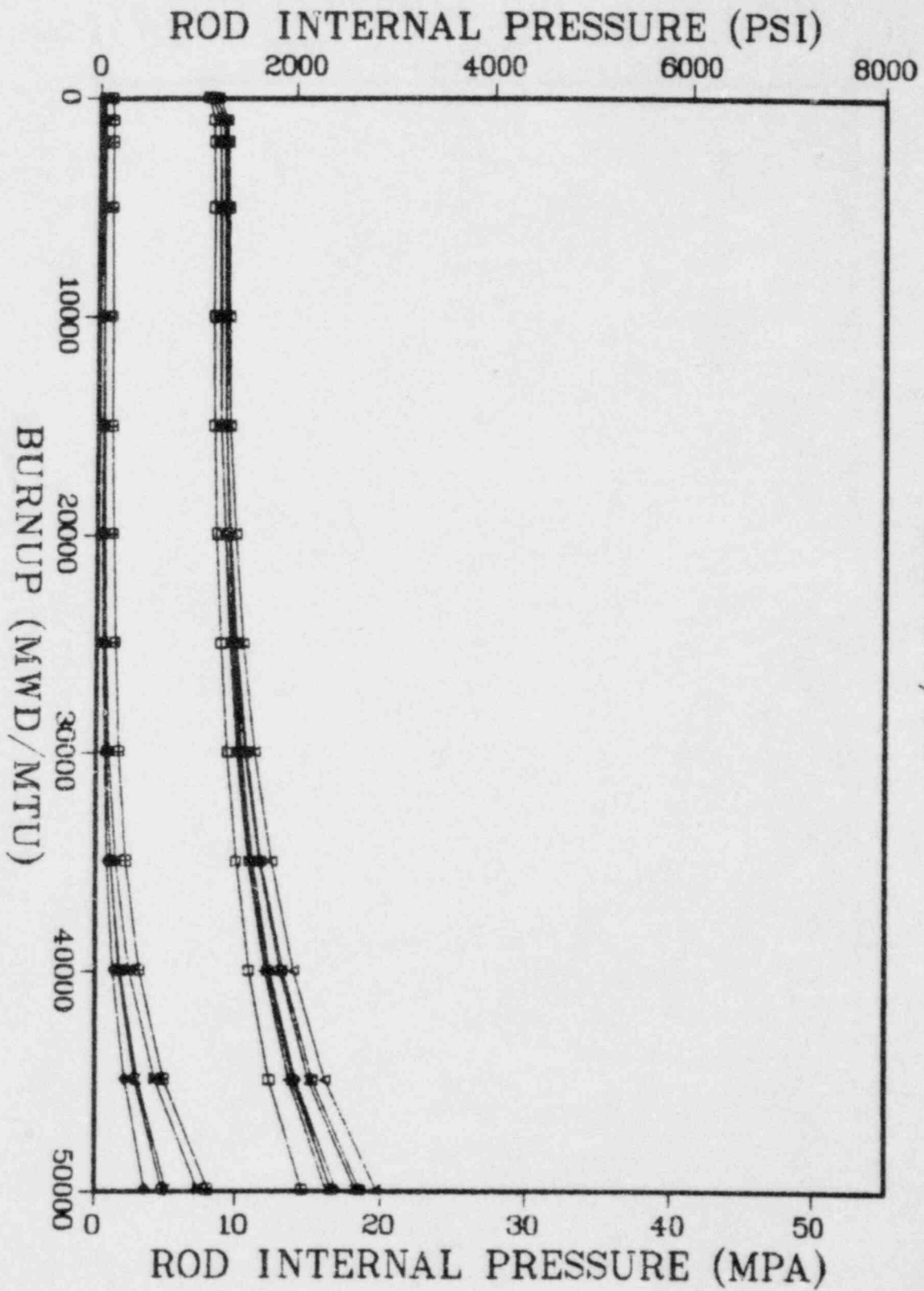


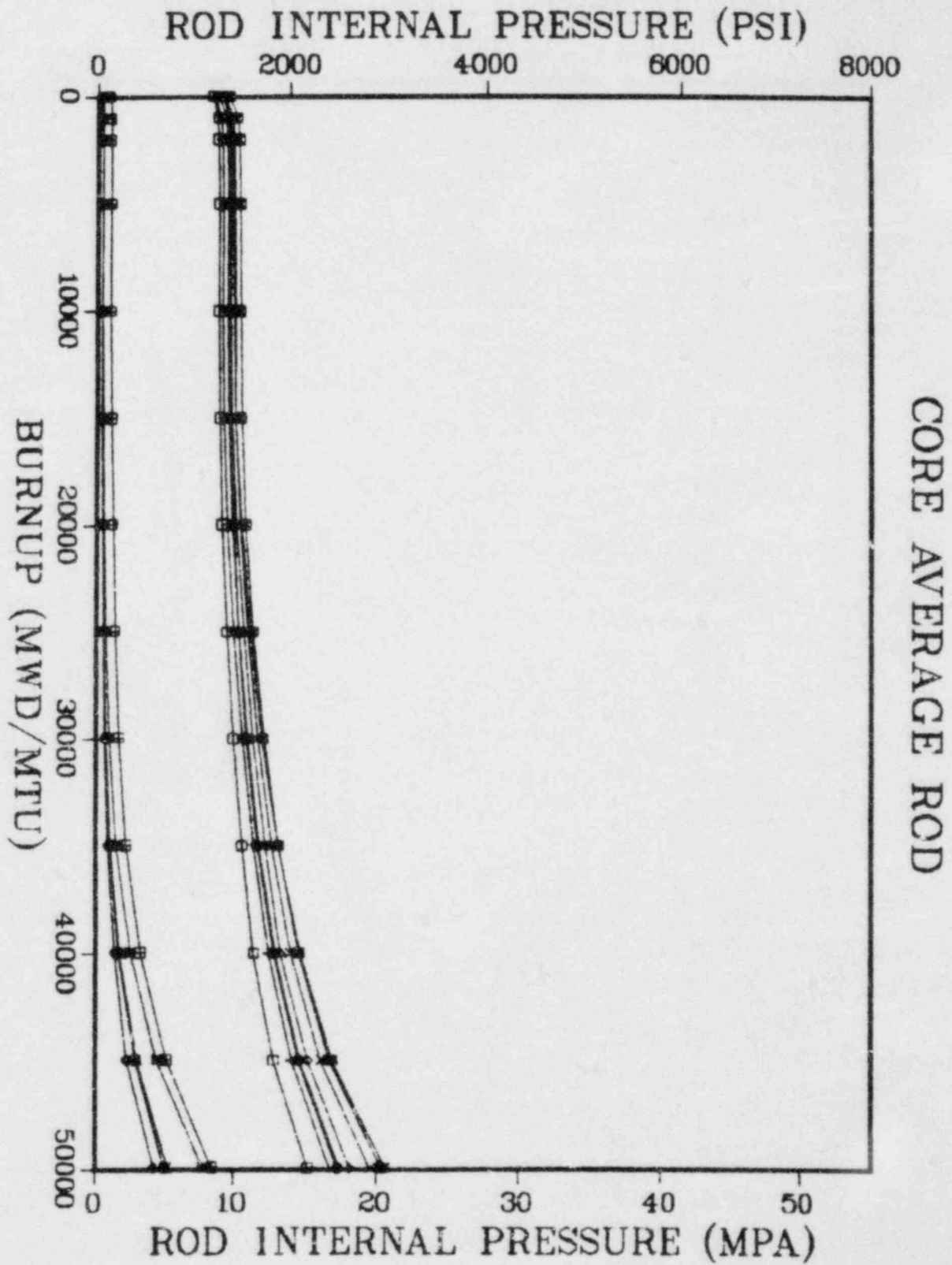


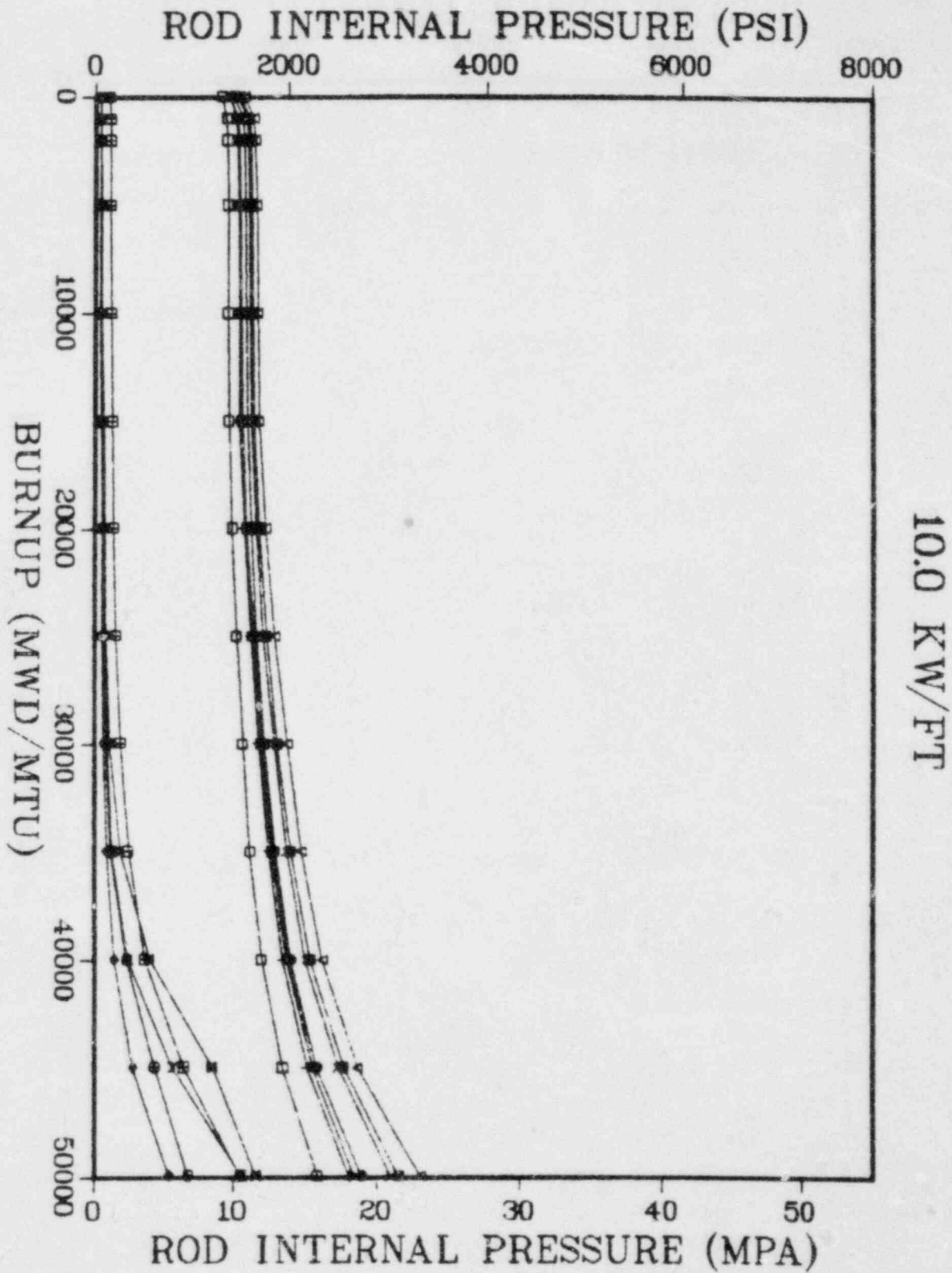
G.E. 8X8R



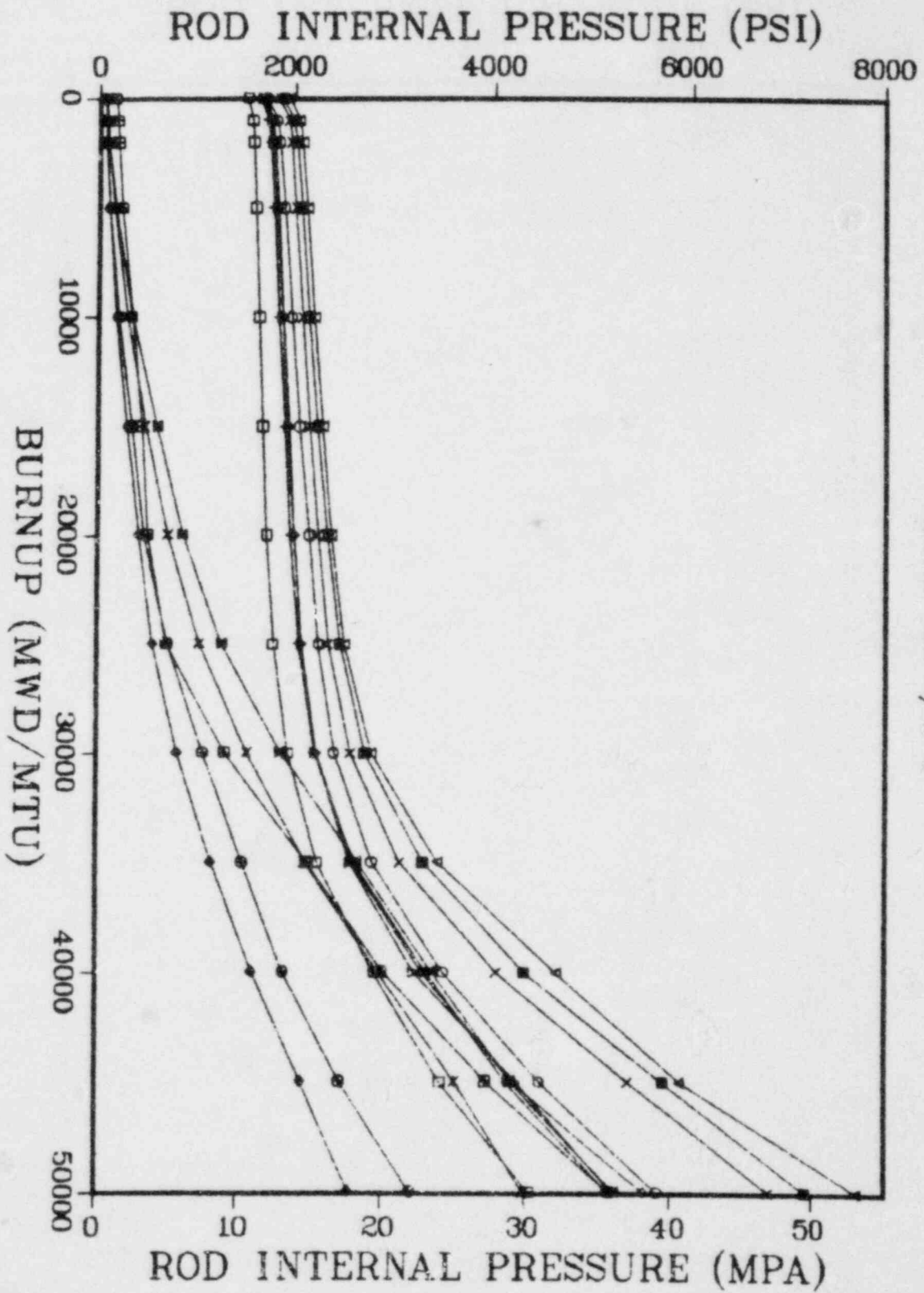
G.E. 8X8R-P











NRC FORM 335 (7-77)		U.S. NUCLEAR REGULATORY COMMISSION BIBLIOGRAPHIC DATA SHEET		1. REPORT NUMBER (Assigned by DDC) NUREG-0559	
4. TITLE AND SUBTITLE (Add Volume No., if appropriate) A COMPARATIVE ANALYSIS OF LWR FUEL DESIGNS				2. (Leave blank)	
7. AUTHOR(S) D. L. ACEY and J. C. VOGLEWEDE				3. RECIPIENT'S ACCESSION NO.	
9. PERFORMING ORGANIZATION NAME AND MAILING ADDRESS (Include Zip Code) Core Performance Branch Division of Systems Integration Office of Nuclear Reactor Regulation U.S. Nuclear Regulatory Commission 20555				5. DATE REPORT COMPLETED MONTH June YEAR 1980	
12. SPONSORING ORGANIZATION NAME AND MAILING ADDRESS (Include Zip Code) Core Performance Branch Division of Systems Integration Office of Nuclear Reactor Regulation U.S. Nuclear Regulatory Commission 20555				DATE REPORT ISSUED MONTH July YEAR 1980	
13. TYPE OF REPORT Technical Report				6. (Leave blank)	
15. SUPPLEMENTARY NOTES				8. (Leave blank)	
16. ABSTRACT (200 words or less) <p>The computer code GAPCON-THERMAL-2 was used to generate thermal performance predictions for the spectrum of commercial light water reactor fuel designs at four different steady-state power levels. The input parameters for the code were obtained from design data that are non-proprietary and are tabulated in this report. Calculated values of maximum fuel temperature, average fuel temperature, stored energy, gap conductance, fission gas release and rod internal pressure are plotted as a function of burnup. Radial fuel pellet temperatures are also plotted at one burnup level.</p>				10. PROJECT/TASK/WORK UNIT NO.	
17. KEY WORDS AND DOCUMENT ANALYSIS				11. CONTRACT NO.	
17b. IDENTIFIERS/OPEN-ENDED TERMS				14. (Leave blank)	
18. AVAILABILITY STATEMENT UNLIMITED		19. SECURITY CLASS (This report) UNCLASSIFIED		21. NO. OF PAGES 183	
		20. SECURITY CLASS (This page) UNCLASSIFIED		22. PRICE \$	

UNITED STATES  
NUCLEAR REGULATORY COMMISSION  
WASHINGTON, D. C. 20555

OFFICIAL BUSINESS  
PENALTY FOR PRIVATE USE, \$300

POSTAGE AND FEES PAID  
U.S. NUCLEAR REGULATORY  
COMMISSION

